5-2008

The TTC7$^{FSN/FSN}$ Mutation Results in Hyperactivation of Lymphocytes and Overproduction of IL-4 Leading to the Development of Systemic Autoimmunity

Beth Lindroth Hill

THE TTC7$^{FSN/FSN}$ MUTATION RESULTS IN HYPERACTIVATION OF LYMPHOCYTES AND OVERPRODUCTION OF IL-4 LEADING TO THE DEVELOPMENT OF SYSTEMIC AUTOIMMUNITY

By

Beth Lindroth Hill

B.A. University of Southern Maine/Lewiston Auburn College, 2000

A Thesis

Submitted in Partial Fulfillment of the

Requirements for the Degree of

Doctor of Philosophy

in Biochemistry and Molecular Biology

The Graduate School

The University of Maine

May, 2008

Advisory Committee:

Stephen C Pelsue, Ph.D. Associate Professor of Immunology, Advisor

Kenneth Ault, Ph.D. Presidential Professor of Biomedical Science

Keith Hutchison, Ph.D. Professor of Biochemistry and Molecular Biology

Lucy Liaw, Ph.D. Scientist II, Maine Medical Center Research Institute

Ah-Kau Ng, Ph.D. Professor of Immunology

THE TTC7$^{FSN/FSN}$ MUTATION RESULTS IN HYPERACTIVATION OF LYMPHOCYTES AND OVERPRODUCTION OF IL-4 LEADING TO THE DEVELOPMENT OF SYSTEMIC AUTOIMMUNITY

By Beth Lindroth Hill

Thesis Advisor: Dr. Stephen C. Pelsue

An Abstract of the Thesis Presented
in Partial Fulfillment of the Requirements for the
Degree of Doctor of Philosophy
in Biochemistry and Molecular Biology
May, 2008

Ttc7$^{fsn/fsn}$ mice exhibit systemic autoimmunity characterized by hyperactivated B cells, increased interleukin-4, autoantibodies, kidney disease and reduced lifespan. Because the pathology is similar to systemic lupus erythematosus, Ttc7$^{fsn/fsn}$ mice are a useful model with which to study early events that lead to autoimmune disease.

Although the Ttc7^{fsn} mutation has been identified the gene function is unknown. The phenotype of Ttc7$^{fsn/fsn}$ mice mimics the Th2 autoimmunity of the IL-4 transgenic (Erb et al 1997). It was previously unknown whether the over-production of IL-4 was an intrinsic defect of Ttc7$^{fsn/fsn}$ lymphocytes that led to autoimmunity, or, whether excess IL-4 was produced as a result of hyper-activated lymphocytes, which then drove pathology. Because the transcription factor, signal transducer and activator of transcription (Stat)-6 is unique to the IL-4 pathway and influences both IL-4 production and lymphocyte activation, we evaluated the regulation of Stat6 in B cells as an indication of IL-4 signaling. We examined the activation status and IL-4 production in 4-and 10-week T cells to determine if activation preceded the IL-4-driven pathology.

Immunoprecipitation and Western blot revealed that Stat6 appeared constitutively activated in Ttc7$^{fsn/fsn}$ B cells, however, *ex vivo* functional analysis of Stat6 with confocal microscopy determined that when the IL-4 signal was removed, Stat6 became deactivated.

The use of actinomycin D in mRNA expression studies revealed that IL-4 mRNA stability was increased in Ttc7$^{fsn/fsn}$ T cells which resulted in IL-4 production in unstimulated cells and extended IL-4 production after transcription was blocked as determined by ELISA. Using cyclosporine A in the same assays suggested that IL-4 production was dependent on TCR stimulation. Flow cytometry established that Ttc7$^{fsn/fsn}$ mice have more activated and memory T cells at 4-weeks, suggesting that activation occurs before the over-production of IL-4.

Genetically deleting Stat6 from Ttc7$^{fsn/fsn}$ mice unexpectedly did not improve the disease phenotype but increased the percentage of immature B and activated T cells. The neutralization of IL-4 improved renal pathology but did not alter the status of Ttc7$^{fsn/fsn}$ lymphocytes. Therefore, we suggest that the Ttc7^{fsn} mutation results in autoreactive lymphocytes that are induced to produce IL-4, leading to systemic autoimmunity.

ACKNOWLEDGEMENTS

I would like to thank Dr. Stephen C. Pelsue for his unflagging patience and guidance in this project. I would also like to thank Dr. Lynn Hannum and Cory Ernst for providing Figure 1.10, Nick Matluk III for his work on the anti-DNA ELISAs, Dr. Harini Bagavant for the kidney pathology images and scoring, and Ivy Berquist for assistance in maintaining the mouse colony. I am grateful to Dr. Fred Finkelman for kindly providing the GL113 cell line for use in producing as isotype control antibody in the IL-4 neutralization study. Thank you to Dr. Sara Ballester for permission to use her figure depicting IL-4 production and regulation in T cells (Figure 1 in the introduction). I am extremely grateful to Maine ScienceCorps, The USM Bioscience Research Institute, and The Lupus Research Institute for their financial support during this project.

I would also like to thank my lab-mates and the staff and faculty of the University of Southern Maine for contributing to a positive and friendly environment in which to work. Finally, I am extremely thankful for the love, support and patience of my husband David and my children Jesse, Sophie and Ingrid. This thesis is dedicated to them.

TABLE OF CONTENTS

LIST OF TABLES

LIST OF FIGURES

LIST OF ABBREVIATIONS

Abbreviation	
Act D	Actinomycin D
ANA	Anti-nuclear antibodies
BAFF	B cell activation factor of the TNF family (also known as Blys)
Bcl-6	B cell lymphoma 6
BCR	B cell receptor
BLIMP-1	B lymphocyte induced maturation protein-1
BSA	Bovine serum albumin
CLTA-4	Cytolytic T lymphocyte associated antigen-4
CsA	Cyclosporine A
ELISA	Enzyme linked immunosorbant assay
EMSA	Electrophoretic mobility shift assay
ETn	Early transposon
FBS	Fetal bovine serum
GN	Glomerulonephritis
ICAM	Intercellular adhesion molecule
IFN-γ	Interferon gamma
IL-4	Interleukin-4
IRF-1	Interferon regulatory factor-1
IRS	Insulin receptor substrates
ITIM	Immunoreceptor tyrosine-based inhibitory motif
NFAT	Nuclear factor of activated T cells
NK	Natural killer
PI	Propidium iodide
PI3K	Phosphatidylinositol 3- kinase

PTB	Phosphotyrosine-binding (motif)
RBC	Red blood cell
RT	Reverse transcriptase
RT-PCR	Reverse transcriptase polymerase chain reaction
SH2	Src-homology 2
SLE	Systemic lupus erythematosus
SOCS	Suppressor of cytokine signaling
STAT	Signal transducer and activator of transcription
TBS	Tris-buffered saline
TCR	T cell receptor
TF	Transcription factor
TPR	Tetratricopeptide repeat
Ttc7	Tetratricopeptide repeat protein 7
VCAM	Vascular cell adhesion molecule
WT	Wild type

INTRODUCTION

Autoimmunity results from the production of cells that react to self-antigens during the normal development of a diverse repertoire of cells needed to populate the immune system. Autoimmune disease results when the mechanisms in place to regulate and delete auto-reactive cells fail, helping to set-off a cascade of events leading to pathology that is still not fully understood. Autoimmune diseases affect between 14 to 23 million Americans but remain difficult to study, diagnose and treat due to the underlying complexity of the pathology which drives them and the heterogeneity of the known syndromes. There are over 80 recognized clinically distinct diseases, some that are organ specific such as Type I diabetes and pancreatic beta cells, and some that are systemic such as systemic lupus erythematosus, or SLE (May 2007). SLE, or Lupus, patients often exhibit multi-organ abnormalities and inflammation including skin lesions, vasculitis, immune complex deposition, renal disease and failure, anti-nuclear autoantibodies, arthritis, neurological disorders and cytokine abnormalities. Lupus can affect children as well as the elderly, but is most often diagnosed in women of child-bearing years. There exists great variation between one patient and another, even among genetically similar individuals, suggesting that a complex interaction between environmental agents and disease susceptibility genes determines disease progression and outcome (Kammer, Perl et al. 2002). Some underlying defects contributing to the pathogenesis of SLE have been identified and include impaired clearance of dying cells (Gaipl, Munoz et al. 2007), impaired T cell signaling (Kammer, Perl et al. 2002), cytokine imbalances, abnormal B cell activation, inhibition of apoptosis, and abnormal cell proliferation. These defects may have multiple causes, known or unknown, and

may be genetic and/or acquired during the course of infection or aging, making the diagnosis of autoimmune disease and the study of it difficult and complex. This mutli-factorial etiology therefore requires research in a variety of systems to represent the subsets that exist among the human population (Wakeland, Wandstrat et al. 1999; Marrack, Kappler et al. 2001; Whitelaw and Martin 2001).

A number of mouse models of SLE and systemic autoimmunity have been developed or identified to delineate the pathways critical to the development of disease. MRL-lpr/lpr mice lack functional CD95, which is important for apoptosis and develop a lymphoproliferative disease similar to lupus (Giese and Davidson 1992; Singh, Saxena et al. 2003). The murine New Zealand Black/New Zealand White F1 hybrid develops spontaneous systemic autoimmunity and has been helpful in identifying a number of SLE susceptibility loci (Wakeland, Wandstrat et al. 1999). BXSB/MpJ mice carry the Y-linked autoimmune acceleration gene (*Yaa*) and spontaneously develop autoantibodies and glomerulonephritis similar to human SLE (Singh, Saxena et al. 2003). These models and others have been crossed to produce congenic strains as well as genetically modified to add or delete desired traits. The use of these models have greatly contributed to the pool of knowledge regarding autoimmunity, however, there are still many unanswered questions.

Flaky skin mutant mice display systemic immune dysfunction and autoimmunity which includes lymphadenopathy and splenomegaly, alterations in immunoglobulin profiles, the presence of antinuclear autoantibodies and glomerulonephritis (Pelsue, Schweitzer et al. 1998; Withington, Maltby-Askari et al. 2002). In addition, these mice exhibit an alteration of splenic architecture and cell populations, as well as a substantial

increase in the number of lymphocytes in the spleen and lymph nodes. Flaky skin mice acquired their name from the characteristic thickening and flaking of their skin due to the underlying inflammation of the dermis and epidermal layers. They are anemic at birth, and easily identified by the paleness of their ears and tail, reduced size, hunched stance and hair striations on their bellies.

The flaky skin mutation arose spontaneously in A/J mice at the Jackson Laboratory (Bar Harbor, Maine) and has been maintained on the BALB/cByJ strain (Pelsue, Schweitzer et al. 1998). The mutation in the flaky skin gene has been recently identified as an early transposon (ETn) retroviral insertion in the tetratricopeptide repeat 7 ($Ttc7^{fsn}$) gene located on the distal end of mouse Chromosome 17 (Helms, Pelsue et al. 2005; White, McNulty et al. 2005). Hence, flaky skin mice are presently referred to as $Ttc7^{fsn/fsn}$ mice. Ttc7 codes for an 858 amino acid protein which has seven tetratricopeptide repeat (TPR) sequences. The insertion adds 61 amino acids into one of the TPR domains which is thought to disrupt protein function (Helms, Pelsue et al. 2005). Many proteins with several TPR repeats function as adaptor, scaffolding or chaperone proteins (Das, Cohen et al. 1998; Klee, Ren et al. 1998; Brinker, Scheufler et al. 2002; D'Andrea and Regan 2003; Jordan, Singer et al. 2003; Smith 2004), however, the function of Ttc7 is currently unknown. Tools for studying Ttc7 are not yet available, but are currently being developed by our lab.

One of the hallmarks of $Ttc7^{fsn/fsn}$ mice is the dramatic increase in interleukin-4 (IL-4) production (Pelsue, Schweitzer et al. 1998; Welner, Hastings et al. 2004). The phenotype of $Ttc7^{fsn/fsn}$ mice is consistent with that of the IL-4 transgenic mouse as described by Erb, et al (Erb, Ruger et al. 1997). Both exhibit increased expression of

MHC class II on the surface of hyper-proliferative B cells, increased IgG1, thymic involution, anemia, proteinuria, glomerulonephritis associated with complement and immune deposition in the glomeruli, and show increased production of autoantibodies, particularly anti-DNA. In addition, they each suffer a severely reduced life span of approximately 15 weeks as well as splenomegaly and lymphadenopathy without a coincident increase in the percentage of T lymphocytes as compared to B cells. However, one of the major differences between the IL-4 transgenic and Ttc7$^{fsn/fsn}$ is that Ttc7$^{fsn/fsn}$ mice are anemic at birth, before the onset of the IL-4-driven autoimmune pathology whereas treatment with the neutralizing monoclonal antibody, 11B11, starting at 3 days of age prevents the formation of anemia in the transgenic model, which develops by 4-weeks of age (Erb et al., 1997). In contrast to Ttc7$^{fsn/fsn}$, the IL-4 transgenic as described by Erb et al also has not reported evidence of skin pathology. Because of the complexity of the phenotype of Ttc7$^{fsn/fsn}$ mice and the many factors involved in the progression to autoimmune disease, it is important to have an understanding of the elements that contribute to normal and abnormal regulation and signaling of IL-4 in the immune system.

IL-4: Description and Function

IL-4 is a pleiotropic cytokine whose effects have been found to play a protective role in immunity to extracellular parasites, to suppress a cellular autoimmune response such as that in Type I diabetes, and to have an active role in tumor resistance. Overexpression of IL-4 has been implicated in allergy and humoral-immune related autoimmunity (Parronchi, de Carli et al. 1992; Chan, Brown et al. 1996; Webb,

McKenzie et al. 2000; Li-Weber and Krammer 2003), while underexpression has resulted in autocrine growth of tumors and increased susceptibility to some infectious diseases such as *leishmaniasis* (Miralles, Stoeckle et al. 1994). Variables such as the relative amount expressed, timing of production, site of expression, the presence of other cell signals and the genetic background of an organism influence the effects of IL-4 on physiologic processes.

IL-4 was first identified in 1982 as a B cell growth factor (Howard, Farrar et al. 1982). Since then, the structure and function of this molecule has been studied extensively. IL-4 is predominately produced by activated T lymphocytes, as well as NK1+T cells, mast cells and basophils. It has been shown to mediate numerous effects on many different cell types, including T cells, B cells, monocytes, dendritic cells, mast cells, endothelial cells, keratinocytes, hepatocytes, fibroblasts, astrocytes, and osteoblasts. IL-4 acts as a co-stimulant for growth in B cells as well as in T cells and mast cells, it diminishes the inflammatory functions of monocytes and macrophages while enhancing their antigen-presenting functions, it induces growth and chemotaxis in human fibroblasts and the production of IL-6, extracellular matrix proteins and ICAM-1, it regulates the expression of VCAM-1 on human endothelial cells and VLA-4 on T cells and eosinophils, and reduces chloride ion secretion by intestinal epithelial cells (Keegan 2000). IL-4 is absolutely required for the differentiation of the Th2 subset of helper T cells and is considered to be the hallmark of Th2 cytokines along with IL-5, IL-6, IL-10 and IL-13 (Zamorano, Mora et al. 2001; Ansel, Djuretic et al. 2006). Many signal transduction pathways activated by IL-4 have been studied and dissected, with IL-4 signaling in B cells being a particular area of focus.

Optimal activation of B cells is dependent on two Th2-mediated stimuli, IL-4 and a second signal provided by CD40L (1igand). Together, these stimulate the proliferation of B cells, induce the expression of the low-affinity Fc receptor for IgE (CD23), upregulate major histocompatibility class II molecules on the B cell surface, and stimulate the transcription of un-rearranged immunoglobulin heavy-chain germline Ig-epsilon and Ig-gammaI genes leading to class switching and IgE and IgGI synthesis (in mice) or IgG4 (in humans) (Nelms, Snow et al. 1998). IL-4 also regulates the expression of the co-activation and adhesion molecule Thy-l (CD90) on B cells (Snapper, Hornbeck et al. 1988), and has been shown to exert protective effects on cells, sparing them from spontaneous and induced apoptosis (Rush and Hodgkin 2001; Morris, Dragula et al. 2002; Wurster, Withers et al. 2002; Carey, Semenova et al. 2007). Mice lacking IL-4 have normal T and B cell development but highly reduced levels of IgG1 and completely lack IgE (Kuhn, Rajewsky et al. 1991).

IL-4 is an -20kDa globular secreted glycoprotein comprised of four short alpha helices identified as A,B,C, and D. The IL-4 gene is located on mouse chromosome 11 and on the long arm of human chromosome 5 at q23-31 (Keegan 2000). Although IL-4 production has been considered to be the function of CD4+ Th2 cells and mast cells, it has remained a question which cell type provides the initial production of IL-4 to drive the polarizing response. There is evidence that NK-T1 cells may provide the initial hit (Brown and Hural, 1997), but recent evidence suggests that naïve CD4+ cells themselves transcribe low basal levels of IL-4 that act in an autocrine fashion and poise naïve T cells at the brink of becoming committed to IL-4 production (Dorado, Jerez et al. 2002; Yagi, Suzuki et al. 2002; Grogan, Wang et al. 2003; Baguet and Bix 2004; Omori and Ziegler

2007; Rose, Lichtenheld et al. 2007). Recent evidence has shown that germinal center B cells may also be a possible source of IL-4, at least localized to the tonsilar and colonic mucosa. This was demonstrated to be an antigen-dependent response and was specifically seen in a small percentage of B cells prior to differentiation into memory cells. The regulatory mechanisms of IL-4 production in B cells remain unclear although they appear to require the presence of IL-4 and Th2 cells. Molecular regulatory mechanisms of IL-4 production in B cells are thought to be different than those of T cells as B cells displayed a comparatively high level of production of IL-4 and a low level of mRNA in contrast to the co-localized IL-4 producing T cells in the system that was used to study this phenomenon (Johansson-Lindbom and Borrebaeck 2002; Harris, Goodrich et al. 2005).

The endogenous mechanisms active in potentiating IL-4 activity are unclear, but when injected in experimental murine systems IL-4 is rapidly cleared from the circulation and secreted by the kidneys in a proteolytically degraded form. The clearance of IL-4 is also dependent on the internalization of the IL-4 receptor complex and processing in lysosomes. Additionally, in both mouse and humans a naturally occurring soluble version of the IL-4Ralpha chain exists which may function to extend the half-life of IL-4 in the serum by acting as a carrier protein. Conversely, it may also block the binding of IL-4 to the IL-4 membrane-bound receptor thus reducing IL-4 bio-activity. The exact function of this soluble receptor has not yet been elucidated (Weisman, Creaner et al. 1996; Sang, Ouma et al. 1999; Keegan 2000).

IL-4 Regulation and Signaling

The fate of antigen activated naïve T cells is dictated in part by the surrounding cytokine milieu. IL-4 is generally considered to be a hallmark cytokine for humoral immunity due to its role in skewing T helper cells into the Th2 direction, which then provide B cell help. As mentioned earlier, the cell responsible for the first IL-4 "hit" has yet to be definitively determined, but IL-4 is capable of upregulating its own production and acting as an autocrine growth factor for Th2 cells (Yagi, Suzuki et al. 2002). In fact, recent evidence suggests that neonatal resting CD4+ cells are programmed to very rapidly produce high levels of IL-4 upon activation and remain in such a state of transcriptional permissivity until about 3-weeks of age, where chromatin changes cause transcriptional repression until the proper priming occurs resulting in a more adult-like response. This early response was shown to be signal transducer and activator of transcription-6 (Stat6) independent and cell-cycle independent which is in contrast to the adult CD4+ differentiation program (Baguet and Bix 2004; Rose, Lichtenheld et al. 2007). Differentiation into adult CD4+ IL-4+ cells requires several rounds of cell division (Bird, Brown et al. 1998) during which DNA demethylation (Kim, Fields et al. 2007) and chromatin remodeling occurs to make the IL-4 control region more accessible to transcriptional machinery (Guo, Hu-Li et al. 2002). To gear up for IL-4 production in adult resting CD4+ cells, IL-4 binds to the IL-4 receptor which phosphorylates and activates JAK (Janus kinase) kinases and Stat6. Stat6 translocates to the nucleus, the transcription factor GATA-3 is activated which is absolutely necessary for IL-4 production, chromatin is remodeled and becomes acetylated, and then c-Maf is activated. NFAT and NIP45 are upregulated, which then participate in regulating expression of IL-

4. The absence of Stat6 during this stage of differentiation results in cells that produce markedly reduced levels of IL-4 and lack of differentiation into Th2 effector/memory cells (Kaplan, Wurster et al. 1999; Ansel, Djuretic et al. 2006). However, after CD4+ cells have differentiated into effector memory cells ($CD62L^{lo}/CD44^{Hi}$) or central memory cells ($CD62L^{hi}/CD44^{hi}$) IL-4 production becomes Stat6 and IL-4 independent (Zamorano, Mora et al. 2001; Grogan, Wang et al. 2003; Yamashita, Shinnakasu et al. 2004).

It appears that IL-4 also has a hand in down-regulation of its own expression. When Th2 cells are activated through the TCR receptor, calcium is mobilized to the cytoplasm which activates the calcium-calmodulin dependent phosphatase calcineurin. Calcineurin then dephosphorylates the transcription factor NFAT, which is present in an inactive phosphorylated form in the cytoplasm. NFAT then performs a conformational change that allows it to translocate to the nucleus to promote transcriptional activity. This is a cyclosporine (CsA) sensitive event, as this immunosuppressive drug inhibits calcineurin and blocks IL-4 production. NFAT binds to a region defined as the P1 site in the IL-4 promoter region and is required for the upregulation of IL-4 early in activation. In later phases, Stat6 appears to complex with P1, competing with NFAT for the P1 site (Dorado, Jerez et al. 2002; Rengarajan, Mowen et al. 2002). When Stat6 is bound to P1, inhibitory molecules such as SHP-1, suppressors of cytokine signaling (SOCS) proteins, and B cell lymphoma protein-6 (Bcl-6) are able to be transcribed that help to attenuate IL-4 production (Losman, Chen et al. 1999; Jiang, Harris et al. 2000; Nicola and Greenhalgn 2000; Lyons, Lynes et al. 2003) (Figure 1).

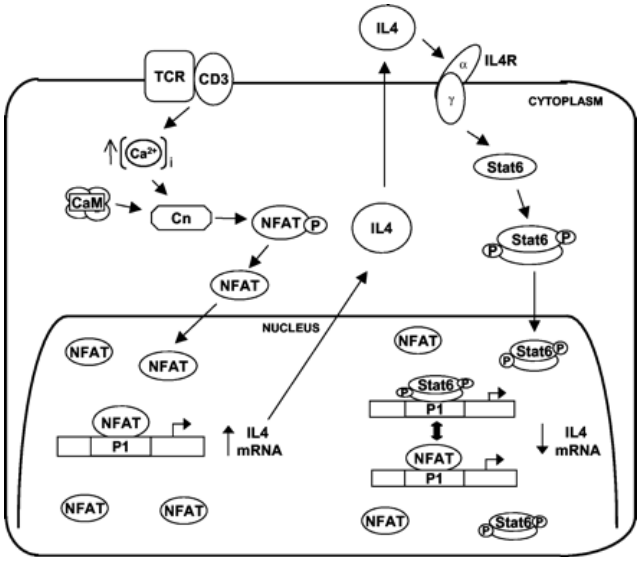

Figure 1. IL-4 Regulation in Th2 Cells
Used with permission (Dorado, Jerez et al. 2002)

The end result of the competition between NFAT and Stat6, i.e. decrease in IL-4 mRNA, depends on the presence of other transcription factors as well as attenuation of the stimulating signal. Low levels of IL-4 transcript continue to be present until the abolishment of signals to induce production (Dorado et al., 2002).

IL-4 Receptor

To produce a biological response, IL-4 must bind to specific high-affinity (K_d = 110-150 pM) receptors present on target cells (Noben-Trauth, Shultz et al. 1997). These are expressed at varying levels on many cell types of both hematopoietic and non-hematopoietic lineage, attesting to the importance of IL-4 in physiologic systems.

Kawakami, et al. (Kawakami, Kawakami et al. 2001), showed receptor densities to be at approximately 300-600 binding sites on basophils, less then 50 on endothelial cells, ~500 on resting T and B cells, and 200-300 on monocytes. Numbers can range up to 5000 receptors per cell however, which can serve as a determinant for IL-4 inducibility. Interestingly, the IL-4R is dramatically upregulated on many tumor cell types.

The IL-4 receptor consists of a ligand-binding 140-kDa alpha chain (IL-4Ra) and a second chain referred to as the common gamma (γc) chain that is shared by cytokine receptors for IL-2, IL-4, IL-7, IL-9 and IL-15. IL-4Ra is a member of the hematopoietin receptor superfamily which shares the presence of type III fibronectin domains in the extracellular region; these motifs include conserved paired Cys residues and a WSXWS motif that has been proposed to maintain the receptor in a conformation favorable for cytokine binding. It is here that helices A and C of the IL-4 molecule associate with the IL-4 receptor alpha chain. Helix D contacts the associating receptor chain, either the common gamma (cy) chain (Type I, more prevalent) or the IL-13 receptor alpha chain (Type II), one of which is needed to form an active receptor complex upon heterodimerization (Leonard and Lin 2000).

The cytoplasmic portion of the murine IL-4Ra chain is 553 amino acids long and contains five, highly conserved tyrosine residues, Y497, Y575, Y603, Y631, and Y713, as well as a short, proline-rich sequence in the membrane proximal region termed a "box motif'. This region has been found to be a site of association with JAK1, a tyrosine kinase critical in the initiation of signaling by hematopoietin receptors. Neither the alpha chain nor the cγ chain have endogenous kinase activity, therefore upon ligand binding to the IL-4R, JAKl (most likely aided by the common gamma chain associated JAK3) must

provide the initial signal to activate the signaling cascade. An adjacent acidic region has been shown to interact with the Src-family kinase, Fes, which has also been shown to be activated by IL-4 stimulation (Nelms, Snow et al. 1998). Activation of the JAK kinases via autophosphorylation or crossphosphorylation between JAKl and JAK3, leads to the tyrosine phosphorylation of the IL-4Ra chain at the appropriate conserved Tyr residues. These are also sites of potential interaction with the Src-homology 2 (SH2) regions or the phosphotyrosine-binding (PTB) domains of downstream signaling molecules.

Biochemical characterizations of pathways activated by IL-4R engagement have identified critical residues that initiate specific signaling cascades. Phosphorylation of Y497 appears to be required for the IL-4 mediated activation of cellular proliferation via interaction with insulin receptor substrate (IRS)-1/2 (Deutsch, Koettnitz et al. 1995). Y575, Y603 and Y631 are critical for the upregulation of IL-4 induced genes through the activation of the IL-4 specific transcription factor, Stat6. Residue Y713 appears to be located within the immunoregulatory tyrosine-based inhibitory motif (ITIM) (Jiang, Harris et al. 2000). Studies have demonstrated the interaction of the phosphatases SHP-1, expressed primarily in hematopoietic tissue, and SHIP with this region. These molecules appear to exhibit an inhibitory role on specific kinases. Research on the mutant mouse strain *motheaten,* in which SHP-1 is defective through the result of aberrant splicing, has shown SHP-1 to be constitutively expressed and to affect JAKl through dephosphorylation and subsequent inactivation (Hilton 1999). SHIP appears to act on the 5' phosphates of phosphotidylinositol (PtdIns)(3,4,5) triphosphate (PI3), thus regulating the phophoinositide (PI)-3 kinase pathway by dephosphorylating the products of this enzyme (Nelms, Snow et al. 1998). However, evidence suggests that SHIP has a positive

effect on B cell proliferation and survival which is in contrast to the proposed inhibitory function of the ITIM. This may reflect a cell type specific role of SHIP that modifies its function depending on location in the cell (Losman, Chen et al. 1999). Each of these pathways will be explored below, with particular emphasis placed on Stat6 regulated signaling in B cells.

IRS-1/2 Pathway

Upon binding of IL-4 to the IL-4 receptor, JAKs 1,2 and 3 potentially become activated and phosphorylate specific tyrosine residues. The phosphorylation of Y497 (Insulin Receptor Motif) on the IL-4Ra chain results in the phosphorylation of Insulin Receptor Substrates (IRS)-1/2 and induces an interaction with the receptor via the N-terminal phosphotyrosine-binding domain (PTB). IRS-1/2 has 20 potential phosphorylation sites, many with SH2 binding domains, as well as pleckstrin homology domains that are thought to allow for interaction with membrane-associated lipids. The regulatory subunit of PI-3K; p85, associates with the activated IRS-1/2 leading to a conformational change in p85, which then activates the catalytic subunit, p 110. The pl10 subunit phosphorylates membrane lipids, mediating the transfer of gamma phosphate from ATP to the D3 position of inositol in membrane-associated phosphotidylinositol producing Ptdlns(3,4,5)P3 or PtdIns(3.4)P2. These molecules act as second messengers to activate downstream kinases such as protein kinase C (PKC) leading to cell proliferation and/or protein kinase B (Akt) which plays a key role in cell survival (Nelms, Snow et al. 1998; Nelms, Keegan et al. 1999).

PI-3K also appears to be able to phosphorylate serine/threonine residues as well as the tyrosine residues involved in activation. Downregulation of this pathway may result from a negative feedback loop put into action by the ser/thr phosphorylation of IRS-1.

Activated IRS-1/2 may alternatively (or also) bind to the adapter molecule, Grb2. This is constitutively associated with the nucleotide exchange protein SOS, which exchanges the GDP of inactive Ras, with GTP to activate Ras. Ras-GTP activates the serine/threonine kinase Raf, which triggers the cascade leading to the mitogen-activated protein kinases, ERK-1/2 in the Ras/MAPK pathway. These translocate to the nucleus to induce gene expression through phosphorylation of transcription factors in the nucleus, such as c-fos. The Jun nuclear kinase, JNK, as well as small GTPases are also Ras activated, which results in upregulation of gene expression through activation of transcription factors such as c-Jun. When c-Jun and c-Fos are activated, they heterodimerize to form the transcription factor complex AP-1, which upregulates genes involved in the entry of the cell into the cell cycle and proliferation and differentiation. The Ras/MAPK pathway is not consistently observed to be upregulated by IL-4 in all cell lines, and in fact IL-4 generally fails to activate the Grb-2 linked Ras/Mapk pathway (Satoh, Nakafuku et al. 1991). However, in keratinocytes, IL-4 induces IL-6 secretion through the rapid activation of p38 MAPK (Wery-Zennaro, Zugaza et al. 2000).

The adapter molecule Shc, may also function to activate the MAPK pathway instead of IRS-1/2. This is a good example of the specificity of signaling being regulated in part by the particular molecules present in various cell types as this pathway was identified specifically in B cells and keratinocytes (Crowley, Harmer et al. 1996). Shc has

a PTB domain which links it to the IL-4 receptor, as well as an SH2 domain linking it to Grb2/Sos and the pathway described above. In B cells, Shc also functions as an adapter molecule in the BCR signaling pathway in which it has been found to associate with Grb2/Sos as well, perhaps resulting in cross-talk between pathways. Another adapter protein, Cbl appears to act in a similar manner to Shc in other cell types, such as T cells, although when hyperphosphorylated Cbl appears to act in an inhibitory manner (Nelms, Keegan et al. 1999).

Downregulation of the Ras pathway may be provided by FRIP, or IL-4 receptor interacting protein, which is a homolog of p62dok(downstream of kinases), a previously discovered phosphoprotein found to bind to Ras-GAP. Phosphorylated FRIP associates with the IL-4Ra chain where it recruits and binds to Ras-GAP (GTPase activating protein), which catalyzes the conversion of Ras-GTP to inactive Ras-GDP. Thus, Ras-GAP functions as an inhibitory protein of the Ras pathway. FRIP is expressed at high levels in T cells; however, it has not been shown to be expressed at high levels in B cells (Nelms, Snow et al. 1998).

Stat6

Upon binding of IL-4 to the IL-4receptor, JAK kinases become activated and phosphorylate tyrosine residues on the receptor alpha chain. Stat6 is recruited to the receptor alpha chain and binds to the cytoplasmic portion of the chain at specific residues via its SH2 domains when the chain is tyrosine phosphorylated on highly conserved residues Y575, Y603, or Y631. Stat6 then becomes phosphorylated on its C-terminal tyrosine residue, Tyr641, by the JAKs. This facilitates the disengagement of the Phospho-

Stat6 (pStat6) from the receptor, which then dimerizes with another pStat6 monomer and activates a cascade that allows for the translocation of the Stat6 dimer to the nucleus. Here, it binds to specific DNA elements on IL-4 responsive genes identified by the recognition sequence TTC-N4-GAA (Quelle, Shimoda et al. 1995; Nelms, Snow et al. 1998).

As mentioned previously, Stat6 is a transcription factor unique to the IL-4 pathway (it may also be active in the IL-13 pathway but evidence is conflicting) (Arinobu, Sugimoto et al. 2000; Andrews, Rosa et al. 2001). Its importance in mediating the effects of IL-4 has been illustrated in studies done with Stat6 deficient mice. Stat6 was found to be required for the surface expression of MHC class II antigens as well as the IL-4 receptor and CD23. Lymphocytes from these Stat6 deficient animals failed to proliferate in response to IL-4 and B cells were unable to produce IgE. T lymphocytes failed to differentiate into Th2 cells in response to IL-4 or IL-13 (Kaplan, Schindler et al. 1996; Mikita, Campbell et al. 1996; Peng, Moslehi et al. 1997).

Regulation of the Stat6 pathway and the mechanisms by which Stat6 initiates transcription are still being elucidated. Natural deletion mutants, the result of alternative splicing of Stat6 transcripts, called Stat6b and Stat6c have been found in some cell types (Patel, Pierce et al. 1998; Hebenstreit, Wirnsberger et al. 2006). There is not much known about these, however, Stat6b contains an N-terminal truncation that still functions when dimerized with a full length Stat6. Stat6c contains a SH2 domain deletion which prevents dimerization with intact Stat6 molecules. This is hypothesized to be an inhibitory measure in the activation pathway, possibly only in mast cells (Patel, Pierce et al. 1998).

Activation of the Stat6 pathway upregulates gene transcription of the SOCS/CIS (cytokine induced SH2)/JAB (JAK binding)/SSI-1 (stat-induced stat inhibitor) family. These inhibitor proteins are specific for the JAK/Stat pathway. Socs-2 and Socs-3 have been shown to be induced by IL-4, while Socs-1 has an inhibitory effect on IL-4 signaling, and may be the primary Socs inhibitor in this pathway (Losman, Chen et al. 1999). The exact mechanism of action has not been worked out, but these proteins appear to function by inhibiting JAK activity by either binding to the JAK activation loop or by functioning as a block between the activated JAK and receptor. In addition, Socs proteins have a conserved Socs box motif located at their C terminus which appears to bind to elongin B and elongin C, molecules that target proteins to the proteasome for ubiquitination and degradation. Thus, a two-step model of inhibition has been proposed, first, inhibition of signaling by binding of Socs to activated proteins, and second, targeting of the signaling components for degradation. This system may also be the way in which inhibitory cross-talk between pathways is conducted (Greenhalgh and Hilton 2001). To complicate matters further, another family of proteins, the Pim kinases, appears to be involved in regulating SOCS proteins in a positive manner. Whether the Pims protect the Socs from degradation or operate by a different mechanism remains unclear (Losman, Chen et al. 1999).

Another family of proteins called protein inhibitors of activated STATs, or PIAS proteins, appear to be constitutively expressed in a number of cell lines. These are thought to act as buffers and bind to active STAT dimers and interfere with DNA binding activity, thus maintaining an equilibrium of available to unavailable STAT dimers (Hilton 1999). The exact mechanism of action has not yet been determined, but it appears that the

methylation state of the STAT dimers influences PIAS' binding activity. Inhibition of methylation enhances the ability of PIAS to bind to activated STATs and reduces their DNA binding capacity (Greenhalgh and Hilton 2001; Chen, Daines et al. 2004).

As mentioned above, the IL-4Ra contains an ITIM, which also functions in an inhibitory capacity. In studies performed with a cell line exhibiting a mutated Y713 site in the IL-4Ra, Stat6 was found to be hyperactivated, showing both higher levels of phosphorylation and longer periods of activation. The effect of the mutated Y713 was not as dramatic on the IRS-1/2 pathway leading researchers to conclude that this was a regulatory measure functioning in gene expression, although they were unsure of the mechanisms involved (Kashiwada, Giallourakis et al. 2001).

The STAT family of transcription factors shares a conserved overall structure which includes a central DNA binding domain, followed by a linker domain and the SH2 domain. The carboxy-portions of the proteins contain a single phosphorylated tyrosine residue absolutely required for DNA binding activity. The C-terminal portion is also required for transcriptional activity but the mechanisms are still poorly understood. However, it has been demonstrated that the C-terminal transactivation domain is regulated independently of the DNA binding activity and that IL-4 induces signals that provide regulation at the transcriptional level. Recent evidence suggests that serine phosphorylation is one of the signals that acts on a transcriptional level. This appears to occur downstream of JAK activation and tyrosine phosphorylation of STAT, and is not regulated by the PI-3K regulated kinases such as Akt, PKC, or p70 S6 (i.e., the IRS-1/2 pathway)(Pesu, Takaluoma et al. 2000).

It is possible that pStat6 dimers may upregulate the expression of IL-4 inducible genes by themselves, however, it is likely that they form complexes and interactions with other transcription factors activated through other signaling pathways. The promoter regions of IL-4 inducible genes contain several cis-acting elements and it appears that the cooperation between different transcription factors (TFs) is critical for efficient regulation of gene transcription. Stat6 appears to be the only TF that is functionally regulated by IL-4, whereas the other factors are either regulated by costimulatory signals, as exemplified by CD-40 regulation of NF-KB, or other signaling pathways. Stat6 cooperates with other TFs through various mechanisms depending on the TFs involved. For example, C/EBP stabilizes the DNA binding of Stat6, while the interferon regulatory factor (IRF)-4 and NF-KB promote transcriptional activation and involve physical interaction with Stat6 (Pesu, Aittomaki et al. 2002).

Recent evidence obtained with gene chip analysis suggests that Stat6 not only cooperates with TFs from other pathways, but upregulates transcription factors at the transcriptional level which then function to modulate Stat6/IL-4 induced effects (Schroder, Pavlidis et al. 2002; Daines, Andrews et al. 2003). These factors include transcriptional repressors, such as Bcl-6, which is needed for germinal center formation in B cells. A lack of Bcl-6 results in an increase in Th2 mediated inflammatory responses. Krox20 is upregulated by Stat6 and has been found to be needed in the CD23 promoter for expression of CD23 in B cells. Other factors induced by Stat6 include NKIL3, IRFs 1 and 4, Stat4, Bcl-3, and Xbp-1. The significance of these factors in IL-4 signaling has not yet been determined, although mice deficient in IRF-4 have profound defects in the

function of mature B and T cells (Schroder, Pavlidis et al. 2002; Hebenstreit, Wirnsberger et al. 2006).

Stat6 may be activated in an IL-4 independent manner through the cross-linking of CD40. CD40 is a glycoprotein receptor on the surface of B cells that interacts with T cells (CD401igand) and mediates immune responses to monomeric protein antigens. CD40 engagement results in cellular activation, homotypic cell adhesion, proliferation, germinal center formation, rescue from apoptosis, and induction of the transcription factors NF-KB, NF-AT and AP-l. It also produces expression of Bcl-2 in germinal centers and (with IL-4) promotes survival of mature B cells and isotype switching (Karras, Wang et al. 1997).

It appears that CD40-CD40L interaction plus IL-4 is necessary for the proper induction of isotype switching in B cells and CD23 expression (Siepmann, Wohlleben et al. 1996; Tinnel, Jacobs-Helber et al. 1998; Rush and Hodgkin 2001). Evidence for the necessity of this was provided when it was discovered that the contributory factors to hyper-IgM syndrome were mutations in the CD40L gene resulting in defective isotype switching (Siepmann, Wohlleben et al. 1996). CD40 induces B cell proliferation that may help drive isotype switching, and it also may open up the Ig locus for transcription of downstream isotypes and augment the responsiveness of the B cells to the effects of IL-4 by helping to increase the level of the IL-4 receptor and modifying the way in which it signals. Preincubation of B cells with anti-CD40, and the subsequent addition of IL-4 seems to result in "pathway switching" which may influence the way the IL-4 receptor signals (Siepmann, Wohlleben et al. 1996). Signaling through CD40 is not well understood but there is evidence for interaction with TRAF proteins, particularly TRAF3

in B cells (Basaki, Ikizawa et al. 2002), as well as JAK3 (Bacharier and Geha 2000; Zhang, Zhang et al. 2002).

Further evidence for the necessity of CD40 cosignals in IL-4/Stat6 signaling comes from Pesu and colleagues (Pesu, Aittomaki et al. 2002) and their examination of p38 mitogen-activated protein kinase (MAPK), which is directly activated by CD40 engagement and is responsible for activating downstream serine kinases. Inhibition of p38MAPK resulted in a block of CD23 expression in a Stat6 dependent manner. p38MAPK was not found to directly phosphorylate Stat6 in B cells, however it appears to regulate the unknown kinase that is involved in the serine-phosphorylation of Stat6 and its subsequent transcriptional activity. This then provides a link to CD4O and IL-4 interaction and the transcriptional activity of Stat6. Zhang and colleagues (Zhang, Zhang et al. 2002) found similar results for the requirement of CD40 activated p38 MAPK in class switching to IgE.

CD23 in B cell signaling and maturation

CD23 is the low affinity IgE receptor which participates in protective responses to helminthic parasites (Oettgen 2000). It is also a marker of B cell maturation and activation and is expressed on splenic Transitional 2 and mature B cells. CD23 is thought to participate with the survival factor BAFF (B cell activation factor of the TNF family) in maintaining the viability of these subsets (Hsu, Harless et al. 2002). Recent work has determined that when IgE is bound to CD23, antigen-capturing by B cells is enhanced which can lead to augmented immune responses (Oettgen 2000). High CD23 expression is a hallmark of B-chronic lymphocytic leukemia (Kneitz, Goller et

al. 2000) and with IgE, participates in inflammatory and allergic responses (Tinnel, Jacobs-Helber et al. 1998; Bacharier and Geha 2000; Oettgen 2000)

CD23, exists in two isoforms (in humans) CD23a, which is exclusively expressed on B cells and CD23b, which is present on a variety of cells of the myeloid lineage as well (Kneitz, Goller et al. 2000). It is encoded by a single gene and is a type II membrane protein which has a cytoplasmic NH2 terminus and a extracellular region that shares a high degree of homology with C-type animal lectins such asialoglycoprotein receptors and rat mannose binding proteins (Richards and Katz 1997). Tinnell et al. (Tinnel, Jacobs-Helber et al. 1998) studied the requirement for Stat6 in the upregulation of CD23. The results of their study showed that while Stat6 enhanced the expression of CD23, it was not absolutely required. They did demonstrate the presence of other Stat family members, namely Stat3 and Stat5 that may act in a similar manner as Stat6 in the CD23 promoter region in the absence of Stat6. However, CD23 expression is a hallmark of IL-4 induced B lymphocyte development and activation and appears to be Stat6 dependent.

Alignment of the CD23 and Ig-epsilon promoters reveal remarkable homology to each other with common response elements suggesting that a similar cassette of transcription factors is activated by IL-4, resulting in the enhanced expression of the two genes. This would make sense in light of the evidence that CD23 surface expression seems to regulate IgE responses in an inverse manner and would work in sync. Richards and Katz (Richards and Katz 1997) divided the Iε and CD23 promoters into 7 functional motifs. Motif 1 appears necessary for CD23 but not IgE induction although a binding element has not been identified. Motif 2 contains a consensus site

CCAAT/enhancer binding protein B (C/EBPB)', needed for IgE but not CD23. Motif 3 is a Stat6 binding site required for both IgE and CD23. Motif 4 contains NF-κB binding sites in both the IgE and CD23 promoters and is required for both. Motif 5 is identified as a stretch of DNA required for CD23, but not entirely necessary for IgE. However, this runs into Motif 6 which has a NF-κB-like sequence in the IgE promoter and there is similarity between both promoters in this region. Motif 7 contains a B cell specific activator protein (BSAP or Pax5) region that is LPS sensitive and present in both promoters. It is not known whether this is a required site however, as evidence is conflicting, but BSAP appears to be constitutively active in B cells and is also activated by CD40. Thus it may help couple the IL-4/CD40 signals to transcription (Thienes, DeMonte et al. 1997). CD40 also appears to be responsible for the activation of NF-κB, possibly at both promoter sites and is required for synergy with IL-4 signaling (Iciek, Delphin et al. 1997). This is also found to be true in the Ig-gamma promoter region. Specificity may be obtained by the combination of NF-κB subunits (Warren and Berton 1995). In fact, Messner and colleagues (Messner, Stutz et al. 1997) determined the composition of two NFκB complexes that were found in the IgE promoter. NFκB1 was of the classical type, or p50/p65. NFκB2 was comprised of p50/relB and appeared to be more functionally significant as an IL-4 response element. Alterations in regulation or function of many of these factors results in loss or expansion of B cell subsets and autoimmunity.

Isotype switching and IgE Production

The process of IgE (and IgG;(Schaffer, Cerutti et al. 1999)) production by B cells involve germline ε (or gamma) transcript expression, IgE class switching (from IgM), clonal expansion of B cells, and differentiation into IgE-secreting plasma cells. These activities are controlled by a variety of cytokines in addition to IL-4, as well as direct cell-to-cell contact between B cells and T cells via CD40/CD40L(CD154). The first signal is cytokine dependent and activates transcription at a specific locus determining isotype specificity, and the second signal activates the recombination machinery. The second signal also upregulates CD80 (B7.1) on B cells which provides a counter signal to T cells via CD28 to upregulate IL-4 (Warren and Berton 1995; Bacharier and Geha 2000).

The Ig heavy chain gene segments encode constant regions that rearrange by class switch recombination resulting in the production of other isotypes. Induction of isotype switching to a particular heavy chain region correlates with the transcriptional activation of that particular gene in the germline configuration. Induction of germline transcripts is necessary to target a switch region for recombination and switching. In the case of IgE class switching, IL-4 activates ε germline transcription through the tyrosine phosphorylation pathway to activate Stat6 and targeting the promoter region described above. Mice deficient in Stat6 fail to produce IgE in response to extracellular pathogens or IL-4/CD40 stimulus (Linehan, Warren et al. 1998). As mentioned previously, the germline ε promoter also contains binding sites for NF-KB, PU.1 and C/EBP transcription factors in addition to Stat6. PU.1 has been shown to be regulated via a separate pathway than Stat6. PKC-δ and PKC-ζ have been implicated in the IL-4-

induced threonine phosphorylation of PU.1; possibly through the IRS 1/2 or Fes kinase pathway and the recruitment of PI3K. PKC activation does not appear to be required for CD23 expression however (Ikizawa, Kajiwara et al. 2001).

Mao and Stavnezer (Mao and Stavnezer 2001) have provided conflicting evidence for the necessity of the presence of C/EBP in the murine ε germline promoter. They have demonstrated through the use of electrophoretic mobility shift assays (EMSA), that AP-1 binds to the putative C/EBP binding site instead. Functional evidence suggests a synergy with Stat6 in transcriptional activation, while C/EBP shuts down promoter activity in reporter gene assays. CD40 has been shown to upregulate c-fos, FosB, JunB and JunD providing the subunits necessary for AP-1 heterodimer formation, which in this case appears to be cFos/JunB. They have not ruled out the possibility of C/EBP acting as a regulatory molecule in this promoter site. Interestingly, their evidence supports the presence of C/EBP in the human ε germline promoter, identifying a possible area of divergence between human and mouse systems. How AP-1 and Stat6 interact has not yet been determined.

Less is known about the negative regulation of transcription and class switch recombination. Bcl-6, a transcriptional repressor upregulated by IL-4/Stat6 competes for Stat6 at the Stat6 binding site and can attenuate transcription (Oettgen 2000). Interferon-gamma induces the activation of Statl, which also competes with Stat6, possibly providing the mechanism by which Thl cells modify Th2 responses (and vice versa). Recently, another transcriptional regulator has been described by Monticelli and colleagues (Monticelli, Ghittoni et al. 2001), Myb, a member of a protein family known to be cell cycle sensors, was shown to overlap the Stat6 binding site of the ε promoter

and compete with Stat6, suppressing ε gene expression in reporter assays. Myb has been shown to interact with nucleolin, a protein important in the CSR machinery, thus it has been proposed that Myb may physically bridge the products of transcription and the recombination machinery (Ying, Proost et al. 2000). How it actually functions to repress transcription is currently unknown.

CD45, via its function as a Janus kinase phosphatase, directly dephosphorylates JAKl and JAK3, thus regulating IL-4 signaling and has a direct impact on class switching by preventing the phosphorylation of Stat6. CD45 is present at all stages of B cell development and has emerged as a potentially important regulatory molecule in the negative regulation of cytokine signaling (Yamada, Zhu et al. 2002). It is thought to also be important in B cell development as CD45-/- B cells have a developmental block in the transition from T 2 to mature follicular FO cells (Monroe and Dorshkind 2007).

The CTLA-4 receptor has been widely described in T cells as having a pleotropic inhibitory effect on activated cells. Less is known about the receptor in B cells. Pioli and colleagues (Pioli, Gatta et al. 2000) found that this receptor is present on the cell surface and in intracellular compartments at a level comparable to T cells in IL-4 and CD40 activated B cells. Furthermore, CTLA-4 engagement inhibits IgGI and IgE production and limits the number of IgG+ and IgE+ cells. This is probably accomplished in a few ways. CTLA-4 inhibits NFκB activation by counteracting the degradation of IκBa in B cells. It may also activate SHP (phosphatase) activity, thus inactivating Stat6 (or not allowing activation). It is speculated to have a counter-regulatory role to CD40 in germinal centers thus influencing the Thl/Th2 polarization as blockage of CTLA-4 accelerates a typical type 2 response. These effects are

mediated through costimulation by CD80 or CD86, which may be provided by other B cells or APCs. It is interesting to note that CTLA-4 engagement does not affect CD23 expression suggesting that CD23 may require less stringent conditions for expression, may be regulated differently or it may be a function of timeliness of activation (Pioli, Gatta et al. 2000).

IgE is believed to be one of the major mediators of immediate hypersensitivity reactions that underlie atopic conditions such as urticaria and eczema, seasonal allergy, food allergy, asthma, and anaphylaxis (Tachibana, Kubo et al. 2001). A mutant Stat6 molecule was identified that may be one mechanism by which IgE is upregulated in an abnormal manner. The mutant Stat6 has two mutations in the SH2 domain that rendered it transcriptionally active even in the absence of IL-4 signaling, was JAK independent for phosphorylation, was resistant to degradation by proteolysis and exhibited an enhanced DNA binding capacity. Other constitutively active forms of Stats have been identified as well, which have been associated with pathological conditions. Gain-of function polymorphisms in the IL-4 gene as well as the IL-4 receptor alpha chain have been shown to be associated with higher serum IgE levels and asthma, hence this may result in a similar phenotype as IgE is Stat6 dependent (Daniel, Salvekar et al. 2000). IL-13 shares many similarities with IL-4 perhaps mediated by the sharing of the IL-4Ra, along with IL- 13Ra, as the functional IL-13 receptor. Andrews (Andrews, Rosa et al. 2001) and colleagues have recently explored the observation that murine B cells are relatively unresponsive to IL-13. This was apparently due to the lack of expression of IL-13Ra1. The functional effect of this was an observed variation in IgE levels in experimental systems depending upon treatment with IL-13. This led them to the

conclusion that IL13Ra may be expressed at various stages of development of B cells and may help to clarify the overlap between IL-4 and IL-13 signaling (Andrews, Rosa et al. 2001).

The "final" step in B cell differentiation is conversion to either a memory cell or an antibody secreting plasma cell. Recent research has focused on a transcription factor known as a transcriptional repressor that appears to be a "master switch" in terminal differentiation and exerts an influence on many of the factors discussed above. IL-4 has been shown to repress the expression of B lymphocyte-induced maturation protein-1 or BLIMP-1, which appears to broadly inhibit gene expression programs controlling mature B cell functions, such as switch recombination, and those driving proliferation (Kallies and Nutt 2007). Among many of the transcription factors found to be influenced by BLIMP-1 are Stat6, Pax5, and Bcl-6 (Schebesta, Heavey et al. 2002). Bcl-6 and BLIMP-1 are thought to antagonize the actions of each other, particularly in germinal centers, where Bcl-6 is highly expressed. Thus, when Bcl-6 is active, cells undergo differentiation and proliferation, when Bcl-6 becomes downregulated, BLIMP-1 expression rises and cells become plasma cells. How this process actually occurs is unknown, but it may be the result of somatic mutations causing the affinity of the BCR to become greater and creating some kind of threshold that leads to loss of Bcl-6 and subsequent upregulation of BLIMP-1 (Shaffer, Yu et al. 2000). At first glance this seems to contradict information presented above. However, work completed in the lab of Paul Rothman and colleagues (Harris, Chang et al. 1999) has fine-tuned the role of Bcl-6 in B cells to be a co-regulator of IgE production which is expressed selectively to control the amount of IgE actually secreted. Thus, when a certain level of transcription has occurred in the IgE promoter,

i.e., a threshold, it would be active to shut down transcription. Since 30% -40% of diffuse large-cell lymphomas have Bcl-6 gene rearrangements, it would seem that Bcl-6 is an important regulator of B cells (Harris, Chang et al. 1999). Considering the wide ranges of influence BLIMP-1 and IL-4 have, other regulatory factors are likely to come into play as well (Knodel, Kuss et al. 2001; Shaffer, Lin et al. 2002).

Protective effects of IL-4 on cell survival

In 2000, the lab of Fred Finkleman reported the results of experiments done in a murine model which demonstrated that IL-4 promoted a dramatic increase in splenic B cells due to the migration of B cells into the spleen as well as increased splenic B cell survival. This was shown to be a Stat6, CD4+T cell, and FcyRII/III independent process but that it was IL-4R dependent (Mori, Morris et al. 2000). Numbers of mature blood and bone marrow B cells decreased, giving credence to this being a redistribution of B cells, and they were able to show that it did not depend on the production of new B cells in the spleen. There were no observable losses of B cells from lymph nodes, Peyer's patches or intestinal lamina propria. They have proposed that the mechanism of action is a retention of B cells in the spleen by the possible upregulation of an adhesion molecule or the loss of a molecule required for exit from the spleen as B cells normally migrate to the spleen, however, this does not account for the reduced number of mature B cells in the bone marrow (enhanced migration out of the bone marrow). They also exhibited an increase in the survival of splenic B cells, determined by the presence of a decrease in B cell expression of HSA, a cell marker that helps to identify the maturity of B cells. Hence, a decrease in HSA indicates an increase in B cell age. There was no mechanism of action offered for this process (Mori, Morris et al. 2000).

The protective effects of IL-4 on cell survival, such as prevention of cell death by neglect after growth factor withdrawal and rendering activated cells insensitive to Fas ligation, is an active area of research and has been mentioned previously. In contrast to T cells (Zamorano, Mora et al. 2001), IL-4 mediated protection from cell-death in B cells

appears to be Stat6 dependent and not directly dependent on IRS-2 activation or Akt activation. Stat6 has been shown to be directly responsible for the upregulation of IL-4 induced transcription of an anti-apoptotic factor, Bcl-xL, which is antagonistic to pro-apoptotic stimuli. This is thought to function by preserving mitochondrial membrane integrity and prevent the release of cytochrome C into the cytoplasm. This doesn't answer the whole question however, as the protection offered from overexpression of Bcl-xL was only ~50%, leading researchers to believe that there are other as yet undiscovered pathways and factors that may be responsible for the IL-4 induced protective effects in B cells (Zamorano, Mora et al. 2001; Wurster, Withers et al. 2002; Carey, Semenova et al. 2007).

One of these undiscovered pathways of IL-4/Stat6 mediated cell-survival may have recently been delineated by Thomas Chiles group at Boston College (Dufort, Bleiman et al. 2007). They discovered that IL-4 increases glucose transport and glycolysis in B cells through a Stat6 dependent mechanism that was independent of IRS-2 and PI3K activity. This effectively links glucose metabolism and apoptosis; if glucose metabolism is impaired, mitochondrial membrane integrity becomes impaired, triggering apoptosis. Thus, in Stat6 deficient B cells, IL-4 induced glycolysis is significantly reduced as is primary B cell viability.

Finkelman and colleagues (2002) have found evidence to support the Stat6 dependence of IL-4 conferred protection in B cells specifically working with autoreactive B cells. They also confirmed evidence that this mechanism is Stat6 independent in T cells, therefore appears to be regulated differently, but a mechanism for this was not offered (Morris, Dragula et al. 2002). Previous work done by Erb et al (Erb, Ruger et al.

1997) suggested that IL-4 did not prevent deletion of autoreactive B cells, but, Finkelman's group, working with soluble, oligovalent self-antigen instead of particulate, multivalent antigen used by Erb and colleagues, found that the ability of IL-4 to prevent Ag-induced B cell deletion decreases as the intensity of the Ag-induced mIg cross-linking increases. Thus, IL-4 might inhibit the deletion of B cells that are specific for soluble, oligovalent self-Ags that are present at low concentration, but not prevent the deletion of B cells specific for polyvalent cell membrane Ags. This appeared to be dependent on the concentration of IL-4 as well. They found that as the amount of IL-4 increased, the protective effects increased even as the intensity of the stimulus required for deletion increased (Morris, Dragula et al. 2002). There has been uncertainty of the role of IL-4 in autoimmunity, as it is difficult to evaluate the local concentrations that cells may be exposed to. However, finding that IL-4 can aid in the survival of autoreactive B cells, and that IL-4 deficient MRL/Mp-lpr/lpr mice show reduced autoreactivity (Peng, Moslehi et al. 1997), as well as the evidence that IL-4 transgenic mice show increased autoreactivity (Erb, Ruger et al. 1997) give credence to the notion that overexpression of endogenous IL-4 can drive autoimmunity in susceptible animals.

IL-4 also seems to have a protective effect on T cells but the picture is foggier than it is for B cells. Past research has shown that when pathways that promote cell survival are activated, cells can be pushed to differentiate into Th2 cells. This also apparently works in reverse as Th2 differentiation appears to result in resistance to apoptosis. The mechanisms involved in these processes are likely to be regulated by caspases, as there is a role for caspase activation in T cell development, proliferation and differentiation. When caspases were inhibited with a pan-caspase inhibitor, T cells were

found to produce IL-4 and differentiate into Th2 cells independently of Stat6 (Sehra, Patel et al. 2005). This may explain the increase in Th2 differentiation and IL-4 production in Bcl6 and Stat6 double knock out mice. When Bcl6, a transcriptional repressor, is knocked out in mice, they develop a Th2-type inflammatory disease. When Stat6, a transcription activator (and repressor, depending on conditions) (Kelly-Welch, Hanson et al. 2005), is also knocked out, mice develop an even more severe Th2-type inflammatory disease (Linehan, Warren et al. 1998). Since Bcl6 functions to inhibit or downregulate the Th2 program, its absence allows for the unregulated expansion of Th2 cells. The additional loss of Stat6 and its contribution to the regulation of IL-4 later in activation, allows for that expansion to become uncontrolled and uninhibited by any Stat6 regulated repressive measures. Interestingly, the same condition ensues in CTLA-4 and Stat6 double knock-out mice (Bour-Jordan, Grogan et al. 2003; Kelly-Welch, Hanson et al. 2005).

Stat6 Related Pathology

Recently, Stat6 has been implicated in the pathology of tumors, lymphoproliferative diseases, and autoimmunity, as well as the previously recognized contribution to asthma and allergy. A gain-of-function mutation in Stat6 was identified by Daniel et al (Daniel, Salvekar et al. 2000) that allowed for a constitutively active and more stable form of Stat6 to signal for an increase in IgE production that could lead to atopic and asthmatic conditions. More recently, Stat6 was found to be constitutively activated in primary mediastinal large B-cell lymphomas as well as certain types of prostate cancers which resulted in the abnormal proliferation of cells (Guiter, I. et al.

2004.; Bruns and Kaplan 2006). The activation of Stat6 was IL-4 independent in these cancers but it was unclear what contributed to it. A lymphoproliferative disorder was recently found in mice expressing a constitutively activated Stat6 in T cells which was characterized by splenomegaly due to an increase in B cells and increased Th2 activity (Kaplan, Sehra et al. 2007). Thus, aberrantly activated Stat6 has been implicated in a number of pathological conditions associated with or without IL-4 signaling.

A mutant Stat6, engineered to be constitutively active in lymphoid cells of mice on a C57BL/6 background, was found to have differing effects on B and T cells. There was an increase in peripheral B cells and in production of IgG1 and IgE. However, even though the B cells had an upregulation of IL-4/Stat6 regulated genes, they did not possess an activated phenotype as they did not proliferate differently than WT B cells and were not larger in size (Bruns, Schindler et al. 2003). In contrast, T cells did have an activated phenotype as they were larger than WT and had increased percentages of $CD62L^{lo}/CD44^{hi}$ cells. In addition, T cells had much greater proliferation than WT cells, but an overall reduction in population due to increased apoptosis.

Many groups have studied the effects of Stat6 deficiency in different model systems. Jacob et al (Singh, Saxena et al. 2003) created a Stat6 deficient NZM 2328 strain of mice. NZM 2328 mice develop spontaneous systemic autoimmunity with altered serum immunoglobulins, autoantibodies and glomerulonephritis. The Stat6 deficient version of this model secreted very little IL-4, had a significant reduction in the level of IgG1, did not upregulate CD23 or MHC II but showed no change in the numbers of splenocytes or distribution of B and T cells. Stat6 deficient NZM 2328 mice showed a significant delay in kidney disease and a decrease in proteinuria and a significantly

prolonged life span. The level of overall Ig was similar and they showed evidence of autoantibodies, but they were of the IgG2a isotype instead of IgG1(Singh, Saxena et al. 2003).

Xu et al (Xu, Duan et al. 2006) also produced a Stat6 deficient version of a lupus-prone mouse designated B6.TC, which is a congenic derivative of the autoimmune-prone IL-4-producing NZM2410 strain. This Stat6 deficient model displayed a significant decrease in spleen cellularity including a reduction in the percentage of effector/memory T cells and a decrease in B cell activation, and the restoration of abnormal follicular architecture. They also had a decrease in IgG levels, with the largest decrease in IgG1, as well as a decrease in anti-chromatin and anti-DNA antibodies. There was a reduction in the severity of glomerular disease and proteinuria, and an increase in survival. In contrast to a Stat6 deficient NZM2410 parental strain, IL-4 production was largely unchanged by Stat6 deficiency in the B6.TC, however, the Stat6 intact B6.TC produced low levels of IL-4 to begin with.

Singh et al.(Singh, Saxena et al. 2003) developed a Stat6 deficient strain of NZM 2410 mice, which in the Stat6 sufficient version overproduce IL-4 (due to unknown causes) and develop severe glomerulosclerosis, have an increase in IgG1 and IgE and produce anti-DNA autoantibodies. NZM2410 Stat6-/- mice have a significant decrease in IL-4 and IgE production, a decrease in proteinuria and kidney disease, an increase in IgG2a, but show no change in the level of anti-DNA antibodies. When these same Stat6 deficient animals are treated with a neutralizing antibody to IL-4 (11B11) they also show a decrease of serum IgG1 and IgE, a decrease in proteinuria and glomerulosclerosis, but an increase in serum IgG anti-DNA antibodies of the IgG1 and IgG2a isotypes. Thus, it

appears that Stat6 plays a pivotal role in maintaining immune homeostasis under normal physiological conditions, and can drive autoimmune pathology in an abnormally activated state, or ameliorate symptoms when inhibited.

Autoantibodies and Renal Disease

It seems that one of the most debated areas of autoimmune research is the role that autoantibodies play in contributing to the pathology, particularly in the renal disease commonly associated with SLE and other systemic autoimmune syndromes. The evidence is often conflicting. In some systems autoantibodies appear to play a very limited role in pathology (Morris, Dragula et al. 2002), or a commonly considered "pathogenic" antibody such as IgG2a may be elevated but there is decreased renal disease (see above, (Singh, Saxena et al. 2003), or there may be a decrease in renal disease but an overall increase in levels of anti-DNA autoantibodies (Singh, Saxena et al. 2003). A recent report by Bizzaro (Bizzaro 2007) analyzed levels of autoantibodies in prospective studies of humans and found the presence of anti-nuclear antibodies (ANA), anti-dsDNA antibodies and many antibodies to cytoplasmic and cell-specific antigens to be predictive of the development of autoimmune disease. Thus, it is difficult to establish the exact role autoantibodies play in any given system, however, there is a strong and consistent correlation with an elevation of self-reactive antibodies and the presence of autoimmune disease (Fields and Erikson 2003; Wardemann, Yurasov et al. 2003; Woetmann, Brockdorff et al. 2003; Yung and Chan 2008).

The generation of B and T cells with self-reactive specificities is a well-accepted result of the need for the immune system to react to a wide-range of antigenic stimuli. In

normal development, these self-reactive cells should be deleted as they pass through a number of tolerance checkpoints in place in the immune system for regulation of autoreactivity. If these cells are erroneously allowed to survive and become activated the B cells can move on to produce self-reactive antibodies with or perhaps even without the help of self-reactive T cells depending on the stimuli (Fields and Erikson 2003). When these antibodies circulate throughout the body, they can react and bind to the cellular antigens of their specificity and form immune complexes. These complexes can block tiny capillaries and induce an inflammatory response, which signals other immune cells to enter the area, leading to the enhancement of inflammation, cell proliferation, tissue remodeling, scarring and the production of inflammatory cytokines that can cause direct damage to cells and tissues. This is particularly true in the glomeruli of the kidney, with its complex network of capillaries needed to filter blood. As the capillaries become damaged they become "leaky" and protein leaks from the serum into the urine. Progressive disease severity then, is often accompanied by increasing proteinuria. Immune complex deposition can be clearly seen in a number of mouse models of autoimmunity, and when the antibodies are eluted, they have been shown to be specific for a number of nuclear as well as cytoplasmic antigens (Daikh 2001; Bagavant, Deshmukh et al. 2006).

It has become increasingly clear recently that the presence of immune complex deposition alone is not enough to drive renal disease, but that the numbers and type of cellular infiltrates present in the glomeruli and surrounding area make a difference in the severity and type of disease that is manifested. T cells have been shown to play a large role in driving the progression of renal disease from acute GN to chronic GN and renal

failure. During a longitudinal study of kidney disease in NZM 2328 mice T cell infiltration into the glomeruli and surrounding area resulted in an increase of disease severity and loss of renal function. The presence of dendritic cells and macrophages were thought to activate these self-reactive T cells and form a localized immune response. This was preceded by the presence of immune complex deposition and inflammatory cytokines which helped to recruit inflammatory cells into the area. (Bagavant, Deshmukh et al. 2006).

Several different types of glomerular disease have been identified but there does not appear to be a clear one-to-one relationship between the potential cause of damage and the type of disease that will occur. There are basically five clinical syndromes associated with nephropathy, which can be acute or chronic, and much overlap between categories. The patterns of glomerular damage are also varied and there is as yet no clear association between a particular genetic background or Th1 vs Th2 skewing of the immune system with a particular type of damage. There is evidence, however, that exaggerated activity of both Th1 and Th2 type responses can lead to equally severe disease.

The importance of renal pathology in the study of autoimmune disease is multi-fold. Current therapies have decreased the high mortality rate associated with renal failure in humans with autoimmune disease but quality of life still remains an issue. For researchers and clinicians the ability to measure protein in the urine has been helpful as a non-invasive marker of disease progression when there are so few consistencies present otherwise (Daikh 2001; Dong, Wang et al. 2007). The presence of renal disease appears to be a constant despite the differing genetic backgrounds and systems used for studying

autoimmunity and for researchers provides a way to evaluate potential therapies and/or genetic manipulations.

The current model of autoimmune development is a three-step process involving hyperactivation, dysregulation of the immune response leading to continued stimulation and the subsequent development of pathogenic inflammatory responses. Since IL-4 functions to induce B cell activation and isotype switching to IgG1 and IgE through a Stat6-dependent pathway, and is thought to contribute to autoimmunity through antibody dependent and independent mechanisms as well (Singh, Saxena et al. 2003), Ttc7$^{fsn/fsn}$ is a useful model to study B cell activation and IL-4 production as they relate to systemic autoimmunity and disease.

AIMS AND HYPOTHESIS

One of the hallmarks of Ttc7$^{fsn/fsn}$ mice is the dramatic increase in IL-4 production. In addition, Ttc7$^{fsn/fsn}$ mice have hyperactivated B cells as has been demonstrated by their increased size, upregulation of MHC II, increased production of serum Ig, especially IgE, and increased proliferative response to mitogens. Ttc7$^{fsn/fsn}$ T cells have also been shown to hyper-proliferate in vitro although less has been done to characterize their phenotype. The transcription factor, Stat6, is a signaling molecule unique to the IL-4 signaling pathway and indispensable for IgE expression. Preliminary work determined Stat6 to be constitutively expressed in Ttc7$^{fsn/fsn}$ B cells. Thus, the aims of this study were to:

- Evaluate IL-4 signaling through Stat6 via the activation and functional responses of Ttc7$^{fsn/fsn}$ B cells
- Evaluate the activation of and IL-4 production in Ttc7$^{fsn/fsn}$ T cells
- Determine the contribution of IL-4 and Stat6 to the pathology of Ttc7$^{fsn/fsn}$ mice.

We hoped to provide insight into our hypothesis that the Ttc7^{fsn} mutation results in the hyperactivation of lymphocytes which leads to the overproduction of IL-4 and systemic pathogenic autoimmunity.

MATERIALS AND METHODS

Mice

Mice were maintained and bred in our barrier and specific pathogen-free research animal quarters at the University of Southern Maine. Mice used in these studies were 4-10 weeks of age. Flaky skin mice (Ttc7$^{fsn/fsn}$) and normal littermate controls (WT) were produced from breeding pairs of Ttc7 heterzygotes originally purchased from The Jackson Laboratory, (Bar Harbor, Maine) and have been maintained on a BALB/c background at our facility since 2001. Mice were maintained in HEPA filtered polycarbonate cages, fed irradiated Harlan-Teklab Rodent diet with food and water available *ad libitum*. The facility strictly adheres to PHS guidelines for animal care and use; all protocols were reviewed and approved by the USM Institutional Animal Care and Use Committee.

Genotyping for breeding pairs was performed in a two-part PCR reaction to detect the presence of Ttc7 WT and Mutant (fsn) alleles. To detect the WT allele a reaction mixture of 5x reaction buffer, 25mM MgCl2, 2.5mM dNTPs, 10µM each of primer E15R and primer I14F, 5% DMSO, 5U/µL Flexitaq DNA polymerase, 1µL genomic DNA and dH2O in a 24 µL volume was reacted in a thermacycler under the following conditions: 95C for 2 minutes, then 94C for 30 seconds, 65C decreasing to 58C for 30 seconds, 72C for 30 seconds for a total of 14 cycles, and 94C for 30 seconds, 60C for 30 seconds and 72C for 30 seconds for a total of 25 cycles. The reaction ended with a final elongation cycle of 72C for 5 minutes. Primers to detect the WT allele included E15R: GAAGAGCAGCGCTAGCAAGT and I14F: ATGGCTTCCTTGGCCATGAT.

To detect the Ttc7 mutant allele a reaction mixture of 5x reaction buffer, 25mM MgCl2, 2.5mM dNTPs, 10μM each of primer I14F and ETnR, 5% DMSO, 5U/μL Flexitaq DNA polymerase, 1μL genomic DNA and dH2O in a 24 μL volume was reacted in a thermacycler under the following conditions: 95C for 2 minutes, then 94C for 30 seconds, 68C decreasing to 60C for 30 seconds, 72C for 1 minute for a total of 16 cycles, and 94C for 30 seconds, 61C for 30 seconds and 72C for 1minute for a total of 30 cycles. The reaction ended with a final elongation cycle of 72C for 5 minutes. Primers to detect the mutant allele included I14F: ATGGCTTCCTTGGCCATGAT and ETnR: GCCAGCAGCTCGACGTGAA.

Generation of Stat6-/- x Ttc7 mice

Stat6 deficient (Stat6^{tm1Gru}) breeding pairs were purchased from The Jackson Laboratory (Bar Harbor, Maine) and maintained in our barrier facility at the University of Southern Maine. Offspring were crossed with Ttc7 heterozygotes (Ttc7+/fsn) produced in our facility. The resulting Stat6+/- x Ttc7+/fsn double heterozygote was backcrossed to a Stat6 (Stat6-/-) deficient Ttc7 WT homozygous (Ttc7+/+) animal resulting in one-quarter of the offspring having a Stat6 deficient Ttc7 heterozygous genotype (Sta6-/-Ttc7+/fsn). These Stat6-/- x Ttc7+/- individuals were intercrossed to produce Stat6-/- x Ttc7$^{fsn/fsn}$ animals for study. All animals were maintained on a BALB/c background. Genotypes were confirmed by PCR for both the Stat6 (protocol and primer sequences: http://jaxmice.jax.org/pub-cgi/protocols/protocols.sh?objtype=protocol&protocol_id=218) and Ttc7 genes for breeding as well as to confirm genotype of the animals used for study.

Evaluation of Stat6 Activation

Splenocytes were isolated from Ttc7$^{fsn/fsn}$ and normal littermate control mice by filtering freshly excised spleens through a nylon mesh biopsy bag (Anatomical Pathology USA, Pittsburgh PA) and enriched for the lymphocyte population by density gradient centrifugation with Lympholyte-M (Cedarlane, Ontario, Canada) following the manufacturer's recommended protocol. Lymphocytes were incubated with 10 ng/mL mouse rIL-4 for 0-30 minutes as indicated in the results and equal numbers of cells per sample were lysed with 0.5% (m/v) SDS, 0.05M Tris-HCl, 0.2 mM $NaVO_4$, 1 mM DTT and 2 µg/mL Protease Inhibitor Cocktail (Sigma), pH 8.0, and resolved by 8% SDS-PAGE. The gel was electrophoresed to a PVDF membrane (Immulon-P, Millipore, Bedford, MA) in Tris-glycine buffer (25 mM Tris, 0.2M Glycine, 20% methanol, pH 8.5) for 2 hours at 75V with cooling and the membrane was blocked with 8% milk in TBS. Immunoblotting was performed using an anti-phosphoStat6 (pStat6) antibody (Cell Signaling Technologies, Beverly MA) at a dilution of 1:2500, incubated 2h at room temperature followed by washing 3 x 15 minutes with TBS (Tris-buffered saline) containing 0.05% Tween-20 (TBST). Horseradish peroxidase-conjugated goat anti-mouse IgG (Southern Biotechnology Associates Inc, Burlingham AL) was diluted 1:20,000 and incubated 2h followed by washing with TBST. Blots were developed with the Super Signal Chemiluminescence Detection System (Pierce, Rockford, IL). Chemiluminescence was detected using a Kodak 440CF Image station (Kodak Scientific Imaging Systems, Rochester, NY).

Immunoprecipitation was performed with rIL-4 (10 ng/mL, R&D Systems) stimulated and unstimulated splenocytes enriched as above. Stat6 was immunoprecipitated from 5 x 10^6 cells using anti-Stat6 (clone S-20, Santa Cruz Biotechnology Inc, Santa Cruz, CA) coupled to the gel component of the Seize Primary Mammalian Immunoprecipation Kit (Pierce, Rockford, IL) as instructed by the manufacturer. Samples were eluted from the immunoprecipitation columns and resolved and transferred to membranes as described above. Immunoblotting and detection were performed as above, first with the anti-pStat6, and then re-probing with the S-20 Stat6 following stripping the blot with 0.2M NaOH and re-blocking. Analysis of pStat6 levels and pStat6/Stat6 ratios were performed using Kodak ID analysis software (Kodak Scientific Imaging Systems) (Welner, Hastings et al. 2004).
Previously published as: Welner, R. W. Hastings, Beth L. Hill and Stephen C. Pelsue. (2004). "Hyperactivation and Proliferation of Lymphocytes from the Spleens of Flaky Skin (fsn) Mutant Mice." Autoimmunity 37(3): 227-235.

B- and T-lymphocyte enrichment

Splenic lymphocytes were enriched using a murine B-lymphocyte or T-lymphocyte negative selection kit (StemCell Technologies, Vancouver, BC, Canada) according to manufacturer's instructions. Briefly, mice were freshly sacrificed and spleens removed for analysis, a cell suspension was then obtained by filtering though a nylon mesh biopsy bag (Anatomical Pathology USA, Pittsburgh PA), followed by Lympholyte-M (Cedarlane, Ontario, Canada) density gradient isolation of total lymphocytes as instructed by the manufacturer. Approximately 1.0x10^8 cells/mL of

purified lymphocytes were then labeled with an antibody cocktail for the enrichment of B- or T-lymphocytes. After completing a wash of the cell suspension, the cells were labeled with the tetrameric complex and the magnetic colloid, then run over a gravity feed column in line with a magnet. The cells collected from the flow-through were washed and counted. Enrichment was approximately 85% to 95% for B- or T-lymphocytes as determined by flow cytometry (data not shown).

Stat6 Analysis in B lymphocytes

B cells were counted on a hemocytometer using the trypan blue exclusion method to monitor cell viability and $2.0x10^6$ cells used per sample. Cells for the Stat6 activation experiment were stimulated with mIL-4 (R&D Systems) at (10ng/mL) for 15 or 30 minutes, or left unstimulated (0 min). Cells were then washed and stained as described below.

Cells for the Stat6 deactivation experiment were stimulated for 30 min with mIL-4. The samples were then washed and processed for staining either immediately after stimulation (0 min) or allowed to incubate for 15 or 30 minutes prior to analysis.

Purified, stimulated or unstimulated, cells were fixed in a 4% paraformaldehyde/0.1M phosphate buffer/0.03M sucrose solution for 20 min and washed 2X with PBS/1% BSA. Cells were then permeabilized with a 0.2% saponin/PBS/0.03M sucrose/1%BSA solution for 5 min, washed 2X 5 min with PBS/1% BSA, blocked for 15 min with 5% rat serum in PBS/1%BSA followed by one wash. Cells were then stained for 60 min with an antibody specific for Stat6 (S-20, Santa Cruz Biotechnology) at 1:200 dilution, a secondary antibody specific for anti-rabbit conjugated with PE at 1:500

(Biosource International, Camarillo, CA) and finally Sytox green (1.0 μM, Molecular Probes, Eugene, Oregon) to identify the nucleus. Following a final spin the cell pellet was suspended in Fluoromount-G (Southern Biotechnology, Birmingham, Al), dropped onto 14mm 3-well slides (Erie Scientific Co), covered with a cover slip and sealed with nail polish. Cells were visualized by laser scanning confocal microscopy (Olympus FV300, Melville, NY), capturing multiple images per sample. Each experiment was repeated three times with separate mice.

Immunofluorescent Staining of Spleen Sections

Spleens of 8-week-old WT and Ttc7$^{fsn/fsn}$ mice were frozen with liquid nitrogen and kept at –70°C until needed. Frozen spleens were embedded in Cryomatrix Frozen Specimen embedding medium (Shandon, Pittsburgh, PA), then sectioned into 8μm sections (Cryotome, Shandon) and laid onto slides charged with poly-l-lysine (Sigma Diagnostics, St Louis, Mo). Slides were fixed for 10 min with ice-cold acetone, dried for 10 min and frozen at -70°C. After warming to room temperature and rehydrating in PBS, slides were first blocked with 5% rat serum/PBS/0.1% Tween, and with Streptavidin/Biotin Blocking Kit (Vector Laboratories, Burlingame, CA, USA). Staining for each molecule was done in individual steps with 4 X 5 min washing in between. Primary antibodies used were a goat polyclonal IgG specific for pStat6 or the Stat6 specific clone S-20, both purchased from Santa Cruz Biotechnology. For IL-4 staining, sections were stained with a hybridoma supernatant containing rat anti-mouse IL-4 (clone 11-B-11). Secondary antibodies used were biotin-sp-conjugated donkey anti-goat IgG and rhodamine-conjugated donkey anti-rabbit IgG both purchased from Jackson

Immunoresearch Lab. Goat anti-rat Ig(H&L)FITC conjugated antibody was obtained from Southern Biotechnology. IgM conjugated Alexa-fluor 633 was purchased from Molecular Probes and CD4-conjugated RPE, biotinylated-CD4 and hamster anti-mouse CD3ε-RPE were all from Southern Biotechnology.

Sections were stained for either phosphorylated-Stat6 with a biotin-conjugated IgG secondary antibody followed by Neutralite Avidin-FITC (Southern Biotechnology), or for Stat6 with a rhodamine-conjugated IgG secondary antibody. To identify B cells, sections were stained for IgM and for T cells using CD4-conjugated RPE on pStat6 slides, or biotinylated-CD4 on Stat6 slides, followed by Neutralite-Avidin FITC (Southern Biotechnology). Finally, slides were washed, a drop of Fluoromount-G was applied to the stained section and a cover slip was added and sealed with nail polish.

To stain for IL-4, slides were prepared as above with the exception of Streptavidin/Biotin blocking. A neat solution of supernatant containing anti-mouse IL-4 was pipetted onto sections and allowed to incubate for 60 min. After washing, a 1:400 solution of anti-rat FITC was added and incubated for 45 min, followed by a washing step, then a 1:400 dilution of anti-CD3ε-RPE for 60 min. Finally, 1:500 anti-IgM was added to stain for B cells and the slides were finished as above.

Slides were visualized with an Olympus FV300 confocal microscope using a 20X objective. Spleen sections from 3 separate Ttc7$^{fsn/fsn}$ and WT mice were stained for each combination of antibodies with similar results.

Immunohistological staining of Spleen Sections

Spleens from eight-week-old mice were sectioned and prepared as above. Antibodies used were biotinylated anti-IL-4 antibody (mouse clone 24G2, Endogen, Rockford, IL), anti-CD3ε-FL (FITC) (clone C363.29B), sheep anti-FL-HRP (horseradish peroxidase) and anti-SA-AP (streptavidin-alkaline phosphatase) which were all purchased from Southern Biotechnology.

Slides were first warmed to room temperature, re-hydrated in PBS 20 min, and blocked with 1% BSA/Tween/PBS for 20 min. A 1:50 dilution of anti-IL-4 antibody was applied to the section and incubated at RT for 60 min. After washing 3 X 10 min, a 1:200 dilution of anti-mouse CD3ε-FL was added, incubated, and washed as above. A secondary antibody solution of 1:200 anti-FL-HRP and a 1:100 dilution of anti-SA-AP was added and incubated as above followed by a washing step. AP was developed using a 20 mg/mL solution of napthol-ASMX-phosphate (Sigma) with 40 mg/mL fast blue BB (Sigma) and 2mM levamisol (Zymed) and incubated for 37 min followed by a wash. HRP was detected using 16 mg/mL of 3-Amino-9-ethylcarbazole with 0.015% H_2O_2 and incubating for 27-40 min. Slides were then washed, sections covered with mounting media and a cover slip and visualized with a light microscope at 40x magnification. (Protocol courtesy of Lynn Hannum)

Expression of IL-4 mRNA by RT-PCR

Cell preparation: T cells from 4- and 10-week-old WT and Ttc7$^{fsn/fsn}$ mice were isolated as described above. Purified T cells were counted and 15-20 million cells used

for each time-point. Cells were either left untreated (0 min) or stimulated with plate-bound anti-CD3 (10μg/mL; clone 145-2C11, Southern Biotechnology) in a 48-well cell-culture plate at 37°C, 5% CO_2. Preliminary experiments indicated that 3 hours of stimulation with anti-CD3 led to optimal IL-4 gene expression for both Ttc7$^{fsn/fsn}$ as well as WT T cells. Thus, after 3 hours of stimulation, the "stimulated" sample was harvested, spun-down to pellet the cells, resuspended in 1mL of Tri®Reagent (Sigma Chemical) and frozen for later RNA extraction. To evaluate RNA stability, Actinomycin D (Act D) (10μg/mL; Sigma) was added to stimulated samples to inhibit mRNA synthesis and incubated for either an additional 2 hours or 4 hours and harvested as above. Cyclosporine A samples were processed as described below.

RNA extraction: Total RNA was isolated from processed cells using the manufacturer's protocol for Tri®Reagent. Briefly, tubes containing cells lysed with Tri®Reagent were centrifuged at 12,000g for 10 min at 4°C to remove high-molecular weight DNA from the supernatant. This was then transferred to a new tube, 200μL of chloroform was added and centrifuged again at 12,000g for 10 min. The aqueous phase containing the RNA was transferred to a new tube, precipitated with 99^{+}% isopropanol and washed with chilled 75% ethanol. The RNA pellet was resuspended with 35μL of sterile dH_20, an aliquot removed for analysis and the remainder frozen until use.

RNA analysis: For RNA quantitation a 1:10 dilution was made and analyzed on a Nanodrop® ND-1000 spectrophotometer (Nanodrop Technologies, Wilmington, Delaware). Three measurements were made per sample and averaged. Two micrograms of RNA per sample were calculated and run on a 1% agarose gel with ethidium bromide (EtBr) to confirm RNA integrity and accuracy of calculations (data not shown).

First strand cDNA synthesis of Poly A mRNA: Two micrograms of purified total RNA were calculated for each sample and added to a mixture of 1.5µL Oligo $dT_{(15)}$ primer (0.5µg/uL, Promega), 1.5nM dNTP mix, and dH_2O to make a 25µL reaction volume. After a 5 min incubation at 70°C, RT buffer, 1.5µL of M-MuLV RT enzyme (200,000U/mL, New England Biolabs), and dH_2O to make a 30µL reaction volume was added and incubated for one hour at 42°C.

PCR of cDNA: PCR (of PolyA mRNA) of reverse-transcribed cDNA was performed as follows. For IL-4 and GADPH expression the same amount of cDNA was added to separate mixtures of 1X PCR Gold Buffer (Applied Biosystems), 2.5µM $MgCl_2$, 1µM dNTP nucleotide mix (Promega), 0.5µM each forward and reverse primers, 0.6µL DMSO, 0.125µL AmpliTaq Gold™ enzyme (5U/µL, Applied Biosystems) and dH_2O to 25µL. The house-keeping genes GADPH, HPRT, and beta-actin were validated experimentally for suitability as a control. GADPH was found appropriate for use as a loading control and for normalization with the type of cells, time-frames and treatments used in these assays. Samples were run in either a BIO-Rad Gene Cycler™ thermocycler (IL-4) or a PTC-100 (GADPH) (MJ Research Inc, Watertown Mass) starting with an activation step of 10 min at 95°C, followed by a touch-down series of 94°C for 45 sec, higher TM + 2° for 1.5 min decreasing to lower TM – 2° for -.5° each cycle, 2 min at 72°C (71°- 66° for 10 cycles IL-4; 69°-62° for 14 cycles GADPH), then repeat cycles of 45 sec at 94°C, 1.5m at 66°C or 62°C and 2 min at 72°C, with a final elongation step of 5 min at 72°C. The amount of cDNA and the number of PCR cycles were selected by pilot experiments and samples of the PCR reactions were taken at multiples points throughout the amplification process for appropriate comparison, thus, PCR was performed in the

linear range of the amplification reaction for each set of primers. The primer set specific for IL-4 was (5'-3') Forward: CGAAGAACACCACAGAGAGTGAGCT and Reverse: GACTCATTCATGGTGCAGCTTATCG (Sigma Genosys, Woodlands Tx) and for GADPH, Forward: GCTCTACATGTTCCAGTATGACTCCAC, Reverse: GGGTCTCGCTCCTGGAAGAT (Operon Biotechnologies, Huntsville AL). Calculated bands sizes are 180bp and 117bp respectively. The PCR products were electrophoresed on a 1.5% agarose gel containing EtBr and visualized with a Syngene Gene Genius imaging system. The relative intensity of bands was determined with ImageJ NIH imaging software (Rasband, W.S., ImageJ, U. S. National Institutes of Health, Bethesda, Maryland, USA, http://rsb.info.nih.gov/ij/, 1997-2006). Results are expressed as the ratio of the intensity of the band for IL-4 to the intensity of the band for GADPH normalized to unstimulated WT control where indicated in the caption. The RNA stability study results are presented as the percent of each residual specific mRNA at each time point relative to the stimulated sample as indicated in the caption.

IL-4 ELISA Measurement

Four- and ten-week WT and Ttc7$^{fsn/fsn}$ T cells were isolated and enriched from spleens of freshly sacrificed animals as described above. Six million cells per sample were resuspended in 400µL of RPMI 1640 culture media supplemented with 10% FCS, 2mM L-glutamine, 0.05% sodium pyruvate, 100U/mL penicillin and 100µg/mL streptomycin. Samples were plated in 48-well culture plates in either uncoated wells (unstimulated samples) or stimulated in wells coated with 10µg/mL anti-CD3 antibody. Plates were cultured at 37°C with 5% CO_2 for 24 hours. To assess protein production

after blocking mRNA synthesis, Act D (10μg/mL) was added to samples after 3-hours of stimulation with plate-bound anti-CD3 and allowed to continue incubating. Cyclosporine A treated samples were processed as described below. After culture, plates were spun and supernatant collected.

IL-4 protein levels were measured from collected supernatants in triplicate samples (100μL) of each individual sample by ELISA using the IL-4 DuoSet kit purchased from R+D systems (Minneapolis, MN) according to the manufacturer's instructions. Optical density readings were obtained using a Packard Instruments Spectracount plate reader (Downers Grove, IL) set at 405nm. IL-4 concentration was determined by converting the mean OD values to picograms per milliliter using an equation determined from standard curves generated with varying concentrations of mouse recombinant IL-4 (5.0- 4,000 pg/mL) and plotting in Excel.

Cyclosporine A Studies

Solid cyclosporine A (CsA) (Alexis Biochemicals, San Diego, CA) was dissolved in DMSO to make a stock solution concentration of 40μg/mL. This was then diluted 1:50 with culture media and added to a cell suspension for a final concentration of 1μg of CsA per mL of cell suspension. DMSO diluted 1:50 in media was used as a control. Cells were pre-treated for 30 minutes before plating onto the prepared 48-well culture plates. Samples were then prepared as above for RT-PCR and ELISA.

Flow Cytometry: Materials and Methods

Reagents And Antibodies Used For Flow Cytometric Analysis Of T Cell Subsets, IL-4 Producing T Cells, Spleen Cell Populations And Cell Cycle Analysis

For intracellular analysis of IL-4 and IFN-γ production Monensin solution (eBioscience, San Diego, CA 92121) was used to inhibit protein transport. Antibodies for intracellular IL-4 analysis include rat anti-mouse IL-4-FITC (clone BVD6-24G2, eBioscience), rat anti-mouse CD4/L3T4-PE (clone GK1.5, Southern Biotechnology, Birmingham, AL.), rat anti-mouse CD44/Pgp-1-APC (clone KM201, Southern Biotech), and rat anti-mouse CD62L-PE/Cy7 (L-selectin clone MEL-14, Southern Biotech). For over-night stimulation, plates were coated with unlabeled hamster anti-mouse CD3e (clone 145-2C11, Southern Biotech). Antibodies for T cell subset analysis (naïve, activated, memory) include hamster anti-mouse CD69-FITC (cloneH1.2F3, Southern Biotech), as well as CD4, CD44 and CD62L mentioned above. Intracellular IFN-γ was assessed with rat anti-IFN-γ- APC (clone XMG1.2, eBioscience) and anti-CD4-PE.

Cell cycle analysis was performed with rat anti-mouse CD4-FITC (clone GK1.5) and hamster anti-mouse CD3-FITC (clone 145-2C11) both purchased from Southern Biotech, and propidium iodide (PI) solution purchased from Becton Dickinson (Franklin Lakes NJ 07417) at 50μg/mL, with added 1 mg/mL RNAse A and 1 mg/mL sucrose (Sigma, St. Louis MO 63178).

Spleen cell populations were determined with goat anti-mouse IgM-AlexaFluor® 633 (μ chain, Invitrogen Molecular Probes, Carlsbad CA 92008), rat anti-mouse IgD-PE (clone 11-26, Southern Biotech), rat anti-mouse CD19-APC (clone 6D5, Southern

Biotech), rat anti-mouse F4/80-PE (clone C1:A3-1 AbD Serotec, Raleigh NC 27604), rat anti-mouse Ter119-PE (erythroid cells y-76 clone Ter119, BD PharMingen, San Diego CA 92121), rat anti-mouse PanNK (CD49b)-PE (clone DX5, Southern Biotech), rat anti-mouse GR1 (Ly-6G)-PE (clone RB6-8C5, Southern Biotech), rat anti-mouse CD8a (Lyt-Z)-APC (clone 53-6.7, Southern Biotech) as well as CD4-PE and CD3-FITC mentioned above. Other markers include rat anti-mouse CD11b (Mac-1) (clone M1/70 Southern Biotech), rat anti-mouse CD11c-APC (clone N418, Caltag Labs, Burlingame CA 94010), rat anti-mouse MHC classII- FITC (clone NIMR-4, Southern Biotech) and rat anti-mouse CD23 (IgE Fc receptor FcεRII)-FITC (clone 2G8, Southern Biotech).

Isotype controls include Rat IgG-APC (BD PharMingen), Rat IgG-RPE and Hamster IgG-FITC, and Rat IgG-FITC, all from Southern Biotech.

Red blood cell (RBC) lysis buffer and Rat serum were purchased from Sigma. Lympholyte-M was obtained from Cedarlane, Ontario Canada. Hank's Balanced Salt buffer came from Mediatech Inc, Herndon VA 20171 and FacsFlow was purchased from BD Biosciences (San Jose, CA). RPMI-1640 (10-040-CV w/L-glut) cell culture media was purchased from Cell-Gro (Mediatech) and supplemented with pen/strep antibiotics (Gibco® Invitrogen, Carlsbad CA 92008), 10% fetal bovine serum (FBS) (Biomedia, Foster City, CA 94404) and 0.05% sodium pyruvate (Gibco® Invitrogen).

Method: Flow Cytometry

Spleens were harvested from freshly sacrificed Ttc7 mice, 11B11- and GL113-treated Ttc7$^{fsn/fsn}$ mice, Stat6-/-Ttc7 mice and designated Ttc7 control mice and single cell suspensions were made by scraping through a mesh biopsy bag (Thermo-Shandon). Cells

were washed with Hank's balanced saline and RBC lysis was performed per manufacturer's protocol using 1-200 million cells per 1mL of lysis buffer. For all analyses except total spleen cell populations, the lymphocyte fraction was separated by gradient density separation with Lympholyte-M per manufacturer's protocol. A cell count was performed using a hemacytometer and the trypan blue exclusion method to measure cell viability, and 2 million cells were used per sample.

Intracellular IL-4 and IFN-γ: To analyze intracellular IL-4 and IFN-γ production in Ttc7 and Stat6-/-Ttc7 mice, cells were resuspended in RPMI-1640 supplemented with 10% FBS, pen/strep, 2% sodium pyruvate and L-glutamine with 1x monensin added to block protein secretion. 6 million cells were plated in either 10µg/mL anti-CD3 coated plates to stimulate or uncoated wells and cultured overnight at 37°C with 5% CO_2. After harvesting and washing, cells were resuspended in 500µL of 2% FBS, 5% rat serum, and FacsFlow buffer to block at 4°C or on ice for 20 minutes. Samples were then spun at 500g for 10 minutes, the supernatant was discarded and cells were washed with 200µL of FacsFlow buffer. Appropriate antibodies for surface markers, CD4, CD44 and CD62L were diluted in FacsFlow with 2% FBS to a working concentration following manufacturer's recommendation for number of cells used, 50µL of the antibody solution was added to each sample and incubated on ice in the dark for 45 minutes.

Following incubation, cells were washed 3x with 200µL FacsFlow/2% FBS, and fixed with 100 µL of 1% paraformaldehyde in PBS (diluted from 4X stock). Samples

were incubated for15 minutes on ice in the dark, 300 µL of FacsFlow was added and samples were stored at 4°C until ready for analysis.

Immediately before analysis, cells were washed 3x with 200 µL of FacsFlow and appropriate samples were resuspended in 100 µL of an antibody solution containing either anti-IL4 or anti-IFN-γ, 0.1% saponin, 2% FBS in FacsFlow and allowed to stain in the dark for 45 minutes. After washing 3x in FacsFlow, all samples were resuspended in 500 µL of FacsFlow and transferred to BD Falcon 2x75mm 5mL round-bottomed polystyrene tubes.

Cell Cycle Analysis: Individual samples of 2 million cells each were blocked and washed as above and then stained for either CD3 or CD4 surface markers by incubating in 50 µL of an antibody solution using the manufacturer's recommended working concentration for number of cells in FacsFlow with 2% FBS on ice for 45 minutes. Samples were washed and fixed in 1% paraformaldehyde as above, 300 µL of FacsFlow was added after 15 minutes of fixation and the samples were stored at 4°C in the dark until ready for analysis.

Immediately before analysis, cells were washed 3x with FacsFlow and either resuspended in 500 µL of FacsFlow and transferred to 5mL polystyrene tubes, or cells to be stained with PI were suspended in 500 µL of a 50µg/mL PI solution supplemented with 1mg/mL of RNAse A and 10% sucrose. Samples were transferred to 5mL polystyrene tubes and allowed to stain for 30 minutes in the dark at RT.

Determination of T cell subsets: Individual samples of 2 million cells each were processed, washed and blocked as above. Four-color staining of cells was accomplished by adding the appropriate concentration per number of cells of antibodies specific for CD69, CD4, CD44 and CD62L as listed under reagents to FacsFlow with 2% FBS. A 50µL volume was added to samples and allowed to incubate for 45 minutes on ice in the dark. After washing and fixing as above, cells were resuspended in 500µL of FacsFlow and transferred to 5mL polystyrene tubes for analysis.

Analysis of Spleen Cell Populations: Spleen cells were processed as above without Lympholyte-M separation. After blocking, individual samples of 2 million cells were stained with antibodies specific for CD3, CD4, CD8a, CD11b, CD11c, CD19, CD23, F4/80, Ter119, PanNK, GR-1, MHC classII and IgM/IgD together to determine ratio as well as individually for controls. All antibodies were added in 50µL volumes of FacsFlow with 2% FBS and then incubated for 45 minutes on ice in the dark. After washing and fixing, cells were resuspended in 500µL of FacsFlow and transferred to 5mL polystyrene tubes for analysis.

Flow cytometric analysis: In addition to the samples described above, single-stained samples of each antibody were prepared in the same manner to use as controls for compensation as well as unstained samples for background fluorescence and isotype controls to determine positive staining. Acquisition of data was conducted on a Becton Dickinson FACSCalibur using CellQuest pro 4.0 Software (BD Biosciences, San Jose, CA) for data collection. Based on lymphocyte gates from forward and side scatter, at

least 50,000 events were recorded for each sample. Data analysis and graphing were accomplished with WinList 6.0 from Verity Software House, Topsham ME 04086.

Production and purification of 11B11 and GL113 monoclonal antibodies

Production of Antibodies: The anti-IL4 producing hybridoma cell line, 11B11 (HB-188™) was originally purchased from American Tissue Culture Collection (ATCC) (Manassas, VA 20110). The isotype matched (IgG1) control monoclonal cell line GL113 was a kind gift from Fred Finkelman, University of Cincinnati, Cincinnati, Ohio. Both cell lines were started in RPMI-1640 (Cell-Gro) supplemented with 2mM L-glut, 10% FBS (Biomedia), 2μL ($5x10^{-5}$ M) 2-Me, pen/strep and 2% sodium pyruvate, all from Gibco® Invitrogen, and incubated at 37°C with 5% CO_2. Cell culture media was gradually changed over to 100% BD Cell™Mab Medium Serum Free Media (BD Biosciences) supplemented with L-glut by resuspending cells in ratios of RPMI to serum free media of 75/25, 50/50, 25/75 and finally to 100%, allowing cells to equilibrate and rebound for several days in each mixture. When required cell density was obtained CELLine™ 1000 System growth chambers (BD Biosciences) were seeded with the hybridoma cells following the manufacturer's recommendations for the 7/21 day procedure. Briefly, cells were suspended at 2 x 10^6 cells/mL in 15 mLs of serum free media and added to the cell compartment with a serological pipet. One liter of pre-warmed (37°C) serum free Mab media was added to the nutrient compartment and the chamber was allowed to incubate for 1 week at 37°C in 5% CO_2. On day 7 cells were removed with a serological pipet to harvest the antibody in the media, and chambers were

re-seeded as before. This was repeated 3x (21 days), whereupon the nutrient chamber was emptied of media, refilled with fresh serum free media and the cell chamber was reseeded for another round of 21-day antibody production. All procedures were conducted in a Hepa-filtered culture hood under aseptic conditions. Cell lines were tested by the Yale University Virology lab using their mouse and rat contaminant panel and found to be negative for mouse and rat viruses and mycoplasma.

Purification of antibodies from supernatant: Cells and supernatants collected above were centrifuged at 1000g for 10 minutes and the supernatants were filtered through a 0.8 μm syringe filter and again through a 0.2 μm filter to remove any cell debris. The filtered supernatants were tested for antibody concentration on a NanoDrop® ND-1000 Spectrophotometer (NanoDrop Technologies Inc., Rockland DE 19732) and the volumes were adjusted to the optimal binding capacity (32 mgs) for use with Ultralink Affinity Pak Immobilized Protein-G 2 mL pre-packed columns (Pierce, Rockford, IL). Purification proceeded following the manufacturer's instructions. Briefly, the supernatants were mixed with an equal volume of de-gassed Immunopure®G IgG Binding Buffer (Pierce), and after equilibrating the columns with addition binding buffer, were passed through the columns 3x. The columns were washed, and the bound antibody was then eluted with de-gassed Immunopure®IgG Elution Buffer (Pierce) into 100μL of 1M Tris neutralization buffer (pH 8.0) in 1 mL fractions. Elution was monitored with NanoDrop® absorbance readings until background values were reached. Purity and binding activity were evaluated with Western blot. The columns were regenerated and stored as recommended.

All collected fractions were measured for absorbance and the fractions with the highest readings were combined and re-measured for total recovered antibody concentration. Buffer exchange into sterile and filtered PBS was accomplished using 10,000 molecular weight cut off 3-12 mL capacity Slide-A-Lyzer Dialysis Cassettes with 3 changes of 2 liters each of PBS per manufacturer's protocol. The recovered buffer-exchanged antibody was again measured for concentration by NanoDrop® absorbance values, all samples were combined and the final concentration was adjusted to 1 mg/mL of 11B11 or GL113 with sterile and filtered PBS, measured into 1 mL aliquots and frozen at -20C for storage.

Treatment of animals with 11B11 and GL113

Five Ttc7$^{fsn/fsn}$ mice from separate litters per each treatment group received 250µg (250µL) of 11B11 anti-IL4 or GL113 isotype control starting at 3 weeks of age, 3 times per week until 10 weeks of age for a total of 7 weeks (Singh, Saxena et al. 2003). All injections were administered intraperitoneally and were approved by the Institutional Animal Care and Use Committee (IACUC) of the University of Southern Maine.

Materials and Methods for Serum Antibody ELISAs

Quantitation of serum immunoglobulin isotype

Sera were collected from 11B11- and GL113-treated mice, Stat6-/-Ttc7 and Ttc7 mice after bleeding from the retro-orbital plexus. Blood was allowed to clot for 1 hr at room temperature and overnight at 4°C. Samples were then spun at 3000g for 15 minutes,

serum was pipetted from each sample, transferred to a new tube and stored at -20°C until analysis by ELISA.

For quantitation of individual Ig isotypes, 96-well microtiter plates were coated overnight at 4°C with 2μg/mL goat anti-mouse IgG1, goat anti-mouse IgG3, goat anti-mouse IgM+IgG+IgA(H&L) (total Ig) or 5μg/mL goat anti-mouse IgE, all purchased from Southern Biotechnology. After washing 3x with 0.01% Tween-20/PBS, plates were blocked for 1 h at RT with 1% BSA in PBS. Dilutions of sera at 1:250 and 1:500 in PBS (IgG1, IgG3 TIg) or 1:20 and 1:50 in PBS (IgE) were incubated in triplicate wells overnight at 4°C. Standard curves were generated with serial dilutions in duplicate wells of mouse IgG1κ (clone 15H6), mouse IgE Balb/c (clone 15.3), both from Southern Biotech, and mouse IgG3κ (KLH, BD PharMingen, San Diego, CA 92121). After washing 3x as above, detection was accomplished by incubating for 30 minutes at RT with horseradish peroxidase-conjugated goat anti-mouse kappa light chain antibody (1:8000) or rat anti-mouse IgE (1:6000, clone 23G3) both from Southern Biotech. Plates were again washed 3x as above and 100μL of the HRP substrate, 1-Step™ Ultra TMB-ELISA (Pierce, Rockford, IL) were added, allowed to develop to a desired color and then stopped with 1N HCl. Colormetric analysis was quantified at 405nm with an EL800 universal microplate reader (BioTek Instruments, Winooski, VT). Quantitation of serum Ig isotypes were calculated into μg/mL using the equation of the line generated by graphing the absorbance/concentration of the standard curves generated with the isotype standards.

Quantitation of IL-4 production by Stat6-/-x Ttc7 splenic lymphocytes

Spleens were harvested from freshly sacrificed Stat6-/-Ttc7 mice. Single cell suspensions were obtained by filtering though a nylon mesh biopsy bag followed by Lympholyte-M (Cedarlane, Ontario, Canada) density gradient isolation of total lymphocytes as instructed by the manufacturer. Six million cells per sample were resuspended in 400µL of RPMI 1640 culture media supplemented with 10% FCS, 2mM L-glutamine, 0.05% sodium pyruvate, 100U/mL penicillin and 100µg/mL streptomycin. Samples were plated in 48-well culture plates in either uncoated wells (unstimulated samples) or stimulated in wells coated with 10µg/mL anti-CD3 antibody. Plates were cultured at 37°C with 5% CO_2 for 24 hours. To assess protein production, supernatant IL-4 protein levels were measured in triplicate 100µL samples by ELISA using the IL-4 DuoSet kit purchased from R+D systems (Minneapolis, MN) according to the manufacturer's instructions. The HRP substrate, 1-Step™ Ultra TMB was added to all wells and allowed to develop to the desired intensity and stopped with 1N HCl. Colorimetric optical density readings were obtained using a BioTek Instruments EL800 Universal Microplate Reader set at 405nm. IL-4 concentration was determined by converting the mean OD values to picograms per milliliter using an equation determined from standard curves generated with serial dilutions of mouse recombinant IL-4 (5.0-4,000 pg/mL) and plotting in Excel.

Material and Methods for Anti-DNA ELISA and Autoantibody Staining

Serum

Blood was collected from all mice used by orbital bleeds. Blood samples were allowed to clot at room temperature, stored overnight at 4°C, and then centrifuged at 3000rpm for 15 min at 4°C. The supernatant (serum) was collected and stored at -20°C.

Antinuclear Antibody (ANA) Determination

Initial ANA detection was performed with a screening ANA ELISA as follows. 100µL of a 5 mg/mL Protamine sulfate (Sigma) capture solution in dH_2O was incubated for 30 minutes at room temperature to coat each well of a 96-well NUNC Polysorp ELISA plate (Nalge Nunc International). Unbound solution was removed and plates were then blocked with 100µL of a 10µg/mL salmon sperm DNA solution in dH_2O for 30 minutes at room temperature. After removing unbound blocking solution, sera titered 1:50, 1:100 and 1:200 in 2% NFDM (non-fat dry milk), 0.2% Tween-20 (Fisher), and PBS was added and incubated for one hour at room temperature, after which sera was removed and plates were washed 3x with 0.2% Tween-20/PBS. Goat anti-mouse IgG- or IgM-HRP (Southern Biotech) at 1:3000 in 2% NFDM/0.2% Tween-20/PBS was added and incubated for 1 hour at room temperature. The antibody was then removed and plates were washed as above, developed with 1-Step™ Ultra TMB substrate (Pierce, Rockford, IL) for 6 minutes, and stopped with 1N HCl. Absorbances were measured on a EL800 Universal Microplate Reader (Biotek Instruments, Winooski, VT 05404) at 450 nm

(Protocol and data kindly provided by Nicholas Matluk III, adapted from Stokes et al., 1982).

Autoantibody Antigen Determination

Slides fixed with HEp-2 cells were commercially obtained from The Binding Site, Inc. (San Diego, Ca.) Serum samples from 11B11- and GL113-treated mice as well as Stat6-/- Ttc7 mice were diluted 1:40 and 1:80 in PBS and added to wells. PBS was used as a negative control and sera from Ttc7$^{fsn/fsn}$ mice were used as positive controls for comparison. Slides were then incubated in a humidified chamber for 30 minutes at room temperature and washed with PBS three times for 5 minutes. Either anti-mouse IgG-FITC or anti-mouse IgM-FITC (both from Southern Biotechnology Inc., Birmingham Al.) was diluted 1:100 and added to designated wells and incubated again for 30 minutes in a humidified chamber at room temperature. Slides were washed as before, Fluoromount-G (Southern Biotech) was applied drop-wise to wells and coverslipped. These were examined with a Olympus 1x71 TH4-100 microscope equipped with epifluorescence and a FITC filter. Photographs were taken with a Photometric "Cool Snap" HQ Digital Roper Scientific 35 mm camera.

Assessment of Renal Disease/ Proteinuria

Renal disease was assessed by colorimetric measurement of proteinuria using Albustix® (Bayer Co., Elkhart In) per manufacturer's protocol. Mild disease was considered less than 100 mg/dL while advanced disease was defined as over 100 mg/dL per Daikh and Wofsy, 2001.

Kidney sectioning and staining

Kidneys were collected immediately upon sacrifice. One kidney half was fixed in 4% paraformaldehyde in PBS and the other half was fixed in 10% formalin. These were sent in fixative to Dr. Harini Bagavant at the University of Virginia, Department of Rheumatology and Immunology for sectioning, staining, and analysis as described in "Materials and Methods" of Bagavant et al., 2006.

Data Analysis

Each individual experiment was repeated with at least 3 separate litters per age group. As all experiments were conducted with primary cells, it was necessary to pool spleens of age and sex-matched littermates to obtain adequate numbers of B or T cells for analysis. For Stat6 activation and fall-off analysis, B cells were counted in a blind fashion by 2 people and the results averaged. All ELISA samples were plated in triplicate and averaged. Arithmetic means are given with standard error of the mean. Statistical comparisons between samples and with controls were made by the Student's unpaired t-test using "Smith's Statistical Package, Version 2.80" © Gary Smith, 2005. Differences were considered significant when P values of <0.05 were obtained.

RESULTS

Results: Section 1: Ttc7$^{fsn/Fsn}$

Previous research on Ttc7$^{fsn/fsn}$ mice had identified high levels of IL-4 in serum as well as an increased capacity for IL-4 production in Ttc7$^{fsn/fsn}$ splenocytes (Pelsue, Schweitzer et al. 1998; Welner, Hastings et al. 2004). The phenotype exhibited by Ttc7$^{fsn/fsn}$ mice is similar to that of the IL-4 transgenic as developed by Erb et al (Erb, Ruger et al. 1997) with hyperproliferative, activated B cells, dramatically increased IgE, anemia, kidney disease, autoantibodies, autoimmune disease and reduced life span. Stat6 is a transcription factor that is unique to the IL-4 pathway which, when constitutively active due to a defect in its regulation, has been shown to have transforming effects on cells leading to lymphoproliferative diseases, as well as high levels of IL-4 and Th2-type inflammation. Since the gene function of Ttc7 was (and is) unknown we undertook this study to determine whether an intrinsic defect in the dysregulation of IL-4 production was the cause of the autoimmune pathology seen in Ttc7$^{fsn/fsn}$ mice or, whether elevated IL-4 was the effect of the increased autoreactivity in Ttc7$^{fsn/fsn}$ which then determined the pathology. Because Stat6 is necessary for high levels of IL-4 production and pivotal in the IL-4 signaling pathway, we first sought to determine the activation status and regulation of Stat6 in Ttc7$^{fsn/fsn}$ mice.

Enhanced Stat6 activation in IL-4 Stimulated Ttc7$^{fsn/fsn}$ Splenocytes

To evaluate IL-4 signaling, splenocytes were collected from Ttc7$^{fsn/fsn}$ and WT control mice and analyzed by Western Blot for Stat6 activation as determined by an

antibody specific for the phosphorylated form of Stat6 (pStat6). Figure1.1 shows the increased level of activated pStat6 in Ttc7$^{fsn/fsn}$ splenocytes following IL-4 stimulation, as compared to WT control splenocytes. All lanes were normalized to 6 million cells per sample. Lower molecular weight fragments were detected by anti-pStat6 in the Ttc7$^{fsn/fsn}$ samples, which were not detected in the WT splenocyte samples, nor were they detected by the S-20 anti-Stat6 antibody (as determined by immunoprecipitation). Proteolytic fragments of Stat6 corresponding to the N-terminal DNA binding domain have also been detected in mast cells cultured in the presence of IL-4 (Sherman 1999; Suzuki 2000). The S-20 anti-Stat6 antibody is reactive with the C-terminus of Stat6 and therefore would not detect these fragments.

To determine if the elevation of pStat6 was a result of increased expression of Stat6, the ratio of pStat6/Stat6 was determined by immunoprecipitation followed by immunoblotting of Stat6 in IL-4 stimulated and unstimulated splenocytes (Figure 1.2). In the WT splenocytes, IL-4 stimulated (30 minutes) versus the unstimulated (0 minutes) show a 12-fold elevation in pStat6 levels. Ttc7$^{fsn/fsn}$ splenocytes did not show a detectable increase in pStat6 levels under the same conditions. In fact, the levels of pStat6 in the unstimulated Ttc7$^{fsn/fsn}$ splenocytes are only 1.3-fold above IL-4 stimulated WT splenocytes. While the levels of Stat6 are not significantly different among all of the samples, the ratio of pStat6 to total Stat6 does vary considerably (Figure 1.3). The pStat6/Stat6 ratios in WT splenocytes were 0.025 and 0.300 respectively for the 0 and 30 minute time points. The pStat6/Stat6 ratios in Ttc7$^{fsn/fsn}$ splenocytes, however, were 0.670 and 0.620 for the same time points, indicating a much higher percentage of Stat6 was

already activated without additional stimulation of Ttc7$^{fsn/fsn}$ splenocytes (Previously published as (Welner, Hastings et al. 2004).

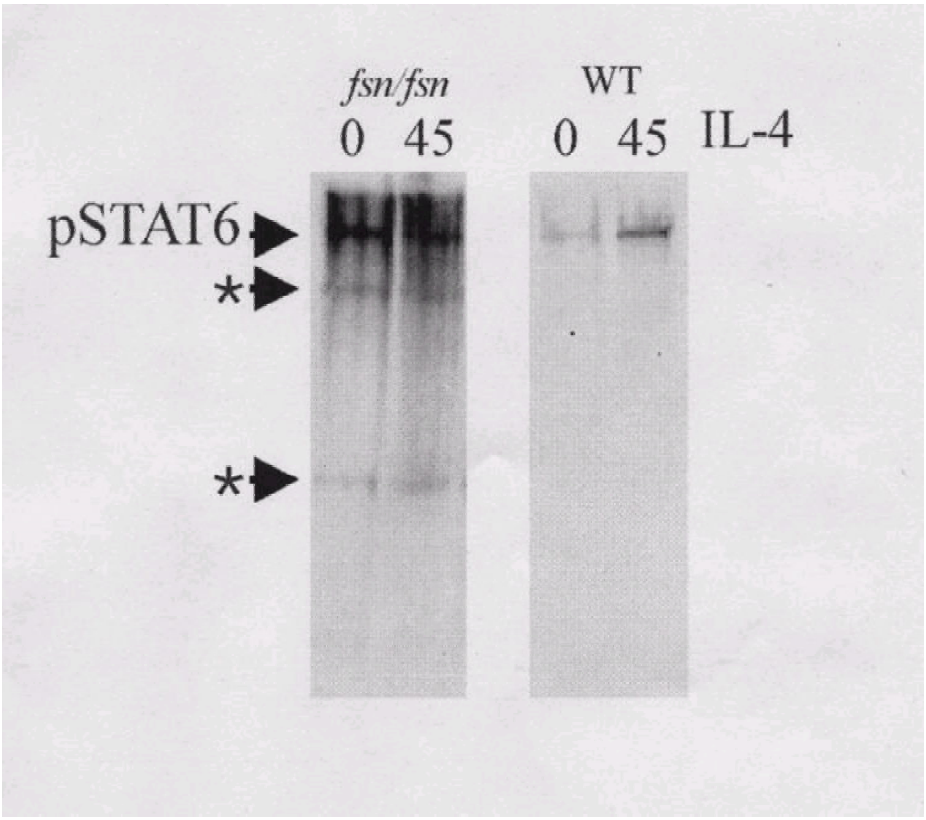

Figure 1.1. Stat6 Activation. Stat6 activation is enhanced in Ttc7$^{fsn/fsn}$ splenocytes. Splenocytes (normalized to 6 x 10^6 cells/lane) were isolated from Ttc7$^{fsn/fsn}$ and WT littermate control mice and stimulated with (10ng/mL) rIL-4 for the time indicated above the lanes. Stat6 analyzed by Western blot for activated (phosphorylated) Stat6 (pStat6). Increased levels of pStat6 are detected from Ttc7$^{fsn/fsn}$ splenocytes even in samples without exogenous IL-4 stimulation. The asterisks indicate possible Stat6 proteolytic fragments.

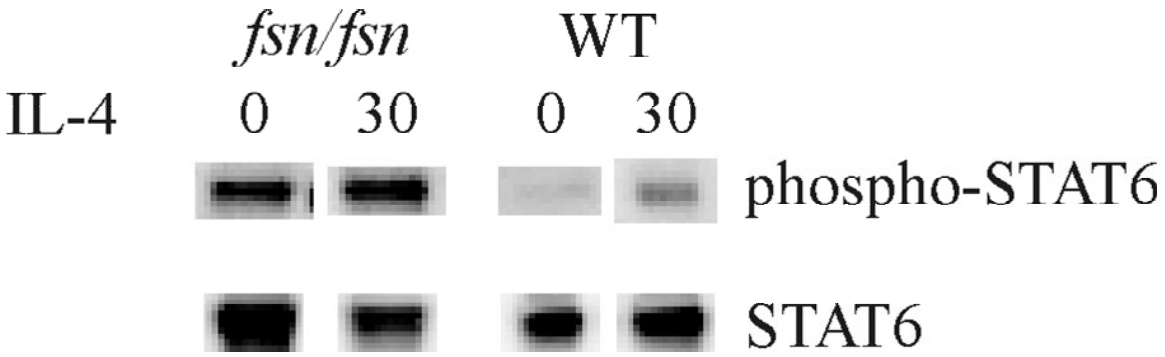

Figure 1.2 Ratio of pStat6 to Stat6. Stat6 was immunoprecipitated with anti-Stat6 antibody and immunoblotted with anti-pStat6 and anti-Stat6 as indicated in the figure. Ttc7$^{fsn/fsn}$ splenocytes show an increase in pStat6 expression as well as in the ratio of pStat6 to Stat6 (see text).

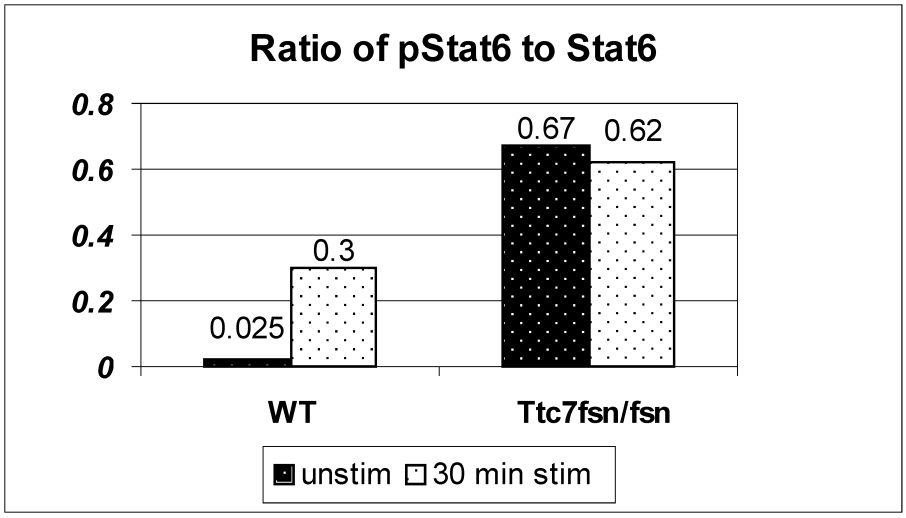

Figure 1.3. The ratio of pStat6 to Stat6 is elevated in Ttc7$^{fsn/fsn}$ splenocytes. In both unstimulated and stimulated samples the ratio of pStat6 to Stat6 is higher in Ttc7$^{fsn/fsn}$ than in WT littermates suggesting more of the total Stat6 pool is activated in Ttc7$^{fsn/fsn}$ mice.

Activation of Stat6 in B lymphocytes

Preliminary work indicated that Stat6 was constitutively activated (phosphorylated) without exogenous IL-4 stimulation in the lymphocyte fraction of Ttc7$^{fsn/fsn}$ splenocytes as compared to their WT littermates, but that the overall expression of unphosphorylated Stat6 between the two was similar. Stat6 is phosphorylated in the cytoplasm upon stimulation of the IL-4 receptor by IL-4 and translocates to the nucleus where it binds to DNA and functions to upregulate IL-4 responsive genes. However, recent research has shown the presence of a factor or factors that may serve to sequester Stat6 in the cytoplasm after phosphorylation whereupon receiving the proper signal will release Stat6 to translocate to the nucleus and perform its role in transcriptional regulation (Daines, Andrews et al. 2003). Thus, to observe the functional regulation of Stat6 during activation in negatively-selected, magnetically-purified splenic B cells, we examined the nuclear localization of Stat6 following IL-4 stimulation. Stat6 (red) and Sytox green (green) double-stained confocal images (Figure 1.4) of unstimulated B cells (0 min) as well as B cells stimulated with IL-4 for 30 minutes, showed that the unstimulated Ttc7$^{fsn/fsn}$ B cell sample exhibited a greater number of activated cells (yellow) than did the unstimulated WT sample, correlating with the previous data that Ttc7$^{fsn/fsn}$ Stat6 was activated *in vivo* (Figure 1.2). Following 30 min of incubation with IL-4, both Ttc7$^{fsn/fsn}$ and WT exhibited an increased number of double-positive cells, but had comparatively similar levels between the groups.

To further analyze the kinetics of activation as well as numbers of activated cells between Ttc7$^{fsn/fsn}$ and WT a minimum of 1500 cells were counted per time point and

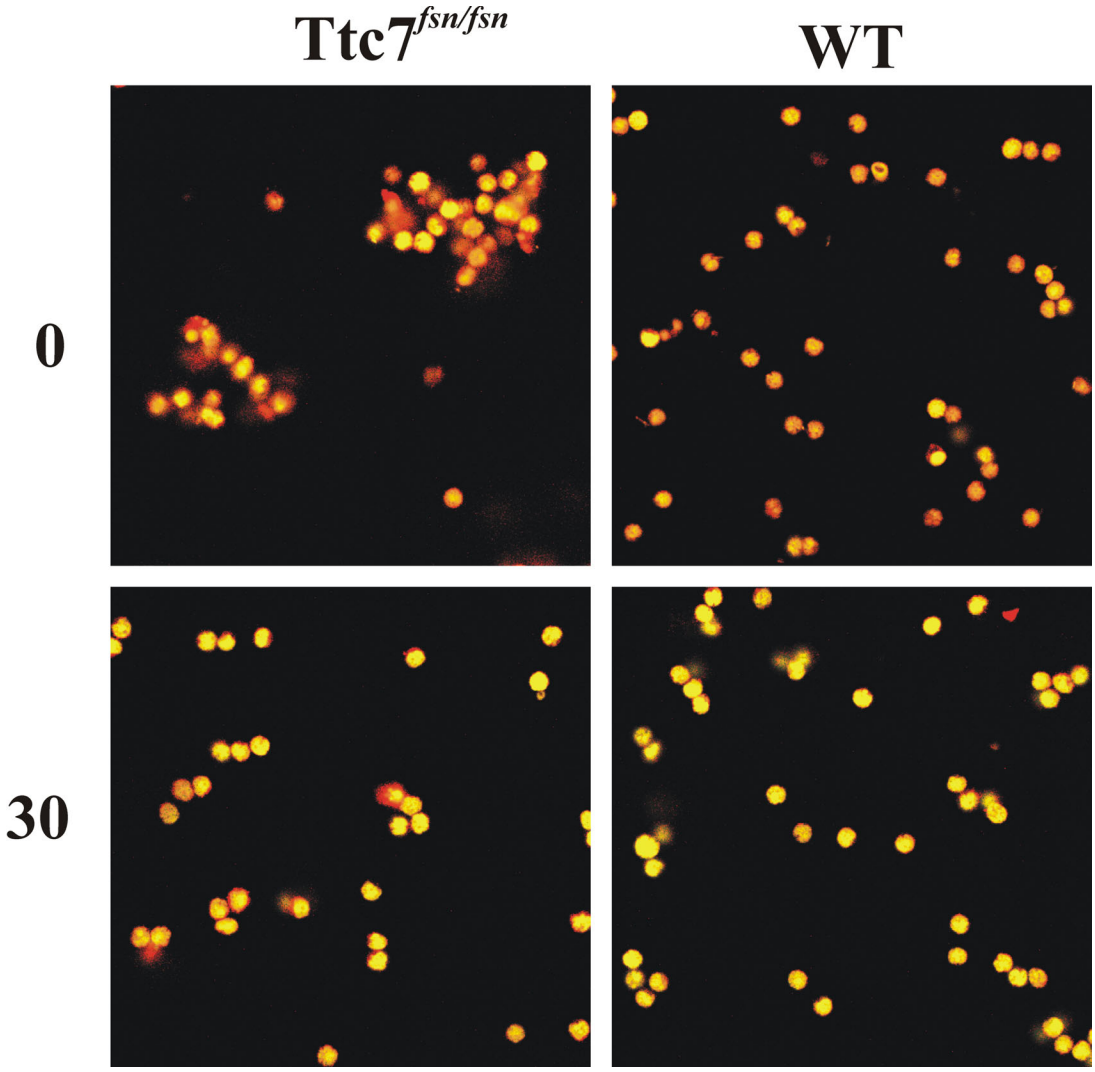

Figure 1.4 Stat6 Localization in B cells. Purified splenic B cells are unstimulted (0) or stimulated with IL-4 for 30 minutes, then stained for Stat6 (red) and the nucleus (green) and visualized with confocal microscopy using a 60x objective. Co-localization of Stat6 with the nucleus, denoting activation, is yellow. Ttc7$^{fsn/fsn}$ B cells show more yellow, activated cells than normal even without stimulation, suggesting preactivation *in vivo*.

scored for percentage of activated cells (Figure 1.5). At 0 min (unstimulated) nearly 30% of the Ttc7$^{fsn/fsn}$ B cells are activated compared to less than 15% of WT. We also saw slightly different kinetics of activation as with 15 minutes of IL-4 stimulation Ttc7$^{fsn/fsn}$ activation slightly declined while WT increased as we would expect. Following 30 minutes of stimulation there was a slight increase in both populations with similar overall levels of activation.

With a P value of 0.09 the difference in Stat6 nuclear localization levels in unstimulated Ttc7$^{fsn/fsn}$ and WT B cells does not reach statistical significance, however, it does suggest a biologically relevant level of pre-activation since B cells have been found to exhibit altered signaling pathways, the upregulation of inhibitory molecules, and a 100-1000 fold increase in responsiveness to subsequent IL-4 stimulation after initial activation (Siepmann, Wohlleben et al. 1996). This warranted further investigation since constitutively active Stat proteins, such as we have seen in Ttc7$^{fsn/fsn}$ mice, have been found to contribute to disease processes such as autoimmunity and lymphomas (Daniel, Salvekar et al. 2000).

Decay of activated Stat6 in B lymphocytes.

The activation state of a protein can be maintained by various mechanisms including continuous signaling, enhanced activity in the binding/behavior of signaling molecules, or the inability of the cell to downregulate the signal after activation. Stat6 decay or inactivation occurs when it becomes dephosphorylated in the nucleus and translocates back to the cytoplasm where it can become reactivated (Andrews, Ericksen et al. 2002; Hanson, Dickensheets et al. 2003). Since Stat6 appeared to be pre-activated

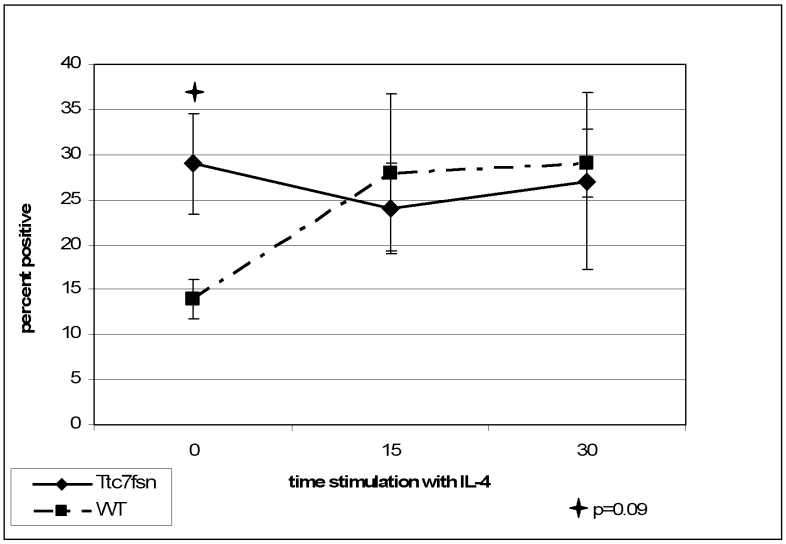

Figure 1.5 Scoring of Stat6 Activation in B cells. 1500 cells per experiment were counted and scored for percent of activated cells. Ttc7$^{fsn/fsn}$ have almost 15% more activated cells B cells without stimulation than WT littermates, although percentages are then similar at 15 and 30 minutes of stimulation. While the 0 time point does not quite reach statistical significance, the p value of 0.09 suggests a biologically significant level of pre-activation. Data are presented as mean ± SEM for three separate experiments.

and constitutively expressed, we needed to determine whether Ttc7$^{fsn/fsn}$ B cells were able to downregulate the activation of Stat6 in the absence of IL-4 (providing evidence that Ttc7$^{fsn/fsn}$ B cells are responding to the exaggerated IL-4 production in Ttc7^{fsnfsn} mice).

To visualize the activation state of Stat6 in Ttc7$^{fsn/fsn}$ and WT B cells when the IL-4 signal is removed, we stimulated isolated B cells for 30 minutes with IL-4 and then removed the IL-4 signal through several washes of the cells and allowed them to rest for either 15 or 30 minutes. Analysis by confocal microscopy (Figure 1.6) suggested that Ttc7$^{fsn/fsn}$ Stat6 was able to move out of the nucleus and achieve an inactive state in the cytoplasm in a similar manner as WT littermates as determined by comparable Stat6 localization outside of the nucleus.

We counted and scored the cells to determine the percentage of activated cells (Figure 1.7). After 30 minutes of IL-4 stimulation (i.e. 0 min resting) the percentages of Stat6 activated Ttc7$^{fsn/fsn}$ and WT B cells were similar; however, after the IL-4 stimulus was removed for 15 minutes both cell populations exhibited decreased activation, with Ttc7$^{fsn/fsn}$ B cells showing a more rapid decline, and after 30 minutes of rest, percentages of activated B cells decreased further and were again similar between Ttc7$^{fsn/fsn}$ and WT. This suggests that Stat6 decay in Ttc7$^{fsn/fsn}$ B cells is similar to WT in both timing of turnover as well as number of cells, and is able to become de-phosphorylated in the nucleus and move into the cytoplasm upon removal of the IL-4 signal. Thus, it seems probable that the constitutively active Stat6 seen in Ttc7$^{fsn/fsn}$ mice (Welner, Swett et al. 2005) was due to a continuous IL-4 stimulation and signaling as described by Andrews et al (Andrews, Ericksen et al. 2002) and Hanson et al (Hanson, Dickensheets et al. 2003), rather than intrinsic defects in Stat6 regulation.

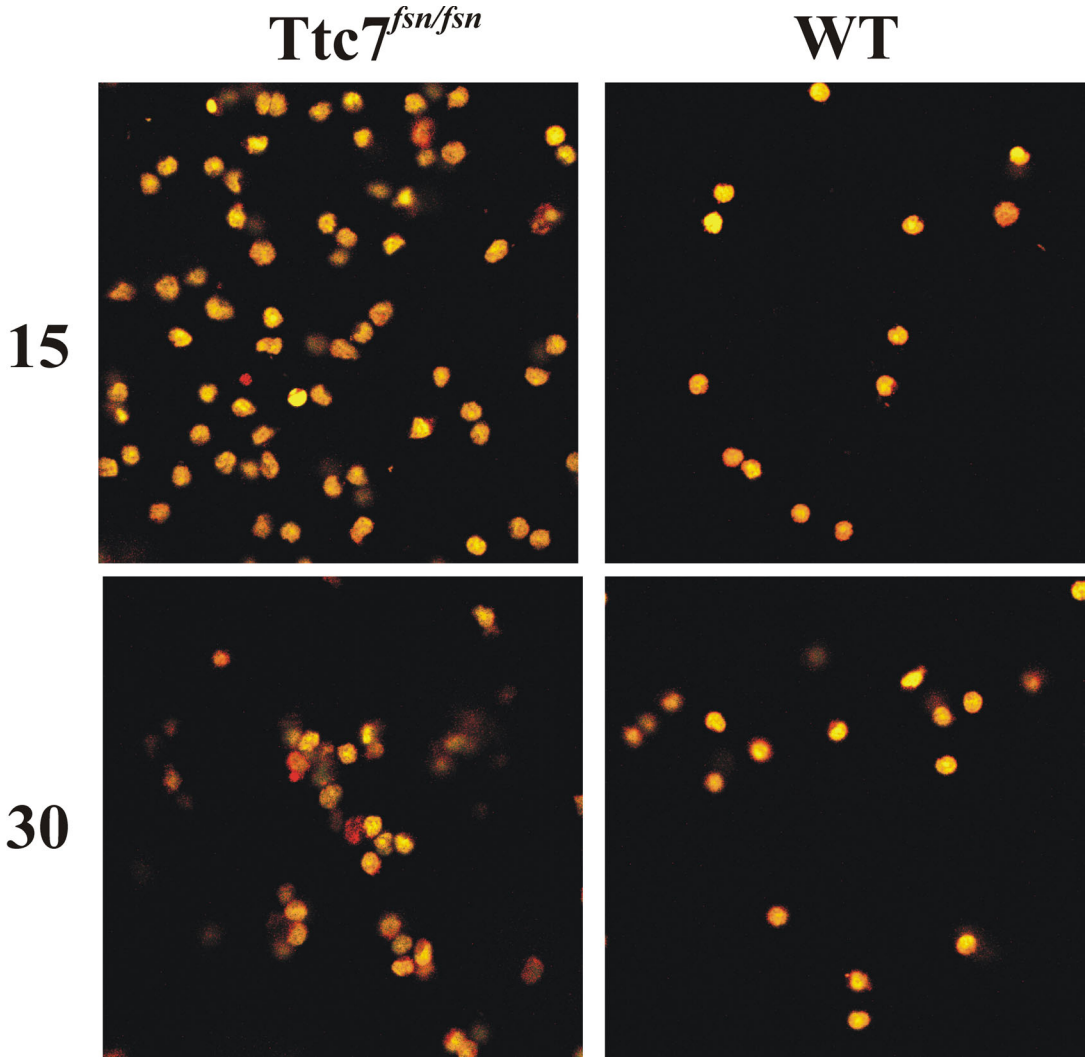

Figure 1.6. Decay of Stat6 activation in B cells. Purified splenic B cells were stimulated with IL-4 for 30 minutes, washed 3X and allowed to rest for 15 or 30 minutes, then stained for Stat6 (red) and the nucleus (green) and imaged with confocal microscopy using a 60x objective. Co-localization of Stat6 with the nucleus, denoting activation, is yellow. Ttc7$^{fsn/fsn}$ cells show a similar trend to WT cells at both time points, indicating they have the inherent ability to down-regulate Stat6 activation when IL-4 stimulus is removed.

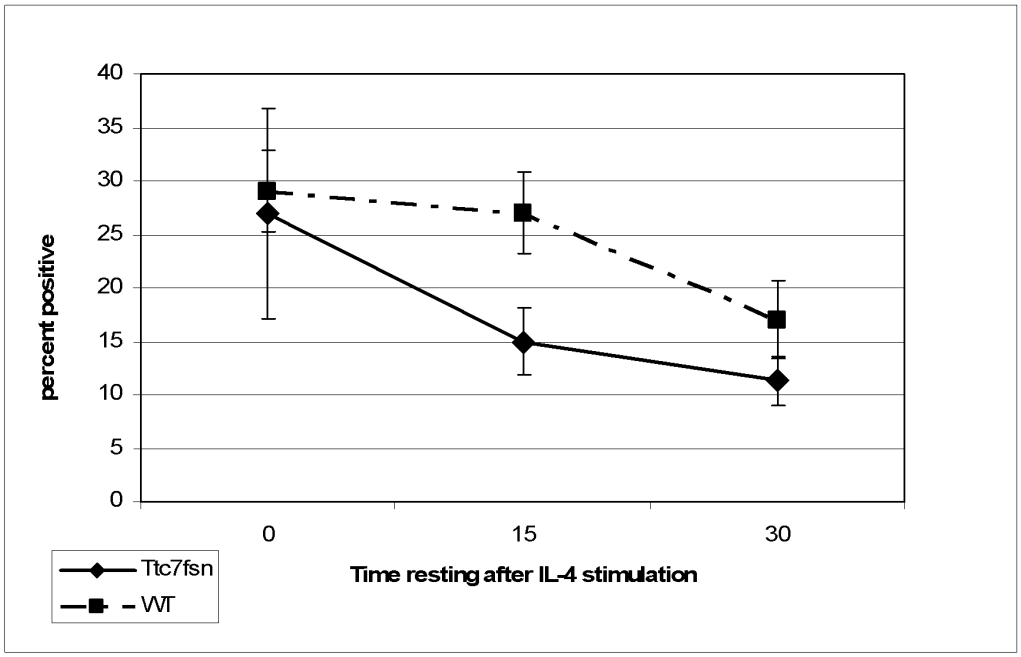

Figure 1.7. Scoring of Stat6 Turnover in B cells. Over 1000 B cells per experiment were counted for each data point and scored for percent of activated cells. Both Ttc7$^{fsn/fsn}$ and normal littermates show similar decay of Stat6 activation indicating turnover is not defective in Ttc7$^{fsn/fsn}$ mice. Data are presented as mean ± SEM for three separate experiments.

Structural location of pStat6 in spleen sections

In addition to the state of activation, it is important to identify the structural location of the Stat6-activated cells in the spleen. Previous studies have shown that the splenic architecture in flaky skin mice becomes increasingly disrupted and chaotic as mice age, which correlates with an increase in autoimmune disease pathology (Sundberg, France et al. 1997; Pelsue, Schweitzer et al. 1998). Normally, lymphocytes are restricted to specific compartments in order to regulate highly specific interactions which instruct cell survival and differentiation or determine if cellular responses are inappropriate which may lead to anergy or death. Because of the loss of follicular structure in Ttc7$^{fsn/fsn}$ spleen we thought it was important to determine the structural localization of Stat6 hyperactivated B cells. Triple staining of 8-week-old Ttc7$^{fsn/fsn}$ and WT mouse spleen sections (Figure 1.8) for IgM, CD4, and Stat6 or pStat6 allowed us to visualize the structural location of the cells exhibiting activated Stat6.

Figure 1.8, A and B were stained for the unphosphorylated form of Stat6 (green). The architectural abnormalities present in the Ttc7$^{fsn/fsn}$ spleen are clearly shown in section B. This leads to the aberrant expression of Stat6 shown in what remains of the follicle, where Stat6 is excluded in WT littermates (Figure 1.8A), although the intensity and total cellular area of Stat6 staining appears similar.

Sections stained for pStat6 (green, C and D) indicate that the cells expressing the activated form of pStat6 in Ttc7$^{fsn/fsn}$ mice are likely extrafollicular immature B cells or plasmablasts as these cells also stain brightly for IgM (red) (Loder, Mutschler et al. 1999; William, Euler et al. 2005). In addition, the number of pStat6 positive B cells in Ttc7$^{fsn/fsn}$

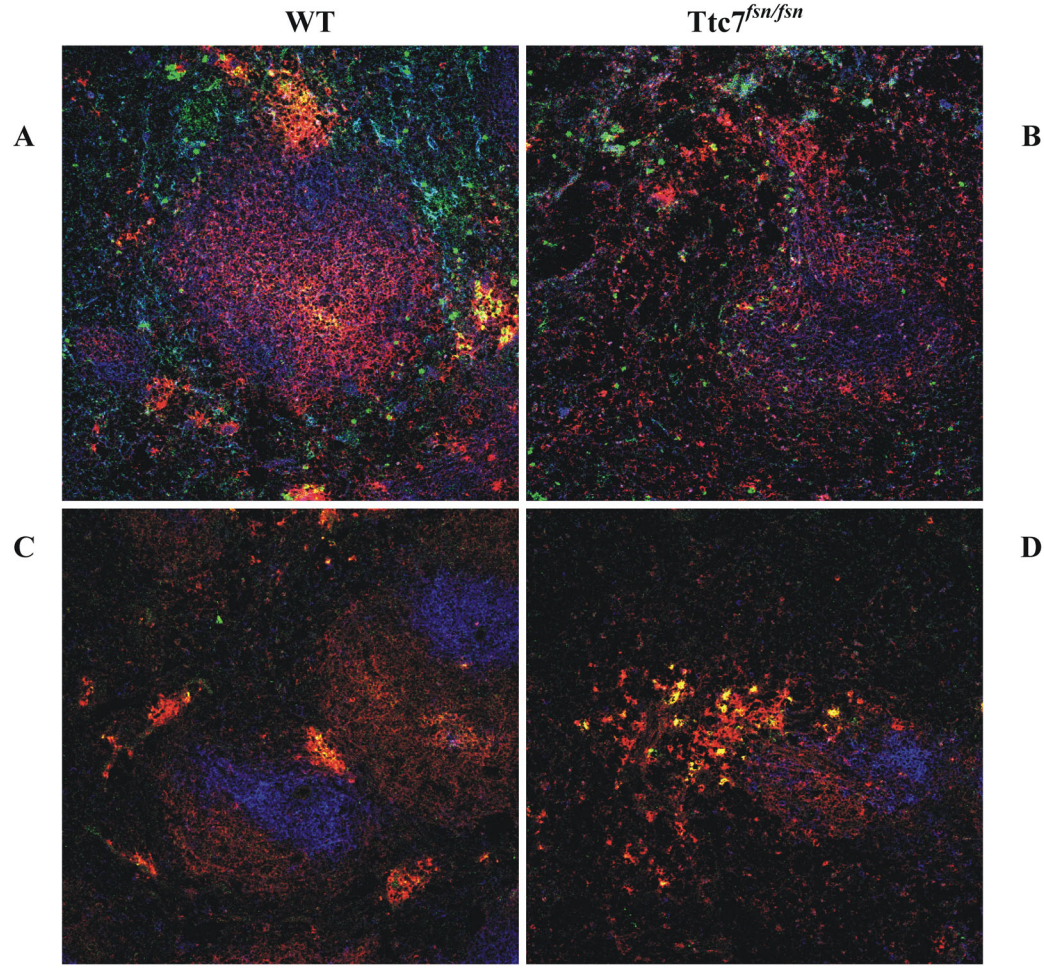

Figure 1.8 Expression of Stat6 and pStat6 in Spleen. Visualized by confocal microscopy using a 20x objective. A-D, Spleen sections from 8-week-old normal (left) and Ttc7$^{fsn/fsn}$ (right) mice stained with anti-Stat6 or anti-pStat6 (green), anti-CD4 (blue), and anti-IgM (red). Yellow indicates co-localization of B cells with Stat6. A and B: Overall expression of Stat6 is similar in both Ttc7$^{fsn/fsn}$ and WT. However, due to the break-down of follicular structure in Ttc7$^{fsn/fsn}$ spleen (B), Stat6 is located inside as well as outside of the follicle, whereas WT expression occurs extra-follicularly (A). C and D: Expression of pStat6. Ttc7$^{fsn/fsn}$ spleen (D) exhibits much more activated phosphorylated Stat6 than WT littermate (C), indicating hyper-activated B cells residing outside of follicle, possibly contributing to survival of autoreactive cells.

spleen (D) was elevated over that of WT as we saw very little pStat6 staining on WT spleen sections (C). The expression of pStat6 in WT spleen was found only in the IgM bright B cells outside of the follicle which denote the newly arrived, more immature B cell population or plasmablasts.

Not only did Ttc7$^{fsn/fsn}$ splenic follicles express higher levels of activated Stat6, there were also more pStat6 positive follicles as shown in Figure 1.9. Out of 18 Ttc7$^{fsn/fsn}$ counted, thirteen (72%) were positive for pStat6 as compared to only 2 (9%) out of 22 counted for WT. While 9 WT and 5 Ttc7$^{fsn/fsn}$ follicles were slightly positive for pStat6, none of the Ttc7$^{fsn/fsn}$ follicles were negative for pStat6 whereas 11 (50%) of the 22 WT counted exhibited no pStat6 staining. Thus, we see a higher level of pStat6 in Ttc7$^{fsn/fsn}$ B cells in the spleen.

IL-4 expression is increased in Ttc7$^{fsn/fsn}$ spleen

The extensive distribution of phosphorylated Stat6 in spleen tissue of Ttc7$^{fsn/fsn}$ mice suggested that their splenic B cells are responding to a higher level of IL-4 as Stat6 regulation appears to be normal in Ttc7$^{fsn/fsn}$ B cells (Figure 1.7). IL-4 generally acts locally in tissues, being produced by one cell type and exerting its influence on another cell near-by. Under normal physiological circumstances, tightly controlled splenic structure provides the proper context for the interaction of cells and cytokines for normal development, tolerance induction, and the immune response (Roy, Chang et al. 2005; Yurasov, Wardemann et al. 2005). Because it has previously been noted that Ttc7$^{fsn/fsn}$ mice have disrupted spleen structure

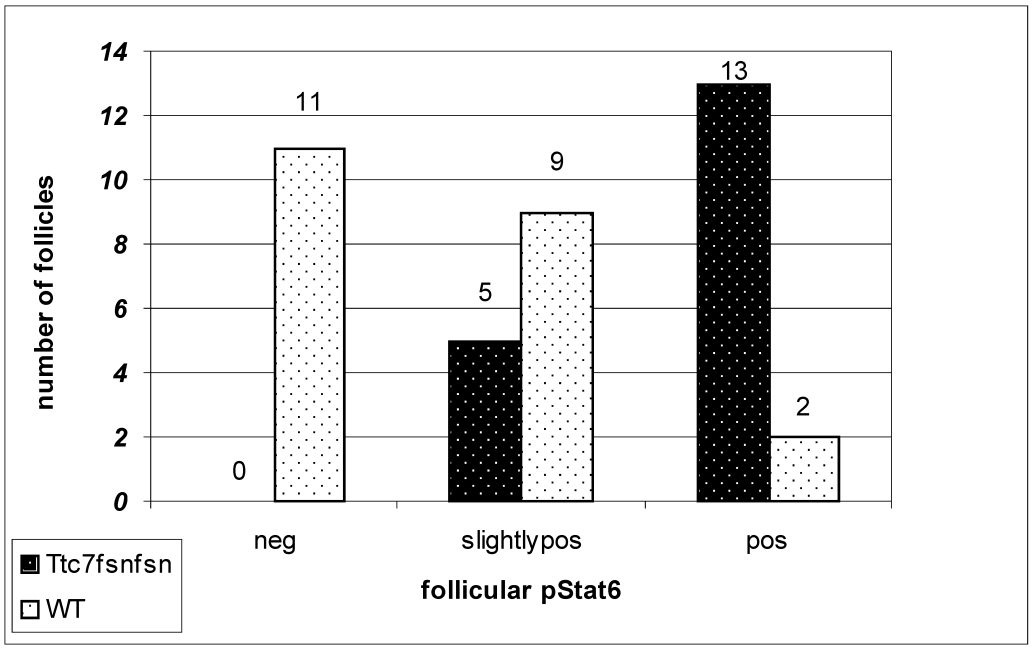

Figure 1.9. Number of splenic follicles positive for pStat6. Eighteen *Ttc7*$^{fsn/fsn}$ and 22 WT follicles were counted and scored for the presence of phosphorylated Stat6 in 8-week spleen sections as shown in Figure 1.8, C and D. Scoring was designated as negative if sections did not show staining for pStat6, slightly positive if there were one to eight positive areas of staining and positive if over eight positive areas were counted. Thirteen positive follicles were counted for *Ttc7*$^{fsn/fsn}$ whereas WT demonstrated only two.

(Pelsue, Schweitzer et al. 1998; Mattsson, Duzevik et al. 2005), it is possible that abnormal IL-4 production contributes to cell survival and activation, leading to a ramping up of autoimmune pathology.

Since we observed that the activated B cells were in close proximity to splenic T cells, and that T cells are a major producer of IL-4 in the spleen, we next wanted to confirm the presence of IL-4 in the spleen and compare its expression to that in WT. Figure 1.10A depicts a spleen section from an 8-week-old WT mouse that has been stained for IL-4 (blue) and CD3 T cells (red). The section clearly showed virtually no detectable IL-4 as expected. Analysis of a Ttc7$^{fsn/fsn}$ spleen section (Figure 1.10B) was accomplished in four sections due to the enlarged spleen of these mice. We saw a dramatic increase in IL-4 staining throughout the spleen, especially in the CD3 positive regions (see arrows) (Staining and image kindly provided by Lynn Hannum and Cory Ernst).

A closer examination of follicular structure in Ttc7$^{fsn/fsn}$ spleen using immunofluorescent staining to detect IL-4 (green), IgM (blue), and CD3 (red) (Figure 1.11B) revealed that IL-4 positive T cells (yellow) were located in the same extrafollicular region where the pStat6 positive B cells were identified in Figure 1.8, depicted here as blue (IgM staining). Wild type spleen showed few, if any IL-4^{+} T cells (yellow) (Figure 1.11A). Thus, newly arriving immature B cells in Ttc7$^{fsn/fsn}$ mice are subjected to IL-4 exposure at a time in their development when they are normally being educated in immune tolerance to self-antigen (Norvell, Mandik et al. 1995), which would likely alter their future responses and support antibody production.

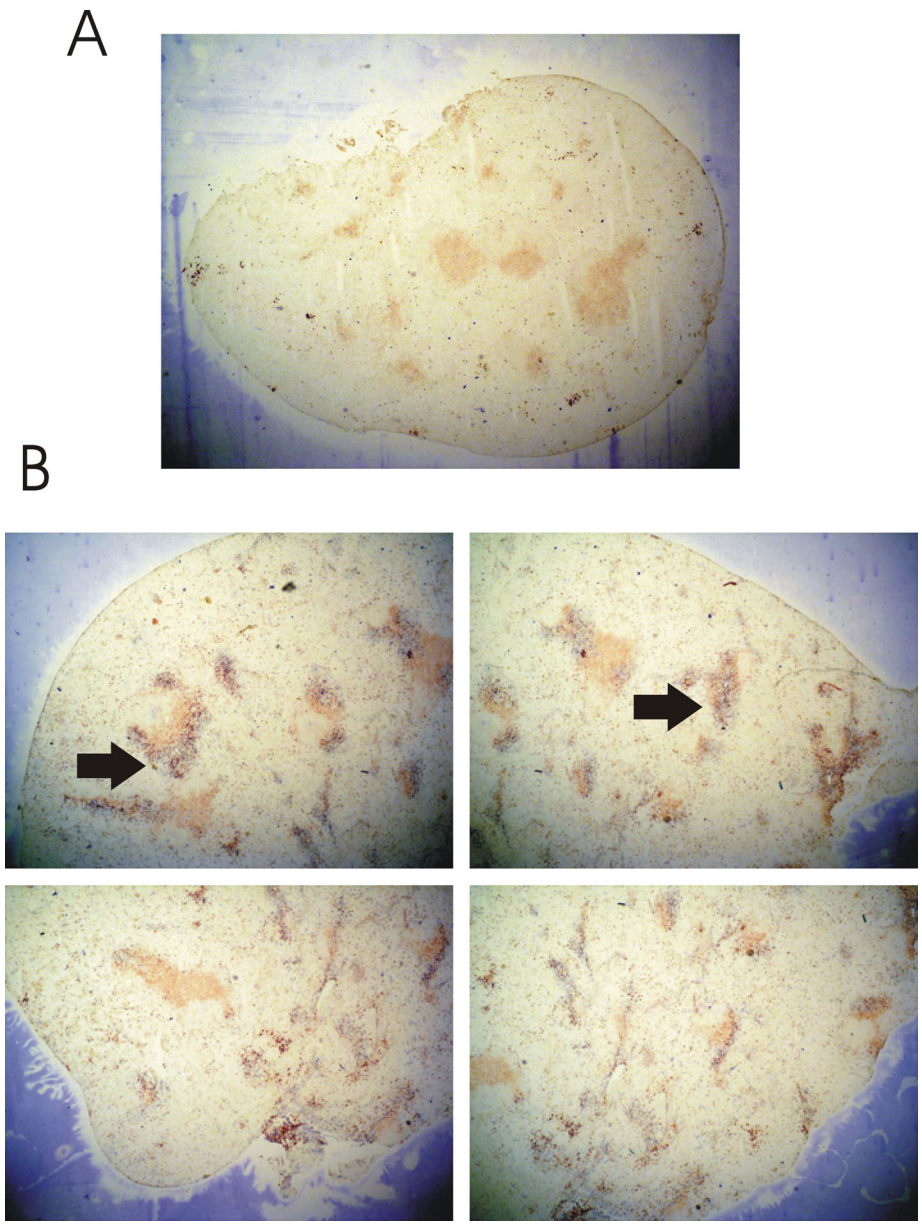

Figure 1.10 IL-4 in Spleen. Gross structure of spleen longitudinal sections showing IL-4 production (blue) and CD3 positive cells (red). A, WT 8-week section showing normal follicular structure, red-stained T cell zones and non-detectable IL-4. B, 8-week section divided into 4 parts of Ttc7$^{fsn/fsn}$ spleen showing dramatic enlargement of organ size, breakdown of regular follicular structure and disintegration of distinct T cell zones. Highly increased and detectable production of IL-4 is shown throughout spleen, but especially in follicles as indicated by arrows. 40x magnification. (Courtesy of Lynn Hannum and Cory Ernst)

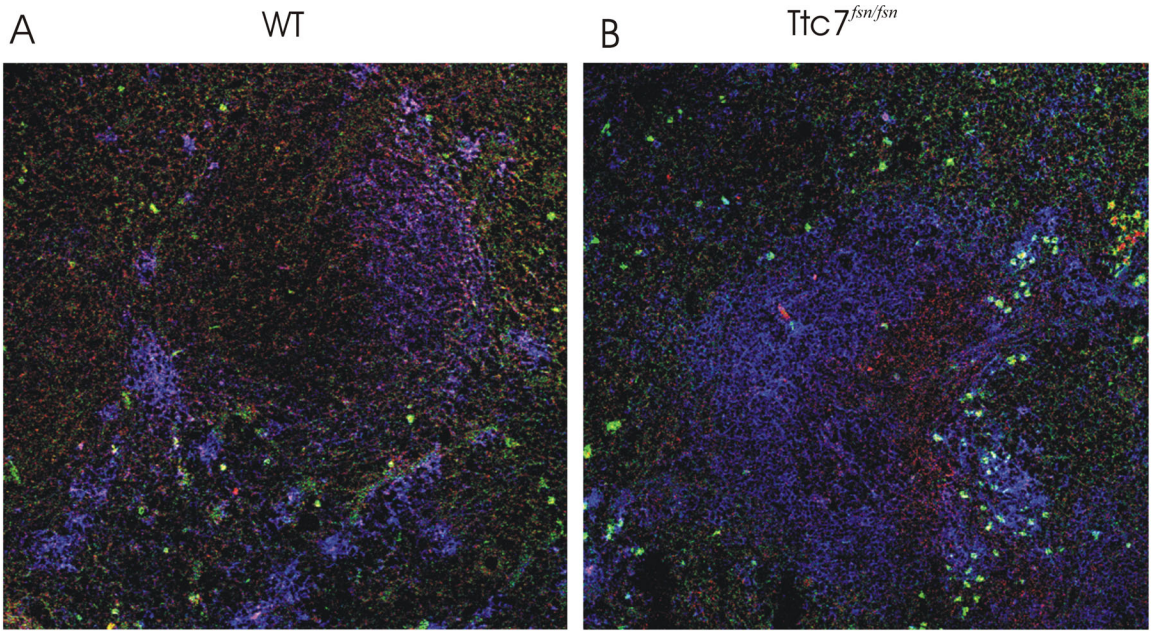

Figure 1.11 IL-4+ Cell Specific Staining in Spleen. IL-4 expression in 8-week spleen visualized with fluorescent scanning confocal microscopy using 20x objective. Spleen sections stained for IL-4 (green), $CD3^+$ T cells (red) and IgM^+ B cells (blue). $Ttc7^{fsn/fsn}$ spleen (B) shows an increase in IL-4-positive intensely stained T cells (yellow) as compared to WT littermate (A). In addition, T cells are located outside of the follicle in the B-cell-rich zone which is consistent with the location of pStat6 positive B cells, possibly exposing newly arrived B cells to IL-4. All staining was repeated three times in three separate animals with similar results.

IL-4 mRNA is upregulated and shows increased stability in Ttc7$^{fsn/fsn}$ mice

Cytokine mRNA stability as well as transcriptional regulation have been demonstrated to play a role in altered cytokine responses (Dokter, Esselink et al. 1993; Naora and Young 1995; Pioli, Pucci et al. 1998; Butler, Monick et al. 2002). T cells have been shown to be a critical contributor to the development of autoimmunity through mechanisms such as: effector functions, B cell co-activation, and production of cytokines. Since one of the hallmarks of Ttc7$^{fsn/fsn}$ mice is a high level of extemporaneous IL-4 production (15X that of normal in the sera) (Pelsue, Schweitzer et al. 1998), we thought it probable that the overproduction of IL-4 by T cells was one of the factors contributing to their severe systemic autoimmunity. Previous work in Ttc7$^{fsn/fsn}$ mice has demonstrated a rapid ramping up of symptoms as well as hyper-activation of lymphocytes in mice past 6-7 weeks of age (Welner, Hastings et al. 2004), thus, we wanted to examine the regulation of IL-4 in T cells before they reach this critical point in disease development.

RT-PCR of IL-4 expression in 4-week-old mice (Figure 1.12A) revealed that in unstimulated Ttc7$^{fsn/fsn}$ T cells IL-4 mRNA expression was actually slightly lower (74%) than that of WT; however, following 3 hours of stimulation with plate-bound anti-CD3 IL-4 mRNA expression jumps to slightly above that of normal (106%). When actinomycin D was added to stimulated samples to block mRNA synthesis and then analyzed at 2 and 4 hours later, we saw an overall decline in expression in both cell populations, but Ttc7$^{fsn/fsn}$ IL-4 mRNA exhibited a more prolonged decline with a slight increase at 2 hours (Figure 1.13A). Designating the mRNA expression level after stimulation as 100%, 2 hours after the addition of Act D there was 95% of WT mRNA

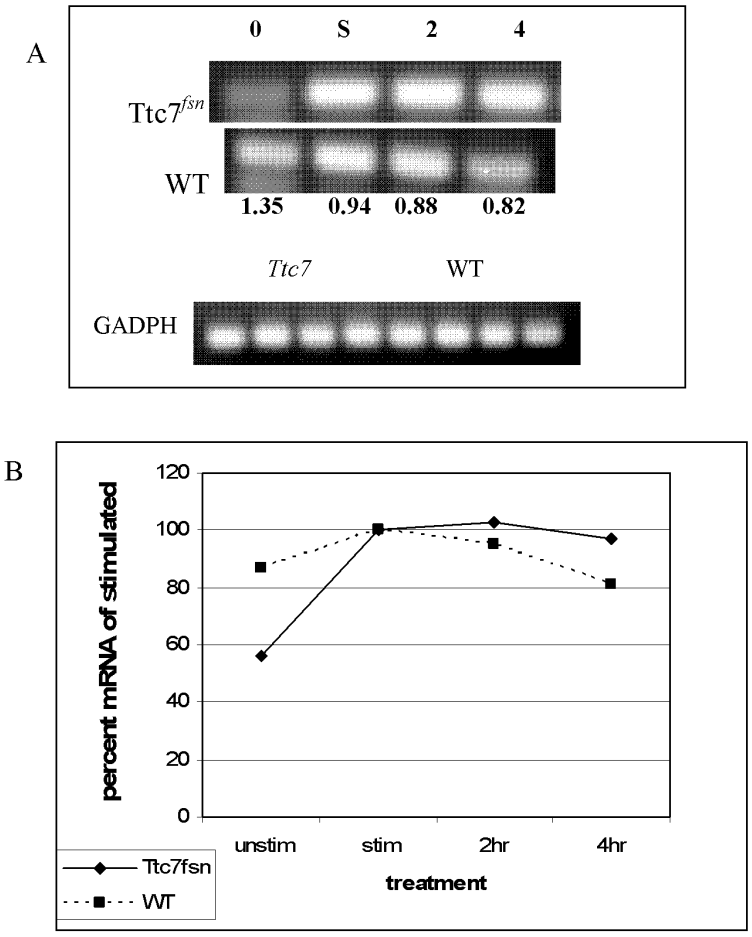

Figure 1.12 IL-4 mRNA expression in T cells. RT-PCR of IL-4 mRNA was performed using purified splenic T cells with RNA normalized to 2μg per sample in reverse transcriptase reaction. Samples include unstimulated cells (0), cells stimulated with plate-bound anti-CD3 (S), and cells stimulated for 3 hours with anti-CD3 before adding actinomycin D to inhibit transcription. These cells were then harvested 2 and 4 hours later as indicated. A, Representative gel of 5 separate experiments demonstrating mRNA turnover. Four hours after inhibition of transcription Ttc7$^{fsn/fsn}$ T cells still exhibit significant presence of IL-4 mRNA. The numbers below IL-4 bands indicate the fold difference of WT over Ttc7$^{fsn/fsn}$ at each time point. Ttc7$^{fsn/fsn}$ exhibits lower initial IL-4 expression whereupon stimulation increases expression over WT and remains higher. GADPH was used as a loading control and to confirm normalization. B, After 3 hours of stimulation, mRNA is designated as 100% and the percentage of mRNA remaining is indicated at designated time points as measured by densitometry. In both Ttc7$^{fsn/fsn}$ and WT cells we see mRNA turnover, but we see a higher percentage of Ttc7$^{fsn/fsn}$ IL-4 mRNA remaining which is still above unstimulated levels at 4 hours, indicating longer half-life of IL-4 mRNA in Ttc7$^{fsn/fsn}$ mice. Data shown as representative of 5 separate experiments with similar results.

A

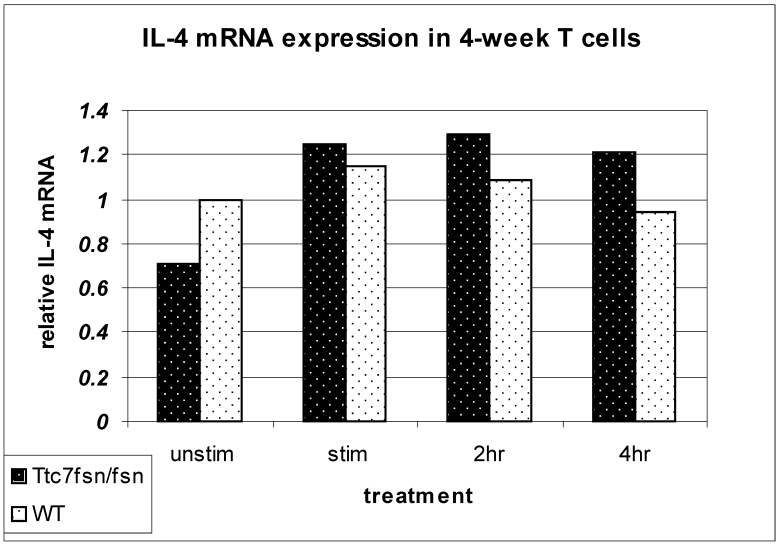

B

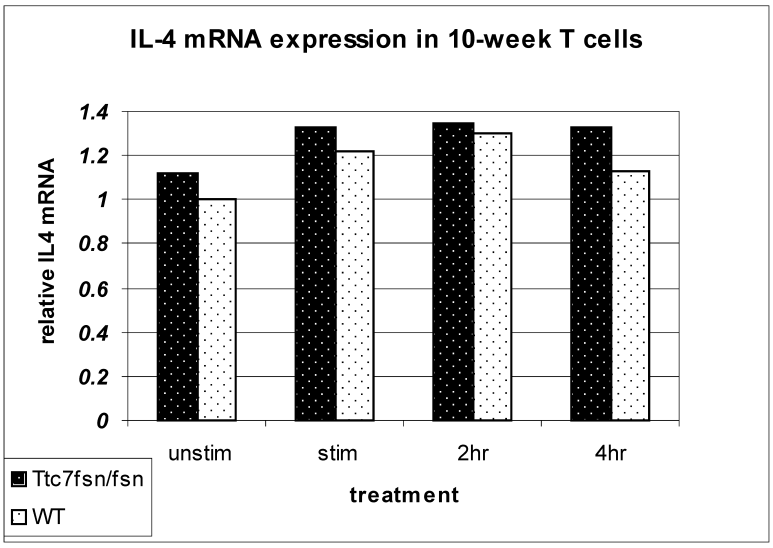

Figure 1.13 IL-4 mRNA Expression in 4- and 10-week T cells. IL-4 RT-PCR of 4- and 10- week T cells presented as the ratio of IL-4 to GADPH, normalized to unstimulated WT control as measured by densitometry. Graphs represent one data set of five separate experiments with similar results. A, 4-week T cells showing unstimulated Ttc7$^{fsn/fsn}$ expressing IL-4 mRNA below that of WT, increasing upon stimulation with anti-CD3 and mRNA remaining at 2 and 4 hours after treatment with Act D. B, 10-week T cells repeating same experiment as in A, showing unstimulated Ttc7$^{fsn/fsn}$ cells expressing a higher level of IL-4 mRNA than 4-week and WT cells.

remaining compared to 103% of Ttc7$^{fsn/fsn}$, and after 4 hours there was 81% of WT mRNA remaining whereas Ttc7$^{fsn/fsn}$ still had 97% (Figure 1.12B). While these figures did not reach statistical significance, this trend was similar among 5 separate experiments. In addition, when the percentage of mRNA remaining at 4 hours was compared to IL-4 mRNA in unstimulated cells, Ttc7$^{fsn/fsn}$ mRNA was 114% above unstimulated levels while WT mRNA declined to 95% below unstimulated levels indicating differences in mRNA half-life between Ttc7$^{fsn/fsn}$ and WT mice. A single experiment examining mRNA after 10 hours of treatment with Act D revealed Ttc7$^{fsn/fsn}$ IL-4 mRNA was back to baseline while WT was below baseline as shown above (baseline equals mRNA of unstimulated IL-4) which indicated that Ttc7$^{fsn/fsn}$ T cells are able to turn over IL-4 mRNA after a prolonged period of transcriptional inhibition (data not shown).

Interestingly, when the same analysis was performed with T cells from 10-week-old mice, we saw a similar trend in all but the unstimulated samples (Figure 1.13B). Ttc7$^{fsn/fsn}$ IL-4 mRNA was expressed at a higher level (113%) relative to WT and following stimulation increased to 133% relative to unstimulated WT control whereas WT mRNA increased to 123% that of unstimulated control. Four hours after treatment with Act D Ttc7$^{fsn/fsn}$ IL-4 mRNA showed little decline remaining at 133% as compared to WT which was measured at 113% relative to control. Thus, at 10-weeks-of-age Ttc7$^{fsn/fsn}$ IL-4 mRNA was expressed at a higher level in unstimulated T cells as compared to WT but followed a similar trend as that of 4-week-old mice upon stimulation and treatment. A single experiment measuring relative IL-4 mRNA at 6 hours

post-treatment suggested both Ttc7$^{fsn/fsn}$ and WT mRNA was turned over to a pre-stimulated expression level (data not shown).

In order to normalize the concentration of RNA at 2μg per sample for RT-PCR, total RNA concentration was measured by spectrophotometry. Table 1.1 summarizes the raw data for 4-week unstimulated T cells. Measurements indicated that Ttc7$^{fsn/fsn}$ cells had approximately 3X the total RNA content per cell as did WT, suggesting the *in vivo* biological impact of increased IL-4 mRNA stability in Ttc7$^{fsn/fsn}$ may be more significant than demonstrated *ex vivo*.

Cyclosporine A shuts down IL-4 mRNA production

The immunosuppressive agent CsA has been shown to bind to the intracellular protein cyclophillin and inhibit the phosphatase calcineurin which thus blocks a Ca^{++} dependent pathway activated by TCR/CD3 stimulation (Dokter, Esselink et al. 1993; Naora and Young 1995). To investigate the effect of CsA on IL-4 mRNA expression, 4- and 10-week enriched splenic WT and Ttc7$^{fsn/fsn}$ T cells were pre-treated with CsA (1μg/mL) or DMSO control for 30 minutes and then stimulated on anti-CD3 coated plates. As shown in Figure 1.14A, CsA blocked mRNA production completely in 4-week T cells in both Ttc7$^{fsn/fsn}$ and WT. Ten-week T cells (Figure 1.14B) showed a slightly different result where CsA reduced but did not completely block IL-4 mRNA production in both cell populations. This suggests slightly different transcriptional control of IL-4 between 4- and 10-week animals but that a similar pathway is involved in both WT and mutant mice.

Total RNA concentration per 1 million unstimulated T cells from 4-week-old mice as measured by NanoDrop™		
	Ttc7^{fsn}	**WT**
	58.8	24.75
	83	44
	15.75	8.7
	61	16
	94.8	15
N=6	71.7	18.8
MEAN	64.17	21.2
SEM	27.3	12.32

*Raw data from 6 individual mice for each group is presented in ng/mL. The mean total RNA concentration of Ttc7^{fsn} T cells is 3X that of WT

Table 1.1 Total RNA Concentration in Splenic T cells

A

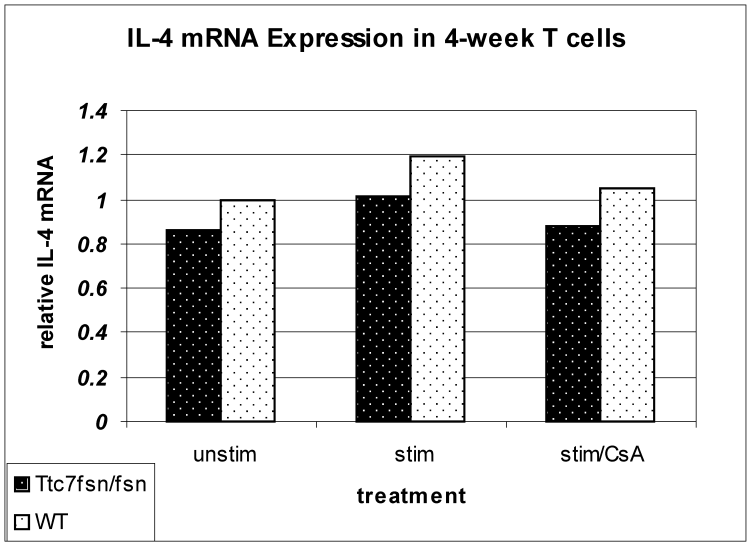

B

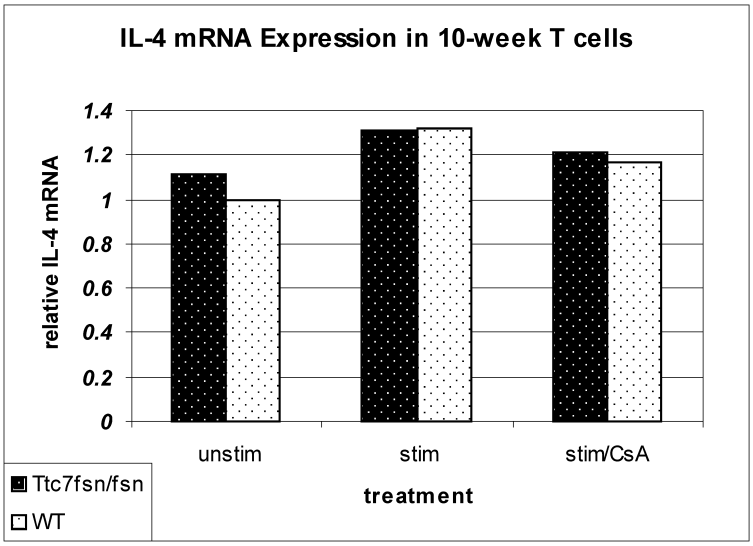

Figure 1.14 IL-4 mRNA Expression in Cyclosporin-Treated T cells. RT-PCR of 4- and 10-week T cells unstimulated, stimulated with anti-CD3 and stimulated with anti-CD3 treated with Cyclosporine A. Data are presented as the ratio of IL-4 mRNA to GADPH mRNA and normalized to unstimulated WT control as measured by densitometry. Graphs are representative of three separate experiments with similar results. A, 4-week T cells demonstrate an increase in IL-4 mRNA upon stimulation but remain at unstimulated levels with the addition of CsA blocking a Ca^{++} induced pathway in both Ttc7$^{fsn/fsn}$ and WT. B, 10-week T cells also demonstrate an increase in IL-4 mRNA upon stimulation but do show a slight increase in mRNA above untreated unstimulated levels when treated with CsA.

T cells from Ttc7^{fsn} mice show an increase in IL-4 protein production that mirrors IL-4 mRNA regulation

Evidence of differentially regulated WT and Ttc7$^{fsn/fsn}$ mRNA expression for IL-4 in splenic T cells suggested that we confirm this effect on protein production. Previous work has shown an increased capacity for IL-4 production in 8-10 week Ttc7$^{fsn/fsn}$ T cells (Welner, Hastings et al. 2004) but 4-week T cells had remained unanalyzed. Thus, 6 x 10^6 cells per sample of 4-week enriched splenic T cells were plated on anti-CD3 coated plates or in uncoated wells for unstimulated samples. Figure 1.15A shows that in unstimulated cells, both Ttc7$^{fsn/fsn}$ and WT produced 61 pg/mL of IL-4 after 24 hours of culture. With anti-CD3 stimulation, Ttc7$^{fsn/fsn}$ cells produced more than WT, at 2790 pg/mL and 2358 pg/mL respectively. After 3 hours of anti-CD3 stimulation the addition of Act D resulted in a much lower IL-4 measurement of 325 pg/mL from Ttc7$^{fsn/fsn}$ T cells and to 81 pg/mL in WT (p=0.0002).

Figure 1.15B shows that 10-week unstimulated Ttc7$^{fsn/fsn}$ T cells out-produced WT by almost 1200-fold, with IL-4 measured at 1198 pg/mL while WT IL-4 was barely detectable at 0.133 pg/mL. Upon stimulation, Ttc7$^{fsn/fsn}$ T cells showed little increase, rising only to 1215 pg/mL agreeing with previous data (Welner, Hastings et al. 2004), while WT increased to 525 pg/mL. When Act D was added after 3 hours of stimulation IL-4 remained high in Ttc7$^{fsn/fsn}$ assays at 1062 pg/mL whereas WT IL-4 was back to background levels at 0.133 pg/mL. All three measurements comparing Ttc7$^{fsn/fsn}$ to WT were statistically significant with p values of 0.00005, 0.0002 and 0.0001 respectively.

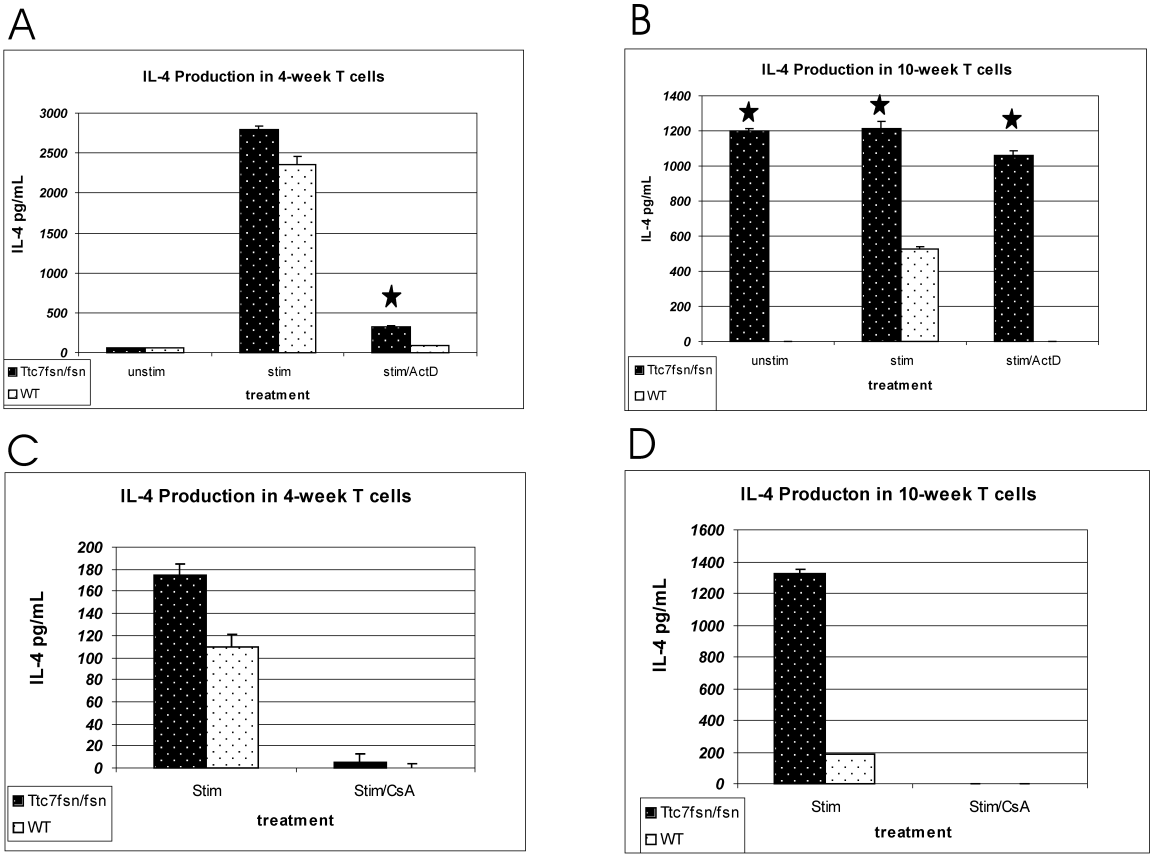

Figure 1.15 IL-4 Production in 4- and 10-week T cells. IL-4 protein production in 4- (A and C) and 10-week (B and D) mice was measured by ELISA using $6.0x10^6$ cells per well of enriched splenic T cells previously cultured for 24 hours in 400uL volume samples in 48-well culture plates. ELISA samples assayed in triplicate with 100uL samples. A and B: IL-4 was produced upon plate-bound anti-CD3 stimulation in both WT and *Ttc7*$^{fsn/fsn}$, although at higher levels in *Ttc7*$^{fsn/fsn}$. *Ttc7*$^{fsn/fsn}$ cells produced IL-4 at 10 weeks even without stimulation. After three hours of stimulation, actinomycin D was added to sample to inhibit transcription. In both 4- and 10-week *Ttc7*$^{fsn/fsn}$ mice, IL-4 protein remained elevated, suggesting altered mRNA stability and regulation. Graphs represent one data set of four separate experiments with similar results. See text for p values.

C and D: IL-4 protein production is shut down by the addition of Cyclosporine A to culture of T cells. Enriched splenic T cells are pre-treated with CsA or the same concentration of DMSO (stim) for 30 minutes and then plated at $6.0x10^6$ cells per well into an anti-CD3 coated culture plate and allowed to stimulate for 24 hours. In both C, 4-week, and D, 10-week T cells, CsA shuts down production of IL-4. This indicates that *Ttc7*$^{fsn/fsn}$ mice respond to TCR stimulation through a calcium-dependent pathway as do WT, suggesting IL-4 production is not being induced through an alternate pathway. Graphs present one data set of two separate experiments with similar results.

Previous flow cytometry data has shown a slight increase in the ratio of $CD4^+$ T cells over that of $CD8^+$ T cells (2.8/2.0) in the spleens of Ttc7$^{fsn/fsn}$ mice (Pelsue, Schweitzer et al. 1998) which may explain some of the increase in IL-4 that we see over that of WT. However, the similar expression of IL-4 in stimulated and unstimulated samples of the 4-week data suggests that this ratio may not affect the magnitude of IL-4 expression as much as other regulatory measures. In addition, there were no detectable differences in cell viability between Ttc7$^{fsn/fsn}$ and WT during and after 24-hour cell culture as measured by Trypan blue exclusion (data not shown).

To measure the effect of CsA on IL-4 protein production, T cells were plated with either CsA (1μg/mL) or DMSO for stimulated control samples. In both 4-week (Figure 1.15C) and 10-week (Figure 1.15D) T cells CsA shut down production of IL-4 at background or non-detectable levels. This suggests that in both Ttc7$^{fsn/fsn}$ and WT at 4- and 10-weeks IL-4 production is stimulated by a CsA sensitive, Ca^{++} dependent pathway.

Ttc7$^{fsn/fsn}$ mice show an increase in activated and memory T cells as compared to WT littermates

Differences in IL-4 production and IL-4 mRNA stability between Ttc7$^{fsn/fsn}$ and WT T cells suggested the possibility of differences in T cell subsets as well. It has previously been demonstrated that naïve T cells produce IL-4 mRNA rapidly upon TCR stimulation which then degrades more quickly than the IL-4 mRNA in effector/memory cells (Carter and Malter 1991). The presence of more total RNA in Ttc7$^{fsn/fsn}$ mice also suggested the presence of more activated T cells. Since the full-blown effects of autoimmunity develop at 5-6 weeks of age in Ttc7$^{fsn/fsn}$ mice, we decided to examine the

distribution of splenic T cells in naïve, activated and memory subsets at 4-weeks-of-age to see if changes in T cell phenotype occur before full-blown disease, and at 10-weeks to examine phenotypic changes in T cells as disease progresses.

Using four-color flow cytometry and previously identified CD4+ cell surface markers to designate subset phenotypes as naïve: $CD44^{lo}$/ $CD62L^{hi}$; activated: $CD44^{hi}$/ $CD62L^{hi}$; memory: $CD44^{hi}$/$CD62L^{lo}$; (Bingaman and Farber 2004); (DeRyckere and DeGregori 2005); Eaton-Bassiri et al, 2000; Lynch and Ceredig, 1989; Swain et al, 1990; Yagi et al., 2001) we examined the distribution of CD4+ T cells. A representative example of the gating done to identify these subsets is shown in Figure 1.16. These data are summarized in Table 1.2.

At 4-weeks-of-age $Ttc7^{fsn/fsn}$ mice have a significantly different distribution of CD4+ T cells in all subsets with 13.4% fewer naïve cells, 15.2% more activated cells, and 16% more memory cells than their wild-type littermates (Figure 1.17). This trend continues with 10-week $Ttc7^{fsn/fsn}$ mice having 6.3% fewer naïve cells, 9.03% more activated cells, and 11.24% more memory cells than their wild-type littermates (Figure 1.18). The actual CD4+ population of gated lymphocytes is different between the two ages with CD4+ T cells comprising 13.7 ± 2.42% of the gated lymphocytes in 4-week WT animals while $Ttc7^{fsn/fsn}$ only make up 5.16 ± 1.5% of gated cells. In 10-week animals WT CD4+ T cells make up 23 ± 3.08% of gated lymphocytes while $Ttc7^{fsn/fsn}$ mice are 14.4 ± 3.9%.

Even though the percentages of CD4+ T cells are reduced in the spleens of $Ttc7^{fsn/fsn}$ mice as compared to WT, Pelsue and colleagues (1998) have previously demonstrated that due to the increased cellularity of the spleens of $Ttc7^{fsn/fsn}$ mice there

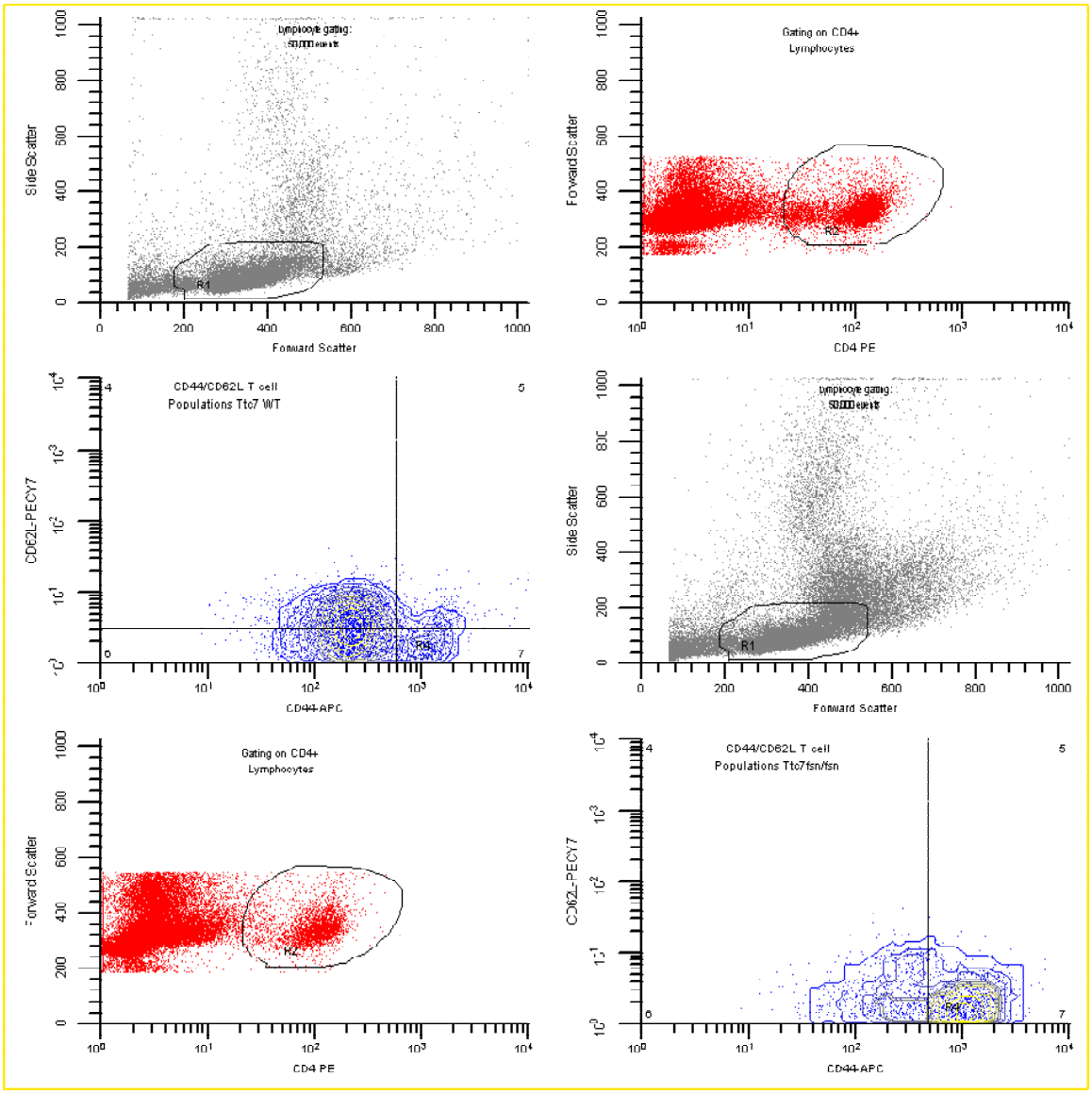

Figure 1.16. Representative CD62L/CD44 dot plots of CD4+ T cell, lymphocyte gating of Ttc7*fsn/fsn* and WT splenocytes. Data from this analysis was used to generate Table 1.2, where naïve cells were $CD62L^{hi}/CD44^{lo}$ (upper left quadrant), activated cells were $CD62L^{hi}/CD44^{hi}$ (upper right quadrant) and memory cells were $CD62L^{lo}/CD44^{hi}$ (lower right quadrant). The results presented are representative of all mice examined where n=5 for each age and genotype. 50,000 lymphocyte events were recorded for each analyses. IL-4+ cells were analyzed similarly with the addition of a gate on each quadrant identifying the IL-4+ cells in that quadrant (Eaton-Bassiri, 2000).

4- and 10-Week Splenic CD4+ T cell Populations				
		Naïve %	**Activated %**	**Memory %**
4-Week		CD62Lhi/CD44lo	CD62Lhi/CD44hi	CD62Llo/CD44hi
	Ttc7WT	35.0 ± 9	9.6 ± 2.39	15.0 ± 2.39
	Ttc7$^{fsn/fsn}$	21.6 ± 9.4*	24.8 ± 6.6*	31.0 ± 9.53*
		p=0.049	p=0.0046	p=0.0175
10-Week				
	Ttc7WT	33.4 ± 3.7	8.07 ± 4.3	16.53 ± 6.2
	Ttc7$^{fsn/fsn}$	27.1 ± 6	17.1 ± 6.6*	27.77 ± 4.7*
			p=0.038	p=0.014
n=5				

Table 1.2 4- and 10-Week Splenic CD4+ T cell Populations
Summary of data from Figure 1.17.

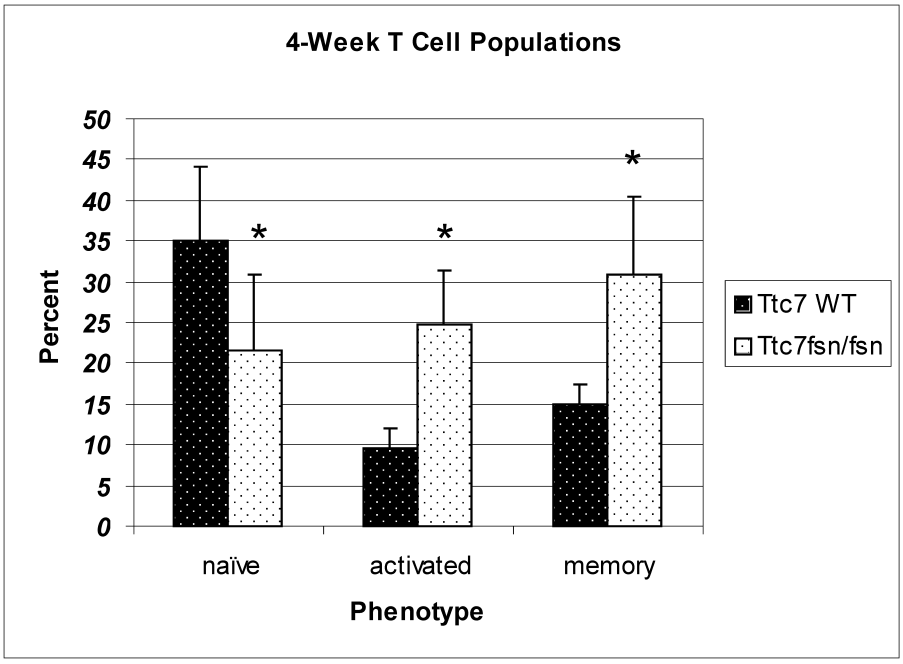

Figure 1.17. 4-Week CD4+ T cell Populations. Distribution of 4-week CD4+ cells by phenotype. Ttc7$^{fsn/fsn}$ mice have a lower percentage of CD4+ naïve cells (p=0.049), and a higher percentage of activated (p=0.0046) and memory (p=0.0175) splenic T cells than WT littermates. Data are presented as the mean percent of five separate experiments ± SEM.

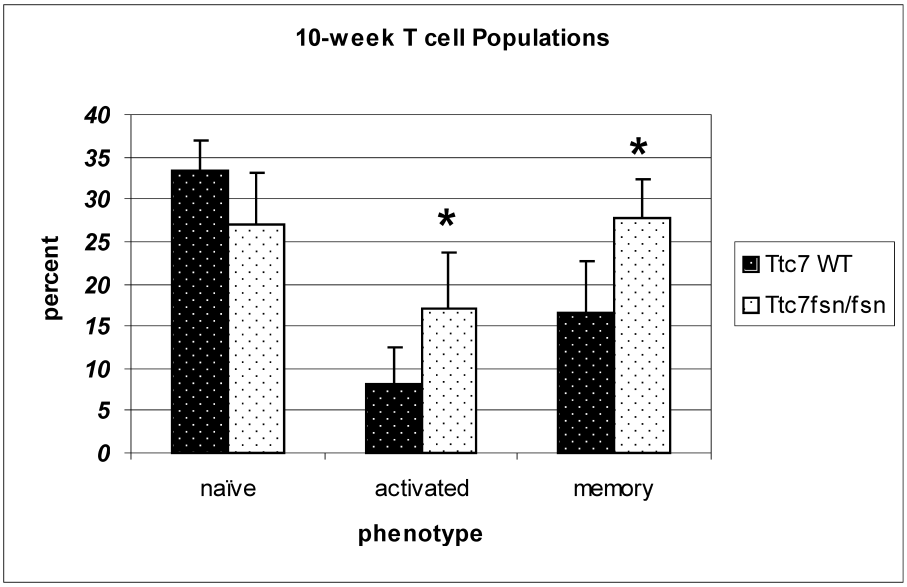

Figure 1.18. 10-Week CD4+ T cell Populations. Distribution of 10-week CD4+ T cells by phenotype. Ttc7$^{fsn/fsn}$ mice have a lower percentage of naïve cells and a higher percentage of activated (p=0.038) and memory (p=0.014) splenic T cells than WT littermates. Data are presented as the mean percent of five separate experiments ± SEM.

was an actual 2.5-fold elevation of total CD3+ T cells. When we calculate the actual numbers of CD4+ cells in spleens of 4-week mice Ttc7$^{fsn/fsn}$ animals have almost twice as many with 6.05 x 10^6 CD4+ cells compared to WT with 3.76 x 10^6 CD4+ cells. 10-week Ttc7$^{fsn/fsn}$ mice have almost 10X more than WT with 1.15 x 10^8 CD4+ cells compared to WT with 1.19 x 10^7 CD4+ cells in their spleens. Thus, the differences in percentages become more magnified when translated into total cell numbers. The functional consequences of elevated total numbers of activated and memory cells can be seen in the elevation of IL-4 production and the difference in IL-4 mRNA.

Ttc7$^{fsn/fsn}$ CD4+ T cells show an increase in the percentage of IL-4 positive cells without exogenous stimulation

Given the differences in CD4+ T cell subsets between Ttc7$^{fsn/fsn}$ and WT mice we next wanted to examine IL-4 expression among the subsets. We used the same activation markers to designate phenotype, i.e. CD62L/CD44, and stained for intracellular IL-4 in unstimulated as well as CD3 stimulated cells in both 4- and 10-week mice. At 4-weeks, in both the unstimulated and stimulated groups Ttc7$^{fsn/fsn}$ mice had higher percentages of IL-4+ cells than their WT littermates (Figure 1.19). In addition, the difference in percentages between the IL-4+ stimulated and unstimulated cells within groups were higher in the Ttc7$^{fsn/fsn}$ mice suggesting that more cells were responding to CD3 stimulation. These data are summarized in Table 1.3. It is important to note that the numbers given are percentages of the subsets designated in the table of splenic T cell populations and not percentages of total T cells. These results suggest that changes in T

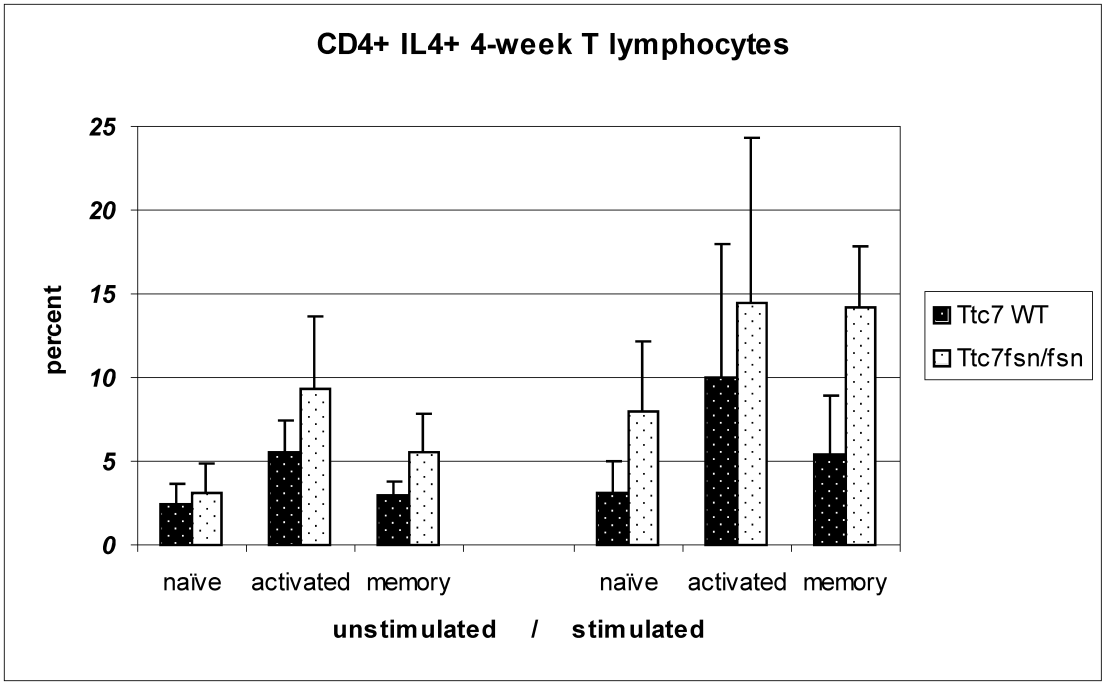

Figure 1.19. 4-Week CD4+ IL-4+ T Lymphocytes. Data presented are the percentage of IL-4+ cells in each indicated subset as shown in Figure 1.17. Stimulated samples were cultured for 24 hours in plates coated with anti-CD3 to trigger IL-4 production in media containing Monensin to prevent protein secretion. In all subsets shown in 4-week cells Ttc7$^{fsn/fsn}$ showed a slightly higher percentage of IL4+ cells in both stimulated and unstimulated samples, but were not statistically significant. These data are summarized in Table 1.3.

4-Week IL-4+ CD4+ T cell Populations				
		Naïve %	**Activated %**	**Memory %**
		CD62Lhi/CD44lo	CD62Lhi/CD44hi	CD62Llo/CD44hi
unstimulated				
	Ttc7WT	2.39 ± 1.3	5.48 ± 1.9	2.95 ± 0.9
	Ttc7$^{fsn/fsn}$	3.05 ± 1.8	9.3 ± 4.4	5.6 ± 2.3
α-CD3 stimulated				
	Ttc7WT	3.14 ± 1.8	10.01 ± 8	5.46 ± 3.4
	Ttc7$^{fsn/fsn}$	7.96 ± 4.2	14.47 ± 9.9	14.2 ± 2.3
n=5				
% Stimulated - % Unstimulated				
	Ttc7WT	0.75	4.53	2.51
	Ttc7$^{fsn/fsn}$	4.91	5.17	8.6

Table 1.3 4-Week IL-4+ T cells. Summary of data presented in Figure 1.19.

10-Week IL-4+ CD4+ T cell Populations							
		Naïve %		**Activated %**		**Memory %**	
		CD62Lhi/CD44lo		CD62Lhi/CD44hi		CD62Llo/CD44hi	
unstimulated			MFI		MFI		MFI
	Ttc7WT	2.22±0.98	6	8.05±6.3	7.4	7.39±5	7.4
	Ttc7$^{fsn/fsn}$	40.79±1.8*	5.5	63.1±45	6.6	51.19±25.2	5.77
		p=0.0042					
Anti-CD3 stimulated							
	Ttc7WT	26.11±5.5	4.1	83.32±0.65	5.37	89.87±5.48	3.78
	Ttc7$^{fsn/fsn}$	34.17±2.7	3.46	63.4±31	4.6	75.5±0.8	3.77
n=5							

Table 1.4 10-Week IL-4+ T cells. Summary of data presented in Figure 1.20.

cell populations occur before the onset of full-blown autoimmune disease with more activated/memory cells in Ttc7$^{fsn/fsn}$ mice poised to produce IL-4.

10-week animals exhibited pronounced differences in percentages of IL4+ CD4+ cells in the unstimulated subsets, especially in the naïve population which reached a statistically significant elevation in Ttc7$^{fsn/fsn}$ mice (Figure 1.20 and table 1.4). With plate-bound anti-CD3 stimulation, WT T cells responded as expected with an increase in IL4+ cells in all subsets, while the percentage of IL4+ Ttc7$^{fsn/fsn}$ CD4+ T cells only increased in the memory population. These results mirror the IL-4 ELISA results presented previously where we showed spontaneous IL-4 production in unstimulated Ttc7$^{fsn/fsn}$ T cells and the presence of IL-4 lingering after shutting down transcription with actinomycin D. An expanded memory population with more cells producing IL-4 would contribute to an increase in more stable IL-4 mRNA seen in Ttc7$^{fsn/fsn}$. This would allow for translation to continue accounting for the increase in IL-4 over WT in Ttc7$^{fsn/fsn}$ after the halt of transcription.

Another important result revealed by this analysis is that this suggests the production of IL-4 *in vivo* may be an antigen-driven process. Foucras et al (Foucras, 2002) demonstrated that the presence of soluble antigens *in vivo* can push naïve cells into activated/memory cells of the Th2 phenotype. This, coupled with a Th2 skewed BALB/c background, may certainly contribute to an increase of IL-4. Thus, we suggest that it is the presence of self-antigens in Ttc7$^{fsn/fsn}$ that induce autoreactive naïve T cells to produce IL-4 and subsequently push them into the expanded populations of activated/memory T cells seen in Ttc7$^{fsn/fsn}$ mice.

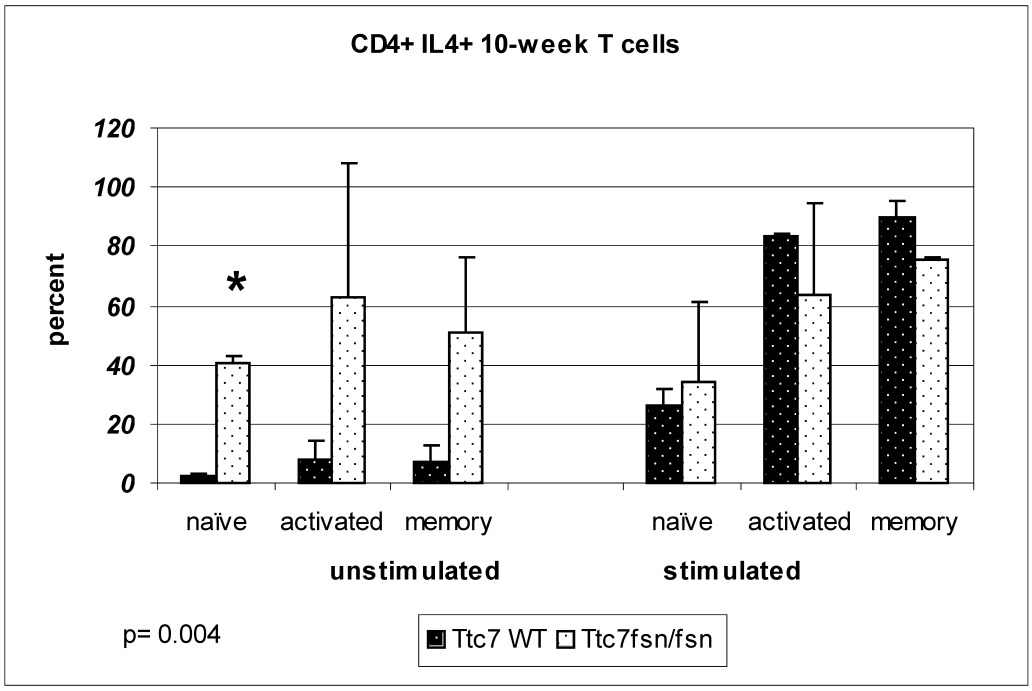

Figure 1.20. 10-Week CD4+ IL-4+ T Lymphocytes. Data presented are the percentage of IL-4+ cells in each indicated subset as shown in Figure 1.18. Stimulated samples were cultured for 24 hours in plates coated with anti-CD3 to trigger IL-4 production in media containing monensin to prevent protein secretion. In the unstimulated 10-week samples, all subsets showed a higher percentage of IL-4+ cells for Ttc7$^{fsn/fsn}$, with the naïve subset having a significantly higher percentage (p=0.004). However, upon 24-hour stimulation with plate-bound anti-CD3 the WT cells had a higher percentage of IL4+ cells in the activated and memory subsets, while Ttc7$^{fsn/fsn}$ was still higher in naïve cells. These data are summarized in Table 1.4.

Results: Section 2: Stat6-/-Ttc7$^{fsn/fsn}$ phenotype and functional study

Stat6-/-Ttc7$^{fsn/fsn}$ mice have severe autoimmunity and inflammation including increased renal disease, splenomegaly, altered subsets of activated B and T cells, and increased production of IL-4

Preliminary data identified the presence of constitutively activated Stat6 in the B cells of Ttc7$^{fsn/fsn}$ mice. This was associated with high serum levels of IL-4 and the upregulation of IL-4/Stat6 responsive genes such as MHC II and CD23. High serum levels of IgE suggested hyper-active B cells, which were responding to IL-4 and help from hyper-active T cells. Many groups have identified similar characteristics in animals with engineered, constitutively active Stat6 (Daniel, Salvekar et al. 2000; Bruns, Schindler et al. 2003; Kaplan, Sehra et al. 2007), and many groups have knocked Stat6 out and reported a dramatic reduction or elimination of these traits (Kaplan, Schindler et al. 1996; Linehan, Warren et al. 1998; Kaplan, Wurster et al. 1999; Mori, Morris et al. 2000; Singh, Saxena et al. 2003). Stat6 deficient animals have also been found to have a dramatic reduction in the amount of IL-4 produced (Kaplan, Schindler et al. 1996; Dorado, Jerez et al. 2002). Thus, we crossed our Ttc7 heterozygotes with Stat6 deficient animals to produce double-mutant animals with the Stat6-/-Ttc7$^{fsn/fsn}$ genotype to analyze the contribution Stat6 made to the phenotype of Ttc7$^{fsn/fsn}$ mice. All genotypes were confirmed with PCR and the lack of functional Stat6 was confirmed with Western blotting. Our expectation was the ameliorization of some of the autoimmune phenotype

displayed by Ttc7$^{fsn/fsn}$ mice, especially that which is associated with hyper-active lymphocytes. We performed a general survey to evaluate the resulting phenotype.

Gross Morphology

Figure 2.1 illustrates the resulting gross morphology of Stat6-/-Ttc7$^{fsn/fsn}$ mice. Shown in the foreground of Figure 2.1A is a 10-week-old male which clearly demonstrates its reduced size, hunched-over stance due to extreme splenomegaly, and the paleness of its ears due to extreme anemia as compared to its Stat6-/-Ttc7WT littermate in the background. Figure 2.1B is the same animal held in a position to display the characteristic distended belly and hair striations indicative of the Ttc7fsn mutation. Figure 2.2A presents an 18-week-old female on the right, again with smaller size and hunched stance, but also clearly showing the characteristic skin pathology around the head, neck and eyes (foreground, Figure 2.2B) from which Flaky Skin was named. Figure 2.3 presents a thirteen-week female with reduced size (Figure 2.3A), a close-up of skin-pathology around the eyes (Figure 2.3B), and the pale ears and distended abdomen (Figure 2.3C) typical to Ttc7$^{fsn/fsn}$ mice. These figures demonstrate some of the typical features seen in Ttc7$^{fsn/fsn}$ mice, and also some of the variation seen between individuals with a genetically identical background. There are no differences typically associated with gender, which appears to be true of Stat6 deficient Ttc7$^{fsn/fsn}$ mice as well. Overall, the appearance of the Stat6-/-Ttc7$^{fsn/fsn}$ and the Stat6WTtc7$^{fsn/fsn}$ animals looks very similar.

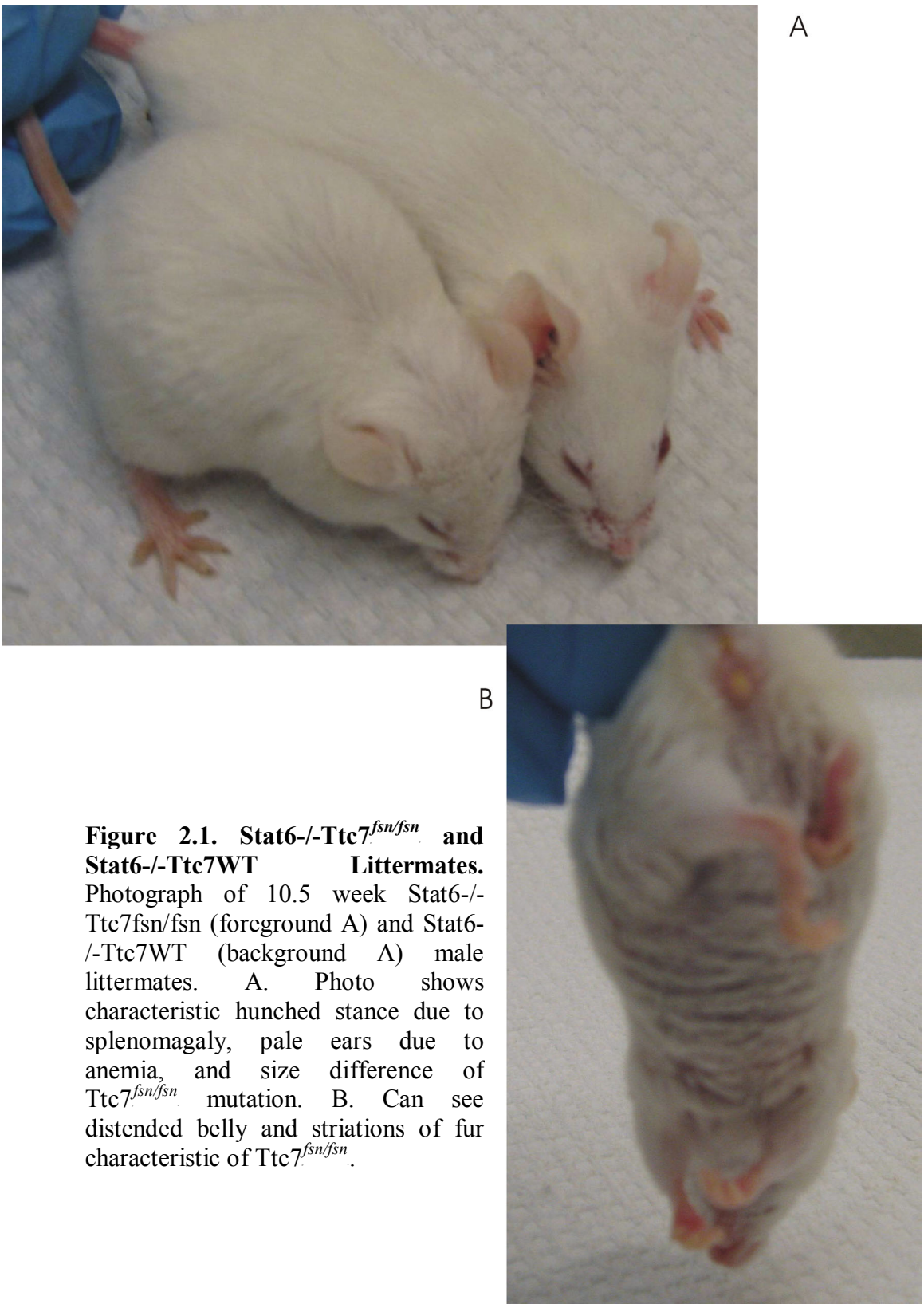

Figure 2.1. Stat6-/-Ttc7$^{fsn/fsn}$ and Stat6-/-Ttc7WT Littermates. Photograph of 10.5 week Stat6-/-Ttc7fsn/fsn (foreground A) and Stat6-/-Ttc7WT (background A) male littermates. A. Photo shows characteristic hunched stance due to splenomagaly, pale ears due to anemia, and size difference of Ttc7$^{fsn/fsn}$ mutation. B. Can see distended belly and striations of fur characteristic of Ttc7$^{fsn/fsn}$.

A

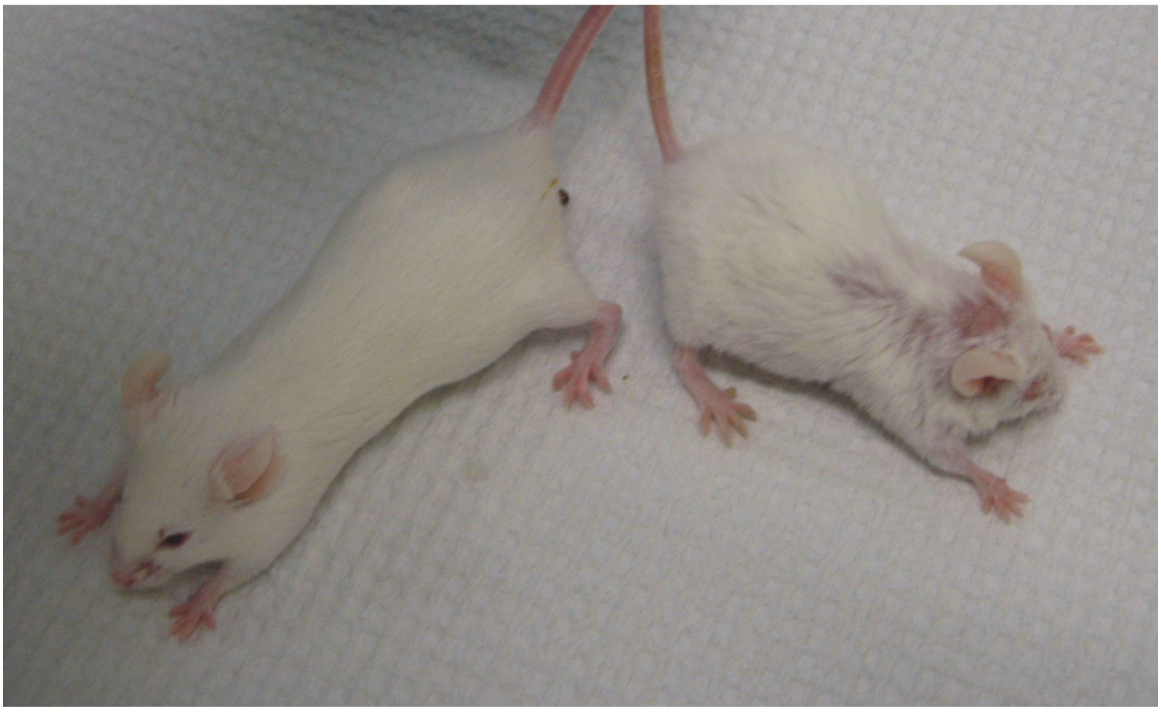

B

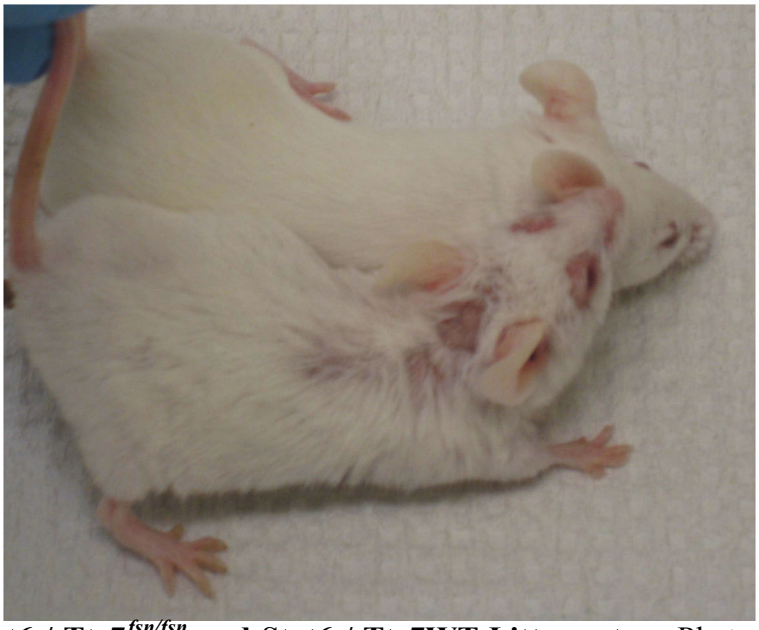

Figure 2.2. Stat6-/-Ttc7$^{fsn/fsn}$ and Stat6-/-Ttc7WT Littermates. Photograph of 18-week Stat6-/-Ttc7$^{fsn/fsn}$ (right A and foreground B) and Stat6-/-Ttc7WT (left A and background B) female littermates. A. Size difference and stance is clearly shown with characteristic Ttc7$^{fsn/fsn}$ skin pathology on head, neck and around eyes. B. Closer view of skin on neck. Fur loss and skin pathology affects males and females equally.

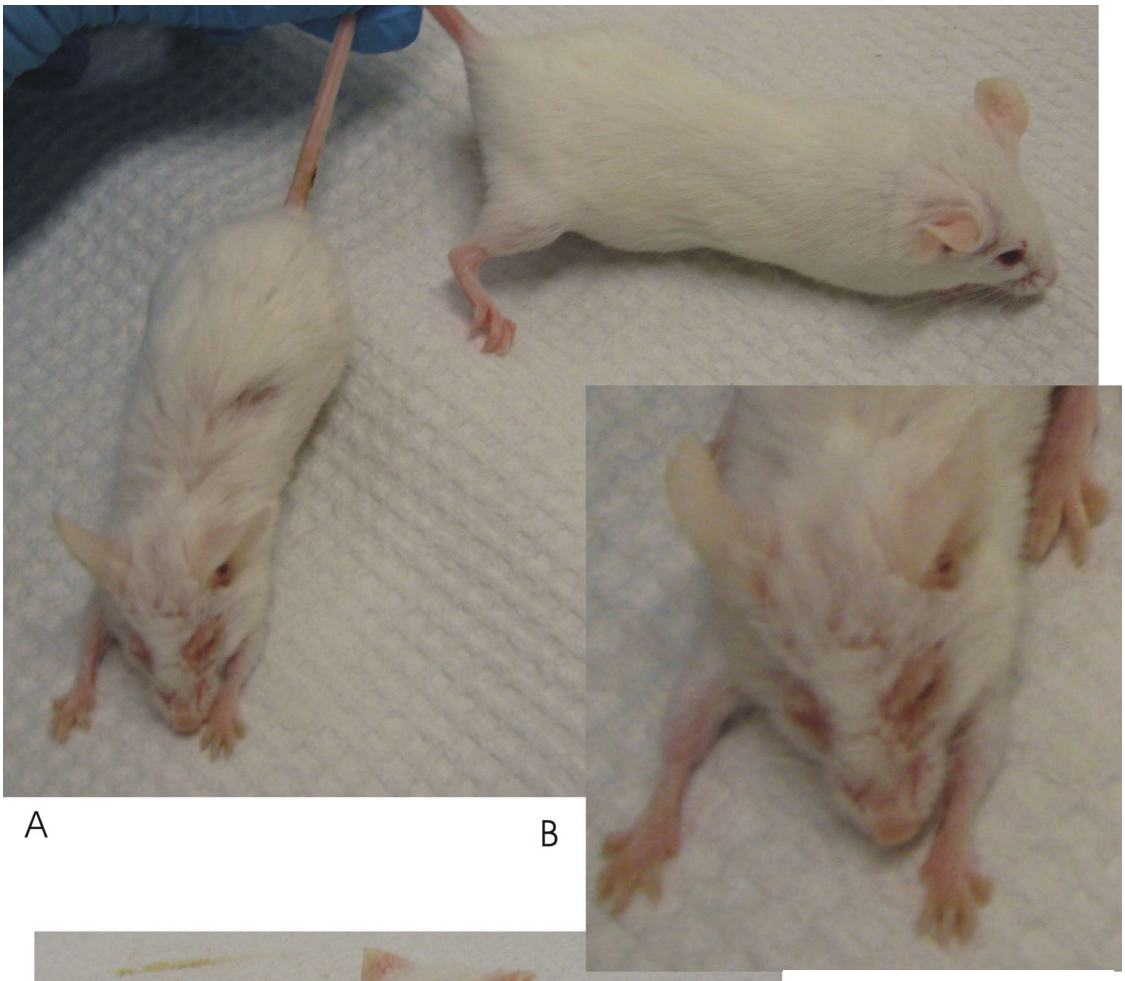

Figure 2.3. Stat6-/-Ttc7$^{fsn/fsn}$ and Stat6-/-Ttc7WT Littermates

Photograph of 13-week Stat6-/-Ttc7$^{fsn/fsn}$ (left A, B, and foreground C) and Stat6-/-Ttc7WT female littermates. A. Characteristic skin pathology of Ttc7$^{fsn/fsn}$ is clearly shown on face, around eyes and in B. close-up. C. Distended belly, fur striations, pale ears, and skin inflammation of Ttc7$^{fsn/fsn}$

Body Weight

Figure 2.4 represents a comparison of body weight of 10-week-old animals, with the females, who are generally smaller, graphed separately from males. Figure 2.4A, left columns, compare Stat6-/-Ttc7$^{fsn/fsn}$ females to Stat6-/-Ttc7WT females, showing the statistically significant reduced body weight of the Ttc7$^{fsn/fsn}$ animals (p=0.03). The right columns compare Stat6-/-Ttc7$^{fsn/fsn}$ males to Stat6-/-Ttc7Wt males showing the reduced body weight of the Ttc7$^{fsn/fsn}$ animals (p=0.0062). Figure 2.4B compares female Stat6-/- animals to Stat6 WT. The left columns compare Ttc7$^{fsn/fsn}$ females, with the Stat6-/- reduced in size from Stat6WT (p=0.0060). The right columns compare Ttc7WT females, with the Stat6-/- also reduced in size from their Stat6WT counterparts (p=0.0019). Thus, Stat6 deficient animals are generally smaller in body weight than their Stat6 intact counterparts, despite their Ttc7 status; however, the double-mutants show a further reduction over WT.

Lifespan

The lifespan of Ttc7$^{fsn/fsn}$ mice is dramatically reduced from their normal WT littermates to about 12-15 weeks of age. They generally start showing severe autoimmune pathology around 5-6 weeks and get progressively sicker until death. We let several Stat6-/-Ttc7$^{fsn/fsn}$ mice age and found no significant difference between these animals and their Stat6 intact counterparts. Figure 2.5 depicts the variation in lifespan of several mice, which closely followed the trend in Stat6 sufficient Ttc7$^{fsn/fsn}$ mice, with the average difference only a few days.

A

B

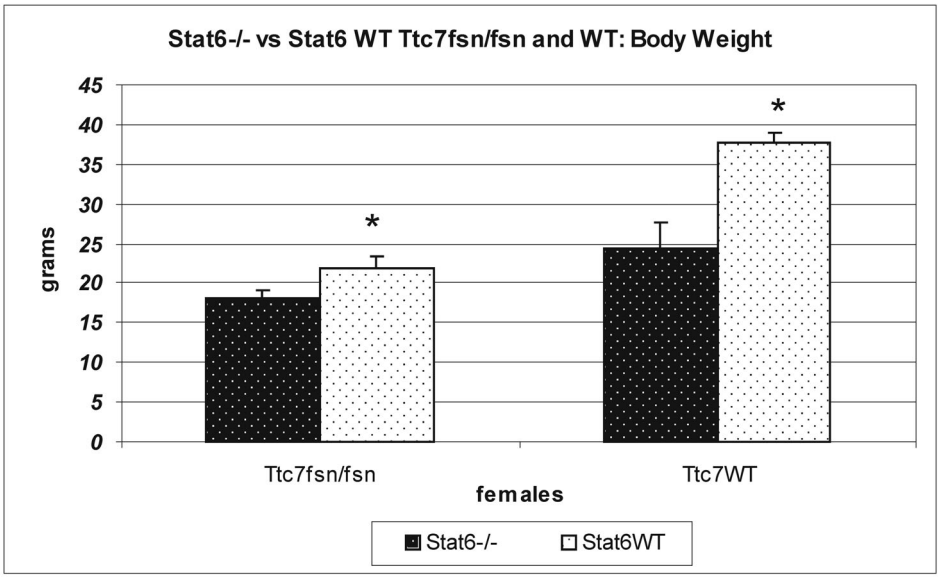

Figure 2.4 Stat6-/-Ttc7 Body Weight. A. Stat6-/-Ttc7$^{fsn/fsn}$ females (left, p=0.03) and males (right, p=0.0062) are significantly smaller than their Stat6-/-Ttc7WT counterparts. B. Female Stat6-/-Ttc7$^{fsn/fsn}$ (p=0.0060)and Stat6-/-Ttc7WT (p=0.0019) are significantly smaller than their Stat6 intact counterparts. N=5 of each animal.

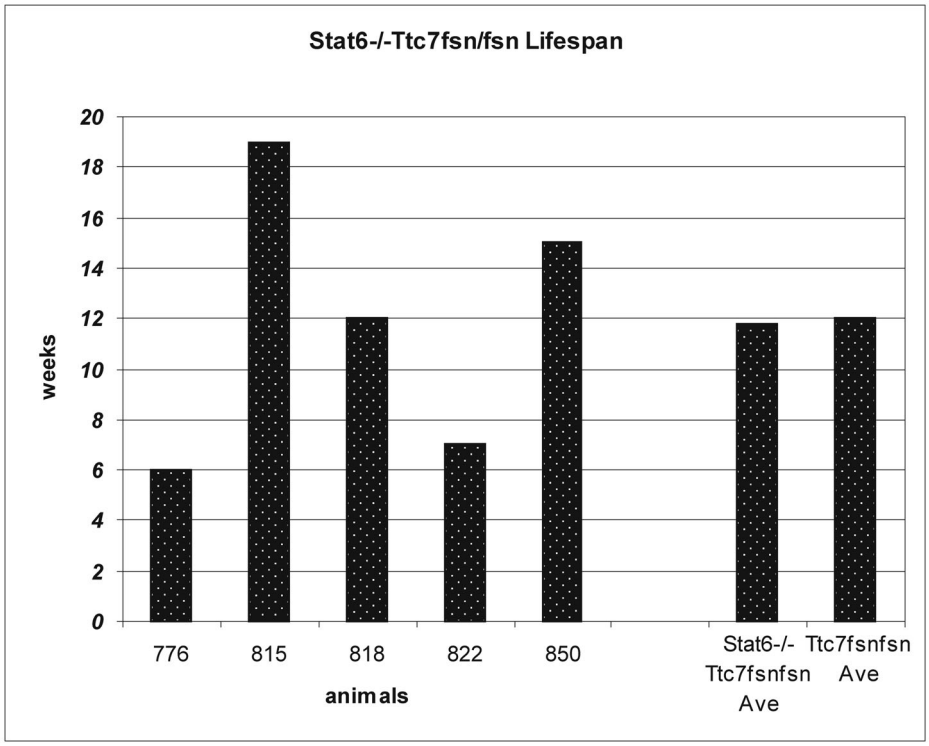

Figure 2.5. Stat6-/-Ttc7 Lifespan. Stat6-/-Ttc7$^{fsn/fsn}$ Lifespan averages 11.5 weeks. The average lifespan of the Stat6 deficient Ttc7$^{fsn/fsn}$ mice (n=8) is similar to the Stat6 intact Ttc7$^{fsn/fsn}$, and varies between animals in a similar manner, an example of which is shown on left side of graph.

Spleen Cellularity

Ttc7$^{fsn/fsn}$ mice have a dramatic increase in spleen cellularity over their WT littermates with altered lymphocyte populations such as a decrease in the percentage of CD3+ cells, a decrease in percentage of CD19+ cells (although increased overall numbers) and an increase in the percentage of immature red blood cells (Pelsue, Schweitzer et al. 1998). We performed flow cytometry on whole Stat6-/- spleens to evaluate any alterations in cell populations due to the absence of Stat6 (data are summarized in Table 2.1)

In Stat6-/-Ttc7$^{fsn/fsn}$ the total spleen cellularity ranges from 0.7 to 3.4 times that of Ttc7$^{fsn/fsn}$ mice; specifically, Stat6-/-Ttc7$^{fsn/fsn}$ cell numbers averaged 25 ± 36.7 x 10^8 cells while Ttc7$^{fsn/fsn}$ averaged 13.0 ± 5.4 x 10^8 cells as determined by cell count with a hemacytometer and the trypan blue exclusion method. (Stat6 deficient and intact Ttc7 WT were both similar, 2.7 ± 0.8 x 10^8 cells). CD3+ cells recovered slightly in Stat6-/-Ttc7$^{fsn/fsn}$ mice to 17.95 ± 3.9 percent (p=0.0003) as did CD4+ cells. The CD8+ data was highly variable due to technical difficulties, but did show an overall recovery. Stat6-/-Ttc7$^{fsn/fsn}$ spleens exhibited a slight reduction in CD19+ cells, although as mentioned above, due to the high cellularity would still have a large CD19+ population. As expected, the Stat6-/-Ttc7$^{fsn/fsn}$ animals expressed very low levels of CD23 (p=0.0007), but surprisingly, MHC II was expressed by over 20% of the cells, however, still below that of Stat6 intact animals (p=0.0005). Interestingly, Stat6-/-Ttc7$^{fsn/fsn}$ animals had a slight decrease (to 15%) in the high level of immature red blood cells (Ter-119)

	CD3			CD4			CD8			CD19			CD23	
	Ttc7fsn		WT	Ttc7fsn		WT	Ttc7fsn		WT	Ttc7fsn		WT	Ttc7fsn	WT
	8wk Pub	8.5±1.2	41.5±3.5	8.7±1.3		32.7±1.6	3.1±1.2		16±6.8	29.0±3.5		37±5.6		
n=5	Stat6-/-	17.85±3.9*1	40.8±1.9	9.9±1.06		29.35±1.2	23.02±5.2		31.83±20.1	26.29±13.7		42.7±3.0	1.27±0.37*2	2.52±1.76
n=3	Ttc7fsn/fsn 10wk												36.27±1.89	6.94±1.13
	MHCII			Ter119			F4/80			GR-1			PanNK	
	Ttc7fsn		WT	Ttc7fsn		WT	Ttc7fsn		WT	Ttc7fsn		WT	Ttc7fsn	WT
	8wk Pub	56.7±4.16	32.3±1.53	17.6±1.1		6.6±0.3	9.5±4.6		1.9±1.2	5.3±2.3		3.4±1.6	3.54	28
	Stat6-/-	20.82±9.9*3	45.1±2	14.87±3.5		11.11±2.7	12.92±17.5		5.78±1.5	14.2±2.8		7.11±1.9	7.45±9.4	12.41±6.8
Ttc7fsn/fsn 10wk		60.1±7.78	63.11±4.9											
	CD11b			CD11c										
	Ttc7fsn		WT	Ttc7fsn		WT								
	Stat6-/-	53.4±16.7	18.17±3.13	56.5±25.7		42.33±29.7								
Ttc7fsn/fsn 10wk		58	36											

*1p=0.0003
*2p=0.0007
*3p=0.0005

Table 2.1. Stat6-/-Ttc7 Spleen Cell Populations. All numbers represent percentages of total spleen.

expressed by their Stat6 intact counterparts (18%). Stat6Ttc7$^{fsn/fsn}$ animals also had a slight increase in F4/80 macrophages and GR-1 granulocytes.

In contrast to our findings, others have reported a decrease of 25% in splenic cellularity in a lupus-prone Stat6-deficient model (Xu, Duan et al. 2006) as well as no change in cellularity in a different lupus-prone Stat6-deficient model (Singh, Saxena et al. 2003). The latter also reported no change in the number of T cells, B cells or CD4 and CD8 distribution. In addition, most reports of Stat6 deficiency declare a dramatic decrease in the percentage and number of CD4+ Th2 cells (Jankovic, Kullberg et al. 2000; Bruns, Schindler et al. 2003; Singh, Saxena et al. 2003). Other reports have indicated an increase in cellularity only when Stat6 is constitutively expressed, with a concomitant increase in CD4+ Th2 T cells (Bruns, Schindler et al. 2003; Kaplan, Sehra et al. 2007). The reason(s) for the opposite effects of Stat6 deficiency in Ttc7$^{fsn/fsn}$ mice is most likely due to the presence of the defective Ttc7 gene, as our Ttc7 WT mice appear to be consistent with published data. However, since the function of this gene is presently unknown, further research will be needed.

Stat6 deficiency increases the percentage of immature, IgD^{lo}/IgM^{hi} B cells in Ttc7$^{fsn/fsn}$ spleen

Previous work in our lab (Farrington 2006) established an alteration in B cell subsets in Ttc7$^{fsn/fsn}$ spleen with an increase in the percentage of immature B cells (IgD^{lo}/IgM^{hi}), a significant decrease in mature B cells (IgD^{hi}/IgM^{lo}, $p=\leq 0.01$), and a decrease in transitional B cells (IgD^{hi}/IgM^{hi}) as compared to Ttc7 WT littermates

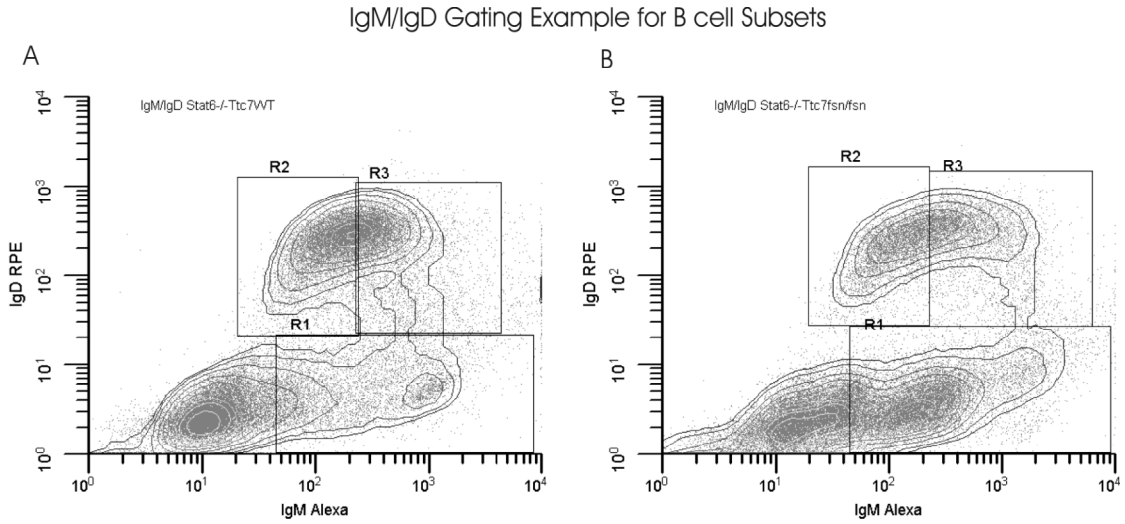

Figure 2.6. IgM/IgD Flow Cytometry Gating Example for B cell Subsets. Flow cytometric gating determination of the ratio of IgM/IgD in splenocytes. Box labeled R1 represents the immature population of B cells with an IgD^{lo}/IgM^{hi} phenotype. The box labeled R2 represents the mature population of B cells with an IgD^{hi}/IgM^{lo} phenotype. The box labeled R3 represents the transitional population of B cells with an IgD^{hi}/IgM^{hi} phenotype. Results from this type of gating are shown in Figure 2.7 for Stat6-/- and Figure 3.2 for anti-IL-4 treated $Ttc7^{fsn/fsn}$ mice.

Figure 2.7 Ratio of IgM/IgD: B cell Subsets. Stat6-/-Ttc6$^{fsn/fsn}$ mice have a significantly increased population of immature B cells than Stat6 intact Ttc7$^{fsn/fsn}$ mice. A. Stat6 intact Ttc7$^{fsn/fsn}$ mice have an increased percentage of immature B cells, a significantly decreased percentage of mature B cells ($p=\leq 0.01$) and a slightly decreased percentage of transitional B cells than their WT littermates. B. Stat6-/-Ttc7$^{fsn/fsn}$ mice have a significantly higher percentage of immature B cells ($p=0.0014$), a significantly decreased percentage of mature B cells ($p=0.049$) and a significantly decreased percentage of transitional B cells ($p=0.0066$) than their Stat6-/-Ttc7WT littermates. C. Stat6-/-Ttc7$^{fsn/fsn}$ mice have a significantly increased percentage of immature B cells (45.19 ± 7.5%, $p=0.0009$) than Stat6 intact Ttc7$^{fsn/fsn}$ mice (20.9 ± 3%) but the mature and transitional populations are unchanged. Data shown are mean percentages of 5 separate experiments ± SEM.

A

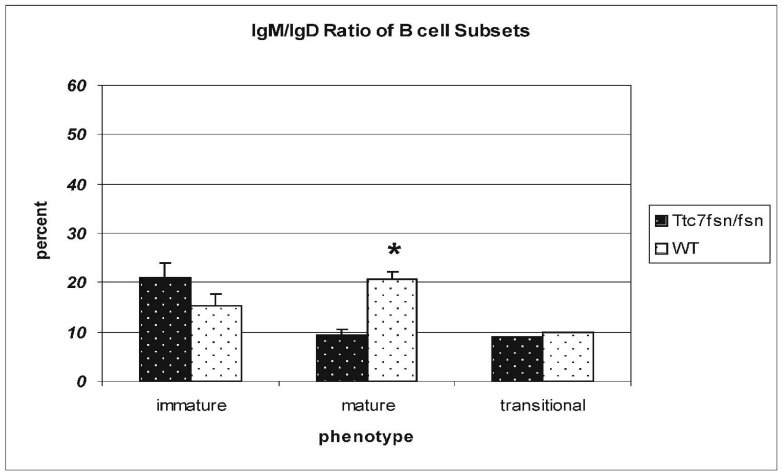
IgM/IgD Ratio of B cell Subsets
percent
60
50
40
30
20
10
0
*
immature
mature
transitional
phenotype
Ttc7fsn/fsn
WT

B

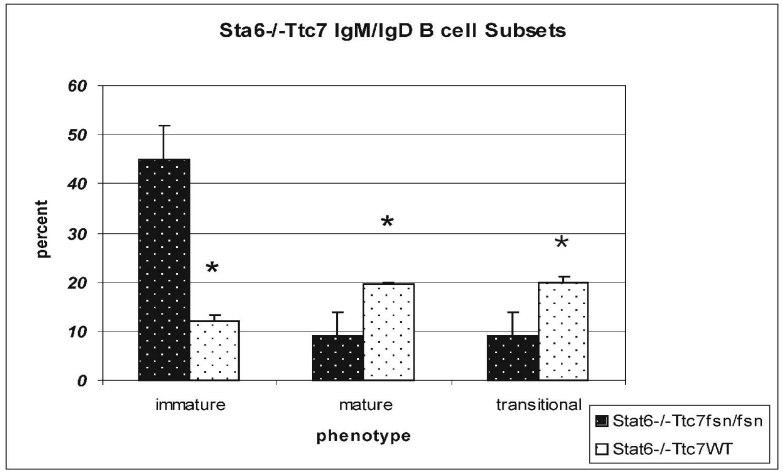
Sta6-/-Ttc7 IgM/IgD B cell Subsets
percent
60
50
40
30
20
10
0
*
*
*
immature
mature
transitional
phenotype
Stat6-/-Ttc7fsn/fsn
Stat6-/-Ttc7WT

C

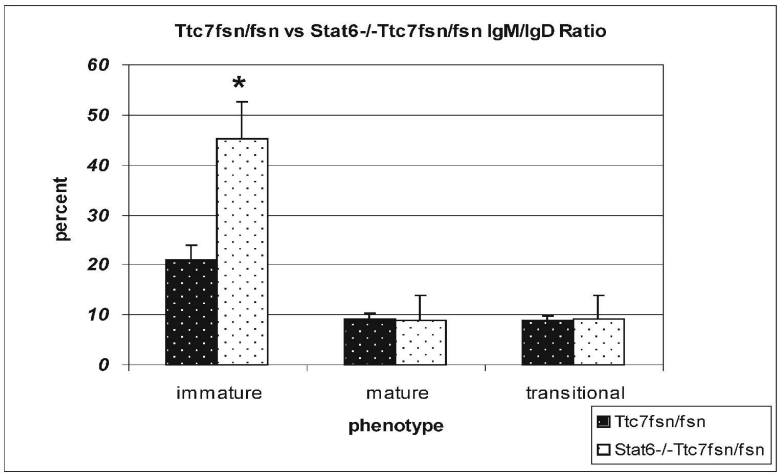
Ttc7fsn/fsn vs Stat6-/-Ttc7fsn/fsn IgM/IgD Ratio
percent
60
50
40
30
20
10
0
*
immature
mature
transitional
phenotype
Ttc7fsn/fsn
Stat6-/-Ttc7fsn/fsn

(Figure 2.7A). Because of the functional differences in these subsets, and the observed increase in spleen cellularity of our Stat6-/-Ttc7$^{fsn/fsn}$ mice, it was important to examine the distribution of B cells in the spleens our Stat6 deficient Ttc7$^{fsn/fsn}$ animals. We performed flow cytometry on single cell suspensions of whole spleen and then gated on the lymphocyte portion of the forward and side scatter plots. Determination of IgM and IgD expression was gated as shown in Figure 2.6.

There was very little difference in the percentage of B cells comprising the mature B cell subset, with Stat6-/-Ttc7$^{fsn/fsn}$ at 8.9 ± 5.1% and Ttc7$^{fsn/fsn}$ at 9.2 ± 1.2%. The transitional subset was also very similar with Stat-/-Ttc7$^{fsn/fsn}$ at 9.06 ± 4.9% and Ttc7$^{fsn/fsn}$ at 9.0 ± 4.6%. However, the immature subset was dramatically different. While Ttc7$^{fsn/fsn}$ mice measured 20.9 ± 3%, Stat6 deficient animals measured 45.19 ± 7.5% immature B cells (p=0.0009). The functional consequences of this difference have yet to be determined, but because this subset includes B-1 and marginal zone B cells we can imagine this population to be an active participant in B cell associated pathogenesis as it has been implicated in the production of autoantibodies and autoimmunity (Sato, Ono et al. 1996; Ying, Proost et al. 2000; Wurster, Rodgers et al. 2002; Amano, Amano et al. 2003; Hardy 2006).

Results of Stat6-/- T cell Populations and IL-4 Production

Stat6-/-Ttc7$^{fsn/fsn}$ mice have a statistically significant higher percentage of activated CD4+ T cells than Ttc7$^{fsn/fsn}$ mice

The effect of Stat6 activation on lymphocytes has been well-studied by several groups. When constitutively activated, Stat6 was found to induce an activated phenotype in T cells compared to normal which was found to enhance autoimmune disease in mice (Daniel, Salvekar et al. 2000; Bruns, Schindler et al. 2003). Many groups have also found that knocking out Stat6 results in reduced lymphocyte activation and the dramatic reduction or complete absence of disease pathology (Daniel, Salvekar et al. 2000; Bruns, Schindler et al. 2003; Singh, Saxena et al. 2003; Kaplan, Sehra et al. 2007). Since we found that significantly more Ttc7$^{fsn/fsn}$ T cells exhibited an activated phenotype than WT T cells, we wanted to examine the effect of the absence of Stat6 in Ttc7$^{fsn/fsn}$ using our Stat6-/-Ttc7$^{fsn/fsn}$ cross. Thus, we performed 4-color flow cytometric analysis on 10-week-old animals using the same cell-surface markers as previously described above. These data are summarized in Table 2.2.

Stat6-/- CD4+ T cell Populations			
	Naïve %	**Activated %**	**Memory %**
	CD62Lhi/CD44lo	CD62Lhi/CD44hi	CD62Llo/CD44hi
Stat6-/-Ttc7WT	43.95 ± 1.66	13.97± 0.33	13.03 ± 1.01
Stat6-/-Ttc7$^{fsn/fsn}$	23.37 ± 2.8*	38.76 ± 1.7*	22.25 ± 3.89*
n=3	p=0.0011	p=0.0010	p=0.0467
Ttc7$^{fsn/fsn}$	27.1 ± 6	17.1 ± 6.6	27.77 ± 4.7
Stat6-/-Ttc7$^{fsn/fsn}$	23.37± 2.8	38.76 ± 1.7*	22.25 ± 3.89
		p=0.001	

Table 2.2. Stat6-/-Ttc7 CD4+ Splenic T cell Populations. Summary of data presented in Figure 2.8.

The changes in the populations of naïve and memory T cells were very small; with a slight but not significant reduction in percentages of both naïve and memory Stat6-/-Ttc7$^{fsn/fsn}$ T cells from Ttc7$^{fsn/fsn}$ T cells. To our surprise, however, the absence of Stat6 more than doubled the percentage of T cells with an activated phenotype in Stat6-/-Ttc7$^{fsn/fsn}$ mice (Figure 2.8C). Ttc7$^{fsn/fsn}$ activated T cells represented 17.1% of the CD4+ lymphocyte population while the Stat6-/-Ttc7$^{fsn/fsn}$ T cells were 38.76% of the CD4+ lymphocyte population. This was statistically significant with a p-value of 0.001. The actual number difference may be even greater between the Stat6-/- and Stat6WT animals as the Stat6-/- CD4+ population recovers slightly from the reduced population in Ttc7$^{fsn/fsn}$ from 8.7% of the spleen population to 9.9% of the spleen population in Stat6-/-Ttc7$^{fsn/fsn}$ (see Table 2.1: Stat6-/- spleen cell populations). Since activated T cells have

Figure 2.8. Stat6-/-Ttc7 Splenic CD4+ T cell Populations. Stat6-/-Ttc7$^{fsn/fsn}$ mice have an increased percentage of activated CD4+ T cells. Populations were determined by gating as shown in Figure 1.16. To collect flow data, the lymphocyte population was gated and 50,000 events were recorded per sample. CD4+ cells were gated and then analyzed for CD62L/CD44 surface markers. A. Stat6-/-Ttc7$^{fsn/fsn}$ mice have a significantly lower percentage of naïve T cells, a significantly higher percentage of activated T cells and a significantly higher percentage of memory T cells than their Stat6-/-Ttc7Wt littermates. B. Stat6 intact T cell populations as shown previously in Figure 1.18. C. Stat6-/-Ttc7$^{fsn/fsn}$ mice have a slightly lower percentage of naïve T cells, a significantly higher percentage of activated T cells and a slightly lower percentage of memory T cells than Stat6 intact Ttc7$^{fsn/fsn}$ mice. These data are summarized with p values in Table 2.2. Data shown are mean percentages of 5 separate experiments ± SEM.

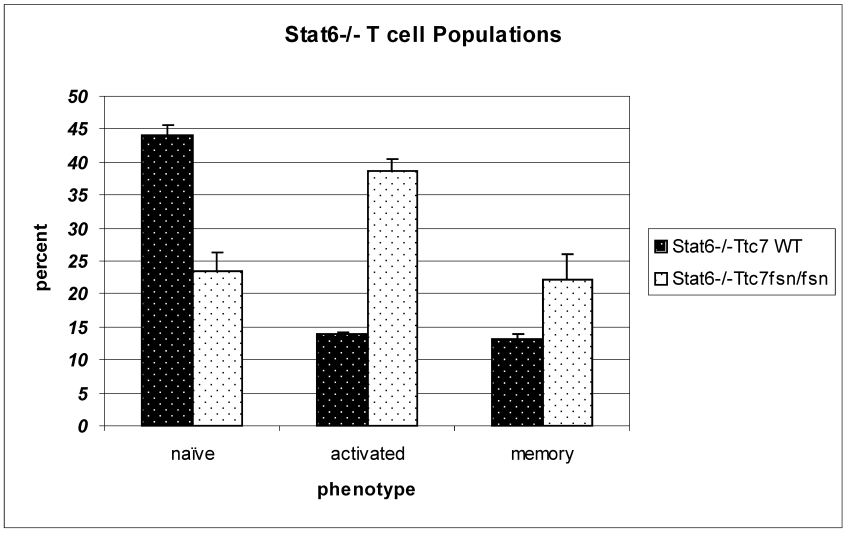
Stat6-/- T cell Populations
50
45
40
35
30
25
20
15
10
5
0
percent
naïve
activated
memory
phenotype
Stat6-/-Ttc7 WT
Stat6-/-Ttc7fsn/fsn

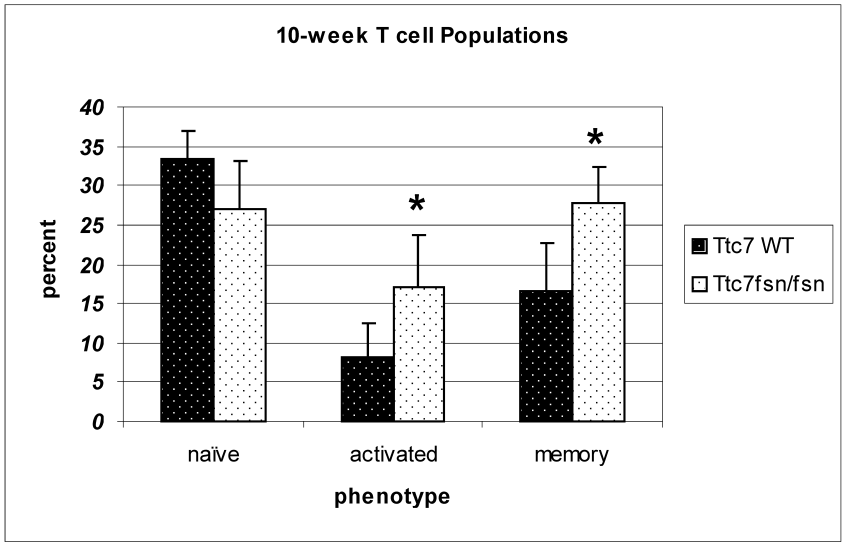
10-week T cell Populations
40
35
30
25
20
15
10
5
0
percent
*
*
naïve
activated
memory
phenotype
Ttc7 WT
Ttc7fsn/fsn

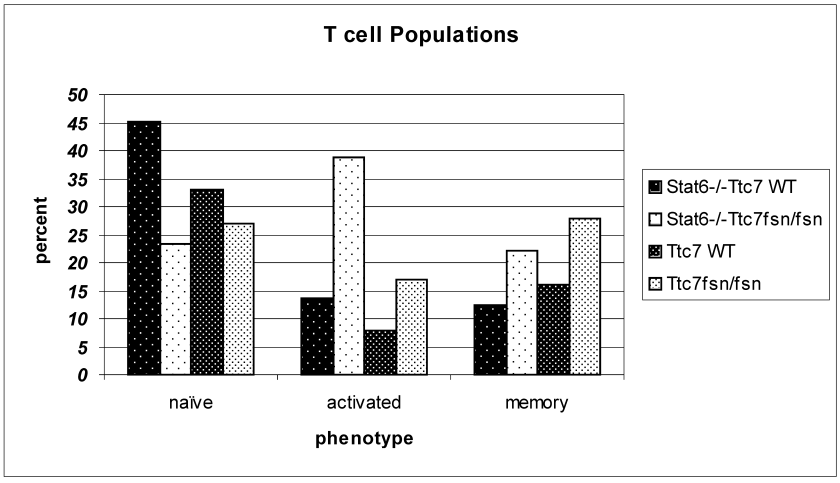
T cell Populations
50
45
40
35
30
25
20
15
10
5
0
percent
naïve
activated
memory
phenotype
Stat6-/-Ttc7 WT
Stat6-/-Ttc7fsn/fsn
Ttc7 WT
Ttc7fsn/fsn

been found to participate in the pathogenesis of autoimmunity directly through cytokine secretion and effector mechanisms as well as indirectly by providing help to autoreactive B cells, this expanded activated T cell population may well be contributing to the severity of disease we find in the Stat6-/-Ttc7$^{fsn/fsn}$ animals.

Stat6-/-Ttc7$^{fsn/fsn}$ CD4+ T cells have a lower percentage of intracellular IL-4+ cells than Ttc7$^{fsn/fsn}$ T cells but when stimulated with plate-bound anti-CD3 exhibit an expanded IL-4+ population

Stat6 has been found to be an important regulator of IL-4 production but the magnitude of IL-4 produced has varied greatly in Stat6-/- animals based on genetic background, experimental design, previous activation, type of activation, stage of cellular differentiation and antigenic specificity (Kaplan, Wurster et al. 1999; Mori, Morris et al. 2000; Dorado, Jerez et al. 2002; Yagi, Suzuki et al. 2002). In general, Stat6 has been found to augment IL-4 production early in activation although it is not absolutely required (Kaplan, Wurster et al. 1999; Mori, Morris et al. 2000), IL-4 production is reduced in Stat6 deficient animals (Bruns, Schindler et al. 2003), and late in activation via CD3 stimulation, Stat6 functions to reduce the IL-4 transcript by competing with the transcription factor NFAT to shut down IL-4 production (Dorado, Jerez et al. 2002). Using 4-color flow cytometry to measure the percentage of IL-4 positive cells we found higher percentages of IL-4+ cells in naïve, activated and memory CD4+ cells of Ttc7$^{fsn/fsn}$ than WT mice in both unstimulated and CD3 stimulated cells. Thus, we wanted to examine how Stat6 deficiency would change the production of IL-4 in CD4+ T cells of

Ttc7$^{fsn/fsn}$ mice that produce high endogenous levels of IL-4. It was not possible to generate sufficient numbers of stimulated CD4+ cells to measure each subtype accurately for a direct comparison as we had great difficulty keeping the Stat6-/-Ttc7$^{fsn/fsn}$ cells alive in culture for the 24 hours necessary for stimulation. However, we were able to analyze the total CD4+ population of both for the presence of intracellular IL-4. These data are summarized in Table 2.3.

In Stat6-/-Ttc7WT animals, the percentage of IL4+ CD4+ cells was reduced in both the unstimulated and stimulated groups as compared to Ttc7WT animals (Figure 2.9A, Table 2.3A). Stat6 deficient cells responded with an increase in the percentage of IL-4+ cells upon stimulation, but at a lower level than Stat6 sufficient cells, which may be expected based on literature reports. However, when we compared Stat6-/-Ttc7$^{fsn/fsn}$ cells to Stat6 sufficient Ttc7$^{fsn/fsn}$ cells we found the same trend in the unstimulated cells, with a lower percentage of IL-4+ cells in the Stat6-/-Ttc7$^{fsn/fsn}$ samples, but when stimulated with anti-CD3 we found an expanded population of IL-4+CD4+ cells in the Stat6 deficient Ttc7$^{fsn/fsn}$ cells (Figure 2.9B and Table 2.3B). Although the actual measured percentages are similar, because the CD4+ population recovers in the Stat6-/-Ttc7$^{fsn/fsn}$ animals, there are over twice as many IL-4+CD4+ cells. We can surmise that this is due to the expanded population of activated T cells found in these animals. As Dorado and colleagues demonstrated in 2002, this expansion may be due to the reduced ability of cells to down-regulate IL-4 production in the absence of Stat6 late in activation. This would be consistent with the pre-activated (hyperactivated) phenotype we find in Ttc7$^{fsn/fsn}$ CD4+ T cells, where, in Stat6 sufficient cells Stat6 may be functioning somewhat normally to reduce IL-4 but overwhelmed by high levels of endogenous

stimulation, and when Stat6 is removed, T cells then are free to produce IL-4 unfettered. This might suggest a cooperative mechanism between Ttc7 and Stat6 in T cell activation and the production of IL-4.

A

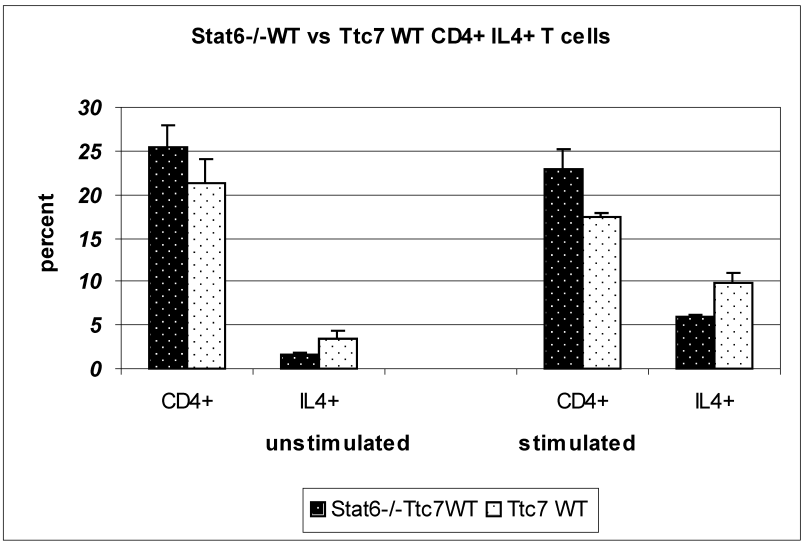

B

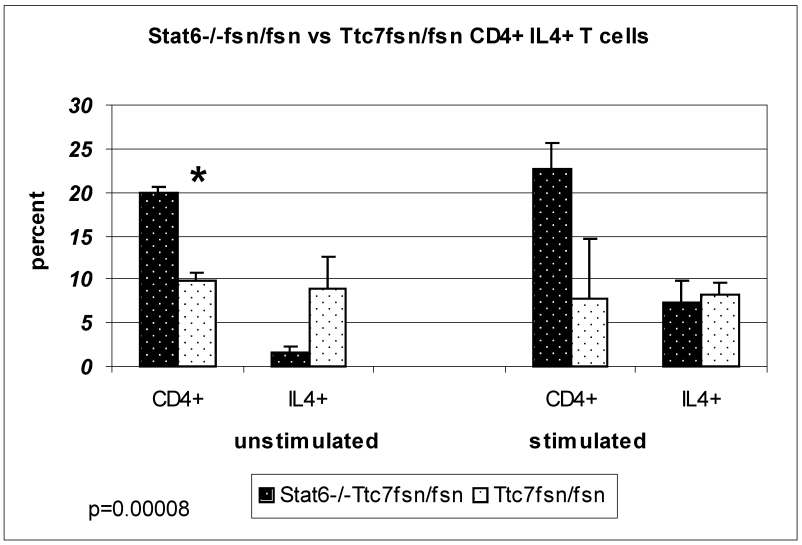

Figure 2.9. Stat6-/-Ttc7 CD4+ IL-4+ T cells Comparison of percentages of IL4+ CD4+ T cells between Stat6-/- and WT animals. Splenic lymphocytes were stained for intracellular IL-4 after culture with or without anti-CD3 stimulation. A. Stat6-/-Ttc7WT versus Stat6 intact Ttc7 WT mice. Stat6-/- have a slightly higher percentage of CD4+ cells but a lower percentage of IL-4+ cells in both the unstimulated and stimulated groups. B. Stat6-/-Ttc7$^{fsn/fsn}$ versus Stat6 intact Ttc7$^{fsn/fsn}$ mice. Stat6-/-Ttc7$^{fsn/fsn}$ mice have a significantly higher percentage of CD4+ cells than Ttc7$^{fsn/fsn}$ Stat6 intact mice but a lower percentage of IL-4+ cells. When stimulated the percentage of Stat6-/- IL-4+ cells rises to almost the same percentage as Ttc7$^{fsn/fsn}$ Stat6 intact mice, suggesting that more cells are producing IL-4 in response to stimulation. These data are summarized in table 2.3 A and B. Data shown are percentages of 5 separate experiments ± SEM.

A

10-Week Stat6-/-Ttc7WT vs. Ttc7WT IL-4+ CD4+ T cells				
		% CD4+	**% IL-4+**	**MFI**
unstim	Stat6-/-Ttc7WT	25.51± 2.5	1.66 ± 0.13	3.34
	Ttc7WT	21.36 ± 2.6	3.48 ± 0.8	3.06
stim	Stat6-/-Ttc7WT	23.0 ± 2.25	5.85 ± 0.35	3.78
	Ttc7WT	17.48 ± 0.31	9.87 ± 1.1	4.93
n=3				

B

10-Week Stat6-/-Ttc7$^{fsn/fsn}$ vs. Ttc7$^{fsn/fsn}$ IL-4+ CD4+ T cells				
		% CD4+	**% IL-4+**	**MFI**
unstim	Stat6-/-Ttc7$^{fsn/fsn}$	19.95 ± 0.6*	1.57 ± 0.7	3.35
	Ttc7$^{fsn/fsn}$	9.82 ± 0.87	8.9 ± 3.6	3.55
		p=0.00008		
Stim	Stat6-/-Ttc7$^{fsn/fsn}$	22.71 ± 2.9	7.44 ± 2.4	3.8
	Ttc7$^{fsn/fsn}$	7.69 ± 6.9	8.35 ± 1.24	5.53
n=3				

Table 2.3. Stat6-/-Ttc7 CD4+ IL-4+ Splenic T cells. A.Summary of Stat6-/- vs. Stat6+/+ Ttc7 WT IL-4+ T cells. B. Summary of Stat6-/- vs. Stat6+/+ Ttc7$^{fsn/fsn}$ IL-4+ T cells. MFI = mean fluorescent intensity

Stat6-/-Ttc7$^{fsn/fsn}$ CD4+ cells do not have an exaggerated IFN-gamma response to CD3 stimulation

Ttc7$^{fsn/fsn}$ T cells have been previously shown to produce similar levels of IFN-gamma, the counter-regulatory cytokine to IL-4, as WT T cells upon anti-CD3 stimulation (Welner, Hastings et al. 2004). Because Stat6 functions to down-regulate IFN-gamma production, we wanted to examine how Stat6-/-Ttc7$^{fsn/fsn}$ T cells responded to stimulation with anti-CD3. We used intracellular staining of IFN-gamma and CD4 to evaluate the percentage of IFN-gamma+CD4+ cells in Stat6-/-Ttc7$^{fsn/fsn}$ and Ttc7$^{fsn/fsn}$ cells in both unstimulated as well as stimulated samples. In the unstimulated cells, the percentage of IFN-gamma+ cells was very similar, with Stat6-/- cells comprising 1.37 ± 0.51% of the CD4+ population while Stat6 sufficient cells were 2.1 ± 1.46% of the CD4+ population (Figure 2.10). When taking the difference in CD4+ percentages between the two groups into consideration, the numbers normalized to 0.36% of the Stat6-/- CD4+ being IFN-gamma+ while Stat6WT were 0.29% IFN-gamma+. Both sets of cells responded to stimulation with anti-CD3 in a similar manner with the Stat6-/- group rising to 2.74 ± 0.57% IFN-gamma + and the Stat6 sufficient group rising to 3.07 ± 1.44% IFN-gamma+. Although the Stat6-/-Ttc7$^{fsn/fsn}$ CD4+ cells had a slightly higher percentage of IFN-gamma+ cells, we did not see the exaggerated response as was shown for IL-4. In addition, the MFIs for both Stat6-/- and Stat6WT, unstimulated and stimulated CD4+ cells were quite similar, suggesting none of the groups were producing higher levels of IFN-gamma than others. Thus, we conclude that the effect we see for IL-4 is specific for IL-4 and not a defect in IFN-gamma regulation.

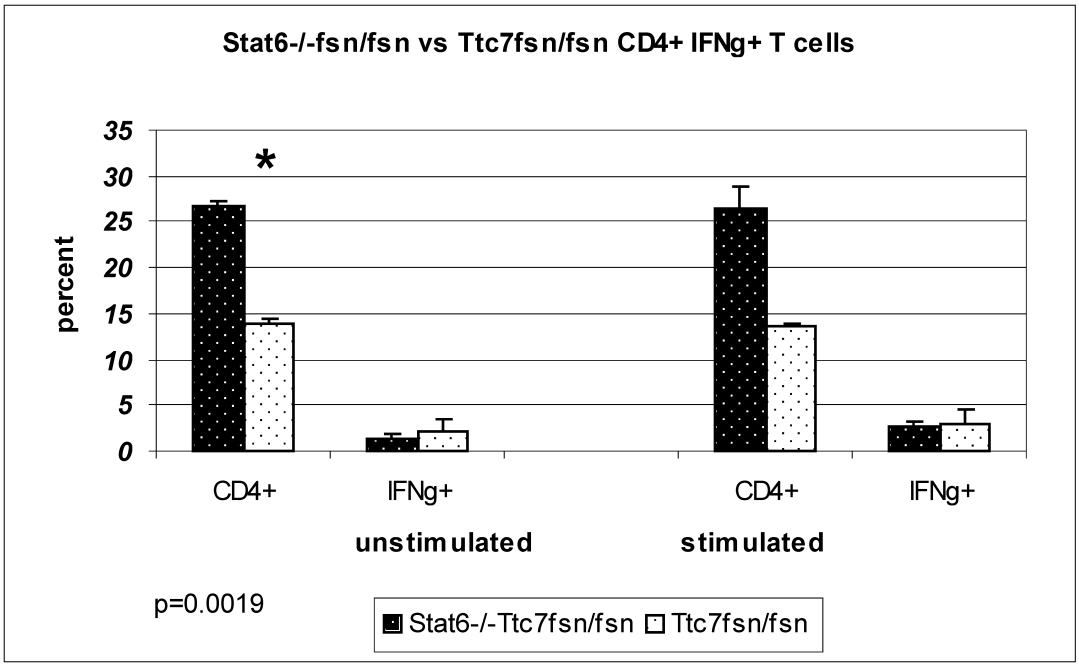

Figure 2.10. Stat6-/-Ttc7$^{fsn/fsn}$ and Ttc7$^{fsn/fsn}$ CD4+ IFN-γ+ T cells. Comparison of percentages of IFN-γ+ CD4+ cells between Stat6-/-Ttc7$^{fsn/fsn}$ and Ttc7$^{fsn/fsn}$ Stat6 intact mice. Splenic lymphocytes were stained for intracellular IFN- γ after culture with or without anti-CD3 stimulation. Stat6-/-Ttc7$^{fsn/fsn}$ mice have a significantly higher percentage of CD4+ cells than Ttc7$^{fsn/fsn}$ Stat6 intact mice but have similar percentages of IFN- γ+ cells in both unstimulated and stimulated groups. Data are summarized in Table 2.4. Data shown are mean percentages of 2 separate experiments ± SEM.

Stat6-/-Ttc7$^{fsn/fsn}$ vs. Ttc7$^{fsn/fsn}$ CD4+ IFN-γ+ T cells				
		% CD4+	**% IFN-γ+**	**MFI**
unstim	Stat6-/-Ttc7$^{fsn/fsn}$	26.79 ± 0.59*	1.365 ± 0.51	3.14
	Ttc7$^{fsn/fsn}$	14.01 ± 0.54	2.1 ± 1.46	3.43
		*p=0.0019		
Stim	Stat6-/-Ttc7$^{fsn/fsn}$	26.32 ± 2,6	2.74 ± 0.57	3.96
	Ttc7$^{fsn/fsn}$	13.5 ± 0.47	3.07 ± 1.44	4.10
n=2				

Table 2.4. Summary of data presented in Figure 2.10.

Results: Stat6-/- ELISAs

Stat6-/-Ttc7$^{fsn/fsn}$ lymphocytes produce 5.8 times the concentration of IL-4 as do Ttc7$^{fsn/fsn}$ lymphocytes

To compare the production of IL-4 between Stat6-/-Ttc7$^{fsn/fsn}$ splenic lymphocytes and Ttc7$^{fsn/fsn}$ splenic lymphocytes we cultured six million cells per sample for 24 hours with or without plate-bound anti-CD3 (10µg/mL) and then performed an IL-4-specific ELISA with the harvested supernatants. The concentration of IL-4 in the unstimulated samples was similar between the two groups with Ttc7$^{fsn/fsn}$ lymphocytes producing 98.5 ± 66 pg/mL IL-4 and the Stat6-/-Ttc7$^{fsn/fsn}$ lymphocytes producing 32 ± 0.001 pg/mL (Figure 2.11). However, after 24 hours of stimulation with anti-CD3, the Stat6-/-Ttc7$^{fsn/fsn}$ lymphocytes produced 22,912 ± 2697 pg/mL of IL-4 while Ttc7$^{fsn/fsn}$ lymphocytes produced 3946 ± 71 pg/mL. The level of IL-4 produced by the Stat6-/-Ttc7$^{fsn/fsn}$ lymphocytes was surprising, which prompted us to repeat the ELISA two additional times; both of which confirmed the results. Thus, it appears that Stat6-/-Ttc7$^{fsn/fsn}$ lymphocytes produce almost 6-fold more IL-4 than the already high levels of IL-4 produced by Ttc7$^{fsn/fsn}$ lymphocytes.

The reason for this is presently unclear. The expansion of activated T cells may certainly account for some of the elevation of IL-4 production noted in the Stat6-/-Ttc7$^{fsn/fsn}$ IL-4 ELISA. It is also possible that the lack of Stat6 fails to induce negative regulatory measures that function to down-regulate IL-4 production, which may already be overwhelmed or defective in Ttc7$^{fsn/fsn}$ mice.

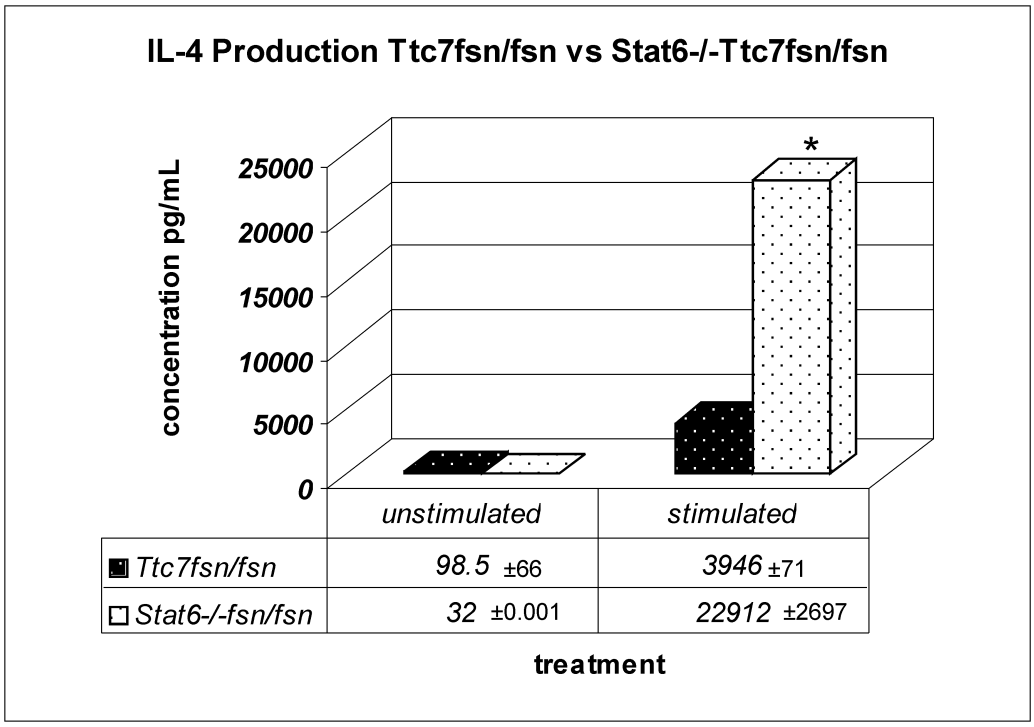

Figure 2.11. Stat6-/-Ttc7$^{fsn/fsn}$ IL-4 Production. Stat6-/-Ttc7$^{fsn/fsn}$ lymphocytes produce almost 6X the amount of IL-4 as do Ttc7$^{fsn/fsn}$ splenocytes. Purified splenic lymphocytes from 10-week Stat6 intact and deficient Ttc7$^{fsn/fsn}$ animals were cultured for 24 hours with plate-bound CD3 and an ELISA was performed on the supernatant. Stat6-/-Ttc7$^{fsn/fsn}$ lymphocytes produced 22,912 ± 2697 pg/mL of IL-4 (p=0.044) compared to 3946 ± 71 pg/mL produced by Stat6 intact Ttc7$^{fsn/fsn}$ lymphocytes. Data shown are mean percentages of 2 separate experiments ± SEM.

It is interesting to note that Dent et al (Linehan, Warren et al. 1998), also noted a dramatic increase in the production of IL-4 when their Stat6 deficient mice were crossed with a Bcl-6 deficient line. Isolated T cells from these mice produced levels of IL-4 that were 7- to 1000-fold greater than the single knock-outs alone. These mice also exhibited a severe, Th2-type inflammatory disease and died prematurely at between 5- and 6-weeks of age. The authors concluded that bcl-6 may function as a negative regulator of Th2 differentiation (and Stat6 responsive genes) and that their data suggest an alternative pathway of Th2 development that does not require IL-4 and/or Stat6. Thus, it appears that there may be other, as yet undiscovered, pathways of Th2 differentiation as well.

Stat6-/-$^{fsn/fsn}$ mice have elevated serum IgG1 and total serum Ig, and elevated IgM anti-DNA antibodies

Previous work by Pelsue et al (1998) determined serum immunoglobulin (Ig) levels of Ttc7$^{fsn/fsn}$ mice to be altered from those of Ttc7WT mice. Specifically, total Ig was 1.8 x more than WT; IgG1 was 2.7 x that of WT; IgG3 was 5.6 x lower than that of WT; IgE was 7000 x more than WT; and IgM was 1.9 x that of WT. Other groups have found a constitutively active form of Stat6 to increase the expression of IgG1 and IgE and in fact, Stat6 was found to be essential for B cells to effect this class switching for Ig production (Linehan, Warren et al. 1998; Bruns, Schindler et al. 2003). Stat6 deficient mice have been shown to have a reduction in T and B cell activation, and hence, a reduction in serum levels of IgG1, IgG3 and IgE (Linehan, Warren et al. 1998; Singh, Saxena et al. 2003; Xu, Duan et al. 2006). Because high serum Ig levels, including IgG1 and IgG3, have been associated with increased anti-DNA antibodies, increased renal

disease and autoimmunity, and knocking out Stat6 has been found to reduce the presence of anti-DNA antibodies and kidney pathology, we wanted to examine the serum Ig composition of our Stat6-/-Ttc7$^{fsn/fsn}$ mice. All serum concentrations were measured with isotype-specific ELISAs and described in the Materials and Methods section.

Interestingly, serum IgG1 concentration of Stat6-/-Ttc7$^{fsn/fsn}$, which averaged 112 µg/mL, was largely unchanged from that of the Ttc7$^{fsn/fsn}$ (129 µg/mL) that we tested (Figure 2.12B). Given that IgG1 may be more IL-4 than Stat6 dependent (Mao and Stavnezer 2001) this may not be surprising given the high levels of IL-4 expressed in these animals. However, Stat6-/-Ttc7WT mice showed greatly reduced levels of IgG1 (average 7.2 µg/mL, p=0.0002), even compared to Ttc7WT animals (47 µg/mL) suggesting that Stat6 does exert an influence in the expression of this Ig. Figure 2.12A presents serum data per animal to illustrate the variation typically found among individual animals in murine models of autoimmunity, including Ttc7$^{fsn/fsn}$ mice.

As mentioned above, previous data showed a reduction in serum IgG3 of almost 6-fold in Ttc7$^{fsn/fsn}$ mice from that of Ttc7WT mice. However, Stat6-/-Ttc7$^{fsn/fsn}$ mice actually had a slightly elevated but not statistically significant IgG3 serum concentration of 48.7 µg/mL compared to that of Ttc7$^{fsn/fsn}$ mice at 43 µg/mL and Stat6-/-Ttc7WT animals at 32 µg/mL (Figure 2.13B). IL-4 has been found to decrease production of IgG3, while IFN-gamma increased its production (Snapper, McIntyre et al. 1992), however, it is unknown why IL-4 may exert its influence over Stat6-/-Ttc7$^{fsn/fsn}$ in IgG1 production and have the opposite effect for IgG3. There are evidently more complicated regulatory issues that have yet to be determined. Enhanced IgG3 production has been associated with increased autoimmunity (de Stahl, Dahlstrom et al. 2003), but

A

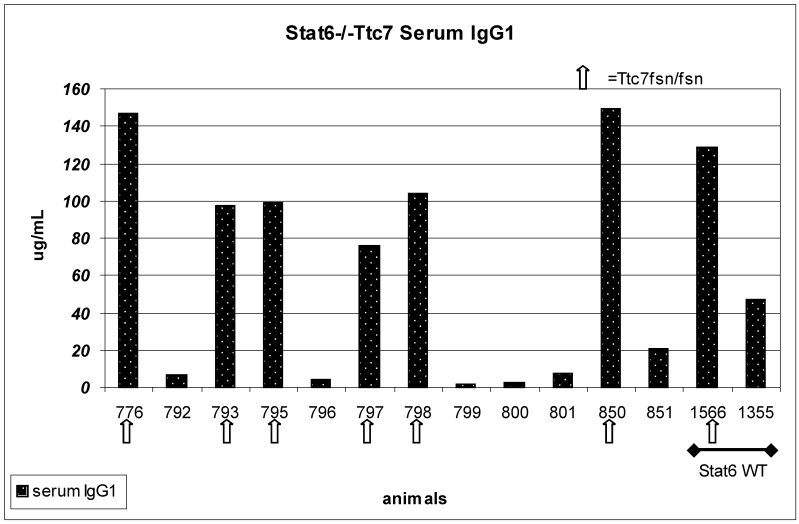

B

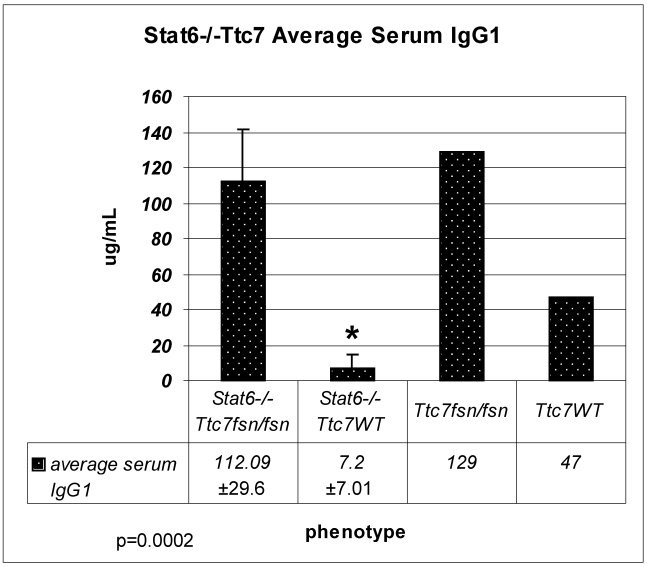

Figure 2.12. Stat6-/-Ttc7 Serum IgG1. Stat6-/-Ttc7 mice were bled at 10-weeks of age and an ELISA specific for IgG1 was performed with serum using Ttc7 Stat6 intact mice as controls. Concentrations were determined by comparing OD numbers to a standard curve generated with IgG1-specific antibody. A. The numbers on the X-axis represent individual animals, gray arrows below denote those with the Ttc7$^{fsn/fsn}$ mutation. Stat6-/-Ttc7WT mice have significantly lower IgG1. B. The average serum IgG1 for Stat6-/-Ttc7$^{fsn/fsn}$ is similar to that of Stat6 intact Ttc7$^{fsn/fsn}$ at 112.09 ± 29.6 µg/mL. Stat6-/-Ttc7WT mice have significantly lower levels of IgG1 (7.2 ± 7.01 µg/mL, p=0.0002) as would be expected in the absence of Stat6 as Stat6 deficient B cells are usually greatly inefficient in class switching to IgG1. Stat6 deficient Ttc7$^{fsn/fsn}$ have 15X more IgG1 than their Ttc7 Stat6 deficient littermates, while Stat6 intact Ttc7$^{fsn/fsn}$ mice produce 2.7X more than Stat6 intact Ttc7 WT littermates.

A

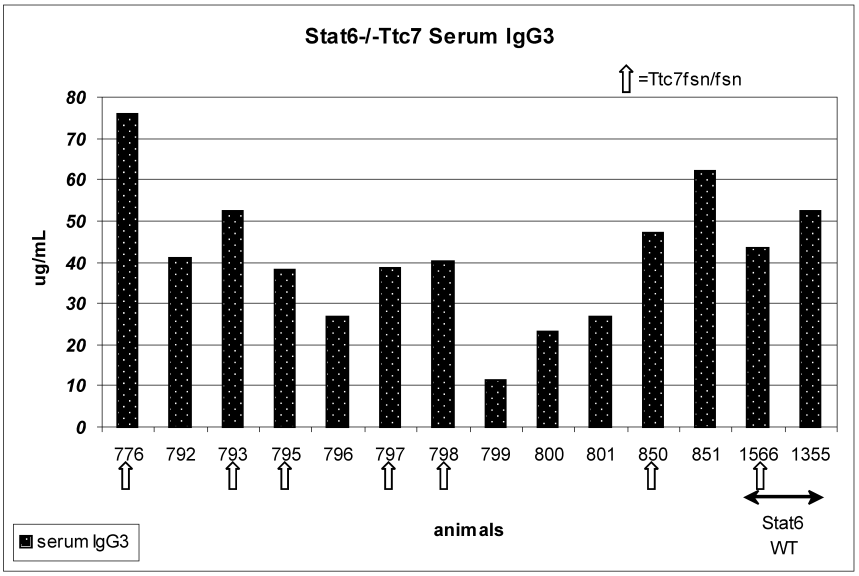

B

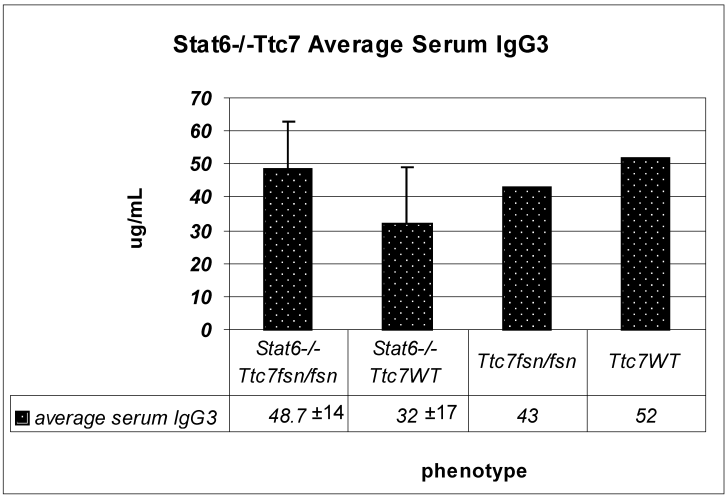

Figure 2.13. **Stat6-/-Ttc7 Serum IgG3.** IgG3 specific ELISA performed with serum from Stat6-/- Ttc7 mice. Animals were bled at 10-weeks and an ELISA was performed using Stat6 intact Ttc7 mice for controls, with an IgG3-specific antibody to generate a standard curve to calculate concentrations. A. As above, individual animals on the X-axis with gray arrows denoting $Ttc7^{fsn/fsn}$. Stat6-/-$Ttc7^{fsn/fsn}$ animals produce slightly more IgG3 than their Stat6-/-Ttc7WT littermates. B. The average serum concentration of IgG3 in Stat6-/-$Ttc7^{fsn/fsn}$ is higher at 48.7 µg/mL than their Stat6-/-Ttc7WT littermates (32 µg/mL) while $Ttc7^{fsn/fsn}$ mice have a lower concentration of IgG3 (43 µg/mL) than their Ttc7 WT littermates (52 µg/mL).

even in the presence of low levels of IgG3, Ttc7$^{fsn/fsn}$ mice exhibit enhanced autoimmunity due to an overall up-regulation of antibody production. It is of note that Stat6-/-$^{fsn/fsn}$ mice have more severe renal disease than do Stat6 sufficient Ttc7$^{fsn/fsn}$ mice, but it is unknown what the contribution of IgG3 may be. Figure 2.13A again presents the data per individual animal.

One of the hallmarks of Ttc7$^{fsn/fsn}$ mice is the huge increase of over 7000-fold in serum IgE spontaneously produced in these animals (Pelsue et al., 1998). Stat6 has been shown to be absolutely required for the production of IgE, whose production has also been shown to be dependent on T cell help (Mao and Stavnezer 2001). Thus, we checked the status of IgE production in Stat6-/-Ttc7$^{fsn/fsn}$ mice to confirm the absence of this Ig. We ran Stat6-/-(Ttc7$^{fsn/fsn}$ and WT) samples against Ttc7WT samples in order to more closely match the anticipated concentration of IgE to better-fit the standard curve. Our results determined an average serum IgE concentration of Ttc7WT mice to be 0.835 ± 0.77 µg/mL while all Stat6-/- samples did not register above background values. Therefore we deduce that Stat6 is not being aberrantly expressed in Stat6-/- mice (which was confirmed by Western Blot previously), but was required for Ttc7$^{fsn/fsn}$ IgE production. In addition, IgE is not contributing to the pathology of Stat6-/-Ttc7$^{fsn/fsn}$ mice, and IgE is being regulated normally in Stat6-/- animals.

Overall, total serum Ig did not differ significantly between Stat6-/-Ttc7$^{fsn/fsn}$ mice and Stat6 sufficient Ttc7$^{fsn/fsn}$ mice (Figure 2.14B). Our measured average value of 4101 ± 186 µg/mL for Ttc7$^{fsn/fsn}$ Stat6 intact mice was not statistically different than the 3479 ± 1080 µg/mL measured for the Stat6 deficient Ttc7$^{fsn/fsn}$ mice. This is in contrast to other Stat6-/- models which generally have significantly reduced Ig over their Stat6 intact

A

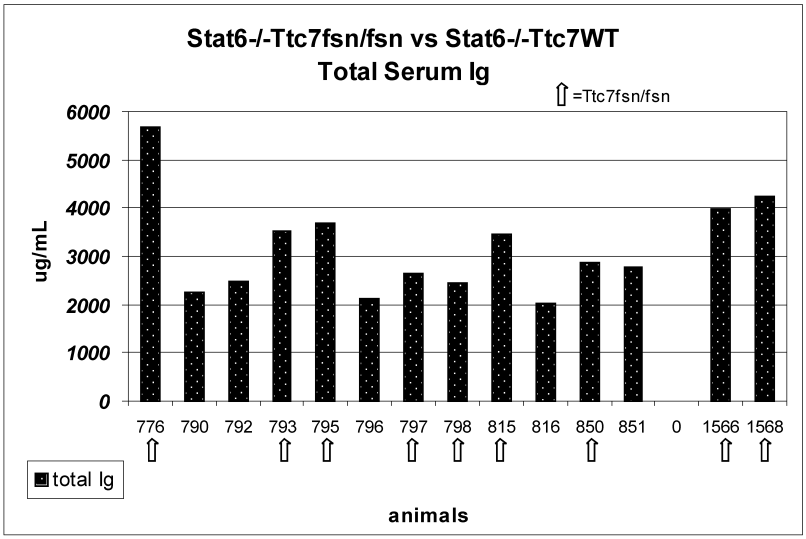

B

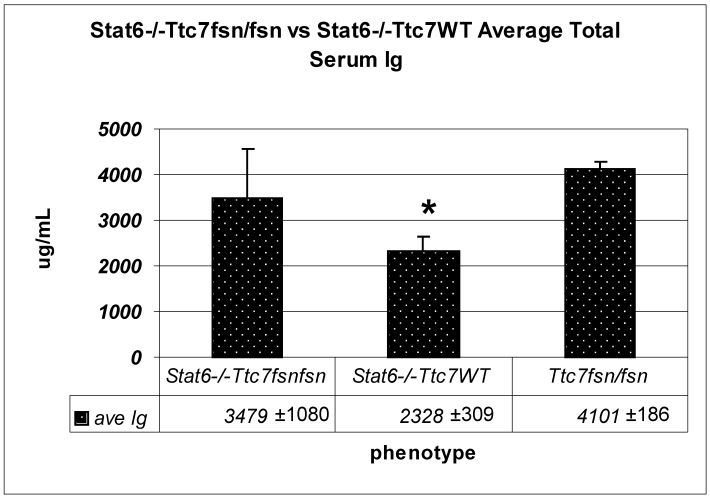

Figure 2.14. **Stat6-/-Ttc7 Total Serum Ig.** Total serum Ig was similar between Stat6 deficient and Stat6 intact Ttc7$^{fsn/fsn}$ mice. 10-week animals were bled and serum was used to perform an ELISA to measure total serum Ig concentration. As above, Stat6 intact Ttc7 animals were used as controls and a standard curve was generated to determine concentration. A. Individual animals showing the variation between serum Ig levels. B. The average concentration of Ig in Stat6 deficient Ttc7$^{fsn/fsn}$ (3479 ± 1080 µg/mL) is not significantly different than that of Ttc7$^{fsn/fsn}$ Stat6 intact animals (4101 ± 186 µg/mL), but is significantly higher than Stat6-/-Ttc7WT littermates (2318 ± 309 µg/mL, p=0.03).

controls (Wurster, Tanaka et al. 2000; Singh, Saxena et al. 2003; Xu, Duan et al. 2006). However, both the Stat6-/- and Stat6 sufficient Ttc7WT groups had similar Ig serum concentrations, which were significantly reduced from their Ttc7$^{fsn/fsn}$ littermates (see Figure 2.14A for values from individual animals). Thus we conclude that the defective Ttc7 gene must have an activating effect on B and T cells that drives Ig production, which Stat6 can only slightly modify.

The significance of variations in serum Ig in autoimmunity is multi-fold. For example, antibodies function to mark cells or debris for clearance which may be defective, they can activate complement for clearance of tissue or which can drive inflammation, and they form immune complexes that can also drive inflammation. The extent and actual mechanism of damage that antibodies contribute to pathology have been the subject of much debate, however it appears that there are self-reactive antibodies that are part of the natural antibody repertoire of an animal that are highly correlated with the disease state. The specificities of these antibodies can be varied, but anti-DNA antibodies seem to be the most well-studied as well as indicative of systemic autoimmunity (Daikh 2001; Bizzaro 2007). Ttc7$^{fsn/fsn}$ mice have been shown previously (Withington, Maltby-Askari et al. 2002) to have anti-nuclear antibodies, including anti-dsDNA antibodies. Also, knocking out Stat6 has been shown in other murine models to significantly reduce the titer of anti-DNA antibodies as compared to their intact Stat6 counterparts (Xu, Duan et al. 2006). Thus, we measured the absorbance values by ELISA of serum anti-DNA antibodies to determine if deleting Stat6 from Ttc7$^{fsn/fsn}$ mice would change the expression of anti-DNA. The result of this study is summarized in Figure 2.15A.

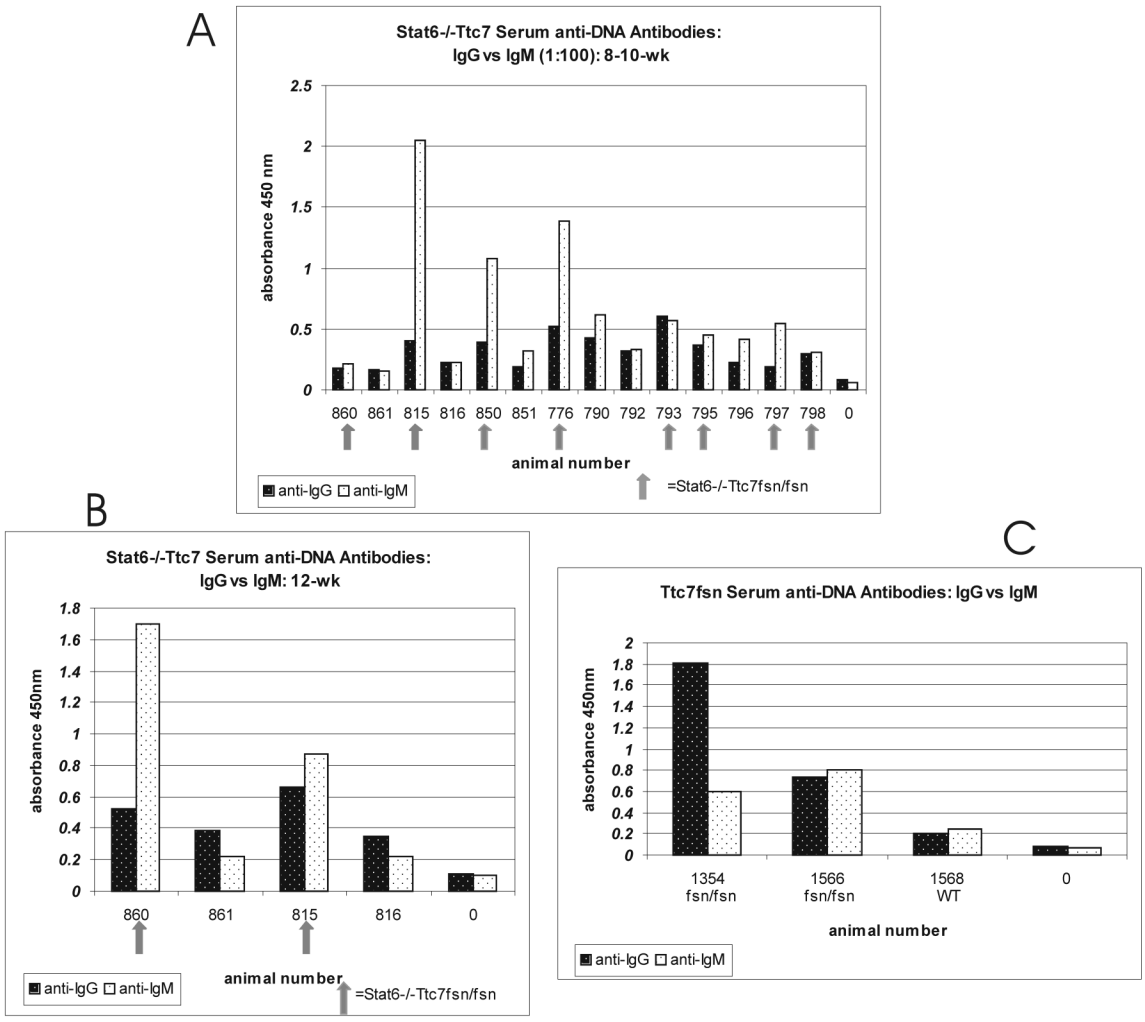

Figure 2.15. Stat6-/-Ttc7 anti-DNA Antibodies. Serum from 8-10 week (A) and 12-week (B) animals was used to perform DNA specific ELISAs to determine the concentration of IgG or IgM anti-DNA antibodies present in Stat6-/-Ttc7 mice. "0" on the X-axis denotes blank well for background fluorescence. Values are given in OD at 450 nm. A. The values for individual animals are graphed to show the variation between individuals, as above, the gray arrows denote Ttc7$^{fsn/fsn}$ mutant mice. Stat6-/-Ttc7$^{fsn/fsn}$ consistently have higher absorbance values than their Ttc7WT littermates for both IgG and IgM. B. Four of the same animals as in A were bled and serum was used to repeat an ELISA to measure anti-DNA antibodies. Animal #860 showed a significant increase in absorbance for IgM anti-DNA while animal #815 actually decreased. C. Stat6 intact Ttc7 anti-DNA absorbance values are mostly higher for IgG, or at a similar value.

Stat6-/-Ttc7$^{fsn/fsn}$ mice consistently showed absorbance values well over those of their Stat6-/-Ttc7Wt littermates, with many also over absorbance values of Stat6+/+ Ttc7$^{fsn/fsn}$ mice (Figure 2.15C). The major difference however, was that the absence of Stat6 changed the class of antibody from IgG in Stat6 sufficient Ttc7$^{fsn/fsn}$ to IgM in Stat6 deficient Ttc7$^{fsn/fsn}$ mice (Figure 2.15A). There is very little research literature on the role of IgM anti-DNA antibodies in the pathology of autoimmunity. However, we suggest that since the autoimmune disease is at least as severe, if not more so, in our Stat6-/-Ttc7$^{fsn/fsn}$ mice as compared to Ttc7$^{fsn/fsn}$ mice, that IgM antibodies are as capable of driving autoimmune disease as IgG. It is difficult to determine the exact contribution these antibodies make, because, as shown in Figure 2.15B, absorbance values in sick animals can spike and decline or vary with age, while their WT littermates stay consistently low.

Stat6-/-Ttc7$^{fsn/fsn}$ sera contain antibodies with mostly cytoplasmic specificities of both IgG and IgM

The presence of anti-DNA antibodies in the sera of Stat6-/-$^{fsn/fsn}$ mice suggested there may be autoantibodies present with specificities directed towards other cellular antigens as has been found in Ttc7$^{fsn/fsn}$ mice (Withington, Maltby-Askari et al. 2002). To analyze auto-reactive antibody staining patterns we used indirect immunofluorescence assays (IFAs) on fixed HEp-2 cells. Previous work in our lab evaluating IFAs had determined the staining pattern of Ttc7$^{fsn/fsn}$ to include several nuclear patterns indicative of SLE as well as a diffuse cytoplasmic pattern more often associated with inflammatory conditions (Withington, Maltby-Askari et al. 2002). Because our anti-DNA ELISA indicated the presence of IgM antibodies, we used both IgG- and IgM-conjugated

detection antibodies to identify the staining patterns of Stat6-/-Ttc7$^{fsn/fsn}$ mice. All Stat6-/-Ttc7$^{fsn/fsn}$ mice had positive staining at dilutions of 1:40 while Stat6-/-Ttc7WT mice were consistently negative. Figure 2.16 shows several representative images of staining identified by this assay. Interestingly, the lack of Stat6 changed the pattern from mostly nuclear in Ttc7$^{fsn/fsn}$ Stat6 intact mice to mostly sub-nuclear and cytoplasmic in the double-mutants. This was true for both IgM and IgG (Figure 2.16A, B and D). Figure 2.16C shows an IgM staining pattern typical of golgi staining, while A, B and D show a more dense, cytoplasmic speckled staining pattern typical of ribosomal or RNA staining, associated with SLE. Only one of 8 Stat6-/-Ttc7$^{fsn/fsn}$ animals (#815) exhibited an IgG nuclear homogeneous staining pattern; IgM detection in this animal identified the cytoplasmic staining typical of the others.

These results suggest that although the absence of Stat6 in Ttc7$^{fsn/fsn}$ mice changes the class and specificity of autoreactive antibodies, it appears that these antibodies may still be contributing to an autoimmune pathology and/or an inflammatory condition. The presence of a higher number of immature B cells in Stat6-/- mice may account for the increase in IgM antibodies.

Figure 2.16 Stat6-/-Ttc7$^{fsn/fsn}$ HEp-2 Slide Staining: IgM and IgG Autoantibodies. HEp-2 cell staining for autoantibody staining patterns of Stat6-/-Ttc7$^{fsn/fsn}$ serum. Commercially prepared HEp-2 slides were incubated with serum from Stat6-/-Ttc7 animals and detected with either IgM or IgG-FITC conjugated antibodies and visualized with Fluorescent microscopy. Images are representative of 8 animals with similar staining patterns. A-C. Three different Stat6-/-Ttc7$^{fsn/fsn}$ animals detected with IgM showing representative cycloplasmic patterns found with all animals analyzed (n=8). C shows a staining pattern typical of autoantibodies to golgi antigens. D and E are 2 different Stat6-/-Ttc7$^{fsn/fsn}$ animals both with IgG detection. Most IgG detection was cytoplasmic (D), but one animal of the eight had a nuclear staining pattern with IgG only (E). Stat6-/-Ttc7WT were negative (shown below). 200X

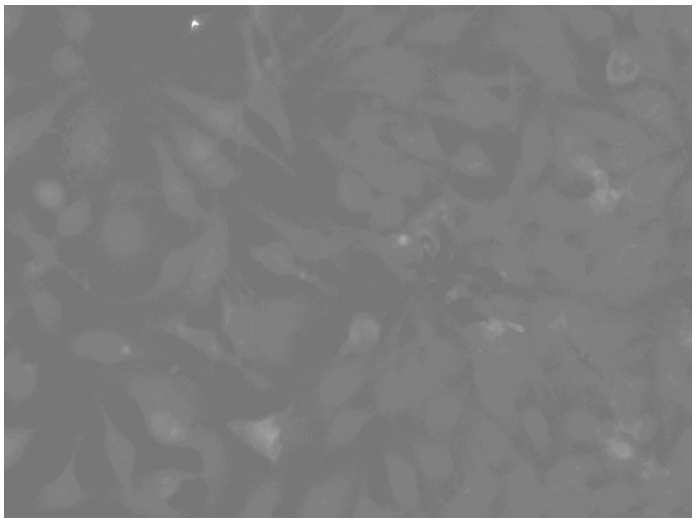

A

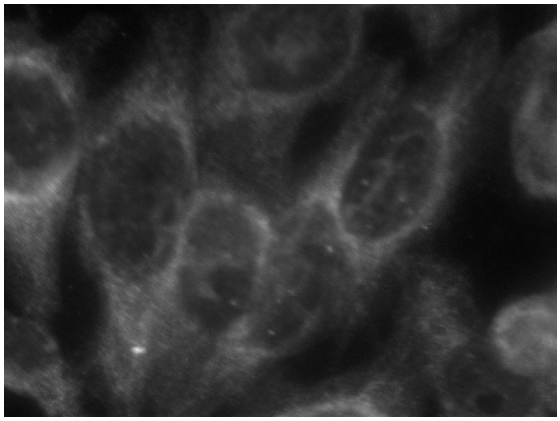

B

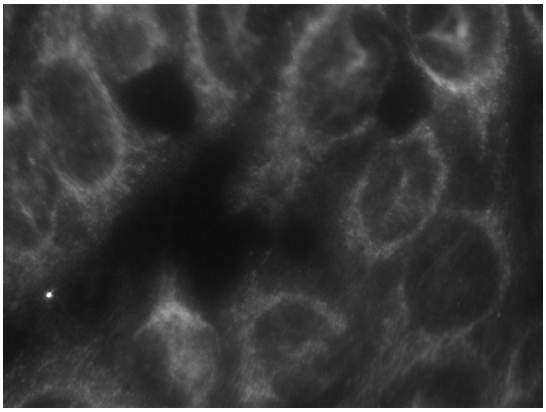

C

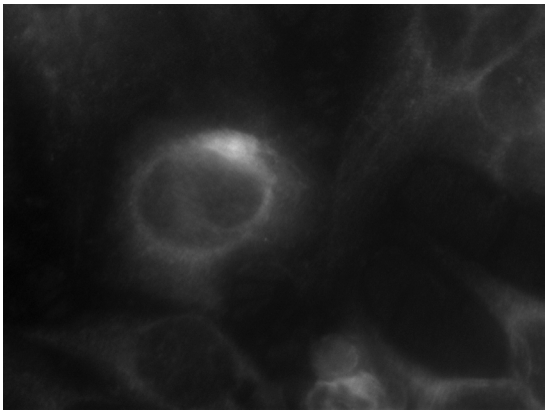

D

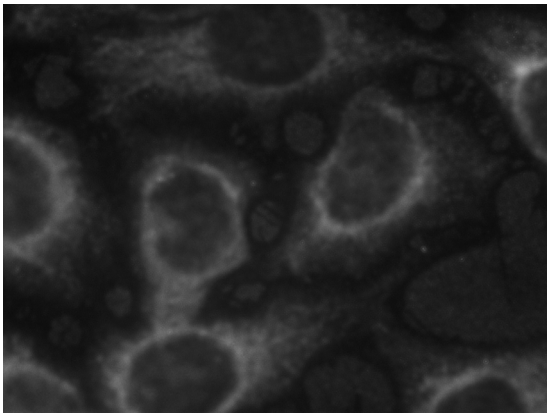

E

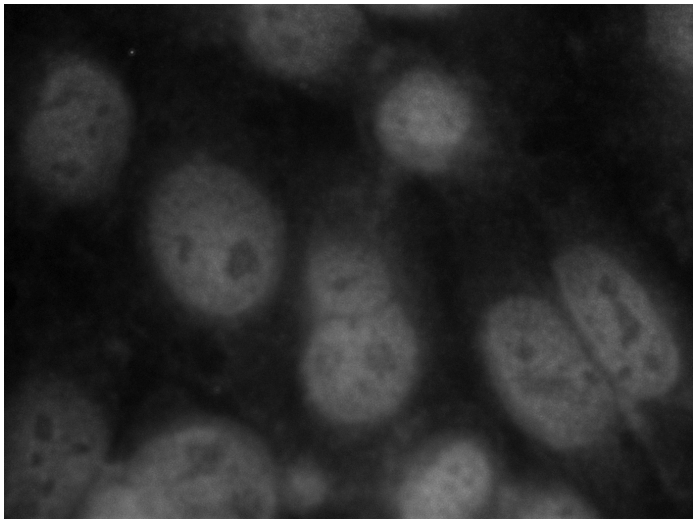

Results: Section 3: Anti-IL-4 Treatment of Ttc7$^{fsn/fsn}$ Mice

Treatment with anti-IL-4 (11B11) reduces CD23 and MHC II expression and alters serum Ig subsets

As mentioned previously, one of the hallmarks of Ttc7$^{fsn/fsn}$ mice is the over-abundance of IL-4 present in vivo, which results in Th2 driven and phenotypic autoimmunity. To assess the contribution of IL-4 to disease expression in Ttc7$^{fsn/fsn}$ mice, we treated 5 mice from separate litters with a neutralizing rat anti-mouse-IL-4 mAB (11B11) for seven weeks, starting at 3-weeks of age. Since the disease pathology starts accelerating at 5-6 weeks of age, we hoped to neutralize endogenous IL-4 before the disease process began. We also treated 5 Ttc7$^{fsn/fsn}$ mice from separate litters with an isotype-matched rat IgG1 mAb (GL113) as an isotype control treatment. All animals were sacrificed at 10-weeks, one day after the final mAb injection whereupon blood and organs were collected for analysis.

At time of sacrifice, there was no obvious difference between treatment groups. The pattern and extent of skin, hair, and eye pathology was similar, as were their size and overall demeanor. Both groups had distended abdomens due to extreme splenomegaly, and the spleens when removed were similar in size. Spleen cellularity was similar, with untreated Ttc7$^{fsn/fsn}$ mice having an average of $13.0 \pm 5.4 \times 10^8$ cells and 11B11-treated mice having an average of $15.1 \pm 6.0 \times 10^8$ cells.

Flow cytometry data of spleen cell populations is summarized in Table 3.1. There is direct evidence that the 11B11-treated group responded to the anti-IL-4 as both IL-4 responsive B cell markers of activation CD23 and MHC II expression had decreased

		CD3		CD4		CD8		CD19		CD23	
		Ttc7fsn	WT	Ttc7fsn	WT	Ttc7fsn	WT	Ttc7fsn	WT	Ttc7fsn	WT
	8wk Pub	8.5±1.2	41.5±3.5	8.7±1.3	32.7±1.6	3.1±1.2	16±6.8	29.0±3.5	37±5.6		
n=5	11B11	18.25±4.6		7.6±1.7		6.68±3.47		22.68±4.9		3.055±0.27*1	
n=4	GL113	15.7±4.7		7.87±0.8		7.4±2.24		31.55±12		31.25±0.91	
n=3	Ttc7fsn/fsn 10wk									36.27±1.89	6.94±1.13
		MHCII		Ter119		F4/80		GR-1		PanNK	
		Ttc7fsn	WT	Ttc7fsn	WT	Ttc7fsn	WT	Ttc7fsn	WT	Ttc7fsn	WT
	8wk Pub	56.7±4.16	32.3±1.53	17.6±1.1	6.6±0.3	9.5±4.6	1.9±1.2	5.3±2.3	3.4±1.6	3.54	2.8
	11B11	12.6±2.29*2		21.1±8.4		8.4±4.7		17.6±8.9		4.9±2.3	
	GL113	43.04±5.8		17.5±5.1		11.6±2.1		20.5±8.3		5.1±4.5	
	Ttc7fsn/fsn 10Wk	60.1±7.78	63.11±4.9								

*1:p=0.0009
*2:p=0.0000006

Table 3.1. Spleen Cell Populations of 11B11-Treated and GL113-treated Ttc7$^{fsn/fsn}$ mice. All numbers represent percentages of total population.

significantly, from 36% to 3% for CD23 (p=0.0009) and from 60% to12% for MHC II (p=0.0000006). The percent of CD19+ cells declined to 22% in the 11B11-treatment group, from approximately 30% in untreated and isotype controls. It also appeared that the percentage of CD3+ cells increased in the 11B11-treatment group, from 8.5% to 18%, however the isotype control group was also elevated (15%) so this may have been a result of antibody treatment and not directly related to IL-4 neutralization.

Anti-IL-4 Treatment alters T cell subsets

To assess the effect of anti-IL-4 treatment on T cell activation we performed 4-color flow cytometry with antibodies to CD69/CD4/CD62L/CD44 cell surface markers and gated as previously described for Ttc7$^{fsn/fsn}$ and Stat6 deficient mice (see Figure 3.1). The percentage of naïve CD4+ cells (CD62L^{hi}/CD44^{lo}) was virtually the same among treated, isotype control and untreated Ttc7$^{fsn/fsn}$ mice. The 11B11 group had a higher percentage of activated (CD62L^{hi}/CD44^{hi}) CD4+ cells (29.1%) than untreated Ttc7$^{fsn/fsn}$ CD4+ cells (17.1%) (Figure 3.1B), however when compared to the isotype control CD4+ cells (34.5%) the percentage was actually slightly lower (Figure 3.1A). Thus, it appeared that the mAb treatment may have had an overall effect on activation, but that neutralizing IL-4 may have slightly reduced the reactivity of the cells to treatment. The memory cell subset (CD62L^{lo}/CD44^{hi}) was also slightly altered, with the percentage of the 11B11-treatment group (18.2%) lower than the isotype control (20.6%) (Figure 3.1A), and even lower than untreated Ttc7$^{fsn/fsn}$ mice (27.77%) (Figure 3.1B). These results suggest that in vivo, IL-4 may serve to help alter the CD4+ T cell population into a more activated state, perhaps augmenting the underlying defect leading to hyperactivation. However, since

A

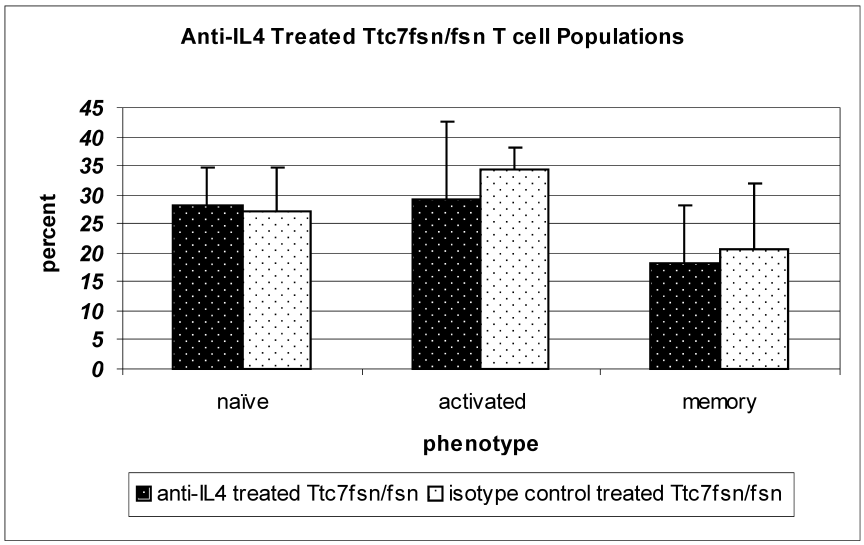

B

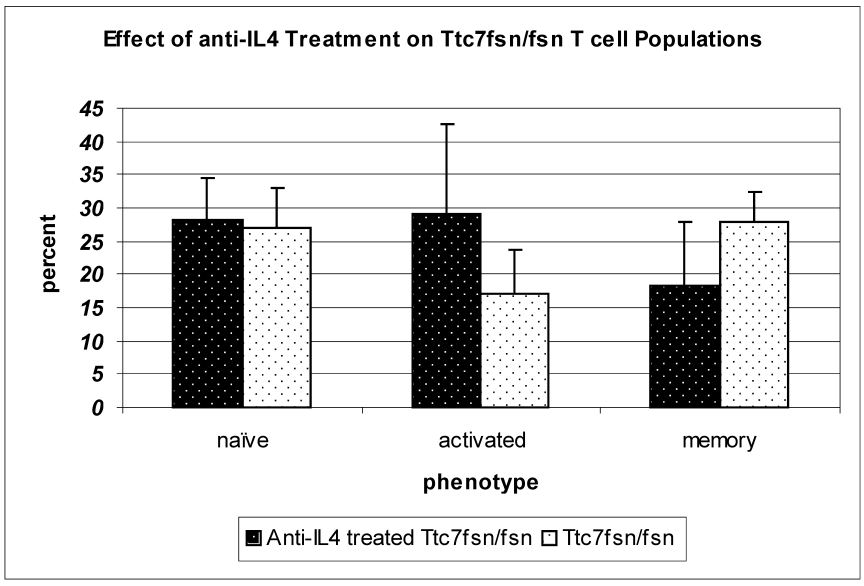

Figure 3.1. Anti-IL-4 Treated Ttc7$^{fsn/fsn}$ T cells. CD4+ T cell subset distribution of anti-IL-4 Treated Ttc7$^{fsn/fsn}$ mice. Lymphocytes were purified from spleen, stained and analyzed by flow cytometry. Gating on CD62L/CD44 surface markers was performed as described in Figure 1.16. A. Comparison of 11B11-treated and GL113-treated isotype control animals showing a slight increase in naïve, a slight decrease in activated and a slight decrease in memory subsets of the 11B11-treated group. B. Comparison of 11B11-treated and untreated Ttc7$^{fsn/fsn}$ showing a slight increase in naïve, an increase in activated (29.1 ± 13.4% vs. 17.1 ± 6.6% respectively), and a decrease in memory (18.2 ± 9.8% vs. 27.77 ± 4.7% respectively) subset of the 11B11-treated group. Data shown is the mean percentage of CD4+ cells of 5 different animals per group ± SEM.

neutralization of IL-4 had no effect on the naïve population it appears that the defect in Ttc7 was more responsible for the reduction in the naïve population.

Anti-IL-4 Treatment decreases the immature B cell subset

Previous work in our lab (Farrington 2006) established an alteration in B cell subsets in Ttc7$^{fsn/fsn}$ spleen with an increase in the percentage of immature B cells (IgD^{lo}/IgM^{hi}), a significant decrease in mature B cells (IgD^{hi}/IgM^{lo}, p=≤ 0.01), and a decrease in transitional B cells (IgD^{hi}/IgM^{hi}) as compared to Ttc7 WT littermates (Figure 3.2C). Because of the functional differences in these subsets, it was important to examine the distribution of B cells in the spleens of our 11B11-treated Ttc7$^{fsn/fsn}$ animals. We performed flow cytometry on single cell suspensions of whole spleen from 11B11- and GL113-treated mice and then gated on the lymphocyte portion of the forward and side scatter plots. Determination of IgM and IgD expression was gated as shown for Stat6-/- in Figure 2.6.

There was very little difference in the percentage of B cells comprising the mature B cell subset, with 11B11-treated at 7.9 ± 3.7% and Ttc7$^{fsn/fsn}$ at 9.2 ± 1.2% (Figure 3.2A). The transitional subset was also very similar with 11B11-treated slightly higher at 11.38 ± 4.7% and Ttc7$^{fsn/fsn}$ at 9.0 ± 4.6%. However, the immature subset was reduced. While Ttc7$^{fsn/fsn}$ mice measured 20.9 ± 3%, 11B11-treated animals measured 14.8 ± 6.0% immature B cells. These data suggest that in vivo IL-4 may be functioning to both drive the proliferation and activation of immature B cells instead of allowing them to differentiate, and/or helping this population to survive to become a functional group able to contribute to the pathogenesis of autoimmunity

Figure 3.2. Anti-IL-4 Treated B cell Subsets. B cell subset distribution of anti-IL-4-treated Ttc7$^{fsn/fsn}$ mice. Splenocytes were stained for IgM and IgD and analyzed by flow cytometry. Gating on IgM/IgD was performed as described in Figure 2.6. A. 11B11-treated Ttc7$^{fsn/fsn}$ mice have a reduction in the percentage of immature B cells, a slight reduction in the percentage of mature B cells and a slight increase in the percentage of transitional B cells as compared to untreated Ttc7$^{fsn/fsn}$ animals. B. 11B11-treated vs. isotype control showed a similar distribution as in A. C. Comparison of untreated Ttc7$^{fsn/fsn}$ vs. Ttc7 WT animals for reference. Data shown is the mean percentage of 5 different animals per group ± SEM.

A

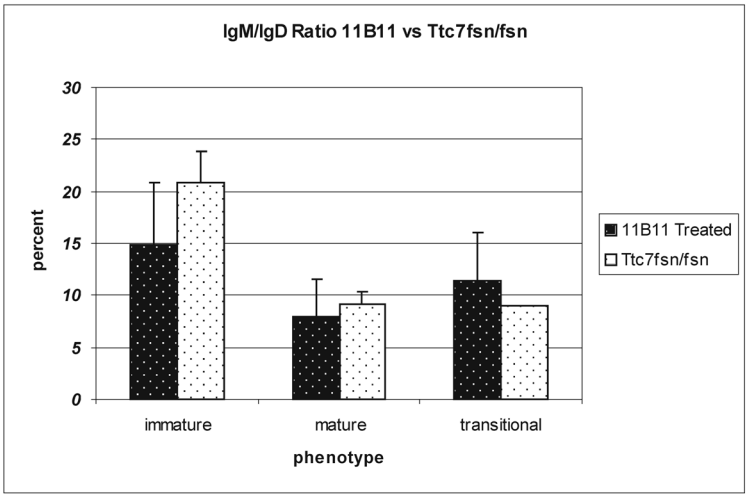
IgM/IgD Ratio 11B11 vs Ttc7fsn/fsn
30
25
20
15
10
5
0
percent
immature
mature
transitional
phenotype
11B11 Treated
Ttc7fsn/fsn

B

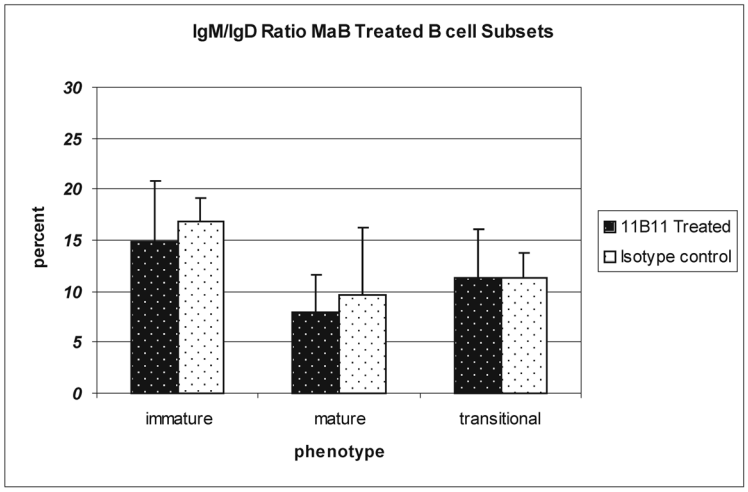
IgM/IgD Ratio MaB Treated B cell Subsets
30
25
20
15
10
5
0
percent
immature
mature
transitional
phenotype
11B11 Treated
Isotype control

C

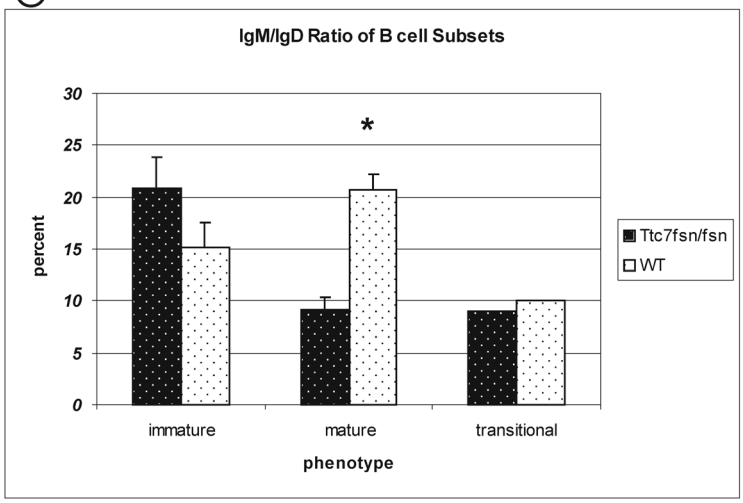
IgM/IgD Ratio of B cell Subsets
*
30
25
20
15
10
5
0
percent
immature
mature
transitional
phenotype
Ttc7fsn/fsn
WT

Anti-IL-4 treated Ttc7$^{fsn/fsn}$ mice have reduced serum IgE, reduced IgG1, slightly reduced IgG3, elevated total serum Ig and slightly reduced anti-DNA serum antibodies

As mentioned previously in the Results section for the Stat6-/- study, Ttc7$^{fsn/fsn}$ mice have elevated total serum Ig, elevated IgE, IgG1, and lower serum IgG3 than their WT littermates. They also have an increase in anti-DNA antibodies and antibody complex deposition in their kidneys. Therefore we performed serum ELISA assays to assess the difference treatment with an IL-4 neutralizing mAb may have on serum antibody production.

The results for serum IgE are shown in Figure 3.3. Overall, there was a reduction in serum IgE in the 11B11 treated group which averaged 6.59 ± 1.26 μg/mL, while the untreated Ttc7$^{fsn/fsn}$ mice averaged 10.64 ± 1.1 μg/mL (Figure 3.3B). Our measurements were actually lower than reported previously by Pelsue et al in 1998 (72 μg/mL). Figure 3.3A presents the data for individual mice. Serum IgG1 was also reduced in the 11B11 treated mice as shown in Figure 3.4B. The average serum IgG1 concentration in the 11B11 treated was 70.8 ± 8.2 μg/mL while the untreated group measured 173 ± 34 μg/mL. Again, the result per individual animal is presented in Figure 3.4A. Since both IgE and IgG1 are influenced by IL-4 we would expect a reduction in production of these antibodies when IL-4 is neutralized.

There was also a slight reduction in IgG3 as shown in Figure 3.5B. The 11B11-treated group averaged 64.79 ± 1.8 μg/mL whereas the untreated group had an average of 85.5 ± 6.72 μg/mL. The average of the isotype control group was in between the two with

A

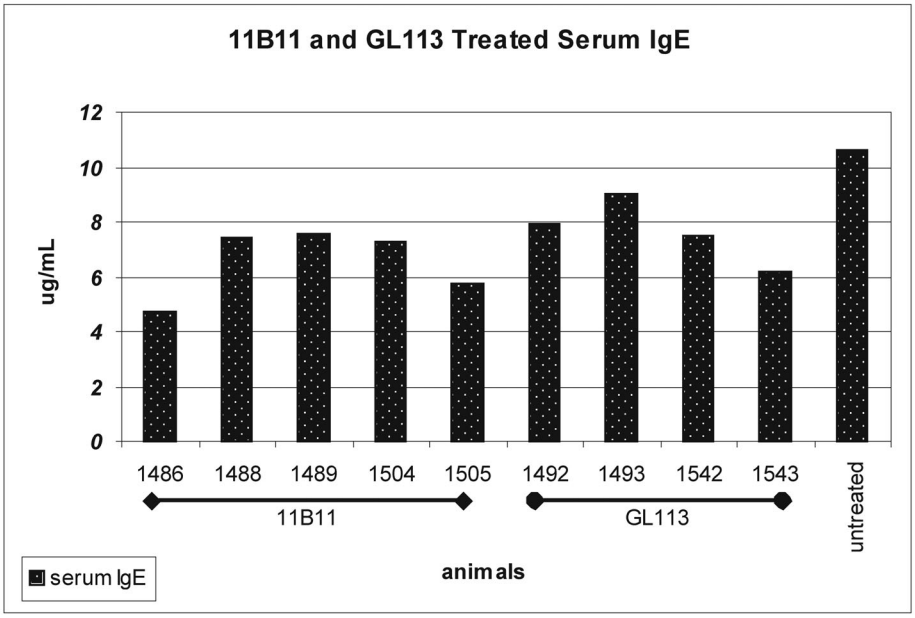

B

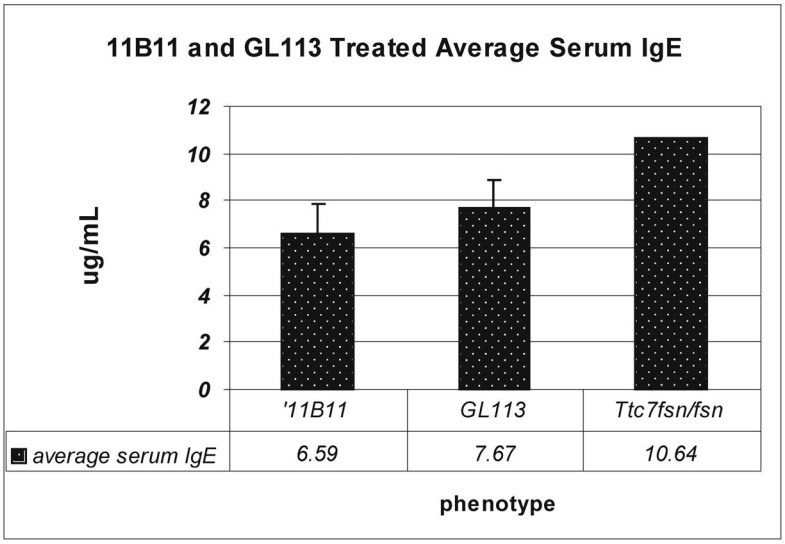

Figure 3.3. 11B11- and GL113-Treated Serum IgE. ELISA specific for IgE was performed on sera collected from 10-week 11B11 or isotype control animals before sacrifice. A. Serum IgE concentrations in µg/mL of individual mice showing variability between animals, but a general trend towards a decrease in IgE in 11B11-treated animals. An untreated Ttc7$^{fsn/fsn}$ was used for a control. B. The average serum IgE concentration from the data in A, showed a reduction in serum IgE concentration in the animals treated to neutralize IL-4.

A

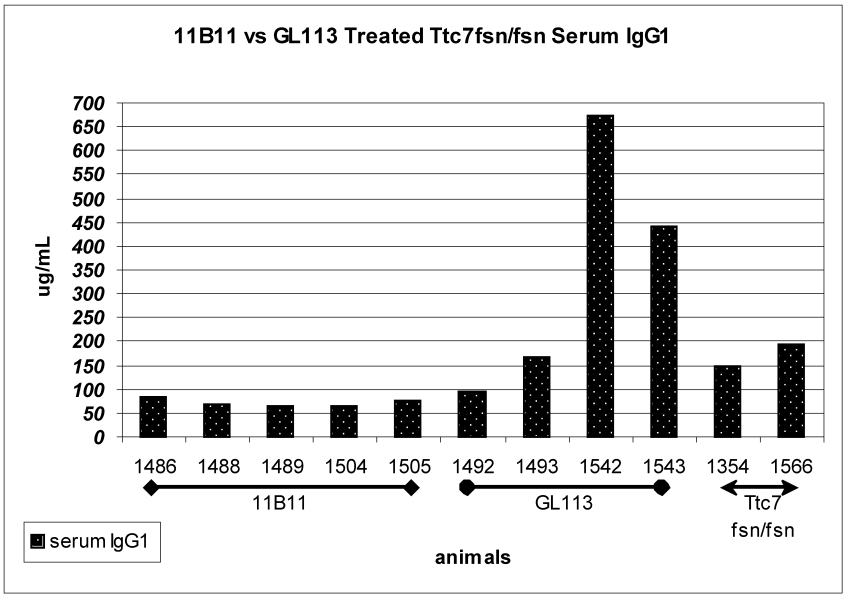

B

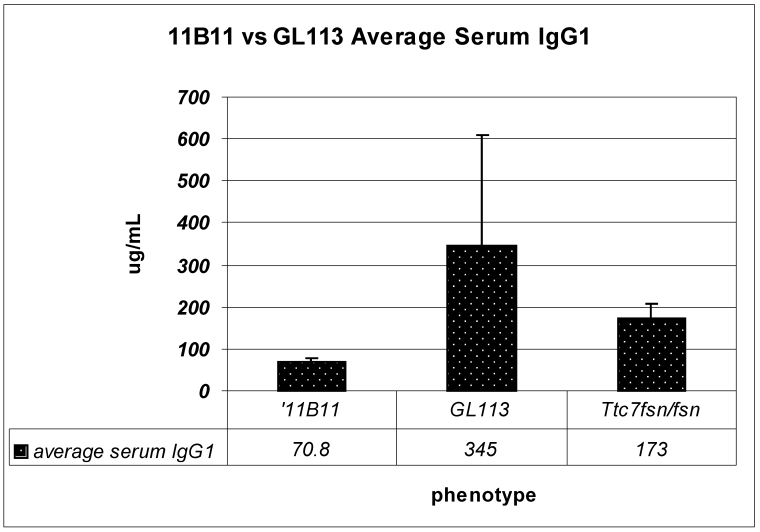

Figure 3.4. 11B11-Treated Serum IgG1. ELISA specific for IgG1 was performed on sera collected from 10-week 11B11 or isotype control animals. A. Serum IgG1 in 11B11-treated animals was reduced from isotype control and untreated Ttc7$^{fsn/fsn}$ mice. Data were fairly consistent among 11B11 treated animals, and more variable among other groups. B. The data from A were averaged, and showed a significant reduction of serum IgG1 in the 11B11-treated group.

A

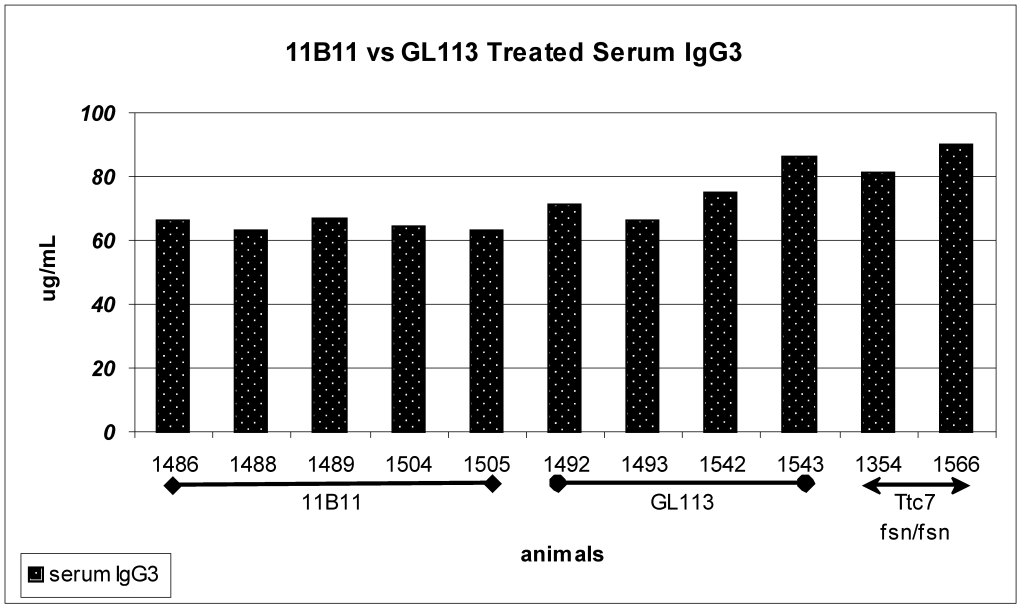

B

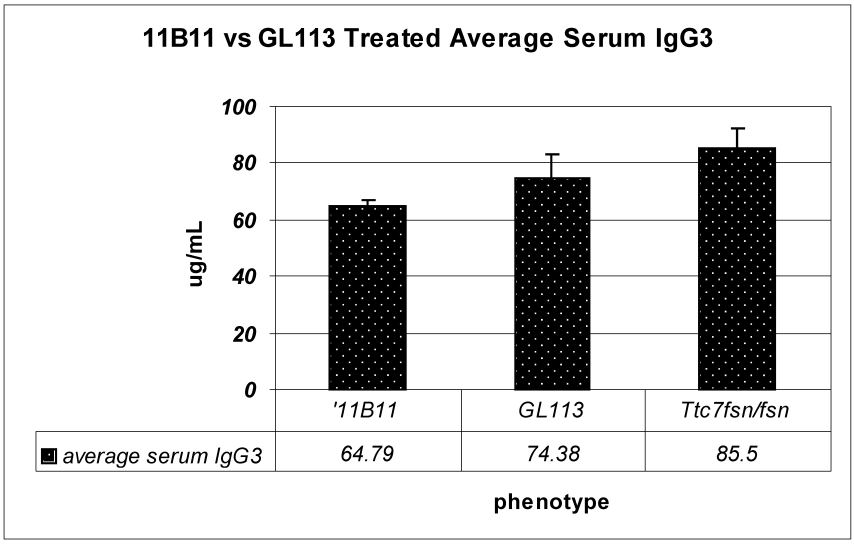

Figure 3.5. 11B11-Treated Serum IgG3. ELISA specific for IgG3 was performed on sera collected from 10-week 11B11 or isotype control animals. A. Serum IgG3 concentration was fairly consistent in all groups. Data shown is from individual animals. B. The data from A were averaged and presented in µg/mL.

74.38 ± 6.72 μg/mL. Thus, it is difficult to determine the effect of 11B11 on IgG3 production.

Interestingly, the average total serum Ig concentration of the 11B11-treated group was slightly more elevated (4567 ± 1000 μg/mL) than the untreated group (3564 ± 489 μg/mL, Figure 3.6B), although highly variable (Figure 3.6A). The average of the isotype control group was similar to the untreated (3515 ± 351 μg/mL). As mentioned previously, the importance of serum antibody measurements lies in the correlation between high serum antibody levels and the presence of autoantibodies and immune complexes. Some antibody isotypes are believed to be more "pathogenic" than others, and the evidence is conflicting about the role immune complexes play in autoimmune pathology (Ebling and Hahn 1989; Rüger, Erb et al. 2000; Morris, Dragula et al. 2002; Deocharan, Marambio et al. 2003; Singh, Saxena et al. 2003). Therefore, the significance of an elevation in total serum Ig must be evaluated in context of the ensuing pathology, and any confounding factors such as the limitations of experimental design and treatment with exogenous antibodies. Ttc7$^{fsn/fsn}$ mice spontaneously secrete high levels of antibody with great variability between animals. It is unknown when this pattern of antibody production is established. Therefore, it appears that anti-IL-4 treatment altered the isotype profile with reduced levels of IgE and IgG1, which are known to be influenced by IL-4, but did not affect the overall level of production of Ig, which is also influenced by the action of IL-4 on B cells, but is more dependent on the activation state of the secreting B cells.

A

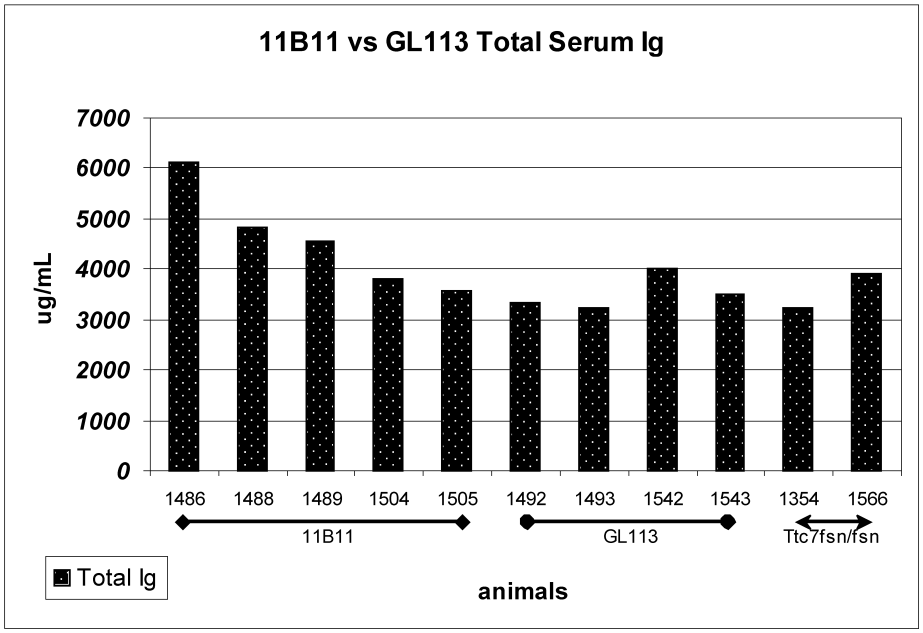

B

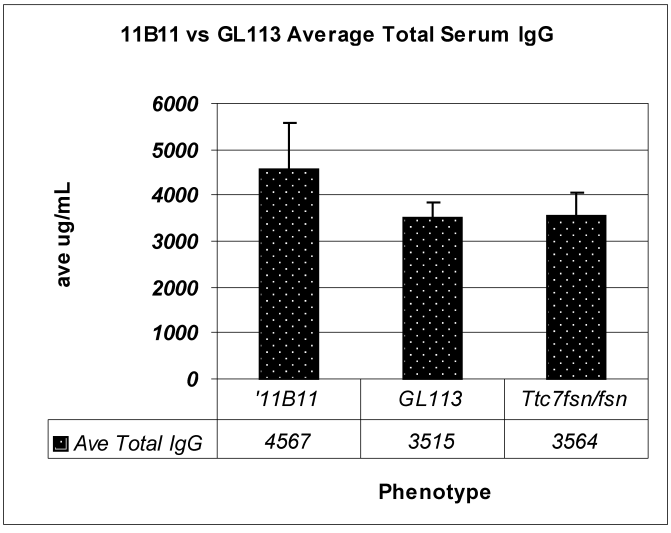

Figure 3.6. 11B11-Treated Total Serum Ig. ELISA specific for total serum Ig concentration in µg/mL. Sera was collected from 10-week 11B11 or isotype control animals before sacrifice. A. Total serum Ig concentrations presented for individual animals showed variability but a general increase in the 11B11 group. B. The data from A were averaged and presented as average µg/mL. All groups had similar concentrations of total Ig. The increase in the 11B11-treated group shown was not significant.

Anti-IL-4 treated Ttc7$^{fsn/fsn}$ mice have lower absorbance values of anti-DNA antibodies than untreated Ttc7$^{fsn/fsn}$ mice

The presence of anti-dsDNA antibodies has been established in Ttc7$^{fsn/fsn}$ mice (Withington, Maltby-Askari et al. 2002), as well as inflammation and immune complex deposition in the kidneys, mild proteinuria, and autoantibodies of other specificities. It is unknown exactly how IL-4 contributes to the extent and pathology of these conditions. Therefore, we performed serum ELISA to evaluate the presence of anti-DNA antibodies in 11B11- treated Ttc7$^{fsn/fsn}$ mice (Figure 3.7).

Treatment with 11B11 lowered the absorbance values in ELISA of both IgM and IgG anti-DNA antibodies from that of untreated Ttc7$^{fsn/fsn}$ mice. Average absorbance values of the 11B11-treated group were 1.13 ± 0.6 for IgG and 0.65 ± 0.35 for IgM while untreated Ttc7$^{fsn/fsn}$ mice averaged 1.26 ± 0.76 for IgG and 0.706 ± 0.14 for IgM. GL113-treated isotype controls averaged 0.87 ± 0.15 for IgG and 0.72 ± 0.36 for IgM anti-DNA antibodies. Interestingly, the reduction in IgM anti-DNA antibodies in the 11B11 group correlates with the reduction in the percentage of immature B cells also found in that group, in contrast to the Stat6 deficient group which had a dramatic rise in anti-DNA IgM absorbance as well as a dramatic rise in the percentage of immature B cells. Perhaps IL-4 is functioning to prolong survival in this group of cells which is then able to produce IgM autoantibodies, which then leads to the ramping up of autoimmunity.

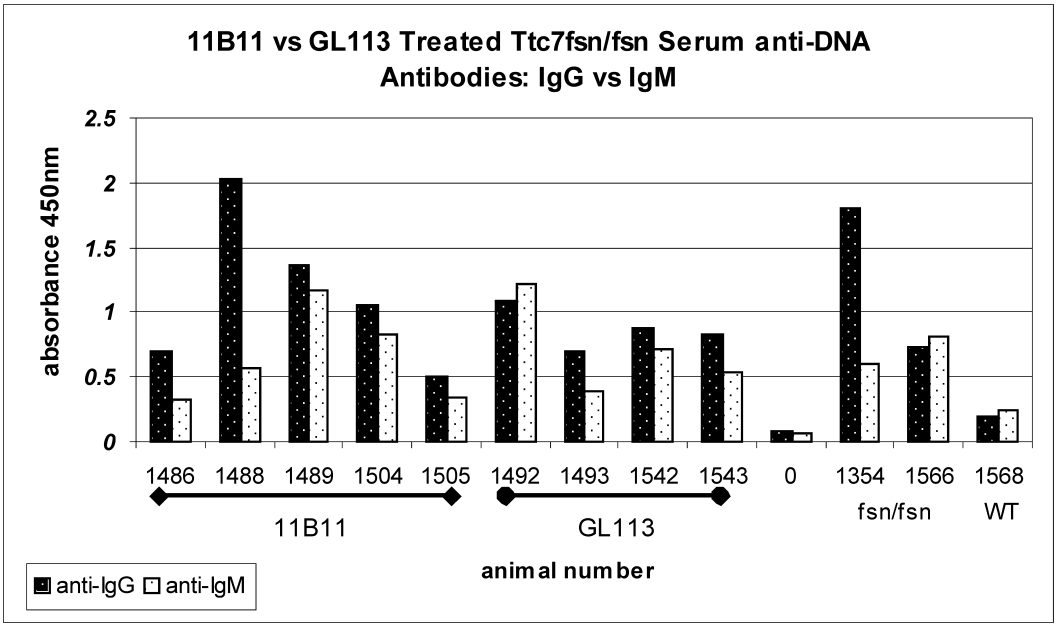

Figure 3.7. 11B11-Treated Serum anti-DNA Antibodies. An anti-DNA ELISA was performed on sera collected at 10-weeks from 11B11-treated, GL113-treated (isotype control) and untreated Ttc7$^{fsn/fsn}$ mice. IgG- and IgM-conjugated antibodies were used for detection. The data are presented in absorbance values obtained per individual animal. In general, anti-DNA IgGs have higher absorbance values than IgM in all groups. "0" represents background absorbance, and WT is a Ttc7 WT age-matched animal with absorbance values just above background.

11B11-Treated Ttc7$^{fsn/fsn}$ mice exhibit autoantibody staining patterns similar to untreated Ttc7$^{fsn/fsn}$

Although we saw a reduction in absorbance values for IgG and IgM anti-DNA in 11B11-treated mice, the absorbance was still well-above background. Therefore, we wanted to examine serum staining patterns in HEp-2 cells to see if treatment with anti-IL-4 altered the staining patterns seen previously in untreated Ttc7$^{fsn/fsn}$ mice (Withington, Maltby-Askari et al. 2002). Representative images of staining from 11B11-treated serum are shown in Figure 3.8A-F. Patterns identified include nuclear homogeneous (A), nucleolar (B), nuclear rim (C), nuclear rim with cyoplasmic staining (D), and cytoplasmic staining (E). These patterns are associated with antibodies to nuclear antigens such as dsDNA, histones, Sm, fibrillarin, and cytoplasmic antigens such as RNA, ribosomal antigens, mitochondrial antigens and cytoskeletal antigens. 11B11-treated animals have both IgM and IgG antibodies in these patterns which are typically found in human systemic sclerosis, overlap syndromes and SLE (Bradwell 1995). For comparison, Figure 3.8A-C shows representative images of untreated Ttc7$^{fsn/fsn}$ serum as well as a GL113 control (3.9C). Most of the patterns associated with the treated animals were also found in the untreated and control, with the exception of the nucleolar pattern (3.8B). This suggests that IL-4 may not influence the specificity of autoantibodies, but may have more of an effect on isotype.

Figure 3.8. 11B11-Treated Ttc7$^{fsn/fsn}$ HEp-2 Slide Staining: Autoantibody Patterns. HEp-2 cell staining for autoantibody staining patterns of 11B11-treated serum. Commercially prepared HEp-2 slides were incubated with serum from 11B11-treated Ttc7$^{fsn/fsn}$ animals and detected with either IgM or IgG-FITC conjugated antibodies and visualized with Fluorescent microscopy. Images are representative of 5 animals with similar staining patterns. A. Nuclear homogenous B. nucleolar staining pattern C. Nuclear rim D. nuclear rim with cytoplasmic staining E. cytoplasmic pattern typical of ribosomal, mitochondrial and RNA antigens F. cytoplasmic with rim. Patterns identified were both nuclear and cytoplasmic with both IgM and IgG. Patterns shown are typically found in human systemic sclerosis, overlap syndromes and SLE. 200X

A

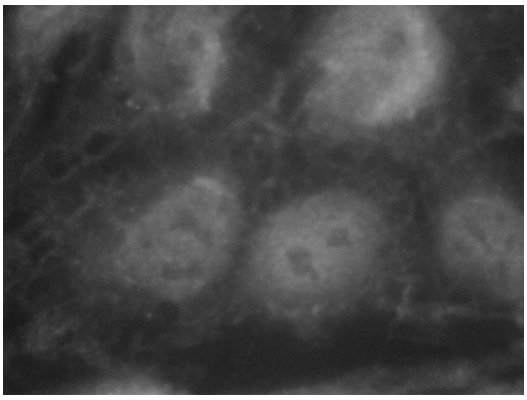

B

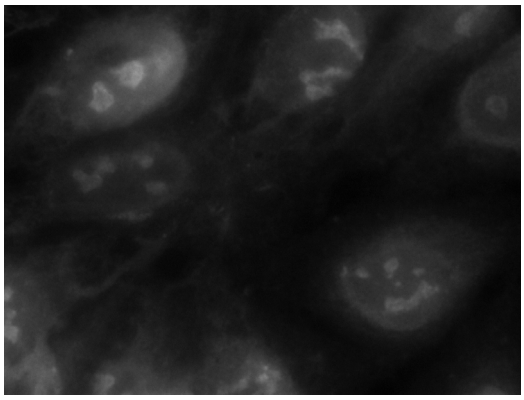

C

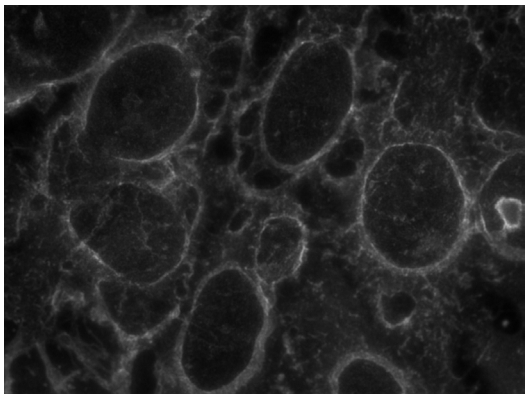

D

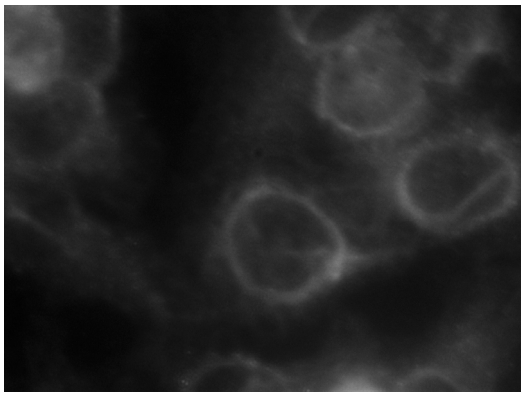

E

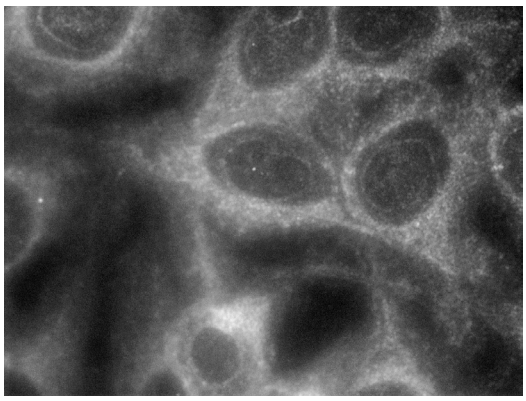

F

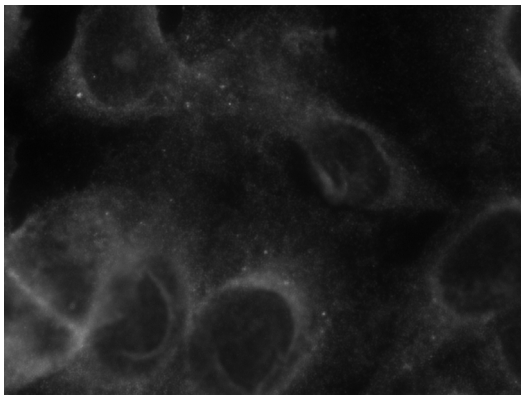

Figure 3.9 Staining of HEp-2 Slides for IgM and IgG Autoantibodies in Ttc7$^{fsn/fs}$ and GL113-treated control animals. HEp-2 cell staining for autoantibody staining patterns of untreated Ttc7$^{fsn/fsn}$ mice (A and B) and isotype control (C). A. nuclear speckled B. nuclear with cytoplasmic C. nuclear rim. Nuclear antigens typically showing these patterns include dsDNA, histones and Sm. Images are representative of staining patterns found in all animals examined. 200X

A

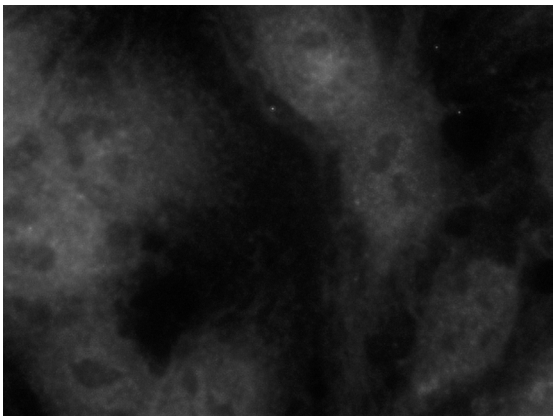

B

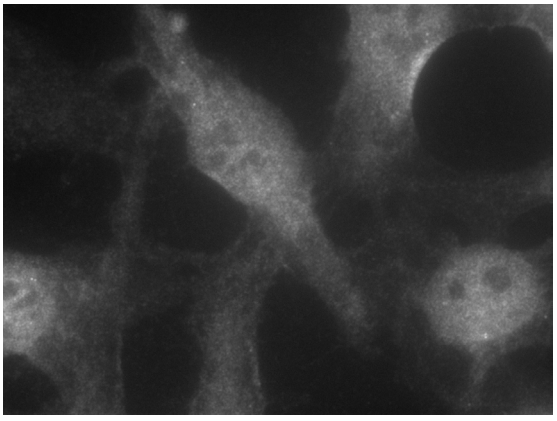

C

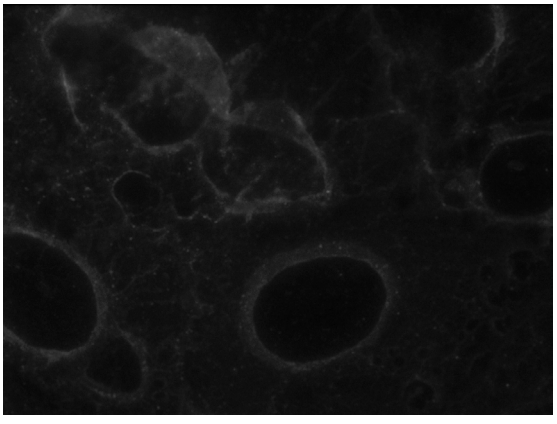

Results: Section 4: Cell Cycle Analysis of Ttc7$^{fsn/fsn}$, Stat6-/-Ttc7$^{fsn/fsn}$, and 11B11-Treated Ttc7$^{fsn/fsn}$ mice

Immune cells are programmed to proliferate when necessary in order to effect a response to an invading pathogen, and then to die off when the threat is over. These cells also proliferate during development and to maintain homeostasis of cell numbers. Thus, proliferation depends on tissue-specific programming and signals provided by extra-cellular proteins produced by other cells, which are controlled by the cell cycle to drive the cell toward a proper response (Morgan 1999 & 2007). IL-4 both drives the cell cycle to induce a proliferative response in many cell types and needs cell cycle activity to upregulate its production. The production of IL-4 depends on a naïve cell to enter into the S phase of the cell cycle upon primary activation and then enter into several rounds of cell division to maintain an IL-4 memory response. Once a memory response is established, IL-4 is produced irrespective of the stage of the cell cycle (Lohning, Richter et al. 2003).

When IL-4 binds to a cell via the IL-4 receptor, signals are transduced that activate proliferation and connect IL-4 to the cell cycle by at least two pathways. Upon phosphorylation of Stat6 and translocation to the nucleus, several cell cycle regulatory genes are upregulated including Cdc25A and members of the minichromosome maintenance (MCM) family (McDonald, Vanscoy et al. 2004). Stat6 activation also decreases the expression of p27Kip which is a cyclin dependent kinase that prevents activation of G1 cyclins and prevents progression through the cell cycle (Carey, Semenova et al. 2007). Stat6 can also bind to the same DNA target sequences as E2F proteins (Weisman, Creaner et al. 1996).

The binding of IL-4 to its receptor also activates the insulin receptor 1/2 pathway independently of Stat6, which leads to cell growth, proliferation and survival through a PI-3K dependent pathway. Proliferation through this pathway appears to function more efficiently when Stat6 is present; however, it has been shown to induce proliferation in the absence of Stat6 as well (Lohning, Richter et al. 2003).

Cell cycle defects have been shown to lead to autoimmune syndromes similar to that of Ttc7$^{fsn/fsn}$ mice (Murga, Fernandez-Capetillo et al. 2001). Since Ttc7$^{fsn/fsn}$ mice have both hyper-proliferative cells and produce high levels of IL-4 we thought it important to examine the status of the cell cycle in Ttc7$^{fsn/fsn}$ T cells. Because the production of IL-4 requires different cell cycle events at different stages of cellular differentiation and we have demonstrated that T cells are distributed differently at 4- and 10-weeks, we looked at both 4- and 10-week T cells to evaluate any changes. Additionally, having both Stat6 deficient T cells and anti-IL-4 treated T cells gave us the ability to examine the cell cycle under different conditions in order to evaluate the response. We used flow cytometry and propidium iodide staining to look at DNA content and determine the percentage of cells in G1/G0, designated as non-cycling cells, as well as the percentage of cells in S, G2 and M, which are designated as cycling cells (Carey, Semenova et al. 2007). We accomplished this by using double-stained cells and gating first on CD3+ cells (or CD4+), then on PI stained cells and gating on the appropriate peaks. An example of our gating is shown in Figure 4.1.

Figure 4.2 represents 4-week CD3+ cells with non-cycling cells in black columns and cycling cells in white. We saw significantly more cycling Ttc7$^{fsn/fsn}$ CD3+ T cells (13.76 ± 5.72%) as compared to WT (8.06 ± 2.01%, p=0.05). Hence, Ttc7$^{fsn/fsn}$ CD3+

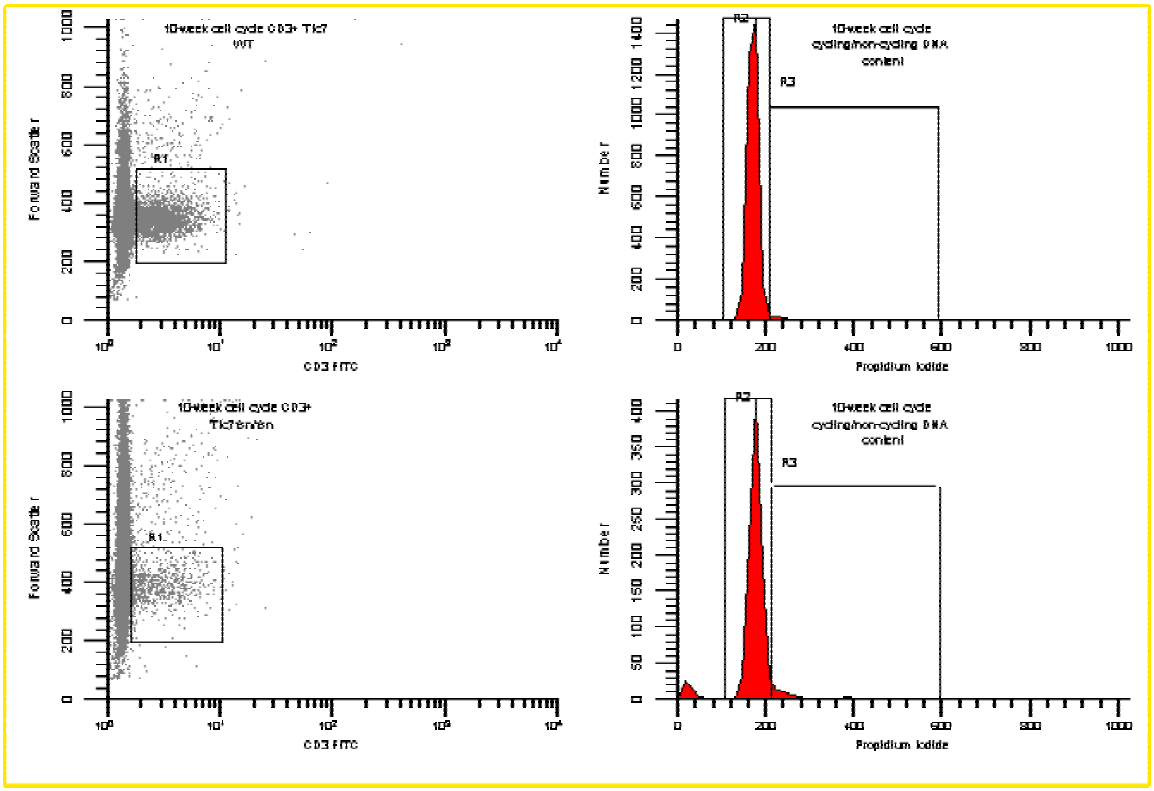

Figure 4.1. Gating Example For Cell Cycle Analysis. Splenocytes were stained with either CD3- or CD4-congugated with FITC and Propidium Iodide. The CD3+ or CD4+ population was gated on as shown (R1) and then a histogram was constructed for PI staining. 65,000 total events were recorded per sample. Gating shown pertains to Figures 4.2-4.5. All data shown is presented as mean percentage of the number of indicated experiments ± SEM.

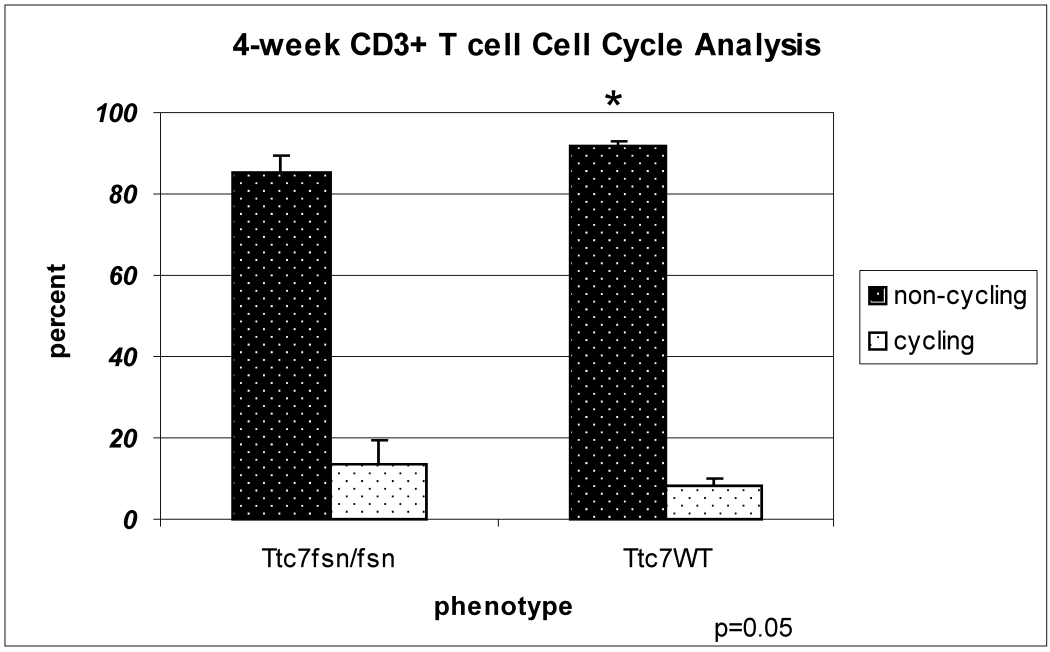

Figure 4.2. 4-Week CD3+ T cell Cell Cycle Analysis. Ttc7$^{fsn/fsn}$ CD3+ cells have a higher percentage of cycling cells (13.76 ± 5.72%) than do WT CD3+ cells (8.06 ± 2.01%). WT animals have a significantly higher percentage of non-cycling cells (91.54 ± 0.79%, p=0.05) than Ttc7$^{fsn/fsn}$ (85.19 ± 4.1%). Data was similar for CD4+ cells (not shown). N=4 for both groups.

cells had a lower percentage of non-cycling cells (85.19 ± 4.1%) than WT (91.54 ± 0.79%).

Ten-week T cell analysis is shown in Figure 4.3A&B. Here again there was a significantly higher percentage of cycling CD3+ cells (6.23 ± 1.01%) in Ttc7$^{fsn/fsn}$ cells than in WT (3.78 ± 0.4%, p=0.03)(Figure 4.3A). Thus, 4-week-old mice in both the Ttc7$^{fsn/fsn}$ and WT animals had a higher percentage of cycling cell than did 10-week mice. Figure 4.3B illustrates CD4+ cells, which follows the same trend as CD3+ cells, with some minor variation in percentages.

Stat6-/- CD3+ and CD4+ cell cycle analysis is shown in Figure 4.4A and B. At 10-weeks, Stat6-/-Ttc7$^{fsn/fsn}$ animals have a higher percentage of cycling CD3+ cells (9.9 %) than do Ttc7$^{fsn/fsn}$ Stat6 intact animals, although they show greater variability. These animals also have a dramatically elevated percentage of activated T cells, (CD62L^{hi}CD44^{hi}) which have been reported to be newly activated and dependent on the cell cycle for IL-4 production (Lohning, Richter et al. 2003). This may account for the high level of IL-4 produced by these animals and the increase in percentage of cycling cells, although the reason for the expansion of this population is unknown.

When Ttc7$^{fsn/fsn}$ mice are treated with anti-IL-4 (11B11) for seven weeks and then sacrificed at 10-weeks-of-age and analyzed, the percentage of cycling CD3+ cells (9.19 ± 0.02%) is actually higher than that of untreated Ttc7$^{fsn/fsn}$ mice (6.23 ± 1.01%)(Figure 4.5). However, when compared to the isotype control treated Ttc7$^{fsn/fsn}$ mice (14 ± 1.25%), the 11B11-treated have a lower percentage of CD3+ cycling cells, suggesting that they are responding to the neutralizing effect of anti-IL-4. Interestingly, the isotype

A

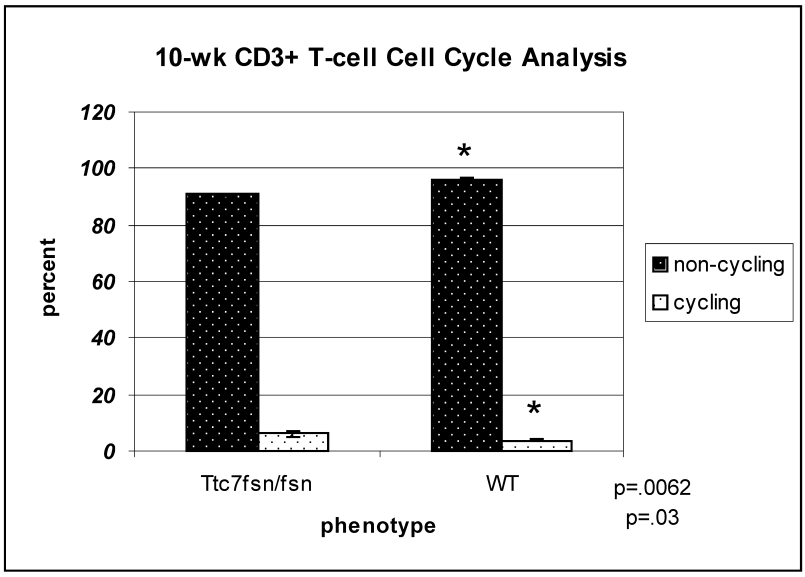

B

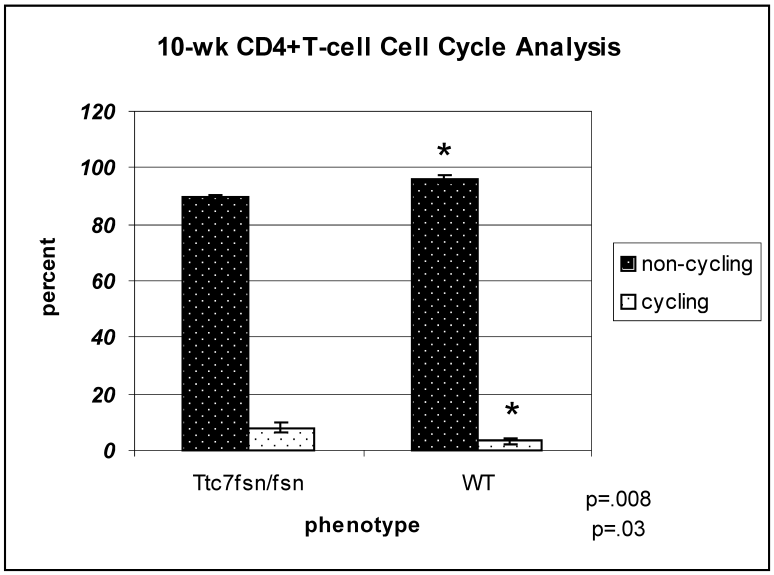

Figure 4.3. 10-Week T Cell Cycle Analysis. A. Ttc7$^{fsn/fsn}$ CD3+ cells have a significantly higher percentage of cycling cells (6.23 ± 1.01, p=0.03) than do WT CD3+ cells (3.78 ± 0.4%). Ttc7$^{fsn/fsn}$ also has a significantly lower percentage of CD3+ cells in G1 (91 ± 0.33%, p=0.0062) than WT (96 ± 0.88%). B. Ttc7$^{fsn/fsn}$ mice also have a significantly higher percentage of cycling CD4+ cells (7.9 ± 1.8, p=0.03) than do WT (3.32 ± 1.0%). N=5 for all groups.

A

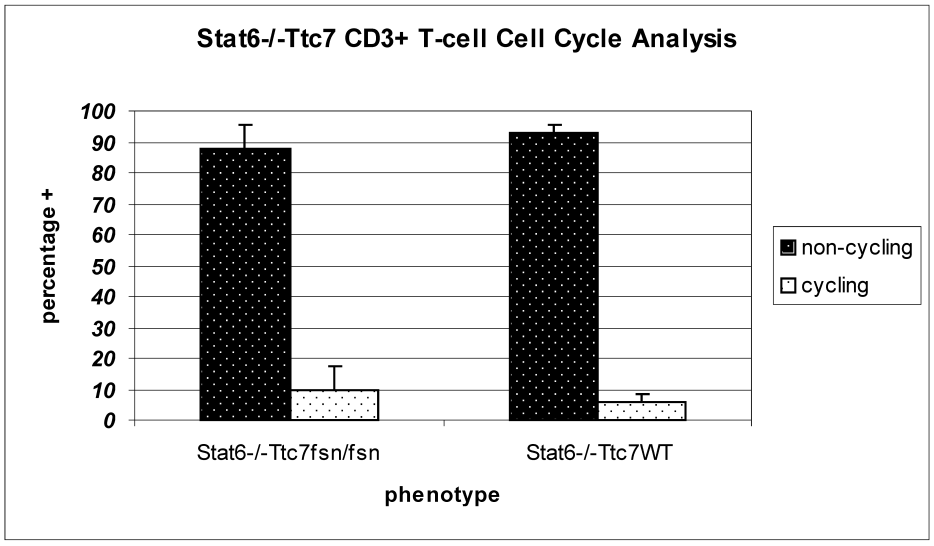

B

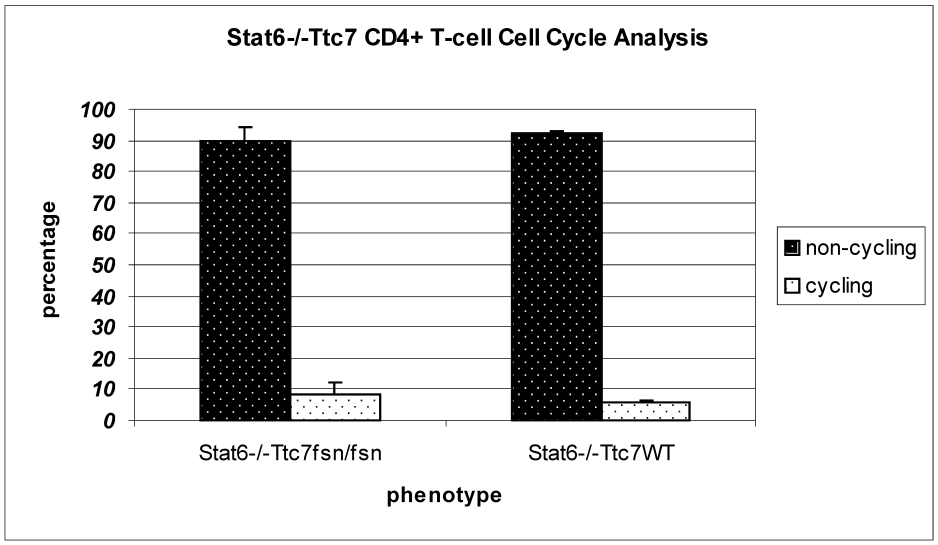

Figure 4.4. Stat6-/-Ttc7 T Cell Cycle Analysis. 10-week Stat6-/-Ttc7$^{fsn/fsn}$ and Stat6-/-Ttc7WT cell cycle analysis. A. Stat6-/-Ttc7$^{fsn/fsn}$ CD3+ cells have a higher percentage of cycling cells (9.9 ± 7.3%) than do Stat6-/-Ttc7WT CD3+ cells (5.6 ± 2.7%). B. Stat6-/-Ttc7$^{fsn/fsn}$ also had a higher percentage of cycling CD4+ cells (8.1 ± 4.4%) than did Stat6-/-Ttc7WT CD4+ cells (6.03 ± 0.45%). N=4 for all groups.

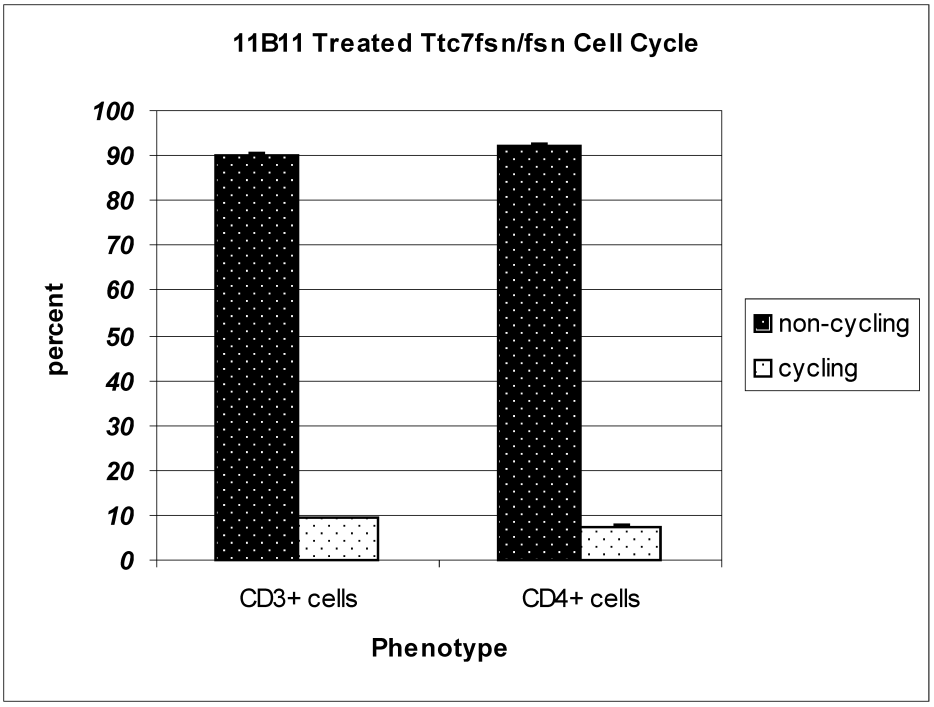

Figure 4.5. 11B11-Treated T Cell Cycle Analysis. Treated animals were sacrificed at 10-weeks, after 7 weeks of treatment with anti-IL-4 and splenocytes were stained for cell cycle analysis. The percentage of cycling CD3+ cells (9.19 ± 0.02%) and cycling CD4+ cells (7.6 ± 0.2%) was similar to untreated Ttc7$^{fsn/fsn}$ (see Figure 4.3). n=5

control-treated mice, have a higher percentage of activated CD3+ cells than do the 11B11-treated, which have a higher percentage of activated CD3+ than the untreated. Even though the antibody was filter-sterilized and tested for contaminants, it is possible that the increase in activation of T cells may be a result of treatment with a rat antibody which can prove to be antigenic in mice.

When comparing all of these groups directly, as shown in Table 4.1 for clarity, we can see a few trends in these data.

Comparison of Ttc7$^{fsn/fsn}$ CD3+ Cells Under Different Conditions

group	G1/G0	S/G2/M
4-week	85.19 ± 4.1	13.76 ± 5.72
10-week	91 ± 0.33	6.23 ± 1.01
Stat6-/-	87.8 ± 7.6	9.9 ± 7.3
11B11	90.03 ± 0.3	9.19 ± 0.02
GL113	80.02 ± 0.86	14.03 ± 1.25

Table 4.1. Comparison of CD3+ Cell Cycle Data

Under the different conditions listed above, the cell cycle, as measured by DNA content, appears to be responding to the changes in ways that can be explained by the activation state of the CD3+ cells. An increase in cycling correlates with an increase in T cell activation state, particularly of the CD62L^{hi}/CD44^{hi} phenotype. We would expect this to be an IL-4 producing population, which at the "activated" stage of cell maturity would still require the cell cycle for IL-4 production. Although Stat6 has been identified as decreasing the cell cycle inhibitory protein p27kip, which seems contrary to the increase in cycling in the Stat6 deficient group, IL-4 is still produced at extremely high

levels and the percentage of CD3+ activated T cells is the highest seen here. Therefore we can imagine that one of the other pathways activated by IL-4, such as the IRS-1/2 pathway, may make up for the deficiency in Stat6. Thus, it appears that the cell cycle in Ttc7$^{fsn/fsn}$ mice is being regulated and responding to changes, however at a higher level of activation than in WT animals.

Results: Section 5: Assessment of Autoimmunity in Ttc7$^{fsn/fsn}$, Stat6-/-Ttc7$^{fsn/fsn}$, and 11B11-Treated Ttc7$^{fsn/fsn}$ Mice: Renal Disease

Stat6-/-Ttc7$^{fsn/fsn}$ mice have increased proteinuria and more severe kidney pathology than Ttc7$^{fsn/fsn}$ Stat6 intact mice, whereas, anti-IL-4 treated mice have improved proteinuria and milder kidney disease

Clinicians and researchers have long used increased urine protein levels as a marker of more severe renal disease in systemic autoimmunity as kidney failure has traditionally been one of the major consequences and outcomes of severe systemic autoimmune disease (Daikh 2001; Bagavant, Deshmukh et al. 2006). As the kidney becomes more diseased, capillaries in the glomeruli become "leaky" and allow serum protein into the urine. This can then be measured using commercially available colorimetric urinalysis. Mild renal disease is defined as proteinuria under 100 mg/mL, with advanced disease measuring over 100 mg/mL (Daikh 2001).

To assess potential kidney pathology, we measured proteinuria in the urine of Stat6-/- animals between 10- and 16-weeks old, and 11B11 and isotype controls at the end-point of treatment at 10-weeks old. All measurements taken of Ttc7$^{fsn/fsn}$ mice (n=12)

were between 30 mg/mL and 100 mg/mL starting at 7-weeks throughout their remaining lifespan. These numbers classify Ttc7$^{fsn/fsn}$ mice as having "mild disease." Interestingly, as these animals advanced in age, proteinuria didn't rise above 100 mg/mL even when their urine output became negligible; consistent with the findings of Daikh and Wofsy, (2001), who had to end their study due to inadequate urine output for further assessment.

Stat6-/-Ttc7$^{fsn/fsn}$ (n=14) mice exhibited advanced to severe disease (over 300 mg/mL) based on proteinuria measurements. Figure 5.1A-C presents data of several individual mice collected at approximately 2-week intervals starting at 10-weeks old. All of the Stat6-/-Ttc7$^{fsn/fsn}$ mice had proteinuria measuring above 100 mg/mL, with several over 300 mg/mL, and even over 1000-2000 mg/mL. The animals with the highest proteinuria measurements died within 1-2 weeks after urinalysis. Stat6-/-Ttc7WT (n=12), as well as Ttc7WT Stat6 intact mice (n=8) consistently had measurements between 0 and trace (10 mg/mL) amounts, except for one Stat6-/-Ttc7WT (#880, B&C) which measured 65 mg/mL throughout the time-course.

The anti-IL-4 treatment appeared to have a mild effect on the amount of proteinuria in Ttc7$^{fsn/fsn}$ mice as only one individual (#1488) in the treatment group (n=5) measured above 30 mg/mL (Figure 5.2). All of the isotype control mice (n=4) were unchanged from that of untreated Ttc7$^{fsn/fsn}$ mice (65 mg/mL).

Figure 5.1. Stat6-/-Ttc7 Proteinuria. Urine was tested with commercial protein detection strips at 2 week intervals for several mice as indicated by animal number for 3 test periods. Stat6-/-Ttc7$^{fsn/fsn}$ and Ttc7$^{fsn/fsn}$ mice are identified with gray arrows below the animal number. A. First test period indicated that Stat6-/-Ttc7$^{fsn/fsn}$ mice had elevated levels of proteinuria, with 2 mice testing for severe renal disease (#850 and # 815). Stat6-/-Ttc7WT tested all had negative readings. Ttc7$^{fsn/fsn}$ mice had consistent measurements of between 30 and 100 mg/mL. B. Test period 2 weeks after A. Mice #850 and 815 had died. Several mice measured previously had elevated levels. New mice were added to test group to replace deceased animals. One Stat6-/-Ttc7WT animal (#880) tested positive for proteinuria, but measurement was under 100 mg/mL. C. Two weeks after test period in B. Some Stat6-/-Ttc7$^{fsn/fsn}$ animals remained at constant but high levels of proteinuria, while 2 mice had elevated levels. One of the animals with elevated proteinuria died immediately after the test period (#869). Mouse number 880 remained constant from 2 weeks prior. One Ttc7$^{fsn/fsn}$ had died over the two-week interval.

A

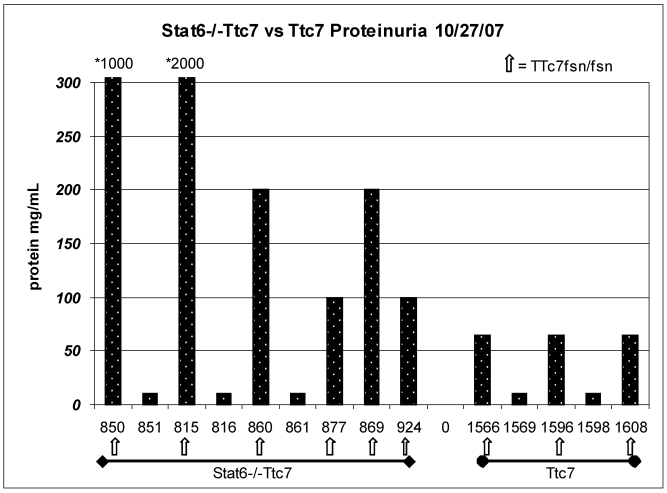
Stat6-/-Ttc7 vs Ttc7 Proteinuria 10/27/07
*1000
*2000
⇧ = TTc7fsn/fsn
protein mg/mL
300
250
200
150
100
50
0
850 851 815 816 860 861 877 869 924 0 1566 1569 1596 1598 1608
Stat6-/-Ttc7
Ttc7

B

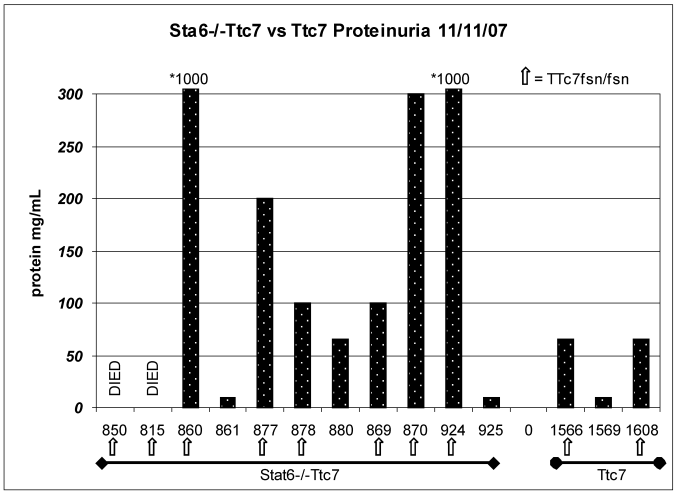
Sta6-/-Ttc7 vs Ttc7 Proteinuria 11/11/07
*1000
*1000
⇧ = TTc7fsn/fsn
protein mg/mL
300
250
200
150
100
50
0
DIED
DIED
850 815 860 861 877 878 880 869 870 924 925 0 1566 1569 1608
Stat6-/-Ttc7
Ttc7

C

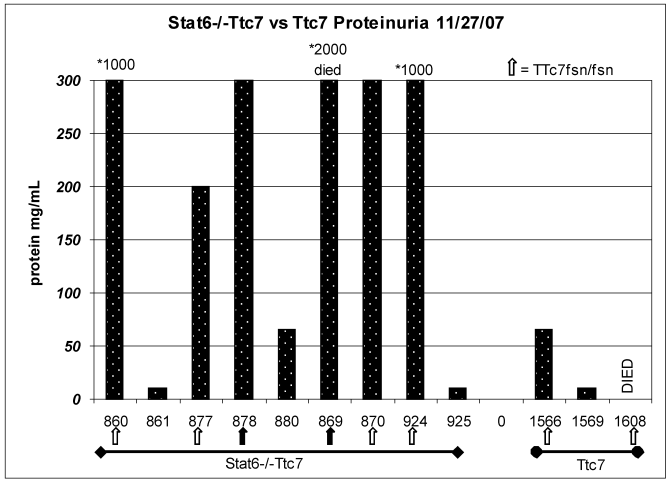
Stat6-/-Ttc7 vs Ttc7 Proteinuria 11/27/07
*1000
*2000
died
*1000
⇧ = TTc7fsn/fsn
protein mg/mL
300
250
200
150
100
50
0
DIED
860 861 877 878 880 869 870 924 925 0 1566 1569 1608
Stat6-/-Ttc7
Ttc7

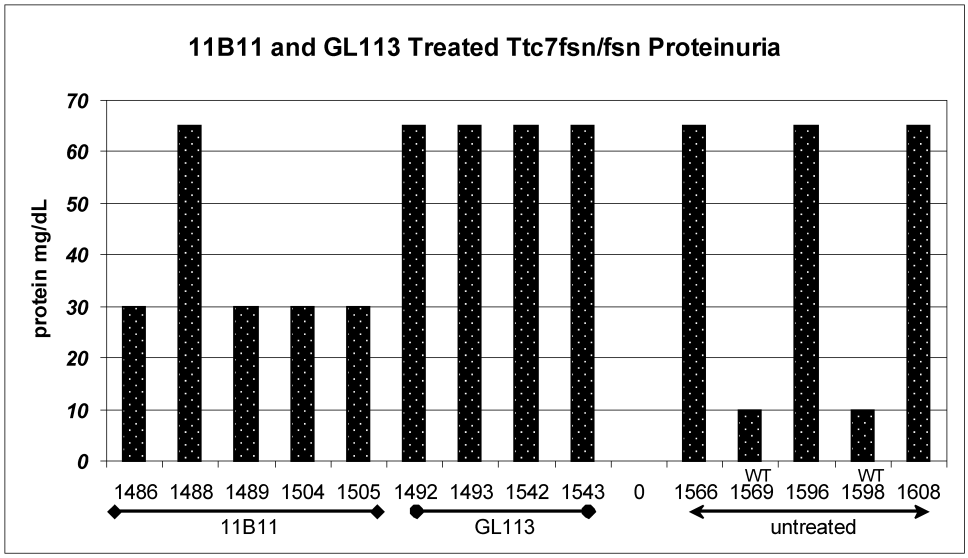

Figure 5.2. 11B11-Treated Ttc7$^{fsn/fsn}$ Proteinuria. Urine from 10-week animals was tested with commercial protein detection strips before sacrifice. 4 out of 5 11B11 treated animals had reduced proteinuria (30 mg/mL) from isotype controls and untreated Ttc7$^{fsn/fsn}$. Isotype controls and untreated values were comparable.

Ttc7$^{fsn/fsn}$ mice have membranoproliferative-glomerulonephritis which increases in severity with the deletion of Stat6

Pathologies of the kidney arise from a variety of maladies such as infection, diabetes, drug reactions and vascular disease, but kidneys are particularly prone to immunological disorders compared to other organs and have been useful in monitoring the progression of immunological disease such as autoimmune diabetes and SLE. In general, there is not a direct one-to-one relationship between a particular mechanism of damage and a histological appearance or clinical syndrome, but glomerular damage can give rise to five clinical syndromes within which a particular glomerular disease may be more commonly associated. SLE, or systemic autoimmune disease, spans all five clinical syndromes and has been associated with deposits of most classes of immunoglobulins and many complement components at any site in the glomerulus (Stevens, Lowe et al. 2002). Recently, immune cell infiltrates, particularly T cells, have been shown to be an important part of the disease process through the local production of cytokines and inflammation (Daikh 2001; Bagavant, Deshmukh et al. 2006).

To assess the type and extent of kidney disease in Ttc7$^{fsn/fsn}$ mice, Stat6-/-Ttc7$^{fsn/fsn}$, and anti-IL-4 treated mice, kidneys from these and WT controls were harvested immediately upon sacrifice and fixed in 4% paraformaldehyde or 10% formalin for PAS and H&E staining. We sent the fixed kidneys, identified only by number, to Dr. Harini Bagavant at the University of Virginia, Division of Rheumatology and Immunology Specialized Center of Research on Systemic Lupus Erythematosus, for staining and blind scoring for kidney disease as described in Bagavant et al., 2006. The images presented herein were supplied by Dr. Bagavant.

Figure 5.3 presents representative images of Ttc7$^{fsn/fsn}$ kidney from 15-week-old mice with membranoproliferative-glomerulonephritis. This type of GN is identified by the thickening of the capillary walls and basement membrane caused by interposition of mesangial cytoplasm into the peripheral capillary loop. This is thought to be in response to subendothelial immune complex deposition which causes new matrix to be laid down resulting in the replication of basement membrane material (Stevens, Lowe et al. 2002). This results in the loops of the glomeruli becoming more globular and enlarged, reducing the urinary space of the Bowman's capsule. The inflammatory cells of this type of GN are seen in the medulla of the kidney instead of the glomeruli as shown in the bottom image.

The next figure (Figure 5.4) focuses on some of the cell types found which included F4/80+ macrophages, CD11c+ dendritic cells, CD5+ T cells, and B220+ B cells. Dr. Bagavant pointed out the unusual presence of dendritic cells and macrophages inside the glomeruli and suggested these may be the pathogenic cells.

It is interesting to note that this type of kidney disease is often associated with normocytic, normochromic anemia, which is exhibited by Ttc7$^{fsn/fsn}$ mice (Beamer, Pelsue et al. 1995), although a specific mechanistic connection has not been identified. In humans, this type of GN is also often associated with hypocomplementemia and a circulating autoantibody identified as C3 nephritic factor, which binds to the C3 convertase of the alternative complement pathway (www.gamewood.net/rnet/renalpath/ch1.htm: site of the University of North Carolina Nephropathology Laboratory).

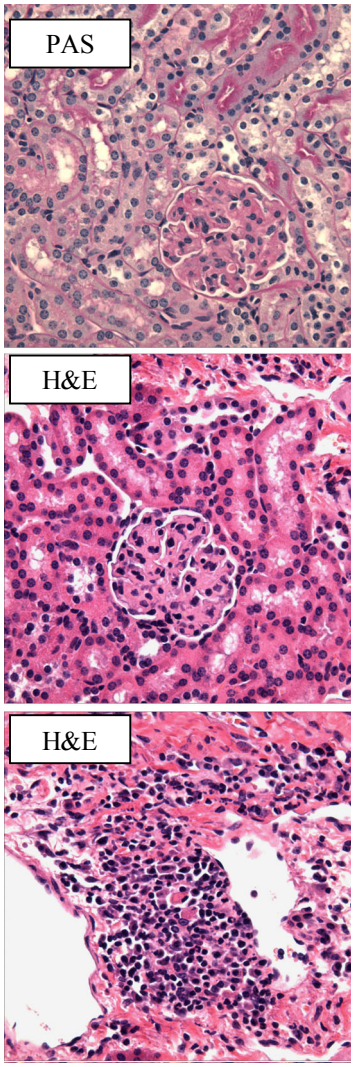

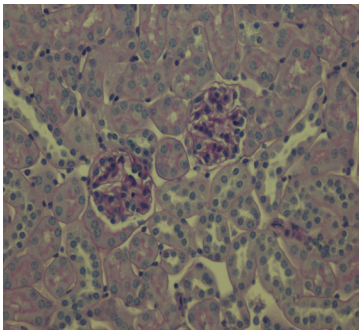

PAS staining of WT: negative for GN

Figure 5.3. Ttc7$^{fsn/fsn}$ Kidney Sections: Membranoproliferative-Glomerulonephritis. The images on the left are from mouse 1356. The glomeruli look like a textbook picture of Membranoproliferative GN. (Lots of mesangium – but little immune cell infiltration). The major distinction from other SLE is the lack of inflammatory infiltrates and the normal looking Bowman's capsule as well as tubules and interstitium. The bottom left picture shows a foci of inflammatory cells in the medulla – seen in all the mice. Areas like these stain for the immune cells shown in Figure 5.4.
Author's note: PAS and H&E stained kidney sections from 20-week Ttc7$^{fsn/fsn}$ mice as indicated in the image. The images and explanation included for the images was written by Dr. Harini Bagavant as indicated in the text. The section in the right column is a Ttc7WT animal without kidney disease for comparison. 200X

Figure 5.4. Immunofluorescent Staining of Kidney Sections. The images below are from Mouse no. 1356 and two pictures from mouse F1337 /F1377. Stained for macrophages (F4/80), dendritic cells (CD11c), T (CD5) and B (B220) cells. Patterns of staining in F1356 were typical and also seen in the other mice F1354, F1362. All the cell types were seen in the medullary regions. T, B and CD11c were seen mainly near large blood vessels in the medulla. Macrophages were abundant in the medullary interstitium – and not only restricted to the peri-vascular regions.T and B cells were infrequent in the cortex. Few T cells were seen near /around glomeruli.CD11c were a little more frequent and seen in the cortical interstitium – mainly around glomeruli. In mouse 1337, CD11c cells were seen INSIDE several glomeruli (one example in the picture). Another very striking feature was that F4/80 macrophages were abundant in the cortex. In our SLE mice we have rarely /almost never seen glomerular infiltration on F4/80+ cells into the glomeruli. However, in these, cells were present infrequently in F1356, but 1337 showed a lot of glomeruli with F4/80+ cells. The lack of T and B cell infiltrates and the presence of CD11c and F4/80 + cells in the gloms is very exciting – especially since you have found that these mice have immune complex deposits. I have not tried double staining on these mice yet but CD11c and F4/80 double positive cells have been described in the kidney in other models and it would be interesting to see if they are the pathogenic cells here.

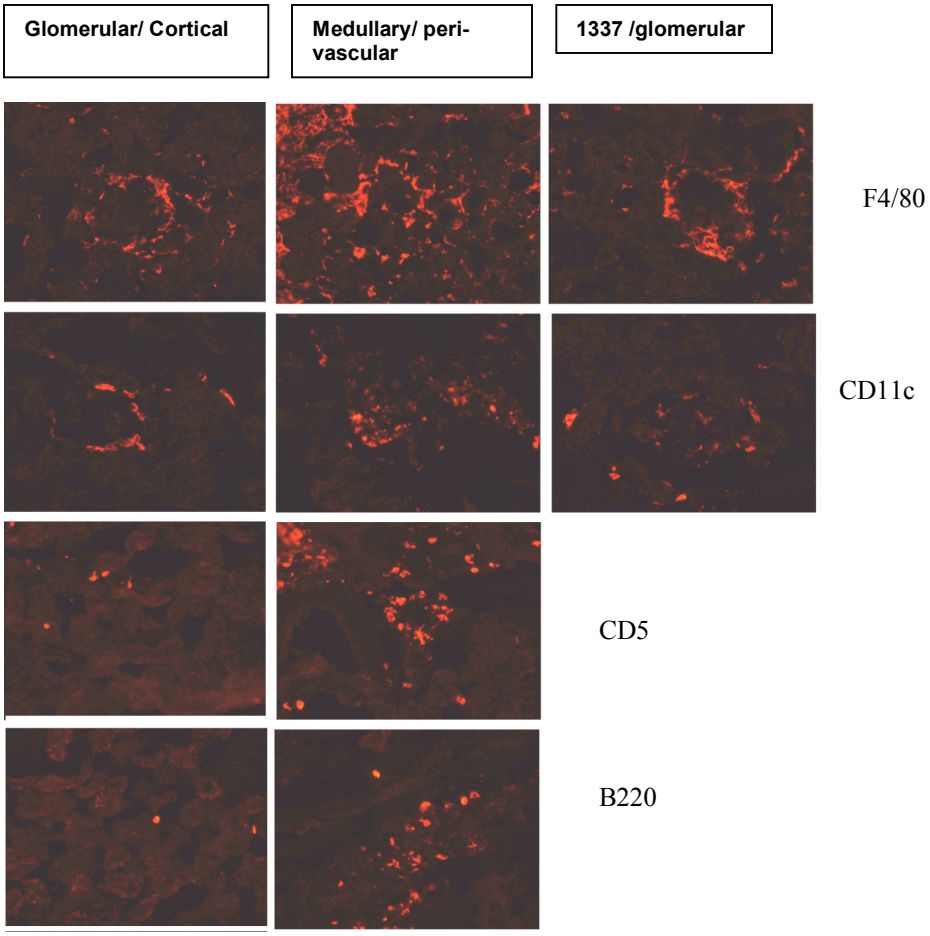

Author's note on Figure 5.4: Fluorescently stained sections above are from the same animals as in Figure 5.3, stained for individual cell types. Explanation in the caption on preceding page and images were provided by Dr. Bagavant. 200X

Figure 5.5 is H&E staining and representative of renal disease found in Stat6-/-Ttc7$^{fsn/fsn}$ (#793 and #797) mice. In images #793 and 797 the thickening of the glomeruli and lobular appearance of the mesangium can clearly be seen. The urinary space of the Bowman's capsule is almost completely gone. Dr. Bagavant indicated that these looked much like the Ttc7$^{fsn/fsn}$ sections and classified them as having more severe glomerular disease (rated 2-3+). The center image, #796, is actually a Stat6-/-Ttc7WT animal (rated 0-0.5+), which showed some mild mesangial changes in some of the glomeruli. Proteinuria information is not available for this animal, but only one Stat6-/-Ttc7WT (n=12) had elevated urine protein. No signs of renal disease or proteinuria have been reported in the literature for Stat6-/- animals of any strain, therefore the mesangial changes may be due to individual variation. It is important to note that the Stat6-/- mice analyzed here were 10-weeks old, hence younger than the Ttc7$^{fsn/fsn}$ above.

Figure 5.6 is PAS staining of 11B11-treated mice on the left and isotype control mice (GL113) on the right. Evidence of glomerular disease was seen in all images, with mesangial proliferation, dilated capillary loops and cellular infiltration. However, slightly less severe changes were evident in the 11B11-treated animals on the left (rated 1+) who exhibited a decrease in cellularity as compared to those on the right (rated 1.5-2+). Therefore, 11B11-treated mice had slightly milder renal disease than the isotype controls, which correlated with the lower proteinuria measurements.

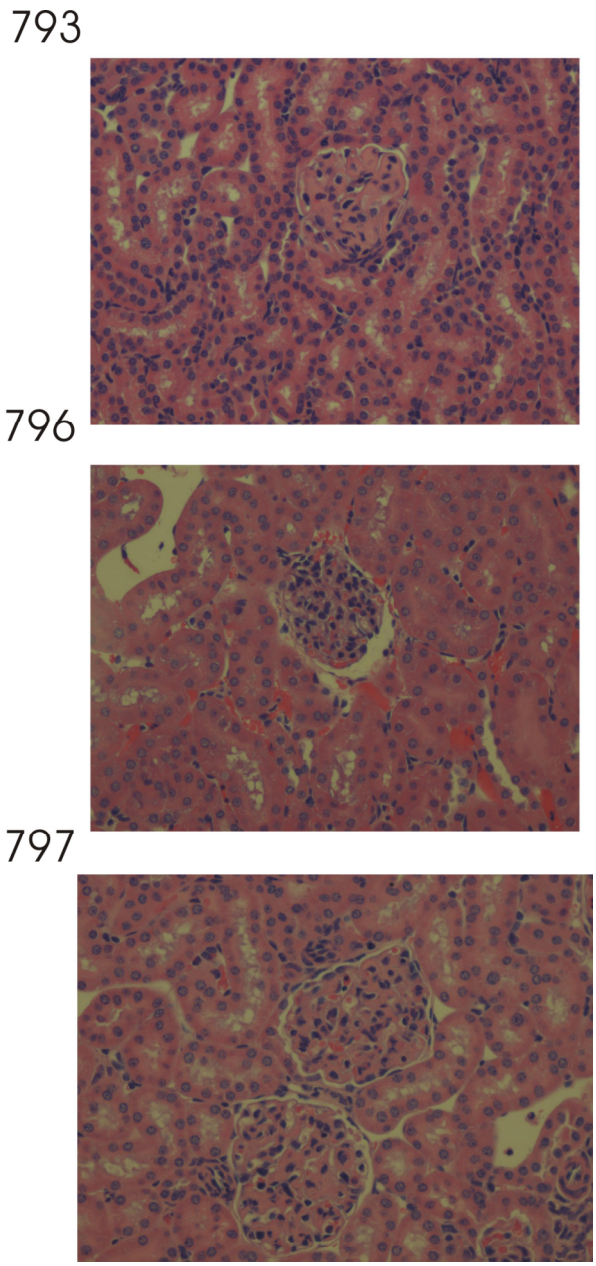

Figure 5.5. H and E Staining of Stat6-/-Ttc7 Kidney Sections. Sections from Stat6-/-Ttc7$^{fsn/fsn}$ (#793 and #797) and Stat6-/-Ttc7WT (#796) kidney stained with H&E. Both Stat6-/-Ttc7$^{fsn/fsn}$ sections show severe glomerular disease as scored by Dr. Bagavant with severity index scores of 2-3+. The increased cellularity, lack of Bowman's space, and thickened mesangium can clearly be seen in the images. #796 had some mild GN; only a few glomeruli had mesangial changes. This section rated a severity index of 0-0.5+. 200X

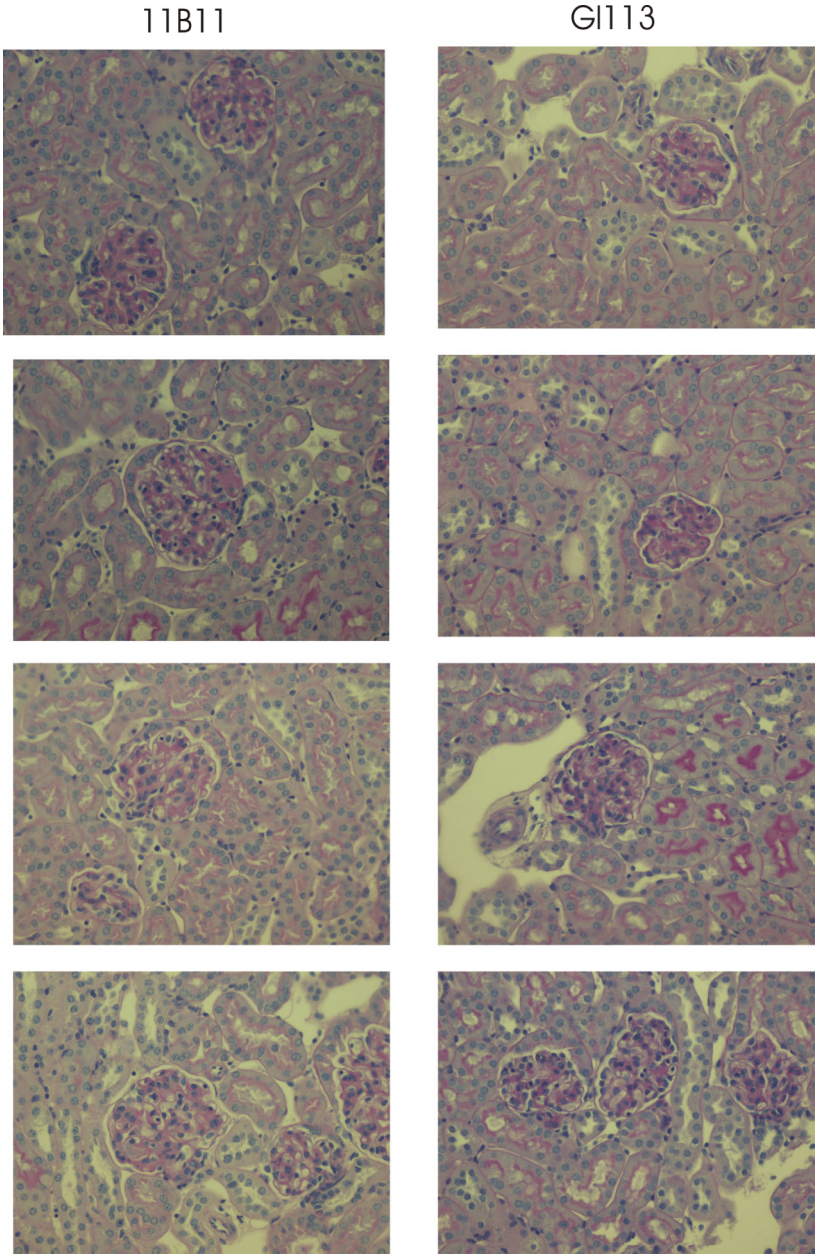

Figure 5.6. PAS Staining of 11B11- and GL113-Treated Ttc7$^{fsn/fsn}$ Kidney Sections. Sections from 10-week 11B11-treated on the left and GL113 isotype-control-treated animals on the right. All sections were stained with PAS. Two animals are shown from each group as representative sections from all animals analyzed with similar results and scores. All of the 11B11-treated animals scored a 1+ on the severity index for mesangial thickening and cell infiltration but had fewer than 100% of the glomeruli effected. The GL113-treated animals all scored 1.5+ except for one which had a score of 2+ for more glomeruli involved, increased cellularity and infiltration and more mesangial thickening than the 11B11 mice. The lobular appearance of the glomeruli capillary loops can be seen clearly with PAS staining. 200X

Thus, from these data, it appears that the lack of Stat6-/- in Ttc7$^{fsn/fsn}$ results in an increase in the severity of autoimmunity as measured by renal disease. The neutralization of IL-4 results in a slight decrease in the severity of autoimmunity. Therefore we suggest that Ttc7$^{fsn/fsn}$ mice exhibit an autoimmune syndrome that is phenotypically-driven by IL-4 due to the background genetic effects of the Th2-skewed Balb/c strain, and results from the dysregulated activation of lymphocytes due to the defective Ttc7 gene. We further suggest that Ttc7 functions to negatively regulate lymphocyte activation and cytokine production and when the downstream inhibitory action of Stat6 is removed in the Stat6 deficient animals, IL-4 production becomes elevated and increases the severity of the pathology. The question of whether Ttc7 and Stat6 interact remains to be answered when the tools for the study of Ttc7 become more readily available for such analysis. However, these data suggest the possibility that Stat6 and Ttc7 may function in a similar or complementary fashion as when both are deficient we see more lymphocyte activation and proliferation, and more autoimmune pathology.

DISCUSSION

Since IL-4 has been shown to have a protective effect on B cells by increasing their survival and proliferative capacity thus contributing to autoimmune disease, and because Stat6 is unique to the IL-4 signaling pathway (Morris, Dragula et al. 2002), the first aim of this thesis was to examine the behavior of Stat6 in Ttc7$^{fsn/fsn}$ lymphocytes to determine the downstream effects of IL-4 signaling. We sought to ascertain whether there is defective signal transduction regulation downstream of the IL-4 receptor in Ttc7$^{fsn/fsn}$ B cells or if overproduction of IL-4 is responsible for the constitutive activation of Stat6. Whereas Ttc7$^{fsn/fsn}$ mice have highly elevated levels of IL-4 we hypothesized that if B cells possessed the inherent ability to deactivate Stat6 when the IL-4 signal was removed (*ex vivo*), then it was likely that the overproduction of IL-4 was driving the autoimmune phenotype of Ttc7$^{fsn/fsn}$.

Preliminary work indicated that Stat6 appeared constitutively activated in 8-week Ttc7$^{fsn/fsn}$ splenic lymphocytes (Welner, Hastings et al. 2004) and (Figure 1.1 and 1.2). Stat6 exists as a latent transcription factor present in the cytoplasm in an inactive monomeric state in IL-4 responsive cells. Upon binding of IL-4 to the IL-4 receptor, Stat6 becomes phosphorylated, forms a homo-dimer with another phosphorylated Stat6 and translocates to the nucleus where it will bind to its recognition sequence on DNA. Here, it cooperates with other transcription factors to initiate transcription of IL-4 responsive genes such as MHC class II, CD23, germline IgE and IgG1, and the IL-4Ra chain. Thus, Stat6 normally becomes activated in the cytoplasm, but is only functional when it has translocated to the nucleus. Daines et al (Daines, Andrews et al. 2003) recently showed that Stat6 is sequestered in the cytoplasm by a detergent-sensitive factor

which may involve the serine phosphorylation of Stat6 mediated through inhibition of protein phosphatase 2A (PP2A). When PP2A is active, the serine is unphosphorylated and Stat6 is able to bind to DNA (Woetmann, Brockdorff et al. 2003). When released, Stat6 is able to enter the nucleus, where it binds to DNA and exerts its influence on gene transcription, then becomes inactivated (dephosphorylated) and is shuttled back to the cytoplasm where it can be recycled for another round of activation. Thus, the overall levels of Stat6 appear to remain stable, but the amount of the activated phosphorylated Stat6 will change with the activation state of the cell. Recently it has been determined that the life cycle of Stat6 is dependant on the duration of the IL-4 signal received and that the shuttling of Stat6 back to the cytoplasm allows for reactivation if continued signaling is present (Andrews, Ericksen et al. 2002).

In experimental models of constitutively expressed Stat6, Stat6 remained phosphorylated even in the absence of IL-4 (Bruns and Kaplan 2006). There existed an exaggerated Th2 cytokine response as well as an increase in IgE and IgG1 antibodies as is the case with Ttc7$^{fsn/fsn}$ mice. T cells appeared to be hyperactivated in the Stat6 transgenic but the researchers concluded that B cells were not as they did not hyperproliferate in response to a mitogen. They indicated that both the bone marrow and thymus showed normal lymphocyte development (Bruns, Schindler et al. 2003; Bruns and Kaplan 2006). Previous work by our group on Ttc7$^{fsn/fsn}$ mice has shown that both splenic T and B cells show enhanced proliferation, increased size, increased surface MHC class II on B cells, and an increase in protein production suggesting that, unlike the Stat6 transgenic, both populations are hyperactivated (Welner et al. 2004). Therefore it

was important to examine the regulation of Stat6 in Ttc7$^{fsn/fsn}$ mice and tease out the contributions that IL-4 and Stat6 make to the phenotype of Ttc7$^{fsn/fsn}$ autoimmunity.

B cell hyperactivation and response to IL-4 was studied by evaluating the expression and function Stat6. Initially, expression levels of phosphorylated and total Stat6 were analyzed as a measure of lymphocyte activation by IL-4 using immunoprecipitation and Western blot and comparing stimulated cells to unstimulated cells. Finding that Stat6 was constitutively activated even without stimulation by exogenous IL-4, we next sought to determine if there was a functional defect maintaining the phosphorylation and activation of Stat6.

Intra-cellular fluorescent staining of Stat6 and the nucleus in purified splenic B cells and visualization with confocal microscopy allowed us to follow the functional translocation of Stat6 to the nucleus to confirm the co-localization of activated Stat6 with the nucleus and the resulting association of localization with activated cells (Figures 1.4 and 1.5). This determined that Stat6 was responding to activation signals by IL-4 as even though the Ttc7$^{fsn/fsn}$ cells had a higher percentage of activated cells without stimulation, the number increased upon stimulation to a level similar to WT although with an altered response curve. The curve exhibited by Ttc7$^{fsn/fsn}$ B cells was reminiscent of previously activated B cells as shown by Andrews et al (Andrews, Ericksen et al. 2002) describing the life cycle of Stat6. They determined that activation and translocation of Stat6 to the nucleus was dependent on the shuttling of Stat6 out of the nucleus, thereby limiting the amount of phosphorylated Stat6 “allowed” in the nucleus at any one time. Therefore, in previously activated B cells which would have a certain amount of pStat6 already occupying the nuclear compartment, the timing of the translocation of newly activated

Stat6 to the nucleus would appear to be delayed from that of previously unstimulated cells.

The inactivation or turnover of Stat6 is an important step in the regulation of gene transcription. Inability to de-activate or inhibit Stat6 activation could result in an uncontrolled activation signal leading to hyperactivation of cells. To study this possibility, negatively selected, magnetically purified B cells were activated with IL-4 and assayed immediately after stimulation and at various time points after washing cells of residual, exogenous IL-4 and then visualized with confocal microscopy to evaluate the kinetics of de-activation (Figures 1.6 and 1.7) . Differences in the fall-off characteristics between Ttc7$^{fsn/fsn}$ and WT cells provided us with information regarding the inherent ability of Ttc7$^{fsn/fsn}$ B cells to downregulate IL-4 signals in the absence of IL-4 stimulus. Our analysis of Stat6 activation in Ttc7$^{fsn/fsn}$ showed that Ttc7$^{fsn/fsn}$ B cells were able to deactivate Stat6 when the IL-4 signal was removed suggesting that an inherent B cell defect of Stat6 regulation was not maintaining Stat6 phosphorylation but that IL-4 was driving the hyperactivation of Stat6. It was interesting to note the difference in the curve of Stat6 decay in Ttc7$^{fsn/fsn}$ B cells, which suggested a sharper initial drop than WT. This also mirrors the behavior of previously activated B cells as shown by Hanson et al (Hanson, Dickensheets et al. 2003) and was most likely due to the activation of Ttc7$^{fsn/fsn}$ cells in vivo.

The information gathered above was then correlated to immunohistofluorescently stained Ttc7$^{fsn/fsn}$ and WT splenic sections to evaluate the cellular activation on a structural level (Figure 1.8). Overall, the amount of staining of total Stat6 in the spleen is similar between Ttc7$^{fsn/fsn}$ and WT, but, as is shown in Figure 1.9, there is an increase in

the number of follicles with phosphorylated Stat6 in Ttc7$^{fsn/fsn}$ mice as well as an increase in the amount of phosphorylated Stat6 within the follicles. The phospho-Stat6 coincides with areas of newly arrived B cells and plasmablasts which are usually outside of the follicle (Mattsson, Duzevik et al. 2005; William, Euler et al. 2005); however, due to the altered architecture of the Ttc7$^{fsn/fsn}$ spleen, these B cells are inside what is left of the follicle in an area where they would be able to interact with T cells. When this is then compared to the IL-4 staining of the spleen (Figures 1.10 and 1.11), we find IL-4 being expressed in these same areas. Thus, it is possible that immature B cells are interacting with T cells at an inappropriate time in development, in an IL-4-rich environment which may enhance their survival and allow for autoreactive B cells to mature into autoantibody producing cells.

Ttc7$^{fsn/fsn}$ mice display an increase in the ratio of CD4^{+} to CD8^{+} T cells in the spleen as compared to WT (Pelsue, Schweitzer et al. 1998) which may likely contribute to the increased levels of IL-4 found in Ttc7$^{fsn/fsn}$ serum and spleen (Figure 1.10 and 1.15). IgM^{+} B cells are also increased, providing an abundant target for the IL-4 released by local T cells. As Ttc7$^{fsn/fsn}$ mice age, we see increasingly disrupted splenic architecture, positioning cells in locations where they may not normally be found thus subjecting them to factors in an untimely and/or at an abnormal level which may result in altered tolerance induction and survival (al-Janadi and Raziuddin 1993).

This study shows that Ttc7$^{fsn/fsn}$ splenic B cells exhibit high levels of activated Stat6 without additional stimulation, but upon stimulation with exogenous IL-4 they follow similar activation trends as wild type (WT) cells. In addition, when these cells are stimulated with IL-4, washed and allowed to rest, Stat6 becomes deactivated in the

nucleus and returns to the cytoplasm in a similar manner to WT. It is important to note that there have been no mutations or polymorphisms associated with the Ttc7$^{fsn/fsn}$ mouse at the "Th2" locus on mouse Chromosome 11 which includes the genes for IL-4, IL-5 and IL-13 nor at the Stat6 locus on mouse Chromosome 10, therefore, we conclude that Stat6 is hyper-activated due to continuous IL-4 signaling and not to inherent defects in Stat6 regulation.

T cell activation and IL-4 production

IL-4 production is regulated in a positive feedback manner in which the presence of IL-4 and IL-4 receptors stimulate more IL-4 to be produced as well as more IL-4 receptors to be upregulated on the cell surface (Dorado, Jerez et al. 2002; Harris, Goodrich et al. 2005). The primary stimulus initiating IL-4 production and the cell type that produces it is an area of intense research with general agreement being that various subtypes of T cells play a big part in production and that skewing towards a Th2 phenotype is genetically determined (Yagi, Suzuki et al. 2002; Yamada, Zhu et al. 2002; Rose, Lichtenheld et al. 2007). IL-4 is produced by T cells upon antigen stimulation or cross-linking of the T cell receptor (TCR). The initial cellular source of IL-4 in an immune response has not been fully determined but it has recently been shown that naïve T cells have a minute pool of IL-4 mRNA, which becomes translated following a signaling event (Rose, Lichtenheld et al. 2007). When secreted, it can bind to the IL-4 receptor of T cells in an autocrine or paracrine fashion to upregulate the production of more IL-4 (Cunningham, Serre et al. 2004). The production of IL-4 is maintained by cells until the initiating signal is discontinued or until inhibitory molecules and mechanisms

are upregulated to attenuate the signal and dampen production. Subsequent production of IL-4 becomes more efficient as chromatin remodeling occurs at the IL-4 locus, allowing for a quicker and more robust response (Dorado, Jerez et al. 2002). This is regulated in part by the presence of particular transcription factors (TFs), including Stat6, that regulate IL-4 gene transcription and drive the polarity of the Th1 and Th2 response (Li-Weber and Krammer 2003). Regulation of IL-4 production is tightly controlled and has been shown to be predominantly via transcriptional regulatory measures, however there has been recent evidence in studies using actinomycin D to block transcription that suggest increased mRNA stability may have an important role in maintaining an IL-4 rich environment (Dokter, Esselink et al. 1993; Norvell, Mandik et al. 1995; Pioli, Pucci et al. 1998). Additional regulatory measures include a change in chromatin structure (Grogan, Wang et al. 2003; Baguet and Bix 2004; Yamashita, Shinnakasu et al. 2004), upregulation of inhibitory molecules such as SOCS and SHP, and a change in signal strength and duration. Initial research into this subject focused on the use of long-term cell lines, whereas recent use of primary cells have noted significant differences between the two (Kelly-Welch, Hanson et al. 2005). Therefore the second aim of this thesis was to examine Ttc7$^{fsn/fsn}$ T cells and determine activation and IL-4 production.

We have shown that altered IL-4 production and regulation due to hyperactivation of the Ttc7$^{fsn/fsn}$ T cells is helping to drive the autoimmune process. When we compared Ttc7$^{fsn/fsn}$ T cells to WT we found an increase in IL-4 mRNA expression upon anti-CD3 stimulation and a slower turnover of IL-4 mRNA when further mRNA synthesis was blocked with Act D (Figures 1.12 and 1.13). As the results shown were given as a ratio of IL-4 mRNA to GADPH, there was not only a larger pool of IL-4 mRNA requiring longer

turn-over time, but also a change in the functional turn-over of the mRNA. Actinomycin D allows for the continued translation of protein, therefore our results demonstrate the effect that an increase in mRNA stability has in the dysregulation of protein production. IL-4 production in Ttc7$^{fsn/fsn}$ T cells was still at a statistically significant higher level 24 hours after the addition of Act D to cell culture of stimulated 4-weeks cells, and even in unstimulated 10-week T cells without Act D (Figure 1.15). Thus, we can imagine that *in vivo* where the signal to produce IL-4 is unchecked by the addition of any exogenous modifiers such as Act D, there exists a strong drive to keep producing IL-4 that is perpetuated by a normal positive feedback loop, whose inhibitory mechanisms may become overwhelmed or are perhaps defective. This is especially evident when examining protein production in 10-week T cells. In other systems it has been shown that IL-4 is regulated differently in cells that have been previously activated and in cells from older mice, which allows for the up-regulation of factors that function to modulate production (Dokter, Esselink et al. 1993). It appeared that there is some attempt in Ttc7$^{fsn/fsn}$ T cells to regulate the magnitude of IL-4 production as stimulated Ttc7$^{fsn/fsn}$ 10-week T cells did not reach the level of IL-4 as do 4-week T cells in a manner similar to WT T cells. However, unstimulated 10-week Ttc7$^{fsn/fsn}$ T cells still produced 1200-fold more IL-4 than WT cells, almost 300-fold more IL-4 in stimulated cells, and there was over 1000-fold more residual IL-4 after treatment with Act D. Therefore, Ttc7$^{fsn/fsn}$ T cells are being pushed to produce IL-4 regardless of any inhibitory signals they may be receiving.

When quantifying RNA to normalize the concentration for each RT-PCR reaction, it was found that unstimulated Ttc7$^{fsn/fsn}$ T cells contain 3X more total RNA on a

per cell basis than do WT cells (Table 1.1). For the experimental method it was necessary to normalize RNA to 2µg per sample in order to determine the relative expression levels of IL-4 mRNA in both populations of T cells. The ELISA protein measurements were based on equal numbers of cells plated per sample. Thus, it was possible that Ttc7$^{fsn/fsn}$ T cells have more IL-4 mRNA which would result in more IL-4. However, when we look at the RT-PCR results which compared equal concentrations of mRNA, at 4-weeks in unstimulated cells the expression of IL-4 mRNA in Ttc7$^{fsn/fsn}$ mice was actually below that of WT. It is only upon stimulation with anti-CD3 that we saw a rise over that of WT. This difference was reflected in protein production as well since at 4-weeks in unstimulated cells both Ttc7$^{fsn/fsn}$ and WT had non-detectable concentrations of IL-4. At 10-weeks in unstimulated cells the situation reversed and Ttc7$^{fsn/fsn}$ T cells had IL-4 mRNA expression above that of WT which was then reflected in the dramatic rise of IL-4 protein that was produced. Thus, we see that there was an increased capacity in Ttc7$^{fsn/fsn}$ T cells for IL-4 gene expression reminiscent of previously activated or "primed" cells (Bird, Brown et al. 1998; Cron, Bort et al. 1999; Grogan, Wang et al. 2003), and a delay in turnover suggestive of increased mRNA stability which had been demonstrated to exert differential control of IL-4 between younger and older mice (Pioli, Pucci et al. 1998; Butler, Monick et al. 2002). An increase in overall RNA also supported the notion that Ttc7$^{fsn/fsn}$ T cells are hyperactivated *in vivo* by as yet undetermined means. This would be expected to exacerbate the condition, which we see reflected in the more severe autoimmune phenotype of 10-week-old mice.

Cyclosporin A is known to inhibit Ca^{++} sensitive pathways by inhibiting the Ca^{++}-calmodulin dependent phosphatase calcineruin (Naora, Altin et al. 1994; Naora and

Young 1995). Our results demonstrated that IL-4 production in enriched T cells (*ex vivo*) is mediated by a Ca^{++} dependant pathway signaled by the TCR/CD3 complex in a similar manner in both Ttc7$^{fsn/fsn}$ and WT. It further demonstrates that IL-4 production actually requires a signal and is not produced in Ttc7$^{fsn/fsn}$ T cells by an alternative mechanism.

Previous work by our group on the Ttc7$^{fsn/fsn}$ mice noted a distinct acceleration of autoimmune pathology starting at about 5-6 weeks of age, leading to death typically at 15 weeks. The results presented here provide a molecular basis for this observation as we also provided evidence that the mRNA and protein differences we see in the 4-week mice have matured in 10-week mice and resulted in exaggerated protein production that is resistant to actinomycin D treatment. Other groups have noted altered IL-4 regulation in T cells that have been previously activated and differentiated into Th2 cells. Dorado et al, (Dorado, Jerez et al. 2002), demonstrated that the initial production of IL-4 in T cells was regulated differently in undifferentiated T helper cells, but once cells were committed to IL-4 production or "primed" they became more efficient in producing IL-4 which, in their system, may have been independent of IL-4 receptor stimulation (Cron, Bort et al. 1999; Grogan, Wang et al. 2003). Committed Th2 cells also produced altered levels of IL-4 mRNA as compared to naïve and exhibited autoregulatory mechanisms involving the competition between Stat6 and NFAT1 for the P1 site of the IL-4 promotor which helped tip the balance between continued production and downregulation (Dorado, Jerez et al. 2002).

The differences observed in IL-4 mRNA stability and protein production between Ttc7$^{fsn/fsn}$ T cells and WT suggested that Ttc7$^{fsn/fsn}$ T cells were phenotypically different than WT. This was confirmed by flow cytometry using published markers for T cell

subsets designated as naïve (CD62L^{hi}/CD44^{lo}), activated (CD62L^{hi}/CD44^{hi}) or memory cells (CD62L^{lo}/CD44^{hi}). There were significantly fewer naïve CD4+ cells and significantly more (2-2.5X) activated and memory CD4+ cells in 4-week Ttc7$^{fsn/fsn}$ mice than WT. The trend in subset alterations was maintained by 10-week mice.

It is interesting that the ramping up of lymphocyte activation and IL-4 production closely correlates with disease progression of the Ttc7$^{fsn/fsn}$ mice as they age. A seemingly slight increase in Stat6 activation in Ttc7^{fsn} B cells (Figure 1.5) resulted in continuous expression of phosphorylated Stat6. The upregulation of Stat6 by IL-4 normally results in the activation of molecules and factors that function to help shut down the production of IL-4. Under normal conditions IL-4 is a tightly regulated cytokine with multiple levels of regulation and has been shown to need continuous stimulation to maintain production. In Ttc7$^{fsn/fsn}$ mice a slight change in IL-4 mRNA expression in T cells became amplified to make a statistically significant difference in actual IL-4 protein production. Experimentally, we could shut off the signal and still see an increased capacity for protein production as well as an increase in mRNA stability, however, *in vivo* it appears that IL-4 is continuously driven by autoreactive activation resulting in a state of overexpression severe enough to cause systemic autoimmune disease resulting in a dramatic decrease in life expectancy.

Ttc7^{fsn} mice in many ways mimic the autoimmune phenotype of the IL-4 transgenic murine model developed by Erb et al (Erb 1994; Erb, Ruger et al. 1997) especially in regards to B cell hyperactivity, increase in self-reactive antibody titers, splenomegaly, anemia and kidney disease. These researchers suggested that the increased expression of MHC class II and costimulatory molecules on B cells contributed to the

activated phenotypes of the T cells. The elevated production of IL-4 in the T cells in turn enhanced the Stat6-induced phenotype of the B cells as well as other IL-4 driven processes. Singh et al (Singh, Saxena et al. 2003) provided evidence of IL-4 overproduction in New Zealand Mixed 2410 mice that resulted in systemic autoimmune pathology in which many of the symptoms were ameliorated when the strain was crossed with a Stat6 knockout. The cause of the dysregulation in IL-4 production was unknown; however, they noticed a significant increase in the number of IL-4 secreting $CD4^+$ T cells.

As mentioned previously, the Ttc7$^{fsn/fsn}$ gene mutation has recently been identified as an ETn retroviral insertion at the distal end of mouse Chromosome 17; however, the gene function is still unknown. Because of the severe phenotype of Ttc7$^{fsn/fsn}$ mice we speculate that the Ttc7$^{fsn/sn}$ gene product has an important function in immune system regulation which is disrupted in these mice. Many of the pathologies seen in Ttc7$^{fsn/fsn}$ have been found to be IL-4 driven in this as well as other systemic autoimmune models. Whereas Ttc7$^{fsn/fsn}$ is on a BALB/c background we would expect a Th2 skewing in cytokine production upon immune activation (Bix, Wang et al. 1998; Butler, Monick et al. 2002; Yagi, Suzuki et al. 2002). What is not yet clear is why on a genetically identical background as WT, except for the Ttc7$^{fsn/fsn}$ mutation, the regulation of IL-4 starts to change early on and becomes so rapidly dysregulated that it leads to such a dramatic reduction in lifespan.

Our results suggested an increased capacity for IL-4 production in Ttc7$^{fsn/fsn}$ T cells that was mirrored by IL-4 mRNA expression. There was a detectable difference in mRNA stability in Ttc7$^{fsn/fsn}$ T cells as compared to WT which resulted in statistically

significant residual protein expression in Ttc7$^{fsn/fsn}$ after transcription was blocked with actinomycin D (Act D). Signaling appeared to be mediated by the TCR/CD3 complex as cyclosporine A (CsA) shut down both mRNA as well as protein production in both WT and mutant T cells. This also supports the idea that the pathology results from an antigen-driven process as both the increased presence of activated T cells, suggesting antigen stimulation, and the ability to block IL-4 production by CsA is mediated by the T cell antigen receptor.

These data suggested that Ttc7$^{fsn/fsn}$ T cells exhibited a "primed" phenotype at 4-weeks of age, a time when WT cells still appeared relatively naïve. These primed cells could then recruit more cells capable of producing IL-4 while they display an increased capacity for production, and may eventually overwhelm the counter-regulatory mechanisms normally in place to prevent IL-4 overproduction. Previous data has shown that both Ttc7$^{fsn/fsn}$ and WT cells produced similar levels of interferon-gamma in response to anti-CD3 stimulation and that regulation of this IL-4-opposing cytokine (So, Park et al. 2000) appeared to be normal with no exaggeration of production. This further suggests that over-production of IL-4 significantly contributes to the development of autoimmunity in Ttc7$^{fsn/fsn}$ mice.

Stat6 deficiency and 11B11-Treatment of Ttc7$^{fsn/fsn}$ Mice

The third aim of this thesis was to evaluate the contribution of Stat6 and IL-4 to the phenotype of Ttc7$^{fsn/fsn}$ mice. Several groups have found that the deletion of Stat6 led to the lessening or elimination of autoimmunity and disease pathology in other mouse models of autoimmunity (Jankovic, Kullberg et al. 2000; Bruns, Schindler et al. 2003;

Singh, Saxena et al. 2003; Xu, Duan et al. 2006). It was determined that a deletion of Stat6 resulted in a concurrent decline in the hyperactivation of lymphocytes, a decline in the production of IL-4 and an alteration in serum Ig levels resulting in a lower expression of autoantibodies. Thus, to determine the contribution of Stat6 to the Ttc7$^{fsn/fsn}$ autoimmune phenotype we developed a Stat6 knock-out X Ttc7$^{fsn/fsn}$ model by crossing Stat6 deficient animals with Ttc7 heterozygotes to fix the Stat6 deficiency with the Ttc7$^{fsn/fsn}$ mutation. The resulting Stat6-/-Ttc7$^{fsn/fsn}$ mice were produced in an expected Mendelian distribution of 1 in 16 animals.

Previous attempts to establish an IL-4 deficient Ttc7$^{fsn/fsn}$ model were unsuccessful, therefore to evaluate the contribution of IL-4 to the pathology of Ttc7$^{fsn/fsn}$ mice we used a monoclonal IL-4-neutralizing antibody (11B11) and injected 250 µg IP, three times per week starting at 3-weeks of age. Another monoclonal antibody, GL113, was used as an isotype control and administered in the same manner as the 11B11. This was continued until 10 weeks of age whereupon mice were bled and sacrificed for analysis (Erb, Ruger et al. 1997; Singh, Saxena et al. 2003).

Previous work by us and others has contributed to a body of knowledge illuminating the autoimmune and inflammatory pathology of the Ttc7$^{fsn/fsn}$ mouse. We used this as a model and frame-of-reference to compare the phenotype of the Stat6-/-Ttc7$^{fsn/fsn}$ as well as the 11B11-treated Ttc7$^{fsn/fsn}$ mice. One of the striking features of the Ttc7$^{fsn/fsn}$ mouse is the marked splenomegaly and altered cell population in the spleen. Therefore we evaluated the identity and percentages of CD3+, B220+, Mac-1+, CD4+, CD8+, F4/80+, Gr-1+ and TER-119+ cells in the spleens of 10-week-old mice using flow cytometry as described previously in Pelsue, et al (1998). In addition, we determined

alterations in T cell subsets as well as B cell subsets using the ratio and expression of cell surface markers to identify subsets categorized here and in other works.

As mentioned earlier in the introduction, B cells play a central role in autoimmune pathology. Thus, we analyzed Stat6-/-Ttc7$^{fsn/fsn}$ and 11B11-Treated mice sera for the production of anti-nuclear antibodies (ANA). This was done in two ways. ELISAs specific for IgM and IgG anti-DNA antibodies and a HEp-2 immunofluorescence assay (IFA) were used to detect the general presence of antibodies against nuclear antigens and characteristic staining patterns of antibodies specific for nuclear and cytoplasmic antigens respectively. Anti-dsDNA is the major component of the anti-DNA measured by the ELISA and is indicative of systemic autoimmunity where higher than normal titers have been correlated with disease activity in humans (Koh, Dunphy et al. 1995; Fields and Erikson 2003; Woetmann, Brockdorff et al. 2003; Craig, Ledue et al. 2006; Stahl, Hoemberg et al. 2006; Bizzaro 2007; Khan, Witsch et al. 2008; Yung and Chan 2008).

In humans with systemic autoimmune disease, kidney pathology is a major cause of morbidity and mortality. Likewise, Ttc7$^{fsn/fsn}$ mutant mice exhibit elevated urine protein levels, infiltrates of immune cells into the kidney and severe glomerulonephritis. Histological studies performed previously with 12-week-old Ttc7$^{fsn/fsn}$ mice show increased size and cellularity of the glomeruli as well as moderate IgG deposits and immune complex formation (Pelsue, Schweitzer et al. 1998). Stat6-/-Ttc7$^{fsn/fsn}$ and 11B11-treated Ttc7$^{fsn/fsn}$ kidneys from 10-week-old mice were sectioned and stained with hemotoxylin and eosin for glomerular size and cellularity, and periodic acid-Schiff for thickening of the basement membrane indicating immune complex deposition. In addition, urinalysis with commercial protein dip-sticks was performed to measure protein

excreted into the urine, a sign of kidney pathology, which correlated the development of glomerulonephritis with renal function. Ttc7$^{fsn/fsn}$ IL-4-competent age-matched mice as well as normal WT littermates were used as controls.

11B11 Treatment

One of the great difficulties in the study of autoimmunity is to determine initiating events that drive the autoimmune process and to distinguish these from downstream events caused by the process itself. Often, these may be the same or similar events, which become dysregulated due to the nature of the intrinsic defect and the fact that there exists many positive feedback mechanisms in the immune system that help to augment an immune response under normal conditions. For example, lymphocytes must become activated by antigen and proliferate and differentiate into effector cells to mount a response against invading pathogens. Cytokines are often secreted under these conditions which may then activate other cell types and drive inflammation to neutralize and clear the unwanted foreigners. When these mechanisms go awry, due to inappropriate activation, defects in regulatory molecules, defects in clearance mechanisms or apoptosis, overproduction of cytokines or other chemical messengers or a number of other means, autoimmunity often results from the lack of resolution of the response. This usually involves a "ramping up" of symptoms and inflammation, which then drives more inflammation and more severe symptoms until the animal of study becomes physiologically overwhelmed and expires. Ttc7$^{fsn/fsn}$ mice exhibit such characteristics of the ramping up of symptoms and inflammation, with hyper-activated lymphocytes and high levels of IL-4. However, the underlying defect is unknown, thus it has been difficult

to determine if the hyperactivation of lymphocytes precedes the over-production of IL-4, or, if a defect in the intrinsic regulation of IL-4 production causes the hyperactivation of lymphocytes due to the ability of IL-4 to behave as a growth factor.

The neutralizing monoclonal antibody, 11B11, was used to treat Ttc7$^{fsn/fsn}$ mice in order to render IL-4 ineffective and tease out some of the downstream effects that IL-4 may be contributing to autoimmunity pathogenesis. This of course, is not as effective as a genetic deletion of IL-4 to halt production, however, as mentioned earlier, attempts to do this were unsuccessful. Treatment with 11B11 began at 3 weeks-of-age before the onset of many of the more severe symptoms of autoimmunity, and continued for 7 weeks until 10-weeks of age in order to compare these animals with the numerous data that were previously collected on 10-week Ttc7$^{fsn/fsn}$ mice. Care was taken in the preparation of the antibody to ensure compatibility with other published data using 11B11 as a neutralizing antibody.

The 11B11-treated Ttc7$^{fsn/fsn}$ mice were essentially unchanged in outward phenotype as they developed skin lesions and distended abdomens in a similar manner to their untreated counterparts. The size of the spleen and number of cells were also similar, however, there was an alteration in the percentages of cell populations indicating that the animals were responding to the IL-4-neutralizing treatment. 11B11-treated Ttc7$^{fsn/fsn}$ mice experienced a rebound of the percentage of CD3+ cells suggesting that neutralization of IL-4 had an effect on either reducing cell death of CD3+ cells or had enhanced their development or survival. The percentages of CD4+ and CD8+ cells remained unchanged.

The effect of 11B11-treatment on CD4+ T cell subsets is difficult to determine. It appeared that the percentage of cells in the naïve population ($CD62L^{hi}/CD44^{lo}$) was essentially unchanged (Figure 3.1) between treated $Ttc7^{fsn/fsn}$, GL113-treated, and untreated $Ttc7^{fsn/fsn}$ animals but that there was a reduction in the percentage of memory cells ($CD62L^{lo}/CD44^{hi}$) in 11B11 mice. This reduction brought the percentage of memory cells in 11B11-treated mice more in line with the percentage of memory cells found in the spleens of 10-week WT mice, with normal levels of IL-4, as shown in Figure 1.18 (18% and 16% respectively). The activated population ($CD62L^{hi}/CD44^{hi}$) however, was actually increased in 11B11-treated mice as compared to untreated $Ttc7^{fsn/fsn}$ mice. The reason for this is undetermined at this time however, when compared to isotype control-treated $Ttc7^{fsn/fsn}$ mice, the percentage of activated CD4+ cells is reduced (Figure 3.1). When compared to untreated $Ttc7^{fsn/fsn}$ mice, the isotype–control treated group also had an increase in activated CD4+ cells, when similar percentages would be expected. Thus, the antibodies used may have caused an immune response and activated T cells in the treated mice as the antibodies were of rat origin and could have been detected by the immune system as foreign antigens. Therefore, it's possible that the 11B11-treatment actually reduced the percentage of activated CD4+ cells aside from the effects of the antibody treatment. If this is true, then the 11B11-treatment had a "normalizing" effect on the percentages of CD4+ cells that we would consider to be "primed" by IL-4 in vivo and thus brought them more in line with the percentages of subtypes found in WT animals. However, the naïve population, which is reduced from WT in $Ttc7^{fsn/fsn}$ mice but similar in $Ttc7^{fsn/fsn}$ treated and untreated animals, would not be expected to change much as this population is more developmentally defined by the Ttc7 defect as opposed to the

downstream effects of a high IL-4 environment which would push activation, and influence proliferation and differentiation.

Flow cytometric analysis of spleen also revealed distinct differences in B cells between 11B11-treated and untreated Ttc7$^{fsn/fsn}$ mice. Interestingly, the 11B11-treated group had a reduction in the percentage of CD19+ cells as compared to untreated. CD19 is part of the BCR signaling system which has a positive role in B cell signaling by increasing the sensitivity of the receptor. An increase in CD19 expression has been shown to make B cells hyper-responsive to antigen signaling and mitogens, while decreased expression renders them hyporesponsive (Sato, Ono et al. 1996). CD19 works in concert with CD22, an inhibitory receptor, to regulate the signaling threshold of the BCR (Marshall, Niiro et al. 2000), a system which, when defective can lead to autoimmunity (Fujimoto and Sato 2007). CD19 expression is important in B cell development and induction of tolerance, and whose expression has been shown to be high in pro-B to mature B cell stages and low in plasma cells (Casola 2007), but does not appear to increase when B cells are activated or in response to activation by mitogens or IL-4 (Sato, Ono et al. 1996). Signals generated through CD19 appear to be important for the development and maintenance of B1 B cells which show increased CD19 expression, in contrast to CD19 deficient mice which have a significant reduction of this cell population (Sato, Ono et al. 1996). CD19 has not been shown to be directly regulated by IL-4, and although CD22 is directly downregulated by signals generated through the IL-4 receptor there is no evidence linking CD22 to the regulation of CD19 expression (Rudge, Cutler et al. 2002). Therefore, we suggest that anti-IL-4 treatment altered the splenic B cell population by decreasing the survival effects that IL-4 exhibited on the expanded

immature population of B cells present in Ttc7$^{fsn/fsn}$ spleens as had previously been shown by Morris et al (Morris, Dragula et al. 2002) and Mori et al (Mori, Morris et al. 2000). In addition, Ttc7$^{fsn/fsn}$ mice have been previously shown by our group to have an increased population of B1 cells in the spleen which is included in the immature B cell subset identified by Mattsson et al, (Mattsson, Duzevik et al. 2005). Thus, the reduction in the percentage of CD19+ cells is probably due to a reduction in the B1 cell population through either induction of an alternate developmental pathway or reduced survival through blocking IL-4.

The functional consequences of an alteration in the B cell subsets have not been determined, however, it appears that there is a significant reduction in activation as CD23 and MHC II, both surface markers of B cell activation were significantly reduced (from 36% to 3% and 60% to 12% respectively, see Table 3.1). These are both directly regulated by IL-4 and provide confirmation that IL-4 signaling was blocked by the 11B11, as well as an indication that B cells were responding to an IL-4 rich or deficient environment in a manner that would be expected (i.e., no intrinsic defects in downstream IL-4 signaling).

The fact that B cells responded to the neutralization of IL-4 was also reflected in a reduction of serum IgE (Figure 3.3) as well as a substantial reduction in serum IgG1 (Figure 3.4) both of which are influenced by IL-4. There was a slight reduction in serum IgG3 (Figure 3.5) but overall, total serum Ig was increased (Figure 3.6). Other isotypes were not measured so it is difficult to determine the type of Ig(s) that may have made up the difference. What is striking however, is that even though IL-4 was neutralized and altered the expression of IL-4-regulated genes, B cells still secreted increased levels of

antibodies that included anti-DNA antibodies as shown in Figure 3.7. This suggested that IL-4 influenced the class of antibody produced by hyperactive B cells, but that the level of antibody secreted and the presence of anti-DNA antibodies were independent of the stimulating and survival effects of IL-4.

11B11-treated mice B cells still produced predominantly IgG anti-DNA antibodies, but had a slight reduction in serum concentration of IgM anti-DNA antibodies as measured by average absorbance (Figure 3.7), probably due to the reduction in the percentage of immature B cells (Figure 3.2A). The 11B11 animals also produced auto-reactive serum antibodies with HEp-2 staining patterns similar to untreated and isotype-control treated Ttc7$^{fsn/fsn}$ mice (Figures 3.8 and 3.9). This attests to the activated nature of the B cells present in the 11B11-treated animals and the presence of autoreactive cells despite the 11B11 treatment.

Overall, this suggests the presence of an underlying defect that heightens lymphocyte activation and autoreactivity, which manifests in an IL-4 driven pathology that changes but does not completely resolve when IL-4 is neutralized. It's possible that starting treatment earlier or prolonged treatment with 11B11 may induce more dramatic changes, but there are additional problems associated with both of these. Early treatment is very stressful for young animals and where they are born with visible indicators of a Ttc7 defect may not change the outcome we observed. Longer treatment increases the risk of treated animals generating an immune response and increased immune complexes to the antibody and would more seriously confound the results. However these data provide evidence that lymphocytes responded to changes in IL-4 modulation that

indicates the downstream regulatory mechanisms of IL-4 signaling are intact in Ttc7$^{fsn/fsn}$ mice.

Stat6 Deficiency

Based on the reports of several research groups, described earlier, we expected that the elimination of Stat6 would possibly lessen the production of IL-4 in Ttc7$^{fsn/fsn}$ mice and reduce the severity of the autoimmune phenotype. However, this was not the case. We were able to identify the presence of the defective Ttc7 gene in Stat6-/- animals early in life by the characteristic belly hair striations, abdominal distention due to the enlarged spleen, and the paleness of the ears, tails and feet due to the presence of anemia. As the mice aged, many, but not all, of them developed similar skin pathology as their Stat6 intact Ttc7$^{fsn/fsn}$ counterparts, and both groups had a similar shortened lifespan, which averaged approximately 12-weeks.

The overall increase in size of the spleen was similar between the Stat6 intact Ttc7$^{fsn/fsn}$ and Stat6 deficient groups, however, there was a change in population distribution. CD23 was virtually eliminated on the surface of splenocytes in the Stat6 deficient animals, attesting to the functional elimination of Stat6 signaling as well as the necessity of Stat6 in the expression of CD23, but MHC II expression was only reduced and not eradicated, suggesting alternate pathways of activation. There was a recovery in the percentage of CD3+, CD4+ and CD8+ expression in the Stat6 deficient group. However, in contrast to other Stat6 deficient animals which had a decrease in T cell activation, there was also a significant increase in the percentage of activated CD4+ T cells from 17% in the Stat6 intact Ttc7$^{fsn/fsn}$ animals to 39% in the Stat6 deficient animals.

The increase in activation of CD4+ cells was not accompanied by an increase in percentage of background intracellular levels of IL-4+ (Figure 2.9) or IFN-γ+ (Figure 2.10) cells, but when these cells were stimulated for 24 hours with anti-CD3, both cytokines showed a percent increase in cells positive for intracellular staining, albeit at slightly lower levels than their Stat6 intact Ttc7$^{fsn/fsn}$ counterparts.

Interestingly, lymphocytes from the Stat6 deficient Ttc7$^{fsn/fsn}$ mice produced almost 6 times more IL-4 than the same number of cells from the Stat6 sufficient Ttc7$^{fsn/fsn}$ mice (Figure 2.11). This is most likely reflective of the expanded activated population of CD4+ cells in Stat6-/-Ttc7$^{fsn/fsn}$ (Table 2.3). It is unlikely that individual cells had an increased capacity for IL-4 production as the mean fluorescent intensity of IL-4+ cells is actually slightly higher in Stat6 intact Ttc7$^{fsn/fsn}$ CD4+ T cells, but given that the percentage of CD4+ cells in Stat6 deficient animals was almost 3X higher, there were that many more cells producing IL-4. Although IFN-γ secretion was not measured by ELISA in Stat6-/- lymphocytes, there was not as significant an increase in CD4+ IFN-γ+ cells upon anti-CD3 stimulation (approximately 1.75 X higher in Stat6-/-Ttc7$^{fsn/fsn}$, Figure 2.10). Stat6 intact Ttc7$^{fsn/fsn}$ CD4+ cells actually had a higher mean fluorescence intensity, which suggested that individual Stat6 intact cells have a slightly increased capacity for IFN- γ production than do Stat6 deficient cells. Therefore, the deficiency of Stat6 in Ttc7$^{fsn/fsn}$ mice does not decrease the production of IL-4 as has been shown in other Stat6 deficient models, nor does it promote skewing towards a Th1 phenotype, but in fact, provides for a significant increase in IL-4 production. One possibility for this increase could be that the loss of Stat6 results in lack of competition for the binding of NFAT to the IL-4 promoter, thereby reducing the negative feedback usually in place to

help downregulate IL-4 production. In addition, it has been shown previously by other groups that CD8+ T cells, CD4/CD8 double-positive T cells and human tonsillar B cells can all be induced into producing IL-4 in other systems, thus it is possible that they may also contribute to the high IL-4 production measured here (Cronin, Stack et al. 1995; Harris, Goodrich et al. 2005; Parel, Aurrand-Lions et al. 2007).

The alteration in B cell subsets in Stat6 deficient Ttc7$^{fsn/fsn}$ splenocytes mainly resided in the significant increase in the percentage of immature B cells as measured by the ratio of IgM to IgD (Figures 2.6 and 2.7). Ttc7$^{fsn/fsn}$ immature B cells made up about 20% of the population, whereas their Stat6 disrupted counterparts increased to 45% of the population. IL-4 has actually been shown to accelerate and promote the maturation and differentiation of B cells; however this was also shown to be Stat6 dependent (Mori, Morris et al. 2000; Morris, Dragula et al. 2002). Therefore, it appears that the disruption of Stat6 had a more significant impact on the maturation of B cells here than did the level of IL-4. Mature and Transitional subsets were very similar between the two groups, as was the percentage of CD19+ cells overall (Table 2.1). It is likely that the population of immature B cells identified here are the IgM bright cells seen in the spleen sections stained for p-Stat6 and IL-4 (Figures 1.8 C&D, and 1.11). These would be the IgM bright cells seen outside of the follicles, that, when exposed to the concentrations of IL-4 seen in the spleen may be induced to survive, escape tolerance and proliferate. This extra-follicular population has recently been shown to contain a population of activated B cells called plasmablasts that participate in the development of autoimmunity through the secretion of autoantibodies and undergo somatic mutation outside of the spleen follicles (William, Euler et al. 2005). Mattsson et al, 2005, from our lab, identified this population

as $CD22^{lo}/IgM^{bright}$ immature B cells which agrees with the description provided by William et al and appears to be the population that is activated early in the induction of autoimmunity which, because of their location, may escape tolerance. These self-reactive cells would then be able to produce autoantibodies, proliferate to form new autoantibody-producing cells, and act as effector cells to activate autoreactive T cells. Thus, a "ramping up" of activated lymphocytes occurs that can go on to mediate the inflammation associated with continuing autoimmunity.

The functional consequences of the presence and activation of auto-reactive, autoantibody-secreting immature B cells were seen in the higher-than-WT concentrations of IgM anti-DNA antibodies (Figure 2.15), higher IgG1 (Figure 2.12), IgG3 (Figure 2.13) and total serum Ig (Figure 2.14), and positive staining for anti-nuclear and cytoplasmic staining patterns in HEp-2 cells (Figure 2.16) in the serum from Stat6-/-$Ttc7^{fsn/fsn}$ mice. Although the concentrations of these antibodies were similar to those of Stat6 intact $Ttc7^{fsn/fsn}$ serum, the switch to a more predominant IgM class reflected the higher percentage of immature B cells in the Stat6 deficient animals. There is little research available describing the significance and pathogenicity of IgM antibodies, however, due to the pentameric structure of the secretory form, IgM is highly efficient in activating complement which can then mediate inflammation. In addition, due to its low affinity, epitope spreading is more likely with IgM resulting in crossreactivity that may become self-reactive, or broaden the reach of primary self-reactive IgM antibodies produced in development. It is interesting that there appeared to be a predominance of cytoplasmic staining of HEp-2 cells from the Stat6 deficient $Ttc7^{fsn/fsn}$ animals. Recently, Wardemann et al. (Wardemann, Yurasov et al. 2003), found that 58.6% of the antibodies expressed by

early immature B cells showed either a nuclear or nuclear/cytoplasmic staining pattern in HEp-2 cells, while 13.8% stained the cytoplasm. The antibodies with nuclear or nuclear/cytoplasmic staining were subsequently removed from the repertoire during developmental checkpoints of tolerance, however, the antibodies reactive with cytoplasmic components were not removed from the B cell pool as efficiently. Thus, it is possible that the increased presence of IgM cytoplasmic autoantibodies represents a "normal" process that, due to the increase in IgM and immature B cells in the Stat6 deficient Ttc7$^{fsn/fsn}$ mice, are not removed and are allowed to survive and undergo isotype-switching to become IgG antibodies that are specific for cytoplasmic antigens. Interestingly, Khan et al (Khan, Witsch et al. 2008) recently described a mechanism by which B cells bearing IgM antibodies specific for cytoplasmic antigens are able to escape tolerance. In their VH56R/Vκ38c transgenic model of anti-DNA specific heavy and light chain combinations they found the IgM antibody produced to be specific for a Golgi-associated antigen, but also cross-reactive with DNA. Because IgM antibodies traffic through the Golgi on the way to the cell surface, specificity for an antigen there caused an intracellular accumulation of IgM which was not degraded. These Golgi-specific B cells were subsequently found in the marginal zone of the spleen. We also identified Golgi-specific IgM autoantibodies in our Stat6-/-Ttc7$^{fsn/fsn}$ HEp-2 staining, as well as other IgM cytoplasmic-specific staining patterns. The mechanism described for central tolerance avoidance may play a role in our system as well.

Assessment of Autoimmunity: Renal Pathology

Researchers and clinicians involved in studying the etiology and pathology of autoimmunity have long used the status of kidney disease to determine disease progression as this is a common element among many different models and types of systemic autoimmunity and for many years was a major source of morbidity and mortality for humans and animals alike. Advancements in treatment options for humans have reduced the mortality rate due to kidney failure among patients, but kidney pathology is still a useful measure of disease progression and severity in animal models of autoimmunity. Because of the ease of measuring protein in urine and the strong association between increased urinary protein and increased kidney disease severity, proteinuria is a useful and non-invasive way to measure the progression of pathology until histological analysis can confirm cellular damage. Prior measurements of proteinuria (unpublished data by Daniel Swett of the Pelsue Lab) and kidney histology have confirmed the presence of renal disease of Ttc7$^{fsn/fsn}$ mice. Proteinuria has generally been measured between 30-100 mg/mL in Ttc7$^{fsn/fsn}$ urine, which stayed in that range as mice aged and succumb to advanced autoimmune disease. The disruption of Stat6 in these mice actually caused a significant increase in proteinuria, with all Stat6-/-Ttc7$^{fsn/fsn}$ mice measured having levels starting at 100 mg/mL and going as high as 2000+ mg/mL (Figure 5.1). When measurements were taken at 2-week intervals, most proteinuria measurements increased, sometimes dramatically. The mice with the highest measured levels of 2000+ died very shortly after the measurements were taken (hours to days).

To correlate the high urinary protein found in both Stat6 deficient and Stat6 intact mice, we harvested kidneys from newly sacrificed animals and sent them to be processed

and scored by Dr. Harini Bagavant, an experienced expert in the evaluation of SLE kidney nephritis at the University of Virginia. Her comments can be read in the "Results" section (Figures 5.3-5.5). Both Stat6 intact and Stat6 deficient, Ttc7$^{fsn/fsn}$ mice were classified as having "severe glomerular disease" of the membranoproliferative-glomerulonephritis-type. This was described as a little different from some forms of GN in SLE due to the lack of inflammatory infiltrates in the glomeruli and the presence of normal looking Bowman's capsules, tubules and interstitium. Both Ttc7$^{fsn/fsn}$ and Stat6-/-Ttc7$^{fsn/fsn}$ were scored as having a rating of 2-3+ on a disease severity index with 4 being the most severe, however, the kidney sections scored from Ttc7$^{fsn/fsn}$ mice were from 20-week-old mice, whereas, the Stat6-/-Ttc7$^{fsn/fsn}$ sections scored were from 10-week-old mice. The number of glomeruli involved was similar in both groups as were the cell-types and location of inflammatory foci. Thus, the absence of Stat6, which in some animal models was shown to reduce renal disease, actually increased and accelerated renal disease in the Stat6 deficient Ttc7$^{fsn/fsn}$ animals. The absence of Stat6 was also accompanied by an increase in activated T cells, which have been found to be important in the pathogenesis of lupus GN and progression to renal failure (Waters, Fu et al. 2001; Bagavant, Deshmukh et al. 2006). This same group has also associated lower levels of proteinuria to distinguish acute GN, and higher levels of proteinuria to distinguish the change to chronic GN and progression to renal failure.

Therefore, these data suggest that the disruption of Stat6 in Ttc7$^{fsn/fsn}$ animals results in an increase in renal pathology, by changing an acute state to a chronic state of GN, with higher percentages of activated peripheral T cells, and immature B cells, leading to a slightly altered, but severe state of systemic autoimmune disease. This is in

contrast to other models wherein the disruption of Stat6 lessens autoimmunity with less lymphocyte activation, milder renal disease, lower levels of serum antibodies including self-reactive antibodies, and lower levels of IL-4.

The neutralization of IL-4 by treatment with 11B11 actually seemed to reduce the severity of renal disease as measured by proteinuria and scoring of kidney sections. Proteinuria was reduced to 30 mg/mL in all but one of the 11B11-treated Ttc7$^{fsn/fsn}$ which was lower than the untreated Ttc7$^{fsn/fsn}$ and isotype control treated groups, but not as low at WT (untreated) animals (Figure 5.2). The kidney sections corresponding to the protein measurements in the 11B11-treated animals all rated a disease severity index score of ~1+ (out of 4, with 4 the most severe).

These data, taken with the 11B11 data given previously suggest that IL-4 definitively contributes to the downstream autoimmune pathology of Ttc7$^{fsn/fsn}$ mice and when neutralized, pathology is reduced. This is demonstrated by the reduction in the population of effector activated and memory T cells, a reduction in the activation markers of B cells, CD23 and MHC II, and a reduction in the immature population of B cells, and lower levels of proteinuria coupled with a lower disease severity index score. That the underlying defect in Ttc7 actually promotes an abnormally activated state in lymphocytes that leads to IL-4 overproduction is supported by the observation that 11B11 did not change the percentage of naïve T cells (which is reduced compared to WT animals) nor did it change the overall level of antibody production or the presence of anti-DNA antibodies, attesting to the hyper-active state of B cells, similar to that seen by Kin and Saunders (Rose, Lichtenheld et al. 2007). Therefore, this indicates that the Ttc7 defect

promotes autoreactivity and autoimmunity, while IL-4 contributes to the expression and progression of the pathology.

Cell Cycle Regulation

Many of the hematopoietic abnormalities associated with Ttc7$^{fsn/fsn}$ mice are similar to those associated with mice engineered to have defects in cell cycle regulatory proteins. This is understandable since the proper regulation of hematopoiesis requires precise regulation of the cell cycle machinery. Entry into the cell cycle is necessary for expansion of cell populations and proliferation, while properly timed exit is necessary for maturation and differentiation to occur (Woetmann, Brockdorff et al. 2003). Thus, prolonged cycling of a cell diminishes its ability to mature and differentiate. Mice with targeted E2F2 mutations for example, (a member of a protein family that regulates proliferation, differentiation, and apoptosis), exhibit an autoimmune syndrome similar to Ttc7$^{fsn/fsn}$ mice, with skin lesions, anemia, splenomegaly and inflammatory infiltrates in many organs, although the E2F2 mice exhibit symptoms much later in life, with life expectancy to 15 months or longer (Murga, Fernandez-Capetillo et al. 2001). Indeed, Th2 differentiation and the production of IL-4 require entry into the cell cycle, and IL-4 itself has been shown to promote the entry of various cell types into the cell cycle. Thus it is difficult to separate a defect in one from a defect in the other.

The differences in the percentages of cycling CD3+ cells, as shown in Table 4.1, suggest that the cell cycle is operating in a predictable manner in Ttc7$^{fsn/fsn}$ which corresponds to the activation and/or differentiation state of the cells. 4-week Ttc7$^{fsn/fsn}$ mice have the highest percentage of naïve cells which are producing IL-4 at a stage when

cycling would be necessary for IL-4 production, as well as having high populations of activated and memory cells. At 10-weeks a higher population of cells would likely have become "primed" and IL-4 production would no longer require entry into the cell cycle. Stat6-/- and 11B11-treated Ttc7$^{fsn/fsn}$ mice both have higher percentages of activated CD3+ cells than 10-week Ttc7$^{fsn/fsn}$ mice and higher percentages of cycling cells. Although DNA content was not examined in B cells, 11B11-treatment reduced the percentage of immature B cells in Ttc7$^{fsn/fsn}$ spleens and resulted in differentiation to a more mature population. Thus, although these data are in no way definitive, they suggest that cell cycle regulation is not the primary defect in Ttc7$^{fsn/fsn}$ mice.

Conclusion

The goal of this thesis project was to evaluate the production of IL-4 and its contribution to lymphocyte activation and autoimmune pathology in Ttc7$^{fsn/fsn}$. This was done in keeping with our general hypothesis that the Ttc7^{fsn} mutation results in the hyperactivation of lymphocytes leading to the overproduction of IL-4 and systemic pathogenic autoimmunity.

Our results suggest that IL-4 plays a major role in the pathology of Ttc7$^{fsn/fsn}$ mice but that the role of Stat6 is more complicated. We have demonstrated that altered IL-4 signaling is not due to defects in IL-4 responsive genes but is influenced by a mutation in the as yet uncharacterized Ttc7 gene which we hypothesize to be important in lymphocyte regulation.

Thus, from these data, it appears that the lack of Stat6-/- in Ttc7$^{fsn/fsn}$ results in an increase in the severity of autoimmunity as measured by renal disease. The neutralization

of IL-4 results in a slight decrease in the severity of autoimmunity. Therefore we suggest that Ttc7$^{fsn/fsn}$ mice exhibit an autoimmune syndrome that is phenotypically-driven by IL-4 due to the background genetic effects of the Th2-skewed BALB/c strain, and results from the dysregulated activation of lymphocytes due to the defective Ttc7 gene. We further suggest that Ttc7 functions to negatively regulate lymphocyte activation and cytokine production and when the downstream inhibitory action of Stat6 is removed in the Stat6 deficient animals, IL-4 production becomes elevated and increases the severity of the pathology. The question of whether Ttc7 and Stat6 interact remains to be answered when the tools for the study of Ttc7 become more readily available for such analysis. However, these data suggest the possibility that Stat6 and Ttc7 may function in a similar or complementary fashion as when both are deficient we see more lymphocyte activation and proliferation, and more autoimmune pathology.

Recently, Heery and colleagues (Heery, Kalkhoven et al. 1997) identified a protein-recognition motif defined by the sequence LxxLL (Leu-Xaa-Xaa-Leu-Leu) that is present on many transcription factors and cofactors that mediate both activation and repression of transcription. Many of the proteins identified with LxxLL sequences have multiple motifs as well as LxxLL binding sites, which are minimally understood, and are thought to possibly mediate transcriptional coactivator complexes (Plevin, Mills et al. 2005). Stat6 has recently been shown to have LxxLL motifs, one of which binds to the cofactor NCoA-1 and is required for IL-4-induced eotaxin-3, with other IL-4 responsive genes still under study (Litterst and Pfitzner 2002). Other LxxLL- containing proteins include cyclic AMP response element-binding protein (CREB)-binding protein (CBP), p300, c-Myb, and several E proteins which are important in lymphocyte development and

regulation of activation. These proteins have been implicated in disease processes as well. For example, Zhang et al (Zhang, Kalkum et al. 2004) identified a fusion protein commonly associated with acute myeloid leukemia, AML1-ETO that binds to an E protein via an LxxLL domain and inhibits the binding of CBP/p300, thus silencing the E protein. We have identified four putative LxxLL domains in the Ttc7$^{fsn/fsn}$ protein, three of which potentially form alpha-helical secondary structures similar to the functional LxxLL motifs identified to date (Razeto, Ramakrishnan et al. 2004). Since the function of Ttc7^{fsnfsn} is unknown, it is interesting to speculate that it may be involved in transcriptional regulation in lymphocytes mediated by its LxxLL motifs through interactions with other cofactors and regulatory proteins, and possibly Stat6.

Interestingly, these data are very reminiscent of reports of Stat6 deficiency combined with the disruption of a negative regulator of lymphocyte activation such as Bcl-6 (Linehan, Warren et al. 1998) or CTLA-4 (BOUR-JORDAN, GROGAN ET AL. 2003) or the combination of a positive and negative regulator of activation such as NFATc2 and NFATc3 (Rengarajan, Mowen et al. 2002). Bcl-6 is a transcription factor that has been shown to be important in Th2 development and when knocked out, mice deficient in Bcl-6 die early from severe lung and heart inflammation. Bcl-6/Stat6 double-knockouts also develop a severe Th2 inflammatory disease with levels of IL-4 from 7 to 1000 times that of Stat6 knock out animals. These animals did not develop a corresponding elevation in the Th1 cytokine, IFN-γ, indicating that they were not pushed into a more inflammatory Th1 phenotype. Thus it appears that Bcl-6 controls an alternate pathway of Th2 differentiation that is independent of Stat6 (Linehan, Warren et al. 1998). This situation also exists in Ttc7$^{fsn/fsn}$ mice which produce high levels of IL-4, but even

higher levels when Stat6 is interrupted. Stat6-/-Ttc7$^{fsn/fsn}$ CD4+ cells do not produce increased levels of IFN- γ but in fact exhibit a reduction in the percentage of IFN- γ+ cells as well as lower levels of cytokine produced per cell. Thus, the Ttc7$^{fsn/fsn}$/Stat6 "double-knockout" does not become skewed towards a Th1 phenotype, but differentiates into Th2 IL-4 producing cells in the absence of Stat6.

Cytolytic T lymphocyte-associated antigen-4 (CTLA-4) is a cytosolic protein that is considered to be an immune attenuator that, when engaged, promotes Th1 differentiation in T lymphocytes. CTLA-4 is considered to function by controlling the strength of the signal after T-cell activation, thus determining the Th1 or Th2 fate of the population. CTLA-4 deficient CD4+ T cells produce increased levels of IL-4 and possess a Th2 phenotype. CTLA-4 and Stat6 double-knock out mice produce elevated levels of IL-4 as compared to CTLA-4 or Stat6 single knock outs. Double knock-out T cells also exhibit an activated phenotype and an expanded population as compared to singly deficient cells (Bour-Jourdan et al., 2003). Thus the CTLA-4/Stat6 double-knockout and Stat6-/-Ttc7$^{fsn/fsn}$ are both able to produce stably differentiated IL-4 producing Th2-driven cell populations that bypass the need for Stat6 in that process. Furthermore, mice with these deficiencies are unable to attenuate activation resulting in fatal lymphoproliferative disease.

Mice with a targeted NFATc2 disruption exhibit an increase in IL-4 production and a skewing towards the Th2 phenotype (Rengarajan, Mowen et al. 2002). They also show an increase in IL-4 mRNA stability, an increase in activated and memory T cells and sensitivity to CsA. When combined with a targeted NFATc3 disruption, doubly-deficient mice show a dramatic increase in IL-4 production, increased IgG1 and IgE

titers, severe inflammation, and differentiate into a Th2 phenotype even in the absence of IL-4. These data suggest that NFATc2 and NFATc3 have inhibitory functions *in vivo* that may regulate negative feedback mechanisms that perturb Th2 polarization. However, these mice do not show a concomitant increase in Th1 cytokines such as IFN-γ, but in fact produce less upon stimulation in Th1 skewing conditions.

What all of these animal models have in common is an intrinsic defect which results in a change in signaling threshold that permits functional activation and alters the cellular response. It is understood that strong TCR signals favor Th2 differentiation while weaker signals push T cells into a Th1 phenotype (Bour-Jourdan et al. 2003). The strength of the signal through the TCR has also been shown to bypass the need for Stat6 in IL-4 production (Sehra, Patel et al. 2005). Thus, in a similar manner, a higher percentage of Ttc7$^{fsn/fsn}$ T cells are activated as compared to WT, due to an intrinsic defect that promotes autoreactivity and allows for a lower threshold of activation. Intracellularly, this translates into a signal strong enough to drive Th2 differentiation and increased levels of IL-4, even in the absence of Stat6. The IL-4-rich environment then, provides the means by which continued activation occurs, resulting in more IL-4 production and a cascade into autoimmune-related pathology.

While the above describes T cell processes there is ample evidence to suggest that B cells are equally activated and participate in the development of the systemic pathology described herein. It is not unreasonable to imagine that the same defect that alters and reduces the signaling threshold in T cells, functions to increase reactivity and autoreactivity in B cells as well. In fact, Gong and Malek (Gong and Malek 2007) and Kallies et al., (Kallies and Nutt 2007), have recently demonstrated a role for B

lymphocyte induced maturation protein -1 (Blimp-1), a protein essential for terminal differentiation in B cells, to be essential for T lymphocyte homeostasis and regulation of activation as well. Interestingly, a role for regulation by Blimp-1 was also determined in some non-hematopoietic cells. In addition, NFATs, originally discovered in T cells, have been found to be present and activated by signals generated through the BCR and important in B cell activation and differentiation (Foucault, Le Bras et al. 2005). Therefore, we suggest that the intrinsic defect in Ttc7 in B cells, increases the autoreactivity and reactivity of Ttc7$^{fsn/fsn}$ B cells. The presence of autoantigens, released through normal cellular turn-over, may participate to activate autoreactive B cells, which respond to increased levels of IL-4 by proliferating and differentiating into autoantibody producing cells, and help to further activate T cells via their antigen-presenting capacity. This is a highly simplified scenario to describe an exquisitely complex process, as there are regulatory and counter-regulatory molecules that are also unique in B and T cells. However, determining the function of Ttc7 will undoubtedly provide valuable insight into lymphocyte regulation and the early changes determining the course of autoimmunity and autoimmune disease.

Future Work

On-going work in our lab seeks to determine the function of Ttc7$^{fsn/fsn}$ and how it contributes to the dysregulation of IL-4 and the hyperactivation of B cells leading to systemic autoimmunity. While a human homologue to Ttc7$^{fsn/fsn}$ has not currently been identified, cytokine dysregulation and B cell hyperactivation have been found to contribute to human systemic autoimmune disease. We propose that the mechanisms

active in Ttc7$^{fsn/fsn}$ will contribute to a greater understanding of IL-4 regulation and T and B lymphocyte activation in humans. Determining these mechanisms will be important in leading to an understanding of the pathology and to ultimately develop effective specifically targeted therapies for those so affected.

REFERENCES

al-Janadi, M. and S. Raziuddin (1993). "B cell hyperactivity is a function of T cell derived cytokines in systemic lupus erythematosus." J Rheumatol **20**(11): 1885-91.

Amano, H., E. Amano, et al. (2003). "The yaa mutation promoting murine lupus causes defective development of marginal zone B cells." J Immunol **170**: 2293-2301.

Andrews, R. P., M. B. Ericksen, et al. (2002). "Analysis of the life cycle of stat6. Continuous cycling of STAT6 is required for IL-4 signaling." J Biol Chem **277**(39): 36563-9.

Andrews, R. P., L. R. Rosa, et al. (2001). "Reconstitution of a functional human type II IL-4/IL13 receptor in mouse B cells : demonstration of species specificity." J Immunol **166**: 1716-1722.

Ansel, K. M., I. Djuretic, et al. (2006). "Regulation of Th2 differentiation and the IL4 locus accessibility." Annu Rev Immunol **24**: 607-56.

Arinobu, Y., R. Sugimoto, et al. (2000). "Augmentation of signal transducer and activation of transcription (Stat)6 and Stat3 expression in stimulated B and T cells." Biochemical and Biophysical Research Communications **277**: 317-324.

Bacharier, L. B. and R. S. Geha (2000). "Molecular mechanisms of IgE regulation." J Allergy Clin Immunol **105**: S547-58.

Bagavant, H., U. S. Deshmukh, et al. (2006). "Role for nephritogenic T cells in lupus glomerulonephritis: progression to renal failure is accompanied by T cell activation and expansion in regional lymph nodes." J Immunol **177**: 8258-8265.

Baguet, A. and M. Bix (2004). "Chromatin landscape dynamics of the IL-4-Il13 locus during T helper 1 and 2 development." PNAS **101**(31): 11410-11415.

Basaki, Y., K. Ikizawa, et al. (2002). "CD40-mediated tumor necrosis factor receptor-associated factor 3 signaling upregulates IL-4 induced germline Ce transcription in a human B cell line." Archives of Biochemistry and Biophysics **405**: 199-204.

Beamer, W. G., S. C. Pelsue, et al. (1995). "The flaky skin (fsn) mutation in Mice: map location and description of the anemia." Blood **86**(8): 3220-3226.

Bingaman, A. W. and D. L. Farber (2004). "Memory T cells in transplantation: generation, function, and potential role in rejection." American Journal of Transplantation **4**: 846-852.

Bird, J. J., D. R. Brown, et al. (1998). "Helper T cell differentiation is controlled by the cell cycle." Immunity **9**(2): 229-37.

Bix, M., Z. E. Wang, et al. (1998). "Genetic regulation of commitment to interleukin 4 production by a CD4(+) T cell-intrinsic mechanism." J Exp Med **188**(12): 2289-99.

Bizzaro, N. (2007). "Autoantibodies as predictors of disease: the clinical and experimental evidence." Autoimmunity Reviews **6**: 325-333.

Boothby, M., A. L. Mora, et al. (2001). "IL-4 signaling, gene transcription regulation, and the control of effector T cells." Immunologic Research **23**(2/3): 1179-191.

Bour-Jordan, H., J. L. Grogan, et al. (2003). "CTLA-4 regulates the requirement for cytokine-induced signals in Th2 lineage commitment." nature immunology **4**(2): 182-188.

Bradwell, A. S. R. J., GD. (1995). Atlas of HEp-2 Patterns. Birmingham England.

Brinker, A., C. Scheufler, et al. (2002). "Ligand discrimination by TPR domains." Journal of Biological Chemistry **277**(22): 19265-19275.

Bruns, H. A. and M. H. Kaplan (2006). "The role of constitutively active Stat6 in leukemia and lymphoma." Crit Rev Oncol Hematol **57**(3): 245-53.

Bruns, H. A., U. Schindler, et al. (2003). "Expression of a constitutively active Stat6 in vivo alters lymphocyte homeostasis with distinct effects in T and B cells." J Immunol **170**(7): 3478-87.

Butler, N. S., M. M. Monick, et al. (2002). "Altered IL-4 mRNA stability correlates with Th1 and Th2 bias and susceptibility to hypersensitivity pneumonitis in two inbred strains of mice." J Immunol **169**(7): 3700-9.

Carey, G. B., E. Semenova, et al. (2007). "IL-4 protects the B-cell lymphoma cell line CD31 from anti-IgM-induced growth arrest and apoptosis: contribution of the PI-3 kinase-AKT pathway." Cell Research **17**: 942-955.

Carter, B. Z. and J. S. Malter (1991). "Regulation of mRNA stability and its relevance to disease." Laboratory Investigation **65**(6): 610-621.

Casola, S. (2007). "Control of peripheral B-cell development." Curr Opin Immunol **19**: 143-149.

Chan, S. C., M. A. Brown, et al. (1996). "Abnormal IL-4 gene expression by atopic dermatitis T lymphocytes is reflected in altered nuclear protein interactions with IL-4 transcriptional regulatory element." J Invest Dermatol **106**: 1131-1136.

Chen, W., M. O. Daines, et al. (2004). "Methylation of Stat6 modulates Stat6 phosphorylation, nuclear translocation and DNA-binding activity." J Immunol **172**: 6744-6750.

Chen, Z., R. Lund, et al. (2003). "Identification of novel IL-4/stat6-regulated genes in T lymphocytes." J Immunol **171**: 3627-3635.

Craig, W. Y., T. B. Ledue, et al. (2006). "Serologic associations of anti-cytoplasmic antibodies identified during anti-nuclear testing." Clin Chem Lab Med **44**(10): 1283-1286.

Cron, R. Q., S. J. Bort, et al. (1999). "T cell priming enhances IL-4 gene expression by increasing nuclear factor of activated T cells." J Immunol **162**(2): 860-70.

Cronin, D. C., 2nd, R. Stack, et al. (1995). IL-4-producing CD8+ T cell clones can provide B cell help. **154:** 3118-3127.

Crowley, M. T., S. L. Harmer, et al. (1996). Activation-induced Association of a 145-kDa Tyrosine-phosphorylated Protein with Shc and Syk in B Lymphocytes and Macrophages. **271:** 1145-1152.

Cunningham, A. F., K. Serre, et al. (2004). "Pinpointing IL-4-independent acquisition and IL-4-influenced maintenance of Th2 activity by CD4 T cells." Eur J Immunol **34**(3): 686-94.

Daikh, D. a. W. D. (2001). "Cutting Edge: Reversal of murine lupus nephritis with CTLA4Ig and cyclophosphamide." J of Immunol **166**: 2913-2916.

Daines, M. O., R. P. Andrews, et al. (2003). "DNA binding activity of cytoplasmic phosphorylated Stat6 is masked by an interaction with a detergent-sensitive factor." J Biol Chem **278**(33): 30971-4.

D'Andrea, L. D. and L. Regan (2003). "TPR proteins: the versatile helix." Trends Biochem Sci **28**(12): 665-662.

Daniel, C., A. Salvekar, et al. (2000). "A gain-of-function mutation in STAT6." J Biol Chem **275**(19): 14255-9.

Das, A. K., P. T. W. Cohen, et al. (1998). "the structure of the tetracopeptide repeats of protein phosphatase 5: implications for TPR-mediated protein-protein interactions." EMBO Journal **17**(5): 1192-1199.

de Stahl, T. D., J. Dahlstrom, et al. (2003). "A role for complement in feedback enhancement of antibody responses by IgG3." J Exp Med **197**(9): 1183-1190.

Dent, A. L., J. Hu-Li, et al. (1998). "T helper type 2 inflammatory disease in the absense of interleukin 4 and transcription factor stat6." Proc Natl Acad Sci U S A **95**: 13823-13828.

Deocharan, B., P. Marambio, et al. (2003). "Differential effects of interleukin-4 in peptide induced autoimmunity." Clinical Immunol **108**: 80-88.

DeRyckere, D. and J. DeGregori (2005). "E2F1 and E2F2 are differentially required for homeostasis-driven and antigen-induced T cell proliferation in vivo." Journal of Immunology **175**: 647-655.

Deutsch, H. H., K. Koettnitz, et al. (1995). Distinct sequence motifs within the cytoplasmic domain of the human IL- 4 receptor differentially regulate apoptosis inhibition and cell growth. **154:** 3696-3703.

Dokter, W. H., M. T. Esselink, et al. (1993). "Transcriptional and posttranscriptional regulation of the interleukin-4 and interleukin-3 genes in human T cells." Blood **81**(1): 35-40.

Dong, J., Q.-X. Wang, et al. (2007). "Activation of the Stat1 signaling pathway in lupus nephritis in MRL/lpr mice." Lupus **16**: 101-109.

Dorado, B., M. J. Jerez, et al. (2002). "Autocrine IL-4 gene regulation at late phases of TCR activation in differentiated Th2 cells." J Immunol **169**(6): 3030-7.

Dufort, F. J., B. F. Bleiman, et al. (2007). "Cutting edge: IL-4-mediated protection of primary B lymphocytes from apoptosis via Stat6-dependent regulation of glycolytic metabolism." J Immunol **179**(8): 4953-7.

Ebling, F. M. and B. H. Hahn (1989). Pathogenic Subsets of Antibodies to DNA, Informa Healthcare. **5:** 79 - 95.

Erb, K. J., Thomas Holtschke Kathrin Muth Ivan Horak Anneliese Schimpl (1994). T cell subset distribution and B cell hyperreactivity in mice expressing interleukin-4 under the control of major histocompatibility complex class I regulatory sequences. **24:** 1143-1147.

Erb, K. J., B. Ruger, et al. (1997). "Constitutive expression of interleukin (IL)-4 in vivo causes autoimmune-type disorders in mice." J Exp Med **185**(2): 329-39.

Farrington, A. R. P. (2006). Analysis of Splenic B cell Subpopulations in the Autoimmune Prone Flaky Skin Mouse. School of Applied Medical Sciences Portland, Maine, University of Southern Maine. **Master of Science** 47.

Fields, M. L. and J. Erikson (2003). "The regulation of lupus-associated autoantibodies: immunoglobulin transgenic models." Curr Opin Immunol **15**(6): 709-17.

Finkelman, F. D., S. C. Morris, et al. (2000). "Stat6 regulation of in vivo IL-4 responses." J Immunol **164**: 2303-2310.

Foucault, I., S. Le Bras, et al. (2005). The adaptor protein 3BP2 associates with VAV guanine nucleotide exchange factors to regulate NFAT activation by the B-cell antigen receptor. **105:** 1106-1113.

Foucras, G., A. Gallard, et al. (2002). "Chronic soluble antigen sensitization primes a unique memory/effector T cell repertoire associated with Th2 phenotype acquisition in vivo." Journal of Immunology **168**: 179-187.

Fujimoto, M. and S. Sato (2007). "B cell signaling and autoimmune disease: CD19/CD22 loop as a B cell signaling device to regulate the balance of autoimmunity." Journal of Dermatological Science **46**: 1-9.

Gaipl, U. S., L. E. Munoz, et al. (2007). "Clearance deficiency and systemic lupus erythematosus." Journal of Autoimmunity **28**: 114-121.

Giese, T. and W. F. Davidson (1992). "Evidence for early onset, polyclonal activation of T cells subsets in mice homozygous for lpr." J Immunol **149**(9): 3097-3106.

Gong, D. and T. R. Malek (2007). Cytokine-Dependent Blimp-1 Expression in Activated T Cells Inhibits IL-2 Production. **178:** 242-252.

Greenhalgh, C. J. and D. J. Hilton (2001). Negative regulation of cytokine signaling. **70:** 348-356.

Grogan, J. L., Z. E. Wang, et al. (2003). "Basal chromatin modification at the IL-4 gene in helper T cells." J Immunol **171**(12): 6672-9.

Guiter, C., D.-F. I., et al. (2004.). "Constitutive Stat6 activation in primary mediastinal large B-cell lymphoma." Blood **104**(2): 543-549.

Guo, L., J. Hu-Li, et al. (2002). "In Th2 cells the IL4 gene has a series of accessibility states associated with distinctive probabilities fo IL-4 production." PNAS **99**(16): 10623-10628.

Hanson, E. M., H. Dickensheets, et al. (2003). "Regulation of the dephosphorylation of Stat6. Participation of Tyr-713 in the interleukin-4 receptor alpha, the tyrosine phosphatase SHP-1, and the proteasome." J Biol Chem **278**(6): 3903-11.

Hardy, R. P. (2006). "B-1 B cell development." J Immunol **176**: 2749-2754.

Harris, D. P., S. Goodrich, et al. (2005). "Cutting edge: the development of IL-4-producing B cells (B effector 2 cells) is controlled by IL-4, IL-4 receptor alpha, and Th2 cells." J Immunol **175**(11): 7103-7.

Harris, M. B., C.-C. Chang, et al. (1999). Transcriptional Repression of Stat6-Dependent Interleukin-4-Induced Genes by BCL-6: Specific Regulation of Ivarepsilon Transcription and Immunoglobulin E Switching. **19:** 7264-7275.

Hebenstreit, D., G. Wirnsberger, et al. (2006). "Signaling mechanisms, interaction partners, and target genes of STAT6." Cytokine Growth Factor Rev **17**(3): 173-88.

Heery, D. M., E. Kalkhoven, et al. (1997). "A signature motif in transcriptional co-activators mediates binding to nuclear receptors." Nature **387**(6634): 733-6.

Helms, C., S. Pelsue, et al. (2005). "The Tetratricopeptide repeat domain 7 gene is mutated in flaky skin mice: a model for psoriasis, autoimmunity, and anemia." Exp Biol Med (Maywood) **230**(9): 659-67.

Hilton, D. J. (1999). "Negative regulators of cytokine signal transduction." Cell Mol Life Sci **55**(12): 1568-77.

Ho, I. C. and L. H. Glimcher (2002). "Transcription: tantalizing times for T cells." Cell **109 Suppl**: S109-20.

Howard, M., J. Farrar, et al. (1982). "Identification of a T cell-derived b cell growth factor distinct from interleukin 2." J Exp Med **155**(3): 914-23.

Hsu, B. L., S. M. Harless, et al. (2002). Cutting Edge: BLyS Enables Survival of Transitional and Mature B Cells Through Distinct Mediators. **168:** 5993-5996.

Iciek, L. A., S. A. Delphin, et al. (1997). CD40 cross-linking induces Ig epsilon germline transcripts in B cells via activation of NF-kappaB: synergy with IL-4 induction. **158:** 4769-4779.

Ikizawa, K., K. Kajiwara, et al. (2001). "PKCdelta and zeta mediate IL-4/IL-13-induced germline epsilon transcription in human B cells: a putative regulation via PU.1 phosphorylation." Biochem Biophys Res Commun **288**(1): 34-41.

Jacob, C. O., S. Zang, et al. (2003). "Pivotal role of Stat4 and Stat6 in the pathogenesis of the lupus-like disease in the New Zealand Mixed 2328 mice." J Immunol **171**: 1564-1571.

Jankovic, D., M. C. Kullberg, et al. (2000). "Single cell analysis reveals that IL-4 receptor/Stat6 signaling is not required for the in vivo or in vitro development of CD4+ lymphocytes with a Th2 cytokine profile." J Immunol **164**: 3027-3055.

Jiang, H., M. B. Harris, et al. (2000). "IL-4/IL-13 signaling beyond JAK/Stat." J Allergy Clin Immunol **105**: 1063.

Johansson-Lindbom, B. and C. A. K. Borrebaeck (2002). "Germinal center B cells constitute a predominant physiological source of IL-4: implication for Th2 development in vivo." J Immunol **168**: 3165-3172.

Jordan, M. S., A. L. Singer, et al. (2003). "Adaptors as central mediators of signal transduction in immune cells. ." nature immunology **4**(2): 110-116.

Kallies, A. and S. L. Nutt (2007). "terminal differentiation of lymphocytes depends on Blimp-1 " Current Opinion in Immunology **19**: 156-162.

Kammer, G. M., A. Perl, et al. (2002). "Abnormal T cell signal transduction in systemic lupus erythematosus." Arthritis Rheum **46**(5): 1139-1154.

Kaplan, M. H., U. Schindler, et al. (1996). "Stat6 is required for mediating responses to IL-4 and for the development of Th2 cells." Immunity **4**: 313-319.

Kaplan, M. H., S. Sehra, et al. (2007). "Constitutively active Stat6 predisposes towards a lymphoproliferative disorder." Blood.

Kaplan, M. H., A. L. Wurster, et al. (1999). "Stat6-dependent and -independent pathways for IL-4 production." J Immunol **163**(12): 6536-40.

Karras, J. G., Z. Wang, et al. (1997). Induction of STAT protein signaling through the CD40 receptor in B lymphocytes: distinct STAT activation following surface Ig and CD40 receptor engagement. **159:** 4350-4355.

Kashiwada, M., C. C. Giallourakis, et al. (2001). Immunoreceptor Tyrosine-Based Inhibitory Motif of the IL-4 Receptor Associates with SH2-Containing Phosphatases and Regulates IL-4-Induced Proliferation. **167:** 6382-6387.

Kawakami, K., M. Kawakami, et al. (2001). "Overexpressed cell surface interleukin-4 receptor molecules can be successfully targeted for anitumor cytotoxin therapy." Critical Reviews in Immunology **21**: 299-310.

Keegan, A. D. (2000). IL-4. Cytokine Reference. J. J. Oppenheim and M. Feldmann, Academic Press.

Kelly-Welch, A., E. M. Hanson, et al. (2005). "Interleukin-4 Pathway." Science Signaling, 2005, from www.stke.org/cgi/content/full/sigtrans;2005/293/cm9.

Khan, S. N., E. J. Witsch, et al. (2008). "Editing and escape from editing in anti-DNA B cells." PNAS **105**(10): 3861-3866.

Kim, S. T., P. E. Fields, et al. (2007). "Demethylation of a specific hypersensitive site in the Th2 locus control region." PNAS **104**(43): 17052-17057.

Kin, N. W. and V. M. Sanders (2007). "CD86 regulates IgG1 production via a CD19-dependent mechanism." J Immunol **179**: 1516-1523.

Klee, C. B., H. Ren, et al. (1998). "Regulation of the calmodulin-stimulated protein phosphatase, calcineurin." Journal of Biological Chemistry **273**(22): 13367-13370.

Kneitz, C., M. Goller, et al. (2000). "Stat6 and the regulation of CD23 expression in B-chronic lymphocytic leukemia." Leukemia Research **24**: 331-337.

Knodel, M., A. W. Kuss, et al. (2001). "Blimp-1 over-expression abrogates IL-4 and CD40-mediated supression of terminal B cell differentiation but arrests isotype switching." Eur J Immunol **31**: 1972-1980.

Koh, W.-H., J. Dunphy, et al. (1995). "Charaterisation of anticytoplasmic antibodies and their clinical associations." Ann Rheum Dis **54**: 269-273.

Kuhn, R., K. Rajewsky, et al. (1991). "Generation and analysis of interleukin-4 deficient mice. ." Science **254**: 707-710.

Leonard, W. J. and J. X. Lin (2000). "Cytokine Signaling Pathways." J Allergy Clin Immunol **105**(5): 877-888.

Li, F. X., J. W. Zhu, et al. (2003). "Defective gene expression, S phase progression, and maturation during hematopoiesis in E2F1/E2F2 mutant mice." Mol Cell Biol **23**(10): 3607-22.

Linehan, L. A., W. D. Warren, et al. (1998). "STAT6 is required for IL-4-induced germline Ig gene transcription and switch recombination." J Immunol **161**(1): 302-10.

Litterst, C. M. and E. Pfitzner (2002). "An LXXLL motif in the transactivation domain of STAT6 mediates recruitment of NCoA-1/SRC-1." J Biol Chem **277**(39): 36052-60.

Li-Weber, M. and P. H. Krammer (2003). "Regulation of IL4 gene expression by T cells and therapeutic perspectives." Nature Reviews Immunology **3**: 534-543.

Loder, F., B. Mutschler, et al. (1999). "B Cell Development in the Spleen Takes Place in Discrete Steps and Is Determined by the Quality of B Cell Receptor–derived Signals." J. Exp. Med. **190**(1): 75-90.

Lohning, M., A. Richter, et al. (2003). "Establishment of memory for IL-10 expression in developing T helper 2 cells requires repetitive IL-4 costimulatioin and does not impair proliferation." PNAS **100**(21): 12307-12312.

Losman, J., X. P. Chen, et al. (1999). "IL-4 signaling is regulated through the recruitment of phosphatases, kinases, and Socs proteins to the receptor complex." Cold Spring Harbor Symposia on Quantitative Biology **LXIV**: 405-416.

Lu, B., M. Reichel, et al. (1997). "Identification of a Stat6 domain required for IL-4 induced activation of transcription." J Immunol **159**: 1255-1264.

Lyons, B. L., M. A. Lynes, et al. (2003). "Mechanisms of anemia in SHP-1 protein tyrosine phosphatase deficient "viable motheaten" mice." Experimental Hematology **31**: 234-243.

Ma, Y., H. E. Hurst, et al. (1996). Soluble cytokine receptors as carrier proteins: effects of soluble interleukin-4 receptors on the pharmacokinetics of murine interleukin-4. **279:** 340-350.

Mao, C.-S. and J. Stavnezer (2001). "Differential regulation of mouse germline Ig gamma1 and epsilon promoters by IL-4 and CD40." J Immunol **167**: 1522-1534.

Marrack, P., J. Kappler, et al. (2001). "Autoimmune disease: why and where it occurs." Nat Med **7**(8): 899-905.

Marshall, A. J., H. Niiro, et al. (2000). "Regulation of B-cell activation and differentiation by the phosphatidylinositol 3-kinase and phospholipase Cgamma pathways." Immunol Rev **176**: 30-46.

Martin, F. and J. F. Kearney (2000). "B-cell subsets and the mature preimmune repertoire. Marginal zone and B1 B cells as part of a "natural immune memory"." Immunological Reviews **175**: 70-79.

Mattsson, N., E. G. Duzevik, et al. (2005). "Expansion of CD22(lo) B cells in the spleen of autoimmune-prone flaky skin mice." Cell Immunol **234**(2): 124-32.

May, M., Ed. (2007). Autoimmunity: Diseases, mechanisms, therapies. Philadelphia, The Scientist.

McDonald, C., S. Vanscoy, et al. (2004). "Induction of genes involved in cell cycle progression by interleukin-4." Journal of Interferon and Cytokine Research **24**: 729-738.

Messner, B., A. M. Stutz, et al. (1997). "Cooperation of binding sites for Stat6 and NFkB/rel in the IL-4-induced up-regulation of the human IgE germline promoter." J Immunol **159**: 3330-3337.

Mikita, T., D. Campbell, et al. (1996). Requirements for interleukin-4-induced gene expression and functional characterization of Stat6. **16:** 5811-5820.

Miralles, G. D., M. Y. Stoeckle, et al. (1994). Th1 and Th2 cell-associated cytokines in experimental visceral leishmaniasis. **62:** 1058-1063.

Monroe, J. G. and K. Dorshkind (2007). "Fate decisions regulating bone marrow and peripheral B lymphocyte development." Advances in Immunology **95**: 1-50.

Monticelli, S., R. Ghittoni, et al. (2001). "Myb proteins repress human Ig e germline transcription by inhibiting Stat6-dependent promoter activation." Molecular Immunology **38**: 1129-1138

Morgan, D. O. (1999-2007). The Cell Cycle: Principles of Control, New Science Press.

Mori, M., S. C. Morris, et al. (2000). "IL-4 promotes the migration of circulating B cells to the spleen and increases splenic B cell survival." J Immunol **164**: 5704-5712.

Morris, S. C., N. L. Dragula, et al. (2002). "IL-4 promotes Stat6-dependent survival of autoreactive B cells in vivo without inducing autoantibody production." J Immunol **169**: 1696-1704.

Murga, M., O. Fernandez-Capetillo, et al. (2001). "Mutation of E2F2 in mice causes enhanced T lymphocyte proliferation, leading to the development of autoimmunity." Immunity **15**(6): 959-70.

Naora, H., J. G. Altin, et al. (1994). "TCR-dependent and -independent signaling mechanisms differentially regulate lymphokine gene expression in the murine T helper clone D10.G4.1." J Immunol **152**(12): 5691-702.

Naora, H. and I. G. Young (1995). "Comparison of the mechanisms regulating IL-5, IL-4, and three other lymphokine genes in the Th2 clone D10.G4.1." Exp Hematol **23**(7): 597-602.

Nelms, K., H. Huang, et al. (1998). "Interleukin-4 receptor signalling mechanisms and their biological significance." Adv Exp Med Biol **452**: 37-43.

Nelms, K., A. D. Keegan, et al. (1999). "The IL-4 receptor: signaling mechanisms and biologic functions." Annu Rev Immunol **17**: 701-38.

Nelms, K., A. L. Snow, et al. (1998). "FRIP, a hematopoietic cell-specific rasGAP-interacting protein phosphorylated in response to cytokine stimulation." Immunity **9**(1): 13-24.

Nicola, N. A. and C. J. Greenhalgn (2000). "The supressors of cytokine signaling (SOCS) proteins: important feedback inhibitors of cytokine action." Experimental Hematology **28**: 1105-1112.

Noben-Trauth, N., L. D. Shultz, et al. (1997). "An interleukin 4 (IL-4)-independent pathway for CD4+ T cell IL-4 production is revealed in IL-4 receptor-deficient mice." Proc Natl Acad Sci U S A **94**: 10838-10843.

Norvell, A., L. Mandik, et al. (1995). "Engagement of the Antigen-Receptor on Immature Murine B Lymphocytes Results in Death by Apoptosis." The Journal of Immunilogy **154**: 4404-4413.

Oettgen, H. C. (2000). "Regulation of the IgE isotype switch: new insights on cytokine signals and the functions of e germline transcripts." Curr Opin Immunol **12**: 618-623.

Omori, M. and S. Ziegler (2007). "Induction of IL-4 expression in CD4+ T cells by thymic stromal lymphopoietin." J Immunol **178**: 1396-1404.

Parel, Y., M. Aurrand-Lions, et al. (2007). "Presence of CD4+CD8+ double-positive T cells with very high interleukin-4 production potential in lesional skin of patients with systemic sclerosis." Arthritis Rheum **56**(10): 3459-3467.

Parronchi, P., M. de Carli, et al. (1992). "Abberant interleukin (IL)-4 and IL-5 production in vitro by CD4+ helper T cells from atopic subjects." Eur J Immunol **22**: 1615-1620.

Patel, B. K. R., J. H. Pierce, et al. (1998). Regulation of interleukin 4-mediated signaling by naturally occurring dominant negative and attenuated forms of human Stat6. **95:** 172-177.

Pelsue, S. C., P. A. Schweitzer, et al. (1998). "Lymphadenopathy, elevated serum IgE levels, autoimmunity, and mast cell accumulation in flaky skin mutant mice." Eur J Immunol **28**(4): 1379-88.

Peng, S. L., J. Moslehi, et al. (1997). "Roles of interferon-gamma and interleukin-4 in murine lupus." J Clin Invest **99**(8): 1936-46.

Pesu, M., S. Aittomaki, et al. (2002). "p38 mitogen-activated protein kinase regulates interleukin-4-induced gene expression by stimulating Stat6-mediated transcription." Journal of Biological Chemistry **277**(41): 38254-38261.

Pesu, M., K. Takaluoma, et al. (2000). "Interleukin-4-induced transcriptional activation by Stat6 involves multiple serine/threonine kinase pathways and serine phosphorylation of Stat6." Blood **95**(2): 494-502.

Pioli, C., L. Gatta, et al. (2000). "Inhibition of IgG1 and IgE production by stimulation of the B cell CTLA-4 receptor." J Immunol **165**: 5530-5536.

Pioli, C., S. Pucci, et al. (1998). "Role of mRNA stability in the different patterns of cytokine production by CD4+ cells from young and old mice." Immunology **94**(3): 380-7.

Plevin, M. J., M. M. Mills, et al. (2005). "The LxxLL motif: a multifunctional binding sequence in transcriptional regulation." Trends Biochem Sci **30**(2): 66-9.

Quelle, F. W., K. Shimoda, et al. (1995). Cloning of murine Stat6 and human Stat6, Stat proteins that are tyrosine phosphorylated in responses to IL-4 and IL-3 but are not required for mitogenesis. **15:** 3336-3343.

Razeto, A., V. Ramakrishnan, et al. (2004). "Structure of the NCoA-1/SRC-1 PAS-B domain bound to the LXXLL motif of the STAT6 transactivation domain." J Mol Biol **336**(2): 319-29.

Rengarajan, J., K. A. Mowen, et al. (2002). "Interferon regulatory factor 4 (IRF4) interacts with NFAT2 to modulate interleukin 4 gene expression." J Exp Med **195**(8): 1003-1012.

Richards, M. L. and D. H. Katz (1997). "Analysis of the promoter elements necessary for IL_4 and anti-CD40 antibody induction of murine FcRII (CD23)." J Immunol **158**: 263-272.

Rose, S., M. Lichtenheld, et al. (2007). "Murine neonatal CD4+ cells are poised for rapid Th2 effector-like function." J Immunol **178**: 2667-2678.

Rothstein, T. L. (2002). "Cutting Edge Commentary: Two B-1 or not to be one." J Immunol **168**: 4257-4261.

Roy, V., N. H. Chang, et al. (2005). "Aberrant IgM signaling promotes survival of transitional T1 B cells and prevents tolerance induction in lupus-prone New Zealand black mice." J Immunol **175**(11): 7363-71.

Rudge, E. U., A. J. Cutler, et al. (2002). "Interleukin 4 reduces expression of inhibitory receptors on B cells and abolishes CD22 and Fc gamma RII-mediated B cell suppression." J Exp Med **195**(8): 1079-85.

Rüger, B. M., K. J. Erb, et al. (2000). Interleukin-4 transgenic mice develop glomerulosclerosis independent of immunoglobulin deposition. **30:** 2698-2703.

Rush, J. S. and P. D. Hodgkin (2001). "B cells activated via CD40 and IL-4 undergo a division burst but require continued stimulation to maintain division, survival and differentiation." Eur J Immunol **31**: 1150-1159.

Sang, D. K., J. H. Ouma, et al. (1999). "Increased Levels of Soluble Interleukin-4 Receptor in the Sera of Patients with Visceral Leishmaniasis." Journal of Infectious Diseases **179**(3): 743-746.

Sato, S., N. Ono, et al. (1996). "CD19 regulates B lymphocyte signaling thresholds critical for the development of B-1 lineage cells and autoimmunity." J Immunol **157**: 4371-4378.

Satoh, T., M. Nakafuku, et al. (1991). "Involvement of ras p21 protein in signal-transduction pathways from interleukin 2, interleukin 3, and granulocyte/macrophage colony-stimulating factor, but not from interleukin 4." Proc Natl Acad Sci U S A **88**(8): 3314-8.

Schaffer, A., A. Cerutti, et al. (1999). "The evolutionarily conserved sequence upstream of the human Ig Heavy chain Sgamma3 region is an inducible promoter: synergistic activation by CD40 ligand and IL-4 via cooperative NF-kB and Stat6 binding sites." J Immunol **162**: 5327-5336.

Schebesta, M., B. Heavey, et al. (2002). "Transcriptional control of B-cell development." Curr Opin Immunol **14**(2): 216-23.

Schroder, A. J., P. Pavlidis, et al. (2002). "Cutting Edge: Stat6 serves as a positive and negative regulator or gene expression in IL-4 stimulated B cells." J Immunol **168**: 996-1000.

Sehra, S., D. Patel, et al. (2005). "A role for caspases in controlling Il-4 expression in T cells." Journal of Immunology **174**: 3440-3446.

Shaffer, A. L., K. I. Lin, et al. (2002). "Blimp-1 orchestrates plasma cell differentiation by extinguishing the mature B cell gene expression program." Immunity **17**(1): 51-62.

Shaffer, A. L., X. Yu, et al. (2000). "Bcl-6 represses genes that function in lymphocyte differentiation, inflammation and cell cycle control." Immunity **13**: 199-212.

Sherman, M. A., Secor, V.H., and Brown, M.A. (1999). "IL-4 preferentially activates a novel Stat6 isoform in mast cells. ." Journal of Immunology **162**(5): 2703-2708.

Siepmann, K., G. Wohlleben, et al. (1996). "CD40-mediated regulation of interleukin-4 signaling pathways in B lymphocytes." Eur J Immunol **26**(7): 1544-52.

Singh, R. R. (2003). "IL-4 and many roads to lupuslike autoimmunity." Clin Immunol **108**(2): 73-9.

Singh, R. R., V. Saxena, et al. (2003). "Differential contribution of IL-4 and STAT6 vs STAT4 to the development of lupus nephritis." J Immunol **170**(9): 4818-25.

Smith, D. F. (2004). "Tetratricopeptide repeat cochaperones in steroid receptor complexes." Cell Stress and Chaperones **09**(2): 109-121.

Snapper, C. M., P. V. Hornbeck, et al. (1988). Interleukin 4 Induces Membrane Thy-1 Expression on Normal Murine B Cells. **85:** 6107-6111.

Snapper, C. M., T. M. McIntyre, et al. (1992). "Induction of IgG3 secretion by interferon gamma: a model for T cell-independent class switching in response to T cell-independent Type 2 antigens." J Exp Med **175**: 1367-1371.

So, E. Y., H. H. Park, et al. (2000). "IFN-gamma and IFN-alpha posttranscriptionally down-regulate the IL-4-induced IL-4 receptor gene expression." J Immunol **165**(10): 5472-9.

Stahl, D., M. Hoemberg, et al. (2006). "Influence of isotypes od disease-associated autoantibodies on the expression of natural autoantibody repertoires in humans." Immunology Letters **102**: 50-59.

Stevens, A., J. S. Lowe, et al. (2002). Wheater's Basic Histopathology. Edinburgh, Churchill Livingstone.

Su, W. and M. P. Madaio (2003). "Recent advances in the pathogenesis of lupus nephritis: autoantibodies and B cells." Semin Nephrol **23**(6): 564-8.

Sundberg, J. P., M. France, et al. (1997). "Development and Progression of Psoriasiform Dermatitis and Systemic Lesions in the Flaky Skin (fsn) Mouse Mutant." Pathobiology **65**: 271-286.

Suzuki, K., Nakajima, H., Watanabe, N., Kagami, S., Suto, A., Saito, Y., Saito, T., and Iwanamoto, I. (2000). "Role of common cytokine receptor gamma chain and JAK3-dependent signaling in the proliferation and survival of murine mast cells. ." Blood **96**(6): 2172-2180.

Tachibana, H., T. Kubo, et al. (2001). "Identification of an inhibitor for interleukin 4-induced epsilon germline transcription and antigen-specific IgE production in vivo." Biochem Biophys Res Commun **280**(1): 53-60.

Thienes, C. P., L. DeMonte, et al. (1997). "The transcription factor B-cell-specific activator protein (BSAP) enhances both IL-4 nd CD-40-mediated activation of the human e germline promoter." J Immunol **158**: 5874-5882.

Tinnel, S. B., S. M. Jacobs-Helber, et al. (1998). "Stat6, NF-kB and C/EBP in CD23 expression and IgE production." Int Immunol **10**(10): 1529-1538.

Wakeland, E. K., A. E. Wandstrat, et al. (1999). "Genetic dissection of systemic lupus erythematosus." Curr Opin Immunol **11**(6): 701-7.

Wardemann, H., S. Yurasov, et al. (2003). "Predominant autoantibody production by early human B cell precursors." Science **301**(5638): 1374-7.

Warren, W. D. and M. T. Berton (1995). "Induction of germ-line gamma 1 and epsilon Ig gene expression in murine B cells. IL-4 and the CD40 ligand-CD40 interaction provide distinct but synergistic signals." J Immunol **155**(12): 5637-46.

Waters, S. T., S. M. Fu, et al. (2001). "NZM2328: A New Mouse Model of Systemic Lupus Erythematosus with Unique Genetic Susceptibility Loci." Clinical Immunology **100**(3): 372-383.

Webb, D. C., A. N. J. McKenzie, et al. (2000). "Integrated signals between IL-13, IL-4, and IL-5 regulate airways hyperactivity." J Immunol **165**: 108-113.

Weisman, R., J. Creaner, et al. (1996). "A multicopy suppressor of a cell cycle defect in S.pombe encodes a heat shock-inducible 40 kDa cyclophilin-like protein." The EMBO Journal **15**(3): 447-456.

Welner, R., W. Hastings, et al. (2004). "Hyperactivation and Proliferation Lymphocytes from the Spleens of Flaky Skin (fsn) Mutant Mice." Autoimmunity **37**(3): 227-235.

Welner, R., D. J. Swett, et al. (2005). "Age-related loss of bone marrow pre-B- and immature B-lymphocytes in the autoimmune-prone flaky skin mutant mice." Autoimmunity **38**(6): 399-408.

Wery-Zennaro, S., J. L. Zugaza, et al. (2000). "IL-4 regulation of IL-6 production involves Rac/Cdc42- and p38 MAPK-dependent pathways in keratinocytes." Oncogene **19**(12): 1596-604.

White, R. A., S. G. McNulty, et al. (2005). "Positional cloning of the Ttc7 gene required for normal iron homeostasis and mutated in hea and fsn anemia mice " Genomics **85**: 330-337.

Whitelaw, E. and D. I. K. Martin (2001). "Retrotransposons as epigenetic mediators of phenotypic variation in mammals." Nature Genetics **27**: 361-365.

William, J., C. Euler, et al. (2005). "Short-lived plasmablasts dominate the early spontaneous rheumtoid factor response: differentiation pathways, hypermutating cell types, and affinity maturation outside the germinal center." J Immunol **174**: 6879-6887.

Withington, S., E. Maltby-Askari, et al. (2002). "Antinuclear Autoantibodies in Flaky Skin (fsn) Mutant Mice." Autoimmunity **35**(3): 175-181.

Woetmann, A., J. Brockdorff, et al. (2003). "Protein phosphatase 2A (PP2A) regulates interleukin-4-mediated STAT6 signaling." J Biol Chem **278**(5): 2787-91.

Wurster, A. L., V. L. Rodgers, et al. (2002). "Interleukin-4-mediated protection of primary B cells from apoptosis through Stat6-dependent up-regulation of Bcl-xL." J Biol Chem **277**(30): 27169-75.

Wurster, A. L., T. Tanaka, et al. (2000). "The biology of Stat4 and Stat6." Oncogene **19**(21): 2577-84.

Wurster, A. L., D. J. Withers, et al. (2002). "Stat6 and IRS-2 cooperate in interleukin 4 (IL-4)-induced proliferation and differentiation but are dispensable for IL-4-dependent rescue from apoptosis." Mol Cell Biol **22**(1): 117-26.

Xu, Z., B. Duan, et al. (2006). "Stat4 deficiency reduces autoantibody production and glomerulonephritis in a mouse model of lupus." Clinical Immunol **120**: 189-198.

Yagi, R., W. Suzuki, et al. (2002). "The IL-4 production capability of different strains of naive CD4(+) T cells controls the direction of the T(h) cell response." Int Immunol **14**(1): 1-11.

Yamada, T., D. Zhu, et al. (2002). "CD45 controls interleukin-4-mediated IgE class switch recombination in human B cells through its function as a janus kinase phosphatase." Journal of Biological Chemistry **277**(32): 28830-28835.

Yamashita, M., R. Shinnakasu, et al. (2004). "Interleukin (IL)-4 independent maintenance of histone modification of the IL-4 gene loci in memory Th2 cells." Journal of Biological Chemistry **279**(38): 39454-39464.

Ying, G.-G., P. Proost, et al. (2000). Nucleolin, a Novel Partner for the Myb Transcription Factor Family That Regulates Their Activity. **275:** 4152-4158.

Yung, S. and T. M. Chan (2008). "Anti-DNA antibodies in the pathogenesis of lupus nephritis- the emerging mechanisms." Autoimmunity Reviews **7**: 317-321.

Yurasov, S., H. Wardemann, et al. (2005). "Defective B cell tolerance checkpoints in systemic lupus erythematosus." J Exp Med **201**(5): 703-11.

Zamorano, J., A. E. Kelly, et al. (2001). "Costimulation of resting B lymphocytes alters the IL-4-activated IRS2 signaling pathway in a STAT6 independent manner: implications for cell survival and proliferation." Cell Res **11**(1): 44-54.

Zamorano, J., A. L. Mora, et al. (2001). "NF-kB activation plays an important role in the IL-4 induced protection from apoptosis." Int Immunol **13**(12): 1479-1487.

Zhang, J., M. Kalkum, et al. (2004). "E protein silencing by the leukemogenic AML1-ETO fusion protein." Science **305**(5688): 1286-9.

Zhang, K., L. Zhang, et al. (2002). "CD40-mediated p38 mitogen-activated protein kinase activation is required for immunoglobulin class switch recombination to IgE." J Allergy Clin Immunol **110**: 421-9.

BIOGRAPHY OF THE AUTHOR

Beth Lindroth Hill was born in Arlington, Mass. and graduated from Burlington High School in Burlington Mass. She moved to Maine at the age of 19 to attend The ApprenticeShop in Bath, Maine, as a boat-building apprentice. Graduating after a two-year apprenticeship, she began her college career at the University of Southern Maine, where she became the longest continuously enrolled student in the history of the University. After 17 years as an undergraduate, during which time she managed a restaurant and a custom jewelry business and raised a family, she returned to USM full-time and completed her BA at USM's Lewiston-Auburn College in Natural and Applied Sciences graduating *Summa cum laude*. Beth is a member of the Phi Kappa Phi and Golden Key National Honor Societies. She entered the Biochemistry and Molecular Biology Graduate Program at the University of Maine in fall of 2001.

After receiving her degree, Beth will be remaining in the Pelsue lab at USM to become a post-doctoral faculty member. Beth is a candidate for the Doctor of Philosophy Degree in Biochemistry and Molecular Biology from The University of Maine in May, 2008.

Publications

Robert Welner, William Hastings, **Beth L. Hill** and Stephen Pelsue. 2004. Hyperactivation and proliferation of lymphocytes from the spleens of flaky skin (*fsn*) mutant mice. *Autoimmunity*, May, 37(3): 227-235.

Thomas A Newton and **Beth Ann Hill**. 2004. Using conductivity devices in nonaqueous solutions I: demonstrating the Sn1 mechanism. *Journal of Chemical Education*, 81: 58.

Thomas A Newton and **Beth Ann Hill**. 2004. Using conductivity devices in nonaqueous solutions II: demonstrating the Sn2 mechanism. *Journal of Chemical Eduction*, 81: 61.

Kim Chamberland, **Beth Ann Lindroth** and Blake Whitaker. 2002. Genotoxicity in Androscoggin River smallmouth bass. *Northeastern Naturalist*, June, 9(2): 203-212.